UNIVERSIDADE ESTADUAL PAULISTA
"JÚLIO DE MESQUISTA FILHO"
INSTITUTO DE BIOCIÊNCIAS - RIO CLARO

PROGRAMA DE PÓS-GRADUAÇÃO EM CIÊNCIAS BIOLÓGICAS
(Biologia Celular e Molecular)

MOLECULAR COMPOSITION AND EVOLUTION OF B CHROMOSOMES IN NEOTROPICAL GRASSHOPPERS: A CYTOGENOMIC APPROACH

DIOGO MILANI

Rio Claro - SP
2021

DIOGO MILANI

MOLECULAR COMPOSITION AND EVOLUTION OF B CHROMOSOMES IN NEOTROPICAL GRASSHOPPERS: A CYTOGENOMIC APPROACH

Orientador: Prof. Dr. Diogo Cavalcanti Cabral de Mello

Tese apresentada ao Instituto de Biociências do Campus de Rio Claro, Universidade Estadual Paulista, como parte dos requisitos para obtenção do título de Doutor em Ciências Biológicas. Área de Concentração: Biologia Celular e Molecular.

Rio Claro - SP
2021

Milani, Diogo
M637m Molecular composition and evolution of B chromosomes in neotropical grasshoppers : a cytogenomic approach / Diogo Milani. -- Rio Claro, 2021
188 p.

Tese (doutorado) - Universidade Estadual Paulista (Unesp), Instituto de Biociências, Rio Claro
Orientador: Diogo Cavalcanti Cabral de Mello

1. Citogenética. 2. Cromossomos supranumerários. 3. Genômica. 4. Gafanhotos. 5. Populações. I. Título.

Sistema de geração automática de fichas catalográficas da Unesp. Biblioteca do Instituto de Biociências, Rio Claro. Dados fornecidos pelo autor(a).

Essa ficha não pode ser modificada.

CERTIFICADO DE APROVAÇÃO

TÍTULO DA TESE: MOLECULAR COMPOSITION AND EVOLUTION OF B CHROMOSOMES IN NEOTROPICAL GRASSHOPPERS: A CYTOGENOMIC APPROACH

AUTOR: DIOGO MILANI

ORIENTADOR: DIOGO CAVALCANTI CABRAL DE MELLO

Aprovado como parte das exigências para obtenção do Título de Doutor em CIÊNCIAS BIOLÓGICAS (BIOLOGIA CELULAR E MOLECULAR), pela Comissão Examinadora:

Prof. Dr. DIOGO CAVALCANTI CABRAL DE MELLO (Participaçao Virtual)
Departamento de Biologia Geral e Aplicada / IB Rio Claro

Profa. Dra. PATRICIA PASQUALI PARISE MALTEMPI (Participaçao Virtual)
Departamento de Biologia Geral e Aplicada / IB Rio Claro

Prof. Dr. JUAN MARTIN FERRO (Participaçao Virtual)
Instituto de Biologia Subtropical / Universidad Nacional de Misiones

Profa. Dra. MAGDALENA VAIO SCVORTZOFF (Participaçao Virtual)
Facultad de Agronomía / Universidad de la República

Prof. Dr. PABLO MORA RUIZ (Participaçao Virtual)
Laboratory of Chromosomics / University of South Bohemia

MORA RUIZ PABLO - 77368717Y

Firmado digitalmente por MORA RUIZ PABLO - 77368717Y
Nombre de reconocimiento (DN): c=ES, serialNumber=IDCES-77368717Y, givenName=PABLO, sn=MORA RUIZ, cn=MORA RUIZ PABLO - 77368717Y
Fecha: 2021.12.08 22:27:46 +01'00'

Rio Claro, 08 de dezembro de 2021

Dedico este trabalho a todos os cientistas, que apesar de todas as dificuldades, continuam sempre em busca do conhecimento.

Agradecimentos

Durante o período da minha formação acadêmica eu tive a oportunidade de conhecer diversos alunos e pesquisadores que atuam na mesma área ou áreas diferentes da ciência. A pós-graduação me fez entender que ao menos 3 coisas são fundamentais para essa jornada: 1) um orientador atuante, ético e presente; 2) um projeto com potencial de produção e potencial para ser cumprido; e 3) ter satisfação com a sua pesquisa.

Hoje, ao fim do meu doutorado eu creio em dizer que fui um sujeito de muita sorte, pois além de ter tido a oportunidade de viver esses três fundamentos eu sempre fui extremamente abençoado por minha família, que sempre me apoiaram e motivaram. Além disso, tive desde a graduação um exemplar orientador, Dr. Prof. Diogo C. Cabral de Mello, que sempre confiou em meu trabalho e me ensinou dois dos maiores valores que adquiri em minha vida profissional, a ética e perseverança.

Além disso, agradeço pela oportunidade de ter realizado um estágio no exterior em Granada/Espanha, o qual fui muito bem recebido pelo Dr. Francisco Ruiz-Ruano, Dr. Prof. Juan Pedro Camacho e colegas.

Agradeço também pela oportunidade de conhecer pessoas extraordinárias em laboratório que começaram como meus colegas e hoje se tornaram grandes amigos.

Agradeço também ao Departamento de Biologia UNESP/Rio Claro pela disposição da realização do meu trabalho e aos colegas do departamento e colaboradores que ajudaram no desenvolvimento do meu trabalho com amostras e materiais científicos.

Agradeço pela enorme felicidade de compartilhar esses anos sempre com o apoio, conselhos e amor de minha parceira, Viviane.

Agradeço à UNESP/Rio Claro e a CAPES pela bolsa de estudos atribuída pelo programa de Pós-graduação em Biologia Celular e Molecular da UNESP de Rio Claro/SP.

O presente trabalho foi realizado com apoio da Coordenação de Aperfeiçoamento de Pessoal de Nível Superior - Brasil (CAPES) - Código de Financiamento 001.

Agradeço pelos auxílios financeiros à pesquisa referente aos seguintes projetos:

- processo nº 2011/19481-3, Fundação de Amparo à Pesquisa do Estado de São Paulo (FAPESP) - (Exigência cláusula 7ª Portaria CTA nº 03/2019 – FAPESP) coordenado pelo Prof. Dr. Diogo Cavalcanti Cabral de Mello;
- Conselho Nacional de Desenvolvimento Científico e Tecnológico – CNPq. Processo de nº 475308/2011-5 coordenado pelo Prof. Dr. Diogo Cavalcanti Cabral de Mello;
- Projeto temático de processo nº 2015/16661-1, Fundação de Amparo à Pesquisa do Estado de São Paulo (FAPESP) - (Exigência cláusula 7ª Portaria CTA nº 03/2019 – FAPESP) coordenado pelo Prof. Dr. Cesar Martins.

E por fim, eu agradeço profundamente a todos vocês que participaram de uma forma ou outra durante esse período do meu doutorado.

“We make a living by what we get, but we make a life by what we give" – Winston Churchill

RESUMO

Cromossomos supranumerários ou Bs são elementos dispensáveis adicionais que estão presentes em alguns indivíduos em uma determinada população de uma determinada espécie. Até agora, estima-se que estejam presentes em mais de 15% dos eucariotos, incluindo plantas, fungos e animais. Uma das principais características dos Bs é que eles não se recombinam com o complemento A, evoluindo independentemente do resto do genoma. Eles também podem se acumular ao longo de gerações por forças evolutivas ainda não muito conhecidas como resultado de impulsos por distorção do padrão normal de herança de Mendel. Uma característica muito comum dos cromossomos B é sua heterocromatinização e acúmulo de DNAs repetitivos, responsáveis por sua evolução e diferenciação em relação ao complemento A. Genes funcionais associados principalmente à divisão e regulação cromossômica também foram documentados. Apesar dos ortópteros apresentarem grande número de espécies portando cromossomos B, estudos com abordagens recentes usando a integração entre sequenciamento genômico e mapeamento cromossômico físico para melhor entendimento sobre origem, composição, evolução e comportamento estão concentrados principalmente em algumas espécies. Aqui, nosso objetivo foi elucidar a composição molecular e possível ancestralidade dos cromossomos B em diferentes gafanhotos neotropicais, com uma extensão para entender a dinâmica populacional do cromossomo B de *Abracris flavolineata*. O presente trabalho teve basicamente três etapas principais apresentadas em três manuscritos. No primeiro, por análise de satDNAs, fornecemos suporte para a origem intraespecífica do cromossomo B de *Rhammatocerus brasiliensis*, *Schistocerca rubiginosa* e *Xyleus discoideus angulatus*, a partir de cromossomos pequenos, o que parece ser uma característica comum para este grupo. O segundo capítulo apresentou o cromossomo B eucromático incomum de *A. flavolineata* que diferentemente a outros Bs poderia ser um elemento jovem, não enriquecido com DNA repetitivo, mostrando padrão C-negativo e alta semelhança com o complemento A. Esses resultados obtidos por sequenciamento genômico, bioinformática e mapeamento cromossômico, sugerem uma origem intraespecífica do cromossomo B a partir do par L1, provavelmente passando por misdivisão e formação de isocromossomo. Finalmente, no terceiro capítulo, mais dois Bs foram encontrados em populações de *A. flavolineata* com frequências diferente e composição altamente diferenciada. As evidências obtidas pela análise do repeatoma reforçaram que os Bs são jovens, mas

em diferentes estágios de heterocromatinização, principalmente devido à intensa amplificação de repetições de satDNA, como observado para o B da população da Argentina. A variante do B da população de Cabo/PE apresentou mais semelhança com a variante de Rio Claro/SP do que a de Posadas/ARG. Além disso, a origem única das variantes de Bs das populações de *A. flavolineata* é discutida.

Palavras-chaves: cromossomos supranumerários, DNA repetitivo, FISH, sequenciamento de DNA, população.

ABSTRACT

Supernumerary chromosomes or Bs are additional dispensable elements that are present in some individuals in a given population of a given species. So far, they were estimated to be present in more than 15% of eukaryotes, including plants, fungi and animals. One of the main characteristics of Bs is that they do not recombine with the A complement, evolving independently of the rest of the genome. They also can accumulate along generations by not well-known evolutionary forces as results of drive by distortion of the normal Mendelian inheritance pattern. A very common feature for the B chromosomes is their heterochromatinization and accumulation of repetitive DNAs, which account for its evolution and differentiation in comparison to A complement. Functional genes mainly associated with division and chromosome regulation were also documented. Despite orthopterans present large number of species harboring B chromosomes, studies with recent approaches using the integration between genomic sequencing and physical chromosome mapping for better understanding about origin, composition, evolution and behavior are concentrated primarily on a few species. Here, our goal was to elucidate the molecular composition and possible ancestry of B chromosomes in different Neotropical grasshoppers, with an extension to understand the populational dynamics of the B chromosome of *Abracris flavolineata*. The present work had basically three main steps presented in three manuscripts. The first one, by satDNAs analysis, we provided support for intraspecific origin of the B chromosome of *Rhammatocerus brasiliensis, Schistocerca rubiginosa* and *Xyleus discoideus angulatus*, from small chromosomes, which appears to be a common feature for this group. The second chapter presented the uncommon euchromatic B chromosome of *A. flavolineata* that differentially to other Bs could be a young element, not enriched with repetitive DNA, showing C-negative pattern and high resemblance with the A complement. These results obtained by genomic sequencing, bioinformatics and chromosome mapping, suggests an intraspecific origin of the B chromosome from L1 pair, probably passing through misdivision and isochromosome formation. Finally, in the third chapter two more Bs were found on *A. flavolineata* populations with different frequency and highly differentiated in composition. The evidences gathered by repeatome analysis reinforced that the Bs are young but in different stages of heterochromatinization, mainly due to intense amplification of satDNA repeats, as for the B from Argentina population. The B variant from Cabo/PE population presented more resemblance to

the variant from Rio Claro/SP than to from Posadas/ARG. Moreover, the unique origin of the B variants of *A. flavolineata* populations is discussed.

Key-words: supernumerary chromosomes, repetitive DNA, FISH, DNA sequencing, population.

SUMARY

1. INTRODUCTION

1.1. Supernumerary chromosomes (B)

In addition to genes that can be directly involved in the adaptability of individuals to environments, eukaryotic genomes have several sequences that are considered selfish genetic elements or genomic parasites. These elements multiply and are transmitted over generations and can, in some cases, have harmful effects on individuals. Among the genomic parasites are known, for example, the transposable elements (TEs) and the supernumerary chromosomes. The supernumerary, extra, or else B chromosomes are outstanding accessory genomic elements discovered in about one century ago (WILSON, 1907), and later described as a selfish and parasitic element (ÖSTERGREN, 1945; NUR, 1966, 1977; JONES, 1985; WERREN et al., 1987). As proposed in the First B chromosome Conference (BEUKEBOOM, 1994), the B chromosomes were classified as additional dispensable elements that originate from A chromosomes (normal complement or karyotype), which do not recombine (CAMACHO, 2005). Another feature of B chromosomes is that they could be accumulated along generations by distorting the normal Mendelian inheritance patterns (JONES, 1995). They may be present in some individuals in a given population of a species exhibiting different morphology and varying in numbers, from one or in multiple copies, as for example in *Zea mays*, which they are present exceeding the number of A complement chromosomes (2n = 20 As + 0–34 Bs) (HOUBEN et al., 2014). As they do not recombine, they follow their own evolutionary fate, accumulating, for example, exclusive mutations and distinct sequences, ultimately causing differentiation of the rest of the genome (BEUKEBOOM, 1994; CAMACHO, 2005; TRIFONOV et al., 2013; HOUBEN et al., 2014; VALENTE et al., 2017).

The occurrence of B chromosomes was reported in previous reviews in at last 1,300 plants, almost 500 animals and many fungi species, and expected to reach about 15% of the eukaryotes (JONES and REES, 1982; JONES, 1995; CAMACHO et al., 2000; 2005). A recent review reported that the number of species harboring B chromosomes raised to 2,828 in total based in 5,760 published manuscripts (D'AMBROSIO et al., 2017) and a new survey by Jones (2017) estimated 406 species carrying B chromosomes discovered since they were last surveyed in 1980. Previous analyses of B chromosomes distribution across species related it to diverse factors as

genome size, breeding system and chromosome differentiation (PALESTIS et al., 2004), moreover, it is reasoning to affirm that the B chromosome frequency among natural populations also depends of distinct evolutionary forces as phenotypic and intragenomic selection, genetic drift and their polymorphism pathway (CAMACHO, 2005).

1.1.1. Repetitive DNAs and their relationship to B chromosomes molecular composition

The nuclear genome of eukaryotes is basically organized in single copy sequences and repetitive DNAs, in low or high number (LÓPEZ-FLORES and GARRIDO-RAMOS, 2012; BISCOTTI et al., 2015a, b). Among the types of repetitive DNA sequences in genomes are the spread repetitive sequences as TEs, and in tandem repetitions that form blocks at one or more locations on chromosomes, including satellite DNA (satDNA) and several genes with multiple copies, such as ribosomal DNAs (rDNAs), genes encoding histone proteins, genes involved in splicing process (snDNAs), MHC genes and immunoglobulins (NEI et al., 1997), olfactory receptor genes (NIIMURA and NEI, 2003; WHINNETT and MUNDY, 2003), among others. For a long time, the non-coding repetitive elements were recognized as “junk DNA” because they do not have known functionality (ORGEL and CRICK, 1980), however the advance in the studies allowed the recognition of multiple functions for these elements, such as regulation of gene expression, replication and repair of genomes (SHAPIRO and STERNBERG, 2005; BIÉMONT and VEIRA, 2006; FESCHOTTE and PRITHAM, 2007; PLOHL et al., 2012). In addition, repetitive DNAs have an important structural function for chromosomes, being the largest components of heterochromatin, constituting the largest fraction of genomes and are the main component of the centromeres (SHAPIRO and STERNBERG, 2005; UGARKOVIĆ, 2005; BIÉMONT and VEIRA, 2006; FESCHOTTE and PRITHAM, 2007; LÓPEZ-FLORES and GARRIDO-RAMOS, 2012; BISCOTTI et al., 2015a).

The satDNAs are highly repetitive sequences with wide structural variability and number of repeats in the genomes that have aroused great importance in research related to chromosomal evolution and genome functionality in different groups of eukaryotes (PALOMEQUE e LORITE, 2008; MACAS et al., 2010; PEZER et al., 2011; LÓPEZ-FLORES e GARRIDO-RAMOS, 2012; CAZAUX et al., 2013;

KOPECNA et al., 2014; NERGADZE et al., 2014; VITTORAZZI et al., 2014; GARCÍA et al., 2015; HEITKAM et al., 2015; RUIZ-RUANO et al., 2016a). These sequences are mainly accumulated in centromeric and telomeric regions of chromosomes, with diverse number of copies and size (CHARLESWORTH et al., 1994; RUIZ-RUANO et al., 2016a). Many studies have shown that satDNAs contributes to important cellular process as chromosome pairing and segregation, regulation and formation of heterochromatin, as well as in the modulation of gene expression (TOPP et al., 2004; UGARKOVIĆ, 2005; PLOHL et al., 2008; PEZER et al., 2011; BRAJKOVIĆ et al., 2012; TSOUMANI et al., 2013; CAMACHO et al., 2015; FELICIELLO et al., 2015; KUHN, 2015). The most accepted proposal on how satDNAs evolve is defined by means of concerted evolution, which is the result of homogenization and fixation of changes among repeats units greater within members of a population than among other species (CHARLESWORTH et al., 1994; UGARKOVIĆ and PLOHL, 2002; PALOMEQUE and LORITE, 2008; PLOHL et al., 2008). This phenomenon could be caused by different molecular mechanisms responsible of spreading new mutations and changes in a repeat family, like DNA turnover, unequal crossing and gene conversion (SMITH, 1976).

The multigene families are groups of genes sometimes classified also as tandem repeats that present essential functional properties emerged mostly by gene duplication (NEI and ROONEY, 2005; EIRIN-LOPEZ et al., 2012; PERVAIZ et al., 2019). Due to its derivation by gene duplication and important functionality, these families present high homology between copies and shares high conservation along the evolutionary pathway, but the processes behind its evolution in genomes comprehends the emergence of diversification, including pseudogenization and spreading of copies (NEI and ROONEY, 2005). The discussion of how the multigene families evolve has been debated for many years, but the most acceptable proposes are known as the concerted and birth-and-death evolution. Contrary to the concerted evolution, the birth-and-death consists that these genes are generated mainly by gene duplication, which could persist in the genome for long periods or be lost, for example, by unequal crossing over. The surviving copies would then pass through modifications that could lead to sub-functionalization or pseudogenization (HUGHES and NEI 1992; NEI and ROONEY, 2005; EIRIN-LOPEZ et al., 2012).

The TEs differs from the others repetitive sequences due to some reasons, but

the most obvious is that they are sequences capable of replicate themselves, alternating its position or inserting additional copies in different regions of the genome. This capacity is basically because they encode proteins with complex multiple activities that promote their transposition, although some TEs loss this capacity (BOWEN and JORDAN, 2002; KIDWELL, 2005; PRITHAM, 2009; BOURQUE et al., 2018; WELLS and FESCHOTTE, 2020). There are diverse types of TE among eukaryotes and they can be classified basically by its transposition mechanisms as Retrotransposons (class I TEs) and DNA transposons (class II TEs) (FINNEGAN, 1989). Additionally, TEs can also be classified according to whether they are able to move by themselves (autonomous) or not (non-autonomous) (KIDWELL, 2005). Non-autonomous TE families require the presence of another TE to move and they are typically noncoding, as for example the short interspersed nuclear elements (SINEs) and miniature inverted-repeat transposable elements (MITEs). More recent classification divided Retrotransposons into three subclasses as, long terminal repeats (LTR) that are mobilized via integrase (IN), the non-LTR elements mobilized via target-primed reverse transcription and the last known subclass YR-elements that its integration is mediated by a tyrosine recombinase in place of a IN (POUTER and BUTLER, 2015). As for the DNA transposons, they can also be divided in four subclasses being the simplest one as DD(E/D) integrase transposons including very known families, such as *Tc1/Mariner* types (YUAN and WESSLER, 2011). The *Cryptons* integrated via YR (KOJIMA and JURKA, 2011), the *Helitrons* known as rolling-circle elements (THOMAS and PRITHAM, 2015), and *Mavericks* or *Polintons* that are capable of self-synthesizing (KAPITONOV and JURKA, 2006; PRITHAM et al., 2007). Due to their great complexity and to present several invasion strategies and to occupy a considerable fraction of the genome in almost all eukaryotes, TEs represent an important source of studies related to genetic variation, genome composition and evolutionary biology. Because they have replicative mobilization mechanisms the frequency of vertical inheritance can be accumulative, thus correlating strongly with genome size among species (TENAILLON et al., 2011; AGREN and WRIGHT, 2011; SUN and MUELLER, 2014; WONG et al., 2019), although functional copies containing protein-coding genes are present in very small amounts (FEDOROFF, 2012).

A very common characteristic for the B chromosomes is their heterochromatinization and accumulation of repetitive DNAs, which account for its

evolution and differentiation in comparison to normal chromosomes (A complement), also suggesting that they could be inert elements (JONES, 1991; CAMACHO, 2005; HOUBEN et al., 2014). Enrichment of satDNAs was well documented in B chromosomes of several species belonging to different groups. In the grasshopper *Eumigus monticola* the ancestry of a B chromosome through an autosome pair was investigated by means of the high-throughput analysis of the satellitome for the first time (RUIZ-RUANO et al., 2016b), and in *Locusta migratoria* a more complete repeat analysis identified that 94.9% content of B chromosome is repetitive mainly by satDNA and TEs (RUIZ-RUANO et al., 2018). For *Drosophila melanogaster* it was documented evidences of a satDNA shared between B chromosome and pair 4 suggesting its origin through isochromosome formation (HANLON et al., 2018). A study of a centromeric-specific satellite CentC in the plant *Zea Mays* revealed evolutionary relationships between copies on the B and A chromosomes (PENG and CHENG, 2011). Moreover, some microsatellites were also described in grasshopper species highlighting that they are part of B chromosomes composition and generally scattered in euchromatic regions (MILANI et al., 2014; RUIZ-RUANO et al., 2015).

Multiple classes of TEs were also identified in distinct species of fish, e.g., *Alburnus alburnus* (ZIEGLER et al., 2003), *Astatotilapia latifasciata* (VALENTE et al., 2014; COAN and MARTINS, 2018), and in fungi *Nectria haematococca* (COLEMAN et al., 2009), and insects as *Eyprepocnemis plorans* (MONTIEL et al., 2014), and in plant species including *Secale cereale* (KLEMME et al., 2013). Moreover, in many species repetitive gene families, including mainly rDNAs, histone genes and U2 snDNA are present (MARSCHNER et al., 2007; POLETTO et al., 2010; TERUEL et al. 2010; OLIVEIRA et al. 2011; KOUR et al. 2013; RUIZ-ESTÉVEZ et al., 2014; SILVA et al. 2014; MENEZES-DE-CARVALHO et al., 2015; JANG et al. 2016; KUMKE et al., 2016; UTSUNOMIA et al. 2016; MILANI et al., 2017).

Since B chromosomes are considered dispensable in many cases, polymorphisms are frequently expected among populations present in different numbers and repetitive DNA molecular composition. As for example, in the fish *Moenkhausia sanctaefilomenae*, two B chromosome variants were found differing in their C-banding patterns, frequency and abundance of repeats (UTSUNOMIA et al., 2016). In the fascinating case of the grasshopper *E. plorans*, more than 40 B chromosome variants were described in different populations (LÓPEZ-LEÓN et al.,

1993; BAKKALI et al., 1999). Several cases of B polymorphisms were also reported in plants, such as *Brachycome dichromosomatica* (HOUBEN et al., 1999), *Crepis capillaris* (PARKER et al., 1991) and *Aegilops speltoides* (BELYAYEV and RASKINA, 2013). However, for rye, besides considered as a young species in evolutionary terms, polymorphic B chromosomes appear to be highly conserved (MARQUES et al., 2013).

1.1.2. Origin

One of the most intriguing questions about B chromosomes is their origin. As mentioned above, one feature of the B chromosomes is that they lack homology with A complement due to interruption of the recombination. However, one of the main theories about its origin points that is from A chromosomes from the same species (intraspecific origin), by simple anomalies during karyotype evolution, as aneuploidy, Robertsonian translocations, misdivision or else by a simple specific A chromosome region duplication (CAMACHO, 2005). Houben et al. (2014) proposed a multi-step model for origin of B chromosomes by formation of an initial proto-B chromosome that emerged possible by cell division anomalies, as translocation derived from duplicated A chromosomes fragments. As a result, this chromosome fragment became more and more incapable of pairing with its donor A chromosome due to the lack of homology. Consequently, the reduced selective pressure on gene integrity with the accumulation of specific repeats, the proto-B would eventually precede a B chromosome and establish a drive mechanism responsible for its persistence. In fact, innumerous works have been reported strong evidences about sequence homology between A and B chromosomes, mainly with repetitive DNAs analysis, such as for the plants *Crepis capillaris* and *Zea mays* (JAMILENA et al., 1994; LAMB et al., 2005; PENG and CHENG, 2011) and for grasshopper species *Eyprepocnemis plorans* and *Locusta migratoria,* or else by different fish species (LÓPEZ-LEÓN et al., 1994; CABRERO et al., 2003; ZIEGLER et al., 2003; POLETTO et al., 2010; TERUEL et al., 2010; FANTINATTI et al., 2011; SILVA et al., 2014). Nevertheless, if B chromosomes arose from A chromosomes, they would become less and less homologous with each other over time due to the higher rate of accumulation of mutation and heterochromatinization process on B chromosomes (GREEN, 1990; CAMACHO, 2005). Supporting this idea, relatively old and heterochromatic B chromosomes, despite sharing sequences with A complement, can accumulate B-

specific repeats (MCALLISTER, 1995; LANGDON et al., 2000; MARTIS et al., 2012; RUIZ-RUANO et al., 2016b; SILVA et al., 2017; HANLON et al., 2018; EBRAHIMZADEGAN et al., 2019; SERRANO-FREITAS et al., 2019).

Intraspecific origin of B chromosomes from sex chromosomes have been proposed, for example, in the fly *Glossina* (AMOS and DOVER, 1981) and in the frog *Leiopelma hochstetteri* (SHARBEL et al., 1998). More recently, an extensive repeats analysis in the fish *Characidium gomesi* pointed to sex chromosomes as B chromosome ancestors (SERRANO-FREITAS et al., 2019). Similar evolutionary process between Bs and sex chromosomes, like chromosome degeneration and inactivation by heterochromatinization (CAMACHO et al., 2000), meiotic behavior, size, morphology, and heteropycnosis, showed to be a strong possibility in many cases, explaining origin of B chromosomes from sex elements or just an evolutionary convergence of this chromosome (HEWITT, 1979; AMOS and DOVER, 1981; JONES and REES, 1982; GREEN, 1990).

Another possibility of B chromosome origin is the interspecific by species hybridization, which basically occurs when B chromosome specific sequences are found in other related species but not in the present host. The most known case of interspecific origin is the PSR chromosome of the wasp *Nasonia vitripennis* that reported some evidence of TE transference through the PSR chromosome of *N. vitripennis* from another species (MCALLISTER and WERREN, 1997). Moreover, additional data showed the possibility of introgression of an external chromosome into another related species of *Nasonia* wasps (PERFECTTI and WERREN, 2001) and between *Partamona* bee species (TOSTA et al., 2014)**.**

Despite all the possibilities of B chromosome origins, an intriguing issue to be resolved is which evolutionary mechanisms are responsible for the B chromosome drive and survive through generations.

1.1.3. Evolution

The most of the studied cases of B chromosome evolution are compatible with the parasitic or selfish model (ÖSTERGREN, 1945; CAMACHO et al., 2000) whose precept the balance between the consequences of B chromosome accumulation and effects that could affect little or has no impact on the host (in low numbers) or causing negative phenotypic differences (in high numbers) (JONES, 1985; SHAW and HEWITT, 1990). Since most of the B chromosomes do not influence in the host

development, they are commonly considered as parasitic and selfish elements that persists in nature, using the hosts cellular machinery that is essential for its maintenance in populations (CAMACHO et al., 2000, 2005; JONES and HOUBEN 2003; HOUBEN et al., 2014). Other model of evolution of B chromosomes is known as the heterotic model (WHITE, 1973), which suggest that the number of B chromosomes influences positively (beneficial fitness) when in low number indicating lack of accumulation and negatively when in high number (not beneficial effects). However, there is almost no case that evidences this model, leaving just the well-known example of the chive *Allium schoenoprasum*, which B chromosomes lacks accumulation and shows that plants with B chromosomes survive longer than plants without B in the natural environment (HOLMES and BOUGOURD, 1989).

The most intriguing fact regarding the evolutionary dynamics of a B chromosome is the mechanism of "*drive*", which promotes its unfair advantage in transmission by not obeying the Mendelian law of equal segregation (CAMACHO 2005, HOUBEN, 2017). In the life cycle of a parasitic B chromosome proposed by Camacho (2005), in benefit of drive, this element would rapidly invade a population increasing its frequency. As the B number rises, it might produce harmful effects in their hosts causing stability in drive selection or reaching its neutralization. In the course of neutralization process, the B chromosome may go to extinction or undergo mutations that convert it into a new variant showing drive or else be eliminated. The "*drive*" mechanism of B chromosomes can occur at several stages during the life cycle, at pre-meiotic, meiotic or post-meiotic divisions in many species (JONES, 1991; CAMACHO et al., 2000). The pre-meiotic drive mechanism was reported in different species of grasshoppers (NUR, 1963; PARDO et al., 1995) and the plant *Crepis capillaris* (RUTISHAUSER and RÖTHLISBERGER, 1966), suggested by the occurrence of mitotic nondisjunction in the germline. The meiotic drive occurs in meiosis, when the B chromosomes succeed its elimination by preferentially migrating to the viable meiotic pole (KAYANO, 1957; HEWITT, 1973; BAKKALI et al., 2002). Otherwise, in several plants, the drive of B chromosomes happens in many cases by nondisjunction in the post-meiotic mitoses (CAMACHO, 2005; HOUBEN, 2017). Despite the cellular mechanism of drive has been very well studied so far, the molecular mechanisms behind this scene still remains unclear and should be the next step to understanding B chromosomes. Interestingly, a study of reactivation of inactive centromeres of B chromosomes in maize by utilizing nondisjunction given by

the presence of B chromosomes brings new perspective in this area (DOUGLAS et al., 2021).

1.1.4. Genes and phenotypic effects

Although B chromosomes are considered as non-essential and present mechanisms that assure their transmission and survival, in the past it was expected that B chromosomes would also carry functional genes. However, external phenotypic effects are rarely seen, with only a few exceptions, like the plant *Haplopappus gracilis* where presence of B chromosomes can alter the color of its achene (JACKSON and NEWMARK, 1960) and *Zea mays* turning striped pattern at their leaves (STAUB, 1987). Moreover, for *Avena sativa*, which the B chromosome presents resistance genes for rust caused by the fungus *Puccinia coronate* (DHERAWATTANA and SADANAGA, 1973). Others striking examples in which the B chromosome changes the phenotype were observed in certain cichlid fish and in the frog *Leiopelma hochstetteri*, in which it was shown that the presence of the B chromosome has an influence on their sex determination (GREEN et al., 1988; YOSHIDA et al., 2011). In the fungus *Nectria haemotococca*, B chromosomes have been reported to have genes that are associated with metabolic processes that appear to be involved with antibiotic resistance and pathogenicity (COLEMAN et al., 2009).

Furthermore, more recently, the presence of genes has been reported in some B chromosome systems, mainly involved with cell division cycle and chromosome related functions (HOUBEN et al., 2014; AHMAD and MARTINS, 2019). However, other genes responsible for diverse important functions associated with metabolism and regulation, development, sexual and nervous system were also documented, such as the *C-KIT* proto-oncogene in canids and deer species (GRAPHODATSKY et al., 2005; YUDKIN et al., 2007; TRIFONOV et al., 2013), the set of genes associated with cellular division in fish species (VALENTE et al., 2014; CLARK et al., 2018; SILVA et al., 2021) and cell division control genes *INCENP* and *SPIRE2* in reptiles (KICHIGIN et al., 2019). Among insects, a comparative analysis of transcriptomes in *Nasonia vitripennis* B chromosome known as PSR (Paternal sex ratio), identified transcripts that are differentially expressed in presence of PSR (AKBARI et al., 2013). In a *Drosophila albomicans* genome sequencing study, it was reported the presence of an enriched actively expressed sequences region on the B chromosome (ZHOU et al., 2012). More recently, for the grasshopper *E. plorans*, a comparative

genomics study revealed the presence of novel truncated and integrated genes on the B chromosome most likely associated with cellular division process, such as, DNA replication, chromosome condensation, mitotic cycle regulation and transcription (NAVARRO-DOMÍNGUEZ et al., 2017).

Among plants, the study of genes on B chromosomes was reported mostly for well-known model species. For example, in maize, transcriptome data showed that expression of genes in A complement is more influenced by the increase of the B chromosome number in samples (HUANG et al., 2016). Likewise in rye, the presence of B chromosomes affected the transcription of A-genome genes (BANAEI-MOGHADDAM et al., 2013), and more than 4000 possible genic sequences were identified on its B chromosome (MARTIS et al., 2012). Besides the activity of coding genes, the transcription of repetitive sequences present on B chromosomes has been also documented, as the case of a retrotransposon in maize (LAMB et al., 2007).

1.2. High throughput sequencing and its contribution to B chromosomes studies

Since B chromosomes were discovered about a century ago (WILSON, 1907) it started to be a subject of more interest over time and consequently became a subject of study by classical cytogenetics and molecular cytogenetics, and nowadays they are studied under the tools of the genomics and bioinformatics era. Moreover, the importance of B chromosomes is represented in a series of scientific meetings that congregates recognized researchers to expose and discourse new findings about this topic, known as B chromosome conferences (1st in 1993, 2nd in 2004, 3rd in 2014 and 4th in 2019) (BEUKEBOOM, 1994; MARTINS et al., 2020).

Before the development of large-scale genomic sequencing, studies of classical and molecular cytogenetics were widely used and tirelessly to illuminates important questions about B chromosome origin, evolution, drive, composition, behavior and phenotypic effects (BEUKEBOOM, 1994; JONES, 1995; CAMACHO et al., 2000, 2005). However, new expanded and reliable data from genomic data have becoming more and more requested. The advances of high throughput sequencing and bioinformatics protocols have led address in more details structural and functional questions about B chromosomes (MARTIS et al., 2012; VALENTE et al., 2014, 2017; KUMKE et al., 2016; RUIZ-RUANO et al., 2016b; NAVARRO-DOMÍNGUES et al., 2017; AHMAD and MARTINS, 2019; MARQUES et al., 2018). For example, new findings related to the understanding the role of repetitive

DNAs in the genomes that harbors B chromosomes received an enormous attention to the study of these elements. Thus, several computer programs for analyzing this fraction of DNA have emerged from sequencing data (SAHA et al., 2008; STATON and BURKE, 2015; WEISS-SCHNEEWEISS, 2015). However, a great difficulty that is still faced is the lack of a database for the reference of known elements for a variety of species, which usually contain information restricted to the most studied species models.

A software currently used to retrieve repetitive portions of the genomes without the need of a database of reference is the RepeatExplorer. The program includes several utilities for prospecting and characterizing repetitive sequences through the formation of clusters based on similarity among sequences, originating from new generation sequencing data specific to eukaryotic genomes, including non-model species (NOVÁK et al., 2013). In addition, other widely used bioinformatics protocols have been applied to supply the repetitive genomic fraction and B chromosome content investigation, such as Repeatmasker and Repeat Landscape (SMIT et al., 2017), satMiner (RUIZ-RUANO et al., 2016a) and dnaPipeTE (GOUBERT et al., 2015). Basically, the repetitive DNA content of genomes from individuals with no B chromosomes and individuals harboring B chromosomes are estimated and compared and the overabundant repeats in +B genome are putatively associated to the B chromosomes. Several works were carried out with the searching and characterization of repetitive sequences and its association with B chromosomes through new generation sequencing, such as for *Secale cereale* where the authors reported the presence of B chromosome specific tandem repeats (MARTIS et al., 2012) and later for *Plantago lagopus* that B-specific sequences were putatively originated from sequence amplification including a 5S rDNA fragments (KUMKE et al., 2016). Moreover, it was reported for the first time in *Sorghum purpureosericeum*, the presence of nine putative B-specific clusters, including centromeric sequences (KARAFIÁTOVÁ et al., 2021). For animals, it was described the first report on B chromosome content in a reptilian species (KICHIGIN et al., 2019), the case of independent origins of B chromosomes in two cervids species (MAKUNIN et al., 2016), and evidences about B chromosome ancestry and content in some grasshopper and fish species (RUIZ-RUANO et al., 2016b; 2018; UTSUNOMIA et al., 2016; SILVA et al., 2017; COAN and MARTINS, 2018).

Apart from the presence of repetitive DNAs, some researches also searched

for genes and their functionality on the B chromosomes, using mostly high-throughput sequencing strategies by genomic and transcriptomic analysis (MAKUNIN et al., 2014; BANAEI-MOGHADDAM et al., 2015; VALENTE et al., 2017; AHMAD AND MARTINS, 2019). In this way, two different strategies are predominantly implemented to investigate the content and biology of B chromosomes. One is achieved by analyzing the directly sequencing of the B chromosomes itself, using flow sorted (KLEMME et al., 2013; MAKUNIN et al., 2016) or microdissected and sequenced B chromosomes (VALENTE et al., 2014; RUIZ-RUANO et al., 2018). The other is by comparative analysis of sequencing data applied in lacking B genomes and carrying B genomes (for a review RUBAN et al., 2017), which, can be done using the similarity-based read clustering method already mentioned above (MARTIS et al., 2012; KUMKE et al., 2016), the coverage ratio analysis (VALENTE et al., 2014; NAVARRO-DOMÍNGUEZ et al., 2017) or else the k-mer frequency ratio analysis (VU et al., 2015). In spite of that, a considerable effort aiming to understand the biological role of genes and its function mapped on B chromosomes have been done, based in different approaches. Valente et al. (2014) followed a method comparing identified B-linked sequences of *A. latifasciata* to a reference databank of genes of closely related species. Otherwise, Navarro-Domínguez et al. (2017) identified several protein coding genes on Bs of *E. plorans* by CDS (coding sequences) counting of mapped reads using a reference transcriptome. Another more recent strategy, is the use of combining different sequencing methods to address more reliable assembles of genomes with and without specific chromosomes, as for example the PacBio and sequencing with Illumina high-throughput sequencing (CLARK et al., 2018).

In short, the integration between genomic sequencing and physical chromosome mapping has been very useful for several genomic projects, in which had led to illuminate the path for better understanding the B chromosomes composition and evolution.

1.3. B chromosomes in Orthoptera

Orthoptera is the groups with largest number of species harboring B chromosomes among insects and the largest representative in number of works related to B chromosomes for animals until now (D'AMBROSIO et al., 2017). According to Palestis et al. (2010), in orthopterans, the presence of B chromosomes was accounted

for about 190 species with higher prevalence in the superfamily Acridoidea. However, in-depth studies on the origin and evolution of supernumerary elements in grasshopper species are concentrated primarily on few species. Studies with different populations, experiments of chromosomal microdissection and mapping of several repetitive sequences including multigene families, satDNAs and TEs have helped to trace the origin of these elements mainly in the species *Eypropecnemis plorans* and *Locusta migratoria* (LÓPEZ-LEÓN et al., 1994; CABRERO et al., 2003, 2014; TERUEL et al., 2009a, b, 2010, 2013; MONTIEL et al., 2012, 2014). In *E. plorans*, a large amount of 45S rDNA and a satellite with 180 bp were observed in different populations (CABRERO et al., 2014), in addition to TEs, *Eplo-GypI*, *EploRTE5*, *EploMar20* (MONTIEL et al., 2012). Interestingly, more recent studies reported the presence of active genes in the B chromosome coding for functions related with cell division, and moreover a genome interaction between the parasitic B chromosome and its host manifested by changes in gene expression (NAVARRO-DOMÍNGUEZ et al., 2017, 2019). In *L. migratoria*, clusters of the histone gene (H3 and H4) were observed on the B chromosome, suggesting origin from pair 8 (TERUEL et al., 2010). Later, with the most complete quantification of the repeat content in a grasshopper, six satDNAs were observed on the B chromosome shared with autosome 9, indicating that this pair together with pair 8 could be the putative ancestors of this species B chromosome (RUIZ-RUANO et al., 2018). In the same work, it was reported that the B chromosome of *L. migratoria* contains 94.9% of repetitive DNA, with a single satDNA comprising 55% of the B chromosome, in addition to carrying a specific B chromosome 17 kb long chimera comprising 29 different TEs (RUIZ-RUANO et al., 2018).

Other less studied species in which the occurrences of repetitive DNA on the B chromosomes were analyzed are two subspecies of *Podisma sapporensis* and *Eumigus monticola*. In *Podisma* subspecies, the probe generated from the microdissected B chromosome revealed shared signals on different chromosomes from complement A (BUGROV et al., 2004), while in *E. monticola*, several satDNAs and multigene families indicate the origin of the B chromosome a from autosome 8 (RUIZ-RUANO et al., 2016b). For South American representatives, some species were better studied in terms of understanding the composition and origin of B chromosomes, including *Rhammatocerus brasiliensis*, *Xyleus discoideus angulatus*, *Eumastusia koebelei koebelei*, *Dichroplus pratensis* and *Abracris flavolineata*

(BIDAU et al., 2004; LORETO et al., 2008; OLIVEIRA et al., 2011; BUENO et al., 2013; ANJOS et al., 2016). In general, the B chromosomes of these species are heterochromatic showing C-positive band patterns with the exception of *A. flavolineata*, in which the B chromosome is totally C-negative (BUENO et al., 2013). In terms of composition, rDNA sequences were found on the Bs chromosomes of *R. brasiliensis* (DNAr 5S) and *D. pratensis* (DNAr 45S) (BIDAU et al., 2004; LORETO et al., 2008), histone H3 genes in *R. brasiliensis* (OLIVEIRA et al., 2011), U2 snDNA genes in *A. flavolineata* (BUENO et al., 2013), and different repetitive DNA sequences in *E. koebelei koebelei* (ANJOS et al., 2016), suggesting intraspecific origin for all cases.

2. OBJECTIVES

2.1. General objectives

The B chromosomes are widespread in nature and their scientific relevance is getting more and more attention as a potential key study related to evolutionary population biology and molecular cytogenetics, besides in genomic evolutionary studies. Among animals the Orthoptera order is one group in which most part of species harboring B chromosomes were described, however there is only a few knowledge with detailed analysis concerning B chromosome molecular composition, origin and evolution. This is an interesting group among insects, because they present large genomes plenty of repetitive DNAs, which could facilitate the occurrence of genome variability. Therefore, the main objective of this thesis was to investigate the structure, molecular composition, origin and evolutionary traces of genomes and specifically B chromosomes of different grasshoppers species by means of comparative cytogenetics, genomics and bioinformatics approaches. For that, it was investigated four species including, *Abracris flavolineata, Rhammatocerus brasiliensis*, *Schistocerca rubiginosa* and *Xyleus discoideus angulatus*. Despite several species of orthopterans has been investigated nowadays, it still clear that these species represent a challenge for genome assemblies projects mainly due to their particular genome features, such as its giant genome size, high abundance in repetitive DNA and the lack of quality and accessibility of genomic sequences in databanks in comparison to other insects. Thus, the effort of this thesis was predominantly on the physical mapping and sequenced genome analysis of the most abundant repetitive DNA families within this group of insects and populations that harbors B chromosomes.

2.2. Specific objectives

- To elucidate the molecular composition and the possible ancestry of B chromosomes in five grasshopper species *Abracris flavolineata*, *Rhammatocerus brasiliensis*, *Schistocerca rubiginosa* and *Xyleus discoideus angulatus* by the isolation and physical mapping of repetitive DNAs combining genomic and cytogenetic analysis;
- To study the occurrence, frequency and repetitive DNA content of possible variants of the B chromosome of *Abracris flavolineata* at an interpopulation point of view, helping to understand its spatial evolutionary dynamics;

3. MATERIALS AND METHODS

3.1. Samples, chromosomal analysis and classical banding

For *Abracris flavolineata*, a total of 37 adult males and 49 adult females were collected in Floresta Estadual Edmundo Navarro de Andrade and in the Campus of UNESP-Universidade Estadual Paulista, Rio Claro/SP-Brazil (SP), 22°24'45''S, 47°31'28''W, 19 male adults in Cabo de Santo Agostinho/Pernambuco (PE), 8°17'15''S; 35°2'7''W, 76 male adults in Santa Bárbara do Pará/Pará (PA), 1°13'27''S; 48°17'38''W and 14 male adults at Posadas/Misiones-Argentina (ARG), 27°25'S; 55°56'W. Additionally, we studied about 10 adult males of each species: *Rhammatocerus brasiliensis* collected at 07°45'00''S; 34°05'10''W Ilha de Itamaracá/PE (Brazil) and 07°50'56''S 35°19'14''W Lagoa do Carro/PE (Brazil); *Xyleus discoideus angulatus* at 07°12'47''S 39°18'55''W from Juazeiro do Norte/CE (Brazil); *Schistocerca rubiginosa* from Levy County/Florida (USA) 29°25.908'N 82°24.060'W. For all male individuals, testes were dissected from anesthetized animals and fixed in 3:1 100% ethanol:glacial acetic acid and stored at −20 °C freezer for chromosomal analysis. Entire animals were immersed in absolute ethanol and stored at −20 °C freezer for genomic DNA (gDNA) extraction. To obtain embryos from *A. flavolineata*, a part of sampled females collected in Rio Claro/SP were maitained in plastic boxes until oviposition. Embryo mitotic cells were obtained from embryo dissection approximately 15 days after oviposition of eggpods, following Webb et al. (1978) method with small modifications in time of colcemid incubation (about 45 minutes) and stored at a temperature of -20°C until use for chromosomal analysis.

Chromosome spreads were done by maceration and spreading of testis follicles and/or embryos in a drop of 50% acetic acid on a slide under a hot plate at 45 °C. For embryos mitotic preparations, the slides were stored in -4°C until use in later fluorescence *in situ* hybridization experiments (FISH) (see section 3.7). For conventional analysis and identification of B chromosome presence the chromosomes were stained with Giemsa 5%. The individuals harboring B chromosomes were selected to be used for subsequently classic and molecular cytogenetic assays. Heterochromatin distribution was analyzed by C-banding according to Sumner (1972).

3.2. DNA extraction and Illumina sequencing

The hind legs of the males that were previously stored in 100% ethanol at -20 °C, were used for genomic DNA (gDNA) extraction following the phenol/chloroform-based protocol (SAMBROOK and RUSSEL, 2001), which was used for genome sequencing and PCR assays.

For gDNA of *X. d. angulatus* and *R. brasiliensis* we used the Illumina HiSeq 4000 platform with 101 bp paired reads in service of Macrogen Inc. service (Seoul, Republic of Korea) with sequencing yielding about 1 Gb DNA per sample (For more details, see section 4.1 Chapter 1). The gDNA Illumina sequencing method used for *S. rubiginosa* specimen was previously described by Song et al. (2017). For gDNA sequencing of *A. flavolineata* belonging to Cabo de Santo Agostinho/PE and Posadas/Misiones-Argentina populations, we used one individual 0B and one individual 1B of each population, following the same Illumina HiSeq 4000 platform service of Macrogen, with sequencing yielding about 1 Gb DNA (per sample) of 101 bp paired reads. Finally, for the *A. flavolineata* population of Rio Claro/SP the gDNA sequencing was performed in seven individuals (three 0B, two 1B and two 2B) with 151 bp paired reads and sequencing yielding about 27-41 Gb DNA (per sample). The genomes from the seven individuals were previously studied by Milani et al. (2021), and Ahmad et al. (2020) and are deposited in the Sequence Read Archive (SRA) under the accession numbers SRX7784770-SRX7784772. For the other species the genomes are deposited in SRA under the numbers, SAMN23009930-SAMN23009933 (*Abracris flavolineata* from other populations), SAMN23009934 (*Xyleus discoideus angulatus*), SAMN23009938 (*Rhammatocerus brasiliensis*), SAMN19103515 (*Schistocerca rubiginosa*). All gDNA sequencing described was performed on libraries constructed as recommended by Illumina using Illumina TruSeq DNA PCR-Free kit (Illumina Inc., San Diego, CA, USA).

3.3. Processing of sequenced reads and identification of repetitive sequences

First, the sequenced paired-end reads of each species were checked for quality using FastQC (ANDREWS, 2012). The pre-processing of the reads was performed following default parameters using the public online platform: https://repeatexplorer-elixir.cerit-sc.cz/galaxy/. Reads were processed following the steps of “quality trimming tool”, “FASTQ interlacer” on paired-end reads and “FASTQ to FASTA” converter using FASTX-Toolkit (GORDON and HANNON, 2010) with the default

options. Differently, for Rio Claro/SP population of *A. flavolineata* that the sequenced genomes were larger and had more samples for each group (three with 0B, two with 1B and two with 2B), we randomly sampled 2 × 5,000,000 reads from each individual using SeqTK (https://github.com/lh3/seqtk) and pooled those belonging to the same type of genome (0B, 1B or 2B) by concatenating them. We then performed sequence pre-processing for each group of reads, using the "rexp_prepare_normaltag.py" script (https://github.com/fjruizruano/ngs-protocols), that uses Trimmomatic (BOLGER et al., 2014) to remove adapters and low-quality nucleotides (Q<20), and finally selects only completely paired reads after trimming, i.e. those read pairs with 151 bp in both members. The script then interleaves forward and reverse reads, and converts them to fasta format.

The RepeatExplorer (RE) clustering pipeline (version 1.0.0) was used for general identification of repeats, but mostly satDNAs families, always following default options (NOVÁK et al., 2013). After, we searched and selected by visual observation the clusters formed by the pipeline that showed high graph density, which corresponds to satDNAs families (NOVÁK et al., 2010). Contigs from the selected clusters were deeply explored and manually searched for sequences with tandem pattern confirmed by the dot plot graphics implemented in Geneious v4.8.5 software (DRUMMOND et al., 2009). The consensus monomer of each satDNA family of each species was used as the query in two databanks, BLAST (http://www.ncbi.nlm.gov/Blast/) and Repbase (http://www.girinst.org/repbase/), to check similarity with another sequence deposited and described.

In order to find and characterize the maximum number of different satDNA families we applied the satMiner protocol (RUIZ-RUANO et al., 2016a) for *A. flavolineata* from different populations, which consists in several rounds of clustering with the RepeatExplorer software (NOVÁK et al., 2013) alternated with the DeconSeq filtering tool (SCHMIEDER and EDWARDS, 2011) to remove those satDNA sequences identified in previous RE rounds, and adding more of the cleaned reads pairs to raise the probability of finding new families (for more details, see section 4.2 Chapter 2).

For TE identification, we also used RE clustering pipeline followed by a re-clustering specific tool available in the Galaxy platform (https://repeatexplorer-elixir.cerit-sc.cz/galaxy/). This tool was used for merging clusters showing homology into larger contigs, which are more prone to improve the TE assembly. Then, we

analyzed all the cluster contigs for sequence extraction with Geneious v4.8.5 software (DRUMMOND et al., 2009). Additionally, for *A. flavolineata* larger sequenced genomes we utilized the dnaPipeTE pipeline (GOUBERT et al., 2015), which uses Trinity (GRABHERR et al., 2011) as assembler, proceeded by TE annotation and quantification in raw reads compared with a custom database that was previously built by Ruiz-Ruano et al. (2018) in *L. migratoria* genomes. Then, we used a custom script (https://github.com/fjruizruano/ngs-protocols/blob/master/dnapipete_createdb.py) that operates dnaPipeTE assembly and annotation to generate a fasta file with annotated contigs in the RepeatMasker format (SMIT et al., 2017) for further analysis.

The multigene families (histone genes, rDNAs and snDNAs) and full mitochondrial DNA (mtDNA) were recovered using MITObim (HAHN et al., 2013) with the seed sequences used for *L. migratoria* in Ruiz-Ruano et al. (2018). At last, redundancy of all repeats obtained was tested and removed by CD-HIT-EST clustering (LI and GODZIK, 2006) using 80% sequence identity level, considering that at least 80% identity were considered the same family.

3.4. Bioinformatics and genomic analysis of repetitive sequences

The satDNA sequences found were classified in subfamilies, families and superfamilies according to an identity criterion proposed by Ruiz-Ruano et al. (2016a). Superfamilies (SF) were considered with at least 50% of identity, families reaching 80% and subfamilies or components (variants) of a family with at least 95% of identity. This homology test between the different satDNA families was performed based on RepeatMasker (SMIT et al., 2017) using the script "rm_homology.py" (https://github.com/fjruizruano/ngs-protocols). Additionally, we checked all the consensus sequences of satDNAs of each species using multiple sequence alignments with Muscle (EDGAR, 2004) implemented in Geneious v4.8.5 software (DRUMMOND et al., 2009) to search for sequence homology.

Sequence abundance and divergence of each repetitive DNA family of each species were determined by means of RepeatMasker (SMIT et al., 2017), using the Cross_match search engine on read pairs of each genome library. SatDNA families were named in decreasing order of abundance following Ruiz-Ruano et al. (2016a). Sequence divergence was estimated by the Kimura 2-parameter (K2P) model, using the calcDivergenceFromAlign.pl script within the RepeatMasker software (SMIT et al., 2017). Abundance for a given repetitive DNA family of a given genome was

calculated as genome proportion, represented by the sum of all mapped nucleotides belonging to it (including all subfamilies) in respect to the total number of nucleotides in the selected reads from each Illumina library.

For *A. flavolineata* from Rio Claro/SP population, the abundance and divergence estimation of each repeat family were done using the previously random selected 2 × 5,000,000 reads from each individual (three with 0B, two with 1B and two with 2B), and separately for each individual, which latter was averaged for 0B (three individuals), 1B (two individuals) and 2B (two individuals) genomes for more accurate comparisons.

Species with genomes sequenced of 0B and +B (1B or 2B) individuals were compared in relation to abundance and divergence of repetitive DNAs isolated with the purpose of verifying overabundant repeats in the B-carrying genomes and to be later validated with physical chromosome mapping. For that, genomes proportion and relative abundance coefficients (1B/0B>1 and/or 2B/0B>1B/0B) were calculated and subtractive satDNA landscapes (2B-0B) were built, showing the level of abundance in relation to divergence (Kimura-2-parameter).

3.5. Repetitive DNA isolation by Polimerase Chain Reaction (PCR)

The sequence for U2 snDNA was obtained using the genomic DNA of *A. flavolineata* with the primers described by Bueno et al. (2013). For other repetitive DNAs we designed primers for PCR amplification either manually or else using the Primer3 software (UNTERGASSER et al., 2012), and PCR mix was composed of: 10× PCR Rxn Buffer, 0.2 mM MgCl2, 0.16 mM dNTPs, 2 mM of each primer, 1 U of Taq Platinum DNA Polymerase (Invitrogen, San Diego, CA, USA), and 50–100 ng/μL of template DNA. The PCR conditions included an initial denaturation at 94 ◦C for 5 min and 30 cycles at 94 ◦C (30 s), 55 ◦C (30 s), and 72 ◦C (80 s), plus a final extension at 72 ◦C for 5 min. For satDNA sequences primers were designed taking in count the size of the monomers to avoid amplification errors, i.e. divergent sets for sequences shorter than 500 pb and convergent for longer sequences. The monomeric bands were isolated and purified using the ZymocleanTM Gel DNA Recovery Kit (Zymo Research Corp., The Epigenetics Company, CA, USA) according to manufacturer's recommendations. The same method was applied for TE isolation with convergent primers, taking care of isolating those fragments showing the size expected from computational annealing of primers. These products were used for re-

amplification using the same PCR conditions. To verify the isolation of sequences of interest, purified PCR products were sequenced by Sanger method in both directions using the Macrogen Inc. service and then compared with consensus sequences obtained by genomic analysis. The sequences already available can be found at NCBI with accession numbers: KC896794 (snDNA U2); MH900339–MH900377 (satDNAs from *S. rubiginosa*, *X. d. angulatus* and *R. brasiliensis*); OL439990-OL440051 (satDNAs from *A. flavolineata*)

3.6. Phylogenetic analysis of COI gene and haplotype network

Aiming to understand the genetic connection between the populations of *A. flavolineata* we reconstructed a haplotype network based in a fragment of cytochrome c oxidase subunit I (COI) gene from 54 individuals, 13 from SP, 13 from PE, 15 PA and 13 from ARG (Accession numbers: OL415778-OL415831). The COI were amplified using the primers A2442 and S1718 (NORMARK, 1996). The PCR products were purified using the ExoSAP-IT (Affymetrix) reagent, following the guidelines of manufacturers, and sequenced by the Sanger method using the service of Macrogen Inc. The sequences were analysed using Geneious v4.8.5 software (DRUMMOND et al., 2009). Phylogenetic and molecular evolutionary analyses were conducted using MEGA v.5 (TAMURA et al., 2011) and DNA polymorphism and haplotype recognition were analysed using the DnaSP v.5.10.01 tool (LIBRADO and ROZAS, 2009). A graphical haplotype network was constructed employing Network 4.6.1.2 software (http://www.fluxus-engineering.com).

3.7. Fluorescence *in situ* Hybridization (FISH)

Repeats including U2 snDNA, satDNAs, TEs and C_0t-DNA were used in FISH experiments for chromosome mapping. The FISH experiments were performed on mitotic chromosome spreads from embryos and testis follicles previously prepared (in section 3.1), using one or two probes simultaneously, according to Cabral-de-Mello et al. (2011) or Cabral-de-Mello and Marec (2021). Probes labeled with digoxigenin-11-dUTP (Roche, Mannheim, Germany) were detected by anti-digoxigenin-rhodamine (Roche) and probes labeled with biotin-14-dATP (Invitrogen) were detected by Streptavidin Alexa Fluor 488-conjugated (Invitrogen), always following the manufacturer's recommendations. The chromosomes were counterstained using 4’,6-diamidine-20-phenylindole (DAPI) and slides mounted in

VECTASHIELD (VECTOR, Burlingame, CA, USA). The preparations were observed and images were captured using a BX61 Olympus microscope equipped with a fluorescence lamp and appropriate filters, and a DP70 cooled digital camera. All images were processed and optimized using Adobe Photoshop CS6.

4. RESULTS AND DISCUSSION

The results of this PhD thesis are presented and discussed in the following manuscripts published or under review in the journals listed below:

Genes. ISSN 2073-4425. Impact factor 4.096 (Published)
https://doi.org/10.3390/genes9110523

Heredity. ISSN 1365-2540. Impact factor 3.821 (Published)
https://doi.org/10.1038/s41437-021-00470-5

Gene. ISSN 1879-0038. Impact factor 3.688 (Under Review)

4.1. Chapter 1

Satellite DNAs Unveil Clues about the Ancestry and Composition of B Chromosomes in Three Grasshopper Species

Diogo Milani, Vanessa B. Bardella, Ana B. S. M. Ferretti, Octavio M. Palacios-Gimenez, Adriana de S. Melo, Rita C. Moura, Vilma Loreto, Hojun Song and Diogo C. Cabral-de-Mello

Published in *Genes* (2018), 9(11), 523.

genes

MDPI

Article

Satellite DNAs Unveil Clues about the Ancestry and Composition of B Chromosomes in Three Grasshopper Species

Diogo Milani [1], Vanessa B. Bardella [1], Ana B. S. M. Ferretti [1], Octavio M. Palacios-Gimenez [1,2], Adriana de S. Melo [3], Rita C. Moura [3], Vilma Loreto [4], Hojun Song [5] and Diogo C. Cabral-de-Mello [1,*]

1 Instituto de Biociências/IB, Departamento de Biologia, UNESP—Universidade Estadual Paulista, Rio Claro, São Paulo 01049-010, Brazil; azafta@gmail.com (D.M.); vbbardella@gmail.com (V.B.B.); anabeatrizferretti@gmail.com (A.B.S.M.F.); octavio.palacios@ebc.uu.se (O.M.P.-G.)
2 Department of Evolutionary Biology, Evolutionary Biology Center, Uppsala University, 75236 Uppsala, Sweden
3 Instituto de Ciências Biológicas, Laboratório de Biodiversidade e Genética de Insetos, UPE—Universidade de Pernambuco, Recife 50100-130, Pernambuco, Brazil; adrianadesouzamelo@gmail.com (A.d.S.M.); ritamoura.upe@gmail.com (R.C.M.)
4 Centro de Biociências/CB, Departamento de Genética, UFPE—Universidade Federal de Pernambuco, Recife 50670-901, Pernambuco, Brazil; vloreto@bol.com.br
5 Department of Entomology, Texas A&M University, 2475 TAMU, College Station, TX 77843-2475, USA; hsong@tamu.edu
* Correspondence: mellodc@rc.unesp.br

Received: 13 September 2018; Accepted: 21 October 2018; Published: 26 October 2018

Abstract: Supernumerary (B) chromosomes are dispensable genomic elements occurring frequently among grasshoppers. Most B chromosomes are enriched with repetitive DNAs, including satellite DNAs (satDNAs) that could be implicated in their evolution. Although studied in some species, the specific ancestry of B chromosomes is difficult to ascertain and it was determined in only a few examples. Here we used bioinformatics and cytogenetics to characterize the composition and putative ancestry of B chromosomes in three grasshopper species, *Rhammatocerus brasiliensis*, *Schistocerca rubiginosa*, and *Xyleus discoideus angulatus*. Using the RepeatExplorer pipeline we searched for the most abundant satDNAs in Illumina sequenced reads, and then we generated probes used in fluorescent in situ hybridization (FISH) to determine chromosomal position. We used this information to infer ancestry and the events that likely occurred at the origin of B chromosomes. We found twelve, nine, and eighteen satDNA families in the genomes of *R. brasiliensis*, *S. rubiginosa*, and *X. d. angulatus*, respectively. Some satDNAs revealed clustered organization on A and B chromosomes varying in number of sites and position along chromosomes. We did not find specific satDNA occurring in the B chromosome. The satDNAs shared among A and B chromosomes support the idea of putative intraspecific ancestry from small autosomes in the three species, i.e., pair S11 in *R. brasiliensis*, pair S9 in *S. rubiginosa*, and pair S10 in *X. d. angulatus*. The possibility of involvement of other chromosomal pairs in B chromosome origin is also hypothesized. Finally, we discussed particular aspects in composition, origin, and evolution of the B chromosome for each species.

Keywords: fluorescent in situ hybridization; Orthoptera; satellite DNA; supernumerary chromosome; RepeatExplorer

1. Introduction

Eukaryotic genomes exhibit repetitive DNA sequences including noncoding tandemly repeated satellite DNA (satDNA). These sequences exhibit extensive variability in copy number and nucleotide sequence, even among phylogenetically related species. Arrays of satDNAs are usually located in the centromeric and telomeric heterochromatin of the chromosomes, although they have also been reported in the euchromatic region. Furthermore, satDNAs are frequently enriched on sex chromosomes and supernumerary (B) chromosomes, as they are greatly enriched in heterochromatin [1–3].

Supernumerary B chromosomes occur in approximately 15% of eukaryotes as dispensable elements (i.e., not required for normal organismal development), frequently heterochromatic and enriched repetitive DNAs, including the satDNAs, which can have implications for B chromosome evolution. Generally, B chromosomes do not recombine with A chromosomes (normal complement), and B chromosome sequences evolve at a higher evolutionary rate than A elements [4,5]. Since the first discovery of the B chromosome [6], the specific ancestry of the studied B chromosomes in eukaryotes has remained largely unknown. For decades, repetitive DNAs have been used to try to ascertain the ancestry and to describe the B chromosome composition in some species. In that way, satDNAs have helped the understanding of the evolutionary history of B chromosomes with intraspecific (from host genome) or interspecific (resultant of species hybridization) origin, for example, in grasshoppers [7,8], wasps [9], fish [10], and plants [11], among others.

Among the grasshoppers, approximately 12% of the species harbor B chromosomes. Some families seem to be hotspots for B chromosome presence, such as Acrididae, with 17.1% of the species harboring B chromosomes, unlike Romaleidae in which only 4% of the species is harboring B chromosomes [12]. As generally observed in eukaryotes, some repetitive DNAs populate the B chromosomes of grasshoppers, like the multigene families for rDNAs [13,14], histone genes [14,15], and U snDNA [16], transposable elements [8,17,18], microsatellites [19], and satDNAs [7,8,13,20]. These sequences shed light on B chromosome composition, variability, and evolutionary dynamics. Concerning satDNAs, their presence in the B chromosomes of grasshoppers is known only in a few species, including *Locusta migratoria* [8], *Abracris flavolineata* [20], *Eyprepocnemis plorans* [13], and *Eumigus monticola* [7].

The search for satDNAs in genomic data was facilitated more recently by analyzing reads from next generation sequencing (NGS) using bioinformatics approaches, like RepeatExplorer software [21]. RepeatExplorer has been a useful tool for detecting satDNAs for probe generation and chromosome mapping in species with B chromosomes, helping to unveil the composition and abundance of satDNAs in those chromosomes as well as their relationships with A elements as well [7,8,11,22].

By combining genomics and cytogenetics, we aimed to elucidate the genome content of satDNAs and used this information to track the possible ancestry of B chromosomes in three grasshopper species, *Rhammatocerus brasiliensis* (Acrididae: Gomphocerinae), *Schistocerca rubiginosa* (Acrididae: Cyrtacanthacridinae), and *Xyleus discoideus angulatus* (Romaleidae: Romaleinae) belonging to two families. The family Acrididae, which is currently most diverse lineage within the orthopteran suborder Caelifera, diverged from its sister lineage, which includes the family Romaleidae, in the late Cretaceous (~78 mya, million years ago) based on a fossil-calibrated divergence time estimate. Two acridid subfamilies included in this study, Gomphocerinae and Cyrtacanthacridinae, each belong to different clades within the family, and they are estimated to have diverged in the late Eocene [23]. For this purpose, we first made a prediction of the most abundant satDNAs in genomes by using the RepeatExplorer tool. Then we recovered the fragments by PCR and designed probes of each satDNA of the three species to use in fluorescent in situ hybridization (FISH) experiments. This allows for the investigation of spatial patterns of satDNAs that have preferentially accumulated in B chromosomes compared to autosomes. We found distinct patterns of satDNA distribution on B chromosomes that are shared with some A chromosomes or with exclusive A chromosomes. Based on these data, it is possible to hypothesize the ancestry of the B chromosome from small autosomes and to discuss aspects of the evolution of B chromosomes in the three species.

2. Material and Methods

2.1. Animal Sampling, Chromosome Preparations, and Genomic DNA Sequencing

Adult animals of *R. brasiliensis* were collected at 07°45′00″ S; 34°05′10″ W Ilha de Itamaracá/PE (Brazil) and 07°50′56″ S 35°19′14″ W Lagoa do Carro/PE (Brazil); *X. d. angulatus* at 07°12′47″ S 39°18′55″ W Juazeiro do Norte/CE (Brazil); *S. rubiginosa* at 29°25.908′ N 82°24.060′ W Levy County/Florida (USA). Testes were fixed with Carnoy's modified solution (3:1, 100% Ethanol:Glacial Acetic Acid) and stored at −20 °C until use for slides preparation. Femurs were immersed in 100% ethanol and stored at −20 °C for genomic DNA (gDNA) extraction.

The genomic DNA sequencing method for the *S. rubiginosa* (male) specimen was previously described [24]. For the *R. brasiliensis* (female) and *X. d. angulatus* (male) specimens DNA extraction was performed using the phenol/chloroform-based procedure described previously [25]. Sequencing was conducted by the Illumina company (Inc., San Diego, CA, USA) with a HiSeq 4000 to obtain paired-ends libraries (2 × 101 bp) using the service of Macrogen Inc. (Seoul, Republic of Korea).

We applied conventional staining with 5% Giemsa for chromosome observation and identification of individuals harboring B chromosomes. The C-banding for heterochromatin identification was performed according to a previously described method [26].

2.2. SatDNAs Searching by Graph-Based Clustering Method

Prior to RepeatExplorer graph-based clustering analysis, we preprocessed and checked the quality of the paired-ends reads of each species using FastQC [27]. Preprocessing of the reads was performed following default parameters using the public online platform: https://repeatexplorer-elixir.cerit-sc.cz/galaxy/. Reads were processed with a "quality trimming tool", "FASTQ interlacer" on paired end reads, "FASTQ to FASTA" converter, and "RepeatExplorer clustering" all with default recommended options [21]. First we searched and selected, by visual observation, the clusters that showed high graph density that indicated proximity with satDNAs families [28]. Contigs from the selected clusters were deeply explored and manually searched for sequences with tandem pattern confirmed by the dot plot graphics implemented using Geneious v4.8.5 software [29]. The consensus monomer of each satDNA family of each species was used as the query in two databanks, BLAST (http://www.ncbi.nlm.gov/Blast/) and Repbase (http://www.girinst.org/repbase/), to check similarity with another sequence deposited and described. Abundance of each satDNA family was calculated with the number of reads of each cluster divided by the total number of reads used in the "RepeatExplorer clustering" protocol [21]. Nucleotide divergence was calculated using the RepeatMasker package with specific parameters provided in the scripts program protocol to calculate Kimura divergence values [30]. Superfamilies (SF) were considered by comparing consensus monomer of each satDNA against all of them from each species independently using the Geneious v4.8.5 software [29] assembly tool, alternating overlap identity following the same considerations as a previous work [31]. We classified each identified satDNA family according to a previous method [31], considering the species name abbreviation and decreasing abundance, followed by the consensus monomer size; they were numbered in decreasing order of abundance. The sequences were deposited in GenBank under the accession numbers MH900339–MH900377.

2.3. Amplification of SatDNAs through PCR, Probes and Fluorescence In Situ Hybridization

We used the consensus sequences of each satDNA family of each species to design divergent primers manually or using the Primer3 tool [32] implemented in Geneious v4.8.5 software [29] (Supplementary Table S1). Polymerase chain reactions (PCRs) were performed using 10× PCR Rxn Buffer, 0.2 mM $MgCl_2$, 0.16 mM dNTPs, 2 mM of each primer, 1 U of *Taq* Platinum DNA Polymerase (Invitrogen, San Diego, CA, USA), and 50–100 ng/µL of template DNA. The PCR conditions included an initial denaturation at 94 °C for 5 min and 30 cycles at 94 °C (30 s), 55 °C (30 s), and 72 °C (80 s), plus a final extension at 72 °C for 5 min. The PCR products were visualized on a 1% electrophoresis agarose

gel. The monomeric bands were isolated and purified using the Zymoclean™ Gel DNA Recovery Kit (Zymo Research Corp., The Epigenetics Company, CA, USA) according to the manufacturer's recommendations and then used as template for reamplification using the same PCR conditions. The monomers were sequenced by the Sanger method using the service of Macrogen Inc. to confirm the amplification of desired sequence.

FISH was performed in meiotic chromosomes using one or two probes according to a method described previously [33] with some adjustments as outlined previously [34]. The probes labeled with digoxigenin-11-dUTP were detected using anti-digoxigenin rhodamine (Roche, Mannheim, Germany), and probes labeled with biotin-14-dATP were detected using Streptavidin Alexa Fluor 488-conjugated (Invitrogen, San Diego, CA, USA). The preparations were counterstained using 4′,6-diamidine-2′-phenylindole (DAPI) and mounted in VECTASHIELD (Vector, Burlingame, CA, USA). FISH results were observed using an Olympus microscope BX61 (Tokyo, Japan) equipped with a fluorescent lamp and the proper filters. Images were obtained using a DP71 cooled digital camera in grayscale and then pseudo-colored in blue for chromosomes and red or green for hybridization signals, merged and optimized for brightness and contrast using Adobe Photoshop CS6. To describe the patterns of satDNA chromosomal distribution distinct cells were analyzed, including diplotene, metaphase I, metaphase II, and mitotic metaphase.

3. Results

3.1. Karyotypes, B Chromosomes, and Heterochromatin Distribution

Occurrence of a karyotype consisting of 2n = 23,X0, and presence of B chromosomes observed here for *R. brasiliensis* and *X. d. angulatus* were previously reported by different authors [14,35], including in the same population, i.e., Juazeiro do Norte/CE for *X. d. angulatus* [36]. We report for the first time the presence of B chromosomes in *R. brasiliensis* from Lagoa do Carro/PE. The karyotype of *S. rubiginosa*, described here for the first time, is also 2n = 23,X0 as observed for other species from the same genus, like *S. gregaria* [37], *S. pallens*, and *S. flavofasciata* [38]. Among the five individuals of *S. rubiginosa,* two presented B chromosomes. We classified autosomal chromosomes of the three species in three distinct groups considering size: three long chromosomes (L1–L3), five medium (M4–M8), and three small (S9–S11).

The B chromosomes of the three species are acrocentric with variable pattern of heterochromatin distribution (Figure 1). For *R. brasiliensis* pericentromeric and distal blocks were observed (Figure 1a) and for *S. rubiginona* pericentromeric and interstitial blocks, close to the centromere, were noticed (Figure 1b). In *X. d. angulatus* the B chromosome was completely heterochromatic with deeper staining in the pericentromeric region (Figure 1c). Heterochromatin blocks restricted to pericentromeric areas were noticed for A chromosomes (Figure 1).

3.2. In Silico SatDNA Analysis

By using RepeatExplorer we predicted the most abundant satDNAs as follows, twelve, nine, and eighteen satDNA families in *R. brasiliensis*, *S. rubiginosa*, and *X. d. angulatus*, respectively. Monomer lengths varied from 36 to 410 nt in *R. brasiliensis*, from 107 to 441 nt in *S. rubiginosa*, and from 8 to 289 in *X. d. angulatus*. The predominance of families with monomer length higher than 100 nt was noticeable. Only for *X. d. angulatus*, satDNA families with monomer length smaller than 50 nt was observed (Table 1). Sequence similarity analysis revealed the presence of two similar satDNAs families in the genome of *R. brasiliensis*, RbrSat01-171 and RbrSat04-168 (superfamily SF1), In *X. d. angulatus* two superfamilies were noticed each composed by two satDNA families, SF1 (XanSat05-267 and XanSat07-279) and SF2 (XanSat09-130 and XanSat14-128). No similarity between satDNAs was noticed between species.

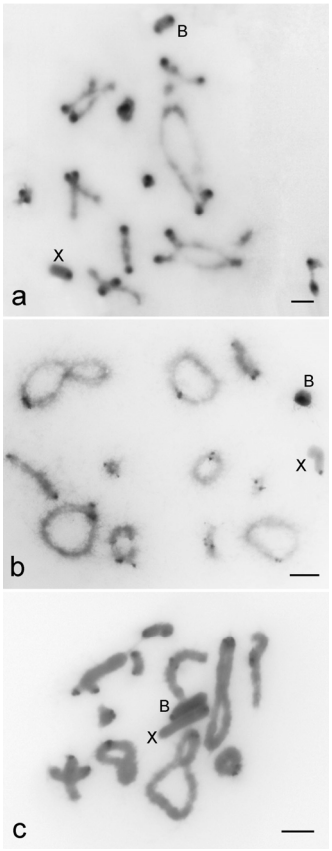

Figure 1. C-banding revealing the heterochromatin location in diplotene chromosomes of *Rhammatocerus brasiliensis* (**a**), *Schistocerca rubiginosa* (**b**), and *Xyleus discoideus angulatus* (**c**). Note the pericentromeric location of C-positive blocks on A chromosomes and the distinct patterns for the B chromosome of the three species, i.e., pericentromeric and distal in *R. brasiliensis*; pericentromeric and interstitial (close to the centromere) in *S. rubiginosa*; along the entire chromosome with darker band in pericentromeric region in *X. d. angulatus*. The X and B chromosomes are indicated. Bar = 5 μm.

A+T content was variable from 44.5% to 63.9% (mean 57.63%) in *R. brasiliensis*, from 48.9% to 61.7% (mean 55.12%) in *S. rubiginosa*, and from 28.6% to 76.2% in *X. d. angulatus* (mean 59.15%). Predominance of A+T-rich satDNA families was observed, ten in *R. brasiliensis*, eight in *S. rubiginosa*, and fifteen in *X. d. andgulatus*. Concerning total abundance, the satDNAs represented 1.499% of the genome of *R. brasiliensis*, 2.172% of *S. rubiginosa*, and 2.322% of *X. d. angulatus* genomes. In all species, even the most abundant satDNA family represented less than 1% of the genome, i.e., 0.766% in *R. brasiliensis*, 0.73% in *S. rubiginosa*, and 0.627% in *X. d. angulatus*. The lowest abundance satDNA in *R. brasiliensis* corresponded to 0.01% of the genome, in *S. rubiginosa* to 0.026%, and in *X. d. angulatus* to 0.013% (Table 1).

3.3. Chromosomal Location of SatDNAs

All satDNA families recognized by RepeatExplorer analysis were accurately amplified by PCR and sequenced; FISH mapping showed signals for most of them (Table 2; Figures 2–4). Six satDNA families revealed signals for *R. brasiliensis* (Figure 2) and *S. rubiginosa* (Figure 3), and for *X. d. angulatus* eleven satDNA families allowed identification of specific marks by FISH (Figure 4), representing clustered satDNAs. For the remaining satDNA families, six for *R. brasiliensis*, three for *S. rubiginosa*, and seven for *X. d. angulatus*, were nonclustered with no FISH signals (Table 2).

Table 1. Characteristics of satellite DNA (satDNA) families isolated from the genomes of three grasshopper species, including their monomer sizes, base pair richness, and genome abundances.

Species	SatDNA Superfamily	SatDNA Family	Monomer Size (nt)	A+T (%)	Abundance (%)	Divergence (%)
R. brasiliensis	SF1	RbrSat01-171	171	59.3	0.766	4.98
	-	RbrSat02-410	410	47.9	0.224	8.94
	-	RbrSat03-36	36	44.5	0.126	8.45
	SF1	RbrSat04-168	168	59.4	0.105	18.14
	-	RbrSat05-179	179	59.1	0.061	4.96
	-	RbrSat06-165	165	59.2	0.056	1.23
	-	RbrSat07-240	240	60.4	0.047	11.56
	-	RbrSat08-176	176	58.0	0.042	6.27
	-	RbrSat09-238	238	63.9	0.025	8.75
	-	RbrSat10-268	268	62.7	0.021	7.79
	-	RbrSat11-233	233	58.0	0.016	7.85
	-	RbrSat12-180	180	57.8	0.010	2.06
Total					1.499	
S. rubiginosa	-	SruSat01-194	194	58.3	0.730	4.30
	-	SruSat02-170	170	54.4	0.476	4.64
	-	SruSat03-170	170	59.9	0.287	7.79
	-	SruSat04-301	301	48.9	0.244	4.77
	-	SruSat05-441	441	50.6	0.135	23.18
	-	SruSat06-363	363	57.1	0.126	9.61
	-	SruSat07-232	232	61.2	0.116	9.23
	-	SruSat08-172	172	58.2	0.032	16.24
	-	SruSat09-107	107	61.7	0.026	10.85
Total					2.172	
X. d. angulatus	-	XanSat01-8	8	62.5	0.627	4.62
	-	XanSat02-21	21	28.6	0.586	4.41
	-	XanSat03-10	10	60.0	0.464	9.38
	-	XanSat04-10	10	60.0	0.228	5.22
	SF1	XanSat05-267	267	56.7	0.087	5.50
	-	XanSat06-168	168	64.3	0.069	4.53
	SF1	XanSat07-279	279	60.2	0.053	11.08
	-	XanSat08-16	16	56.2	0.033	4.38
	SF2	XanSat09-130	130	63.1	0.024	10.61
	-	XanSat10-289	289	60.2	0.022	7.27
	-	XanSat11-51	51	47.1	0.019	3.97
	-	XanSat12-246	246	59.2	0.018	11.81
	-	XanSat13-281	281	56.3	0.018	4.61
	SF2	XanSat14-128	128	62.5	0.017	14.90
	-	XanSat15-228	228	59.7	0.017	5.18
	-	XanSat16-21	21	42.9	0.014	9.79
	-	XanSat17-15	15	53.4	0.013	11.56
	-	XanSat18-21	21	76.2	0.013	6.33
Total					2.322	

The distinct clustered satDNA families were variable in number and position within A chromosomes (Figures 2–4). Only one satDNA was located exclusively on pericentromeric regions of A chromosomes in each species, RbrSat03-36 in *R. brasiliensis* (Figure 2b), SruSat02-170 in *S. rubiginosa* (Figure 3b), and XanSat03-10 in *X. d. angulatus* (Figure 4c). Heterochromatin blocks, like centromeres, were enriched in most satDNAs, but we also noticed a few satDNAs placed on the euchromatin of some chromosomes of *R. brasiliensis*: RbrSat08-176 (Figure 2e) and RbrSat09-238 (Figure 2f), and *S. rubiginosa*: SruSat03-170 (Figure 3c), SruSat06-363 (Figure 3d), SruSat07-232 (Figure 3b), and SruSat08-172 (Figure 3e). We observed that satDNA was more frequently distributed within the interstitial and distal euchromatin of *X. d. angulatus* (Figure 4a,c–g,i). The bias for pericentromeric position of satDNA was noticed by comparing the number of pericentromeric blocks with interstitial

and distal ones for each species: *R. brasiliensis* twenty-eight pericentromeric and three interstitial; *S. rubiginosa* twenty-five pericentromeric, four interstitial, and five distal; *X. d. angulatus* forty-two pericentromeric, ten interstitial, and twelve distal (Table 2).

Table 2. Chromosome location of satDNAs in three grasshopper species. For each species at the bottom is indicated the number of satDNA families per chromosome and the amount of satDNAs shared with the B chromosome. p: pericentromeric, i: interstitial, d: distal, nc: nonclustered.

Species	SatDNA Family	Chromosome Location												
		1	**2**	**3**	**4**	**5**	**6**	**7**	**8**	**9**	**10**	**11**	**X**	**B**
Rhammatocerus brasiliensis	RbrSat01-171	p	p			p		p	p	p		p		p
	RbrSat02-410							nc						
	RbrSat03-36	p	p	p	p	p	p	p	p	p	p	p	p	p
	RbrSat04-168											p		p
	RbrSat05-179							p		p				
	RbrSat06-165							nc						
	RbrSat07-240							nc						
	RbrSat08-176			p	p		p,i	p			p	p	i	p
	RbrSat09-238									i				
	RbrSat10-268							nc						
	RbrSat11-233							nc						
	RbrSat12-180							nc						
Total		2	2	2	2	2	2	4	2	4	2	4	2	4
shared with B		2	2	2	2	2	2	3	2	2	2	4	2	
Schistocerca rubiginosa	SruSat01-194						d							i
	SruSat02-170	p	p	p	p	p	p	p	p	p	p	p	p	i
	SruSat03-170	p,d		p,d		p			p	p	p	p		i
	SruSat04-301							nc						
	SruSat05-441							nc						
	SruSat06-363									i,d				2i
	SruSat07-232									i,d				i
	SruSat08-172			p	i	p	p			p	p,i	p		p
	SruSat09-207							nc						
Total		2	1	3	2	3	3	1	2	5	3	3	1	6
shared with B		2	1	3	2	3	3	1	2	5	3	3	1	
Xylleus discoideus angulatus	XanSat01-8	i	i	d	i	d	i	d	d	d	d	d	2i	
	XanSat02-21	p	p	p	p	p	p	p	p	p	p,d	p	p	
	XanSat03-10	p	p	p	p	p	p	p	p	p	p	p	p	p,i,d
	XanSat04-10			p			p	p						
	XanSat05-267						p				p,i			2i
	XanSat06-168					p	i							
	XanSat07-279	i	d				p							
	XanSat08-16						d							
	XanSat09-130							nc						
	XanSat10-289							nc						
	XanSat11-51		d											
	XanSat12-246	p	p	p	p	p	p	p		p	p	p		
	XanSat13-281							p		d	i			i,d
	XanSat14-128							nc						
	XanSat15-228							nc						
	XanSat16-21							nc						
	XanSat17-15							nc						
	XanSat18-21							nc						
Total		5	6	5	4	5	9	6	3	5	6	4	3	3
shared with B		1	1	1	1	1	2	2	1	2	3	1	1	

SatDNA unique to a specific A chromosome was a rare condition in the three species. It was noticed in *R. brasiliensis* for RbrSat04-168 (Figure 2c) and RbrSat09-238 (Figure 2f) in pair S11 and S9, respectively; SruSat01-194 (Figure 3a) in pair 6, and SruSat06-363 (Figure 3d) and SruSat07-232 (Figure 3b) in pair S9 of *S. rubiginosa*; in *X. d. angulatus* the repeats XanSat08-16 (Figure 4f) and XanSat11-51 (Figure 4g) were exclusive from the pairs M6 and L2, respectively. The number of

satDNAs per specific A chromosome varied from 2 to 4 (mean 2.5) in *R. brasiliensis*, from 1 to 5 (mean 2.42) in *S. rubiginosa*, and from 3 to 9 (mean 5.08) in *X. d. angulatus*.

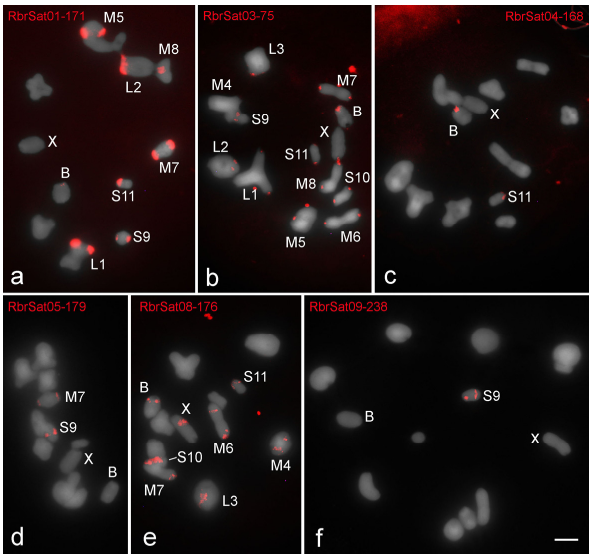

Figure 2. Fluorescent in situ hybridization (FISH) mapping on metaphase I of satDNAs identified in the genome of *R. brasiliensis*. The distinct satDNAs families are indicated. Chromosomes with signals, X and B chromosomes are identified. Note the presence on B chromosome of signals for (**a**) RbrSat01-171 (shared with some A chromosomes), (**b**) RbrSat03-36 (shared with all A chromosomes), (**c**) RbrSat04-168 (shared exclusively with pair S11), and (**e**) RbrSat08-176 (shared with some A chromosomes). For satDNAs (**d**) RbrSat05-179 and (**f**) RbrSat09-238 no signals were observed in B chromosome. Bar = 5 µm.

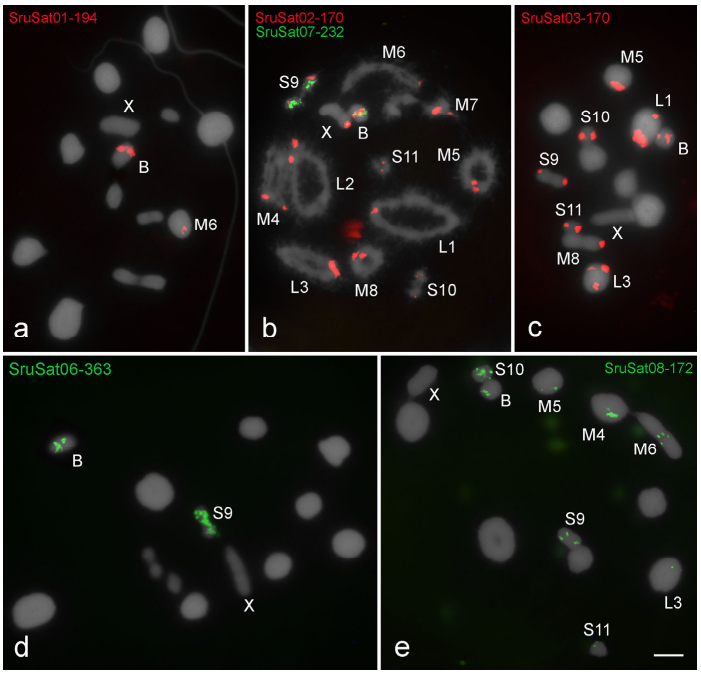

Figure 3. Chromosomal distribution of satDNAs in meiotic cells of *S. rubiginosa* (**a**,**c**,**d**,**e**) metaphase I and (**b**) diplotene. The distinct satDNAs families are indicated. Chromosomes with signals: X and B chromosomes are identified. Observe that the B chromosome harbors all satDNAs families, three of them shared with some A chromosomes (SruSat02-170, SruSat03-170, and SruSat08-172), and three exclusively shared with pair M6 (SruSat01-194) or pair S9 (SruSat06-363 and SruSat07-232). Bar = 5 µm.

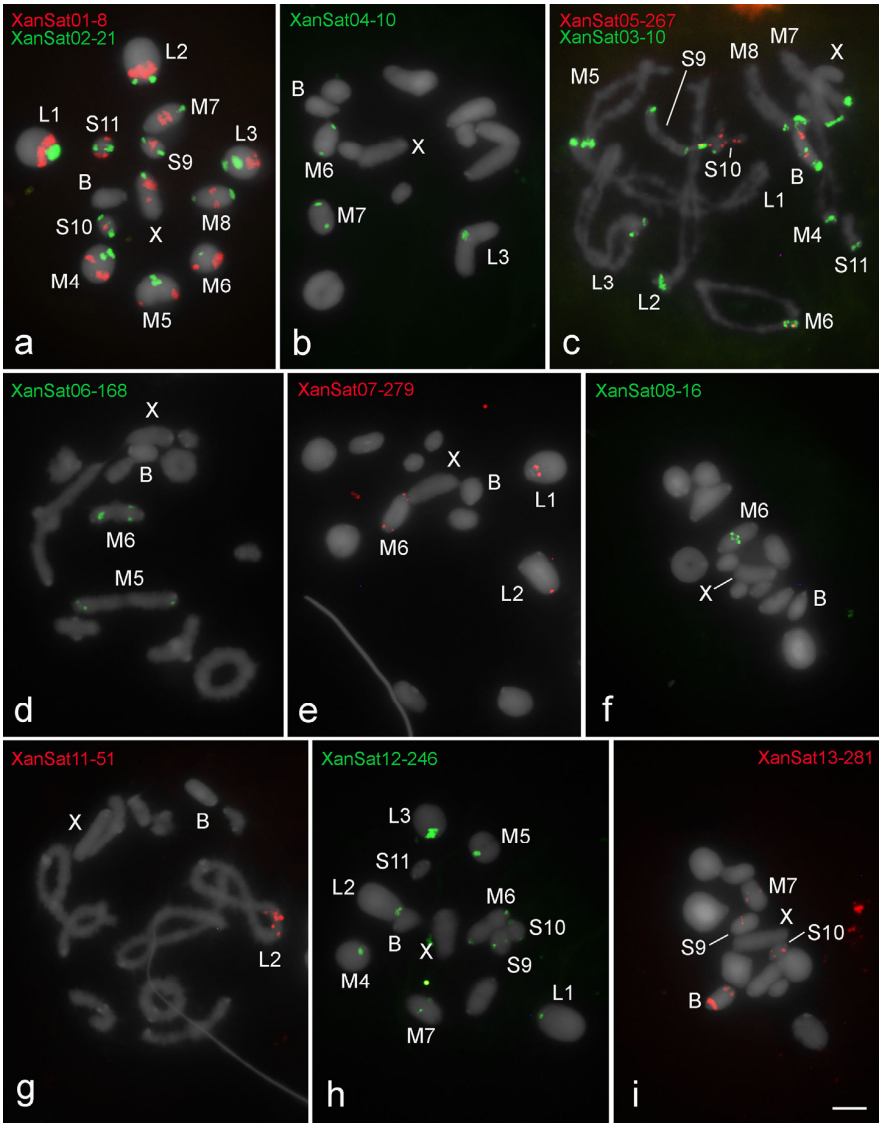

Figure 4. Patterns of chromosomal location revealed by FISH of eleven clustered satDNAs in *X. d. angulatus*. (**a**,**b**,**d**–**f**,**h**,**i**) metaphase I, (**c**,**g**) diplotene. The distinct satDNAs families are indicated. Chromosomes with signals: X and B chromosomes are identified. Note only three satDNA families on the B chromosome, XanSat03-10 (**c**), XanSat05-267 (**c**) and XanSat13-281 (**i**), all of which shared the pair S10. Multiply satDNA sites are observed for all satDNAs (**a**–**e**,**h**,**i**), except XanSat-08-16 (**f**) and XanSat11-51 (**g**). Bar = 5 µm.

The B chromosomes were enriched with distinct satDNA families. All of them were shared with the A chromosomes but show distinct patterns of distribution, such as occurrence in multiple chromosomes or occurrence restricted to one or few elements (Figures 2–5). Four satDNAs occupying pericentromeric regions were seen in the B chromosome of *R. brasiliensis*, RbrSat01-171 (Figure 2a), RbrSat03-36 (Figure 2b), RbrSat04-168 (Figure 2c), and RbrSat08-176 (Figure 2e). These satDNAs were shared with the chromosome S11, which accumulated them in the pericentromeric region. The satDNA RbrSat04-168 was exclusively shared between pair S11 and the B chromosome, while the others were also located in other chromosomes (Figure 2a–c,e and Figure 5a).

The B chromosome of *S. rubiginosa* harbored the six satDNAs that were found clustered in A chromosomes (Figures 3 and 5b). SruSat08-172 (Figure 3e) was located in the pericentromeric region, while the other satellites were interstitially located presenting differences in signal size (Figure 3a–d). The chromosome S9 harbored five of the six satDNAs present in the B chromosome, and among

them two were exclusive of pair S9 and B chromosome, SruSat06-363 (Figure 3d) and SruSat07-232 (Figure 3b). This was the chromosome with highest number of satDNAs shared with the B chromosome. SruSat01-194 was also in the B chromosome but among the A chromosomes this repeat was only in pair 6 (Figure 3a).

Among the eleven repeats mapped by FISH in *X. d. angulatus* chromosomes only three were visualized in the B chromosome, XanSat03-10 (Figure 4c), XanSat05-267 (Figure 4c), and XanSat13-281 (Figure 4i). For these repeats more than one signal was seen in the B chromosome (Figure 4c,i and Figure 5c). Xansat03-10 was located in pericentromeric, interstitial, and distal regions (Figures 4c and 5c), XanSat05-267 presented two interstitial blocks (Figures 4c and 5c) and XanSat13-281 was placed in interstitial and distal areas (Figures 4i and 5c). We observed that none of the satDNAs located on the B chromosome were restricted to one A chromosome, XanSat03-10 (Figures 4c and 5c) was located in all pericentromeric regions, XanSat05-267 (Figures 4c and 5c) was located in pairs M6 and S10, and XanSat13-281 (Figures 4i and 5c) was located in pairs M7, S9, and S10. Chromosome S10 shared the highest amount of satDNAs with the B chromosome (Figure 4c,i and Figure 5c).

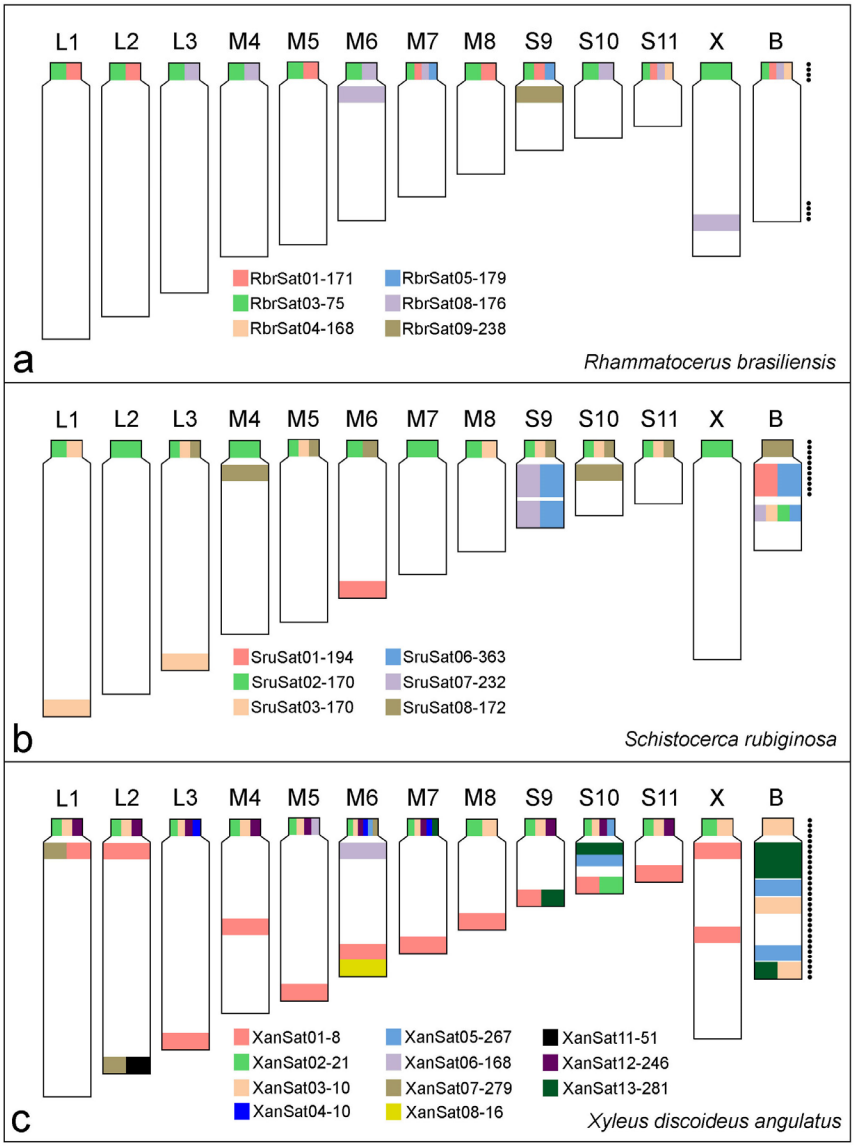

Figure 5. Ideograms summarizing the chromosomal location of clustered satDNAs in the three species of grasshoppers, (**a**) *R. brasiliensis*, (**b**) *S. rubiginosa*, and (**c**) *X. d. angulatus*. Each satDNA family is represented by one color. Black dots next to the B chromosomes indicate heterochromatin distribution in these chromosomes.

4. Discussion

Appling bioinformatic and molecular cytogenetic approaches to determine the content of satDNA allowed for a rapid increase in characterization of these kinds of elements among Orthoptera. High-throughput analysis has allowed the characterization of 234 satDNAs families in seven species [7,31,39–42]. Here we describe for first time the chromosomal organization of the most abundant satDNAs populating the genomes of three grasshopper species from the Romaleidae and Acrididae families. They correspond to a total 39 satDNAs families contributing to the knowledge of chromosomal organization of this kind of repeat on B chromosome.

SatDNAs Reveal Clues about B Chromosome Composition and Ancestry

Even though B chromosomes have been studied for a long time, we know very little about their ancestry in most species. B chromosome ancestry is known only in a few species [7], and therefore its origin still remains intriguing due in part to their high evolutionary rate. In grasshoppers, repetitive DNAs have been used to track B chromosome origin and composition in relatively few species. In *E. monticola* for instance, B chromosome ancestry is attributed to the autosomal pair S8 based on satDNAs analysis [7]. In *A. flavolineata*, the origin of B chromosome from pair 1 is attributed to the unique presence of U2 snDNA genes in these two chromosomes [16]. The ancestry of B chromosome in *L. migratoria* is related to pairs 8 and 9 due to the presence of satDNAs and histone genes in those chromosomes [8,15]. Previous works discussed the composition and putative origin of B chromosomes in two grasshoppers species studied here, *R. brasiliensis* and *X. d. angulatus*. However, it was not possible to elucidate a specific ancestral chromosome (see below). Based on satDNA content and organization we provide some clues about the ancestry of B chromosomes in these species, and additionally in *S. rubiginosa.*

The B chromosome of *R. brasiliensis* harbors four satDNAs, three of them are shared with multiple chromosomes (i.e., RbrSat01-171, RbrSat03-75, and RbrSat08-176) and, because of this, they are not good markers for ancestry determination. Most A chromosomes share two satDNAs with the B chromosome. The A chromosomes that share more satDNAs with the B chromosome are pairs M7 and S11, three and four, respectively, being good candidates to be involved in the origin of B chromosome. Three satDNAs (RbrSat01-171, RbrSat03-75, and RbrSat08-176) shared between pair M7, S11, and the B chromosome are also located on other A chromosomes. Furthermore, the pair S11 harbors the satDNA RbrSat04-168 that is an exclusive sequence shared with the B chromosome. The pericentromeric region of pair S11 fits exactly the composition of pericentromeric region of the B chromosome, supporting the hypothesis of its involvement in B chromosome origin.

Some controversial ideas were proposed for the origin of B in *R. brasiliensis.* First, the authors of a previous paper [35] proposed the origin from one or several chromosomes, including, for example, the pair S11 as supported here by satDNA mapping. Pairs L2, L3, M5, and S11 harbor 5S rDNA clusters that are shared with the B chromosome [35] and could be involved in its origin. Second, the analysis made by the authors of a previous paper [14] did not support the autosomal origin hypothesis, based on the presence of 5S rDNA and H3 gene clusters in the B chromosome that are shared with most A chromosomes (including the X chromosome), except the pair S11. However, the occurrence of these repetitive DNAs in the B chromosome could be more related to transposition events after its origin than ancestry [14]. These data, including the individuals from distinct populations, support the multiregional origin of the B chromosome in *R. brasiliensis* or dynamics for repetitive DNA organization for both A and B chromosomes, causing the emergence of new B chromosome variants. Based on a cytomolecular analysis, multiple B chromosome variants were described, for example, in rye, *Secale cereale* [43], and in the grasshoppers *X. d. angulatus* [36] and *E. plorans* [44].

Although our findings strongly support the ancestry of the B chromosome from the pair S11 in *R. brasiliensis* (at least in Lagoa do Carro/PE population), we should also point attention to the pair M7 that share three satDNAs with the B chromosome. In other populations (including Lagoa do Carro/PE) the chromosome M7 harbors H3 histone gene, which in some individuals is exclusively shared with the

B chromosome [14,45]. This suggests the involvement of M7, besides the pair S11, in B chromosome ancestry. It is similar to *L. migratoria* in which the B chromosome ancestry is putatively from two chromosomes, the pairs 8 and 9 [8], as in rye [46]. On the other hand, we should bear in mind that the pair M7 harbors one satDNA (RbrSat05-179) that is not observed in the B chromosome. Moreover, considering the high dynamism of the H3 histone gene (in number of clusters) in *R. brasiliensis*, it is possible that this gene was acquired later by the B chromosome. To shed light on this possibility, individuals from multiple populations should be studied using the distinct probes.

The satDNA mapping in *S. rubiginosa* suggests an autosomal origin for B chromosome from the pair S9. This chromosome shares five satDNAs with the B chromosome, two of them exclusive for this chromosome (SruSat06-363 and SruSat07-232), thus supporting the ancestry of the B chromosome from this bivalent. Furthermore, the pair S9 also harbors other three satDNAs present in the B chromosome, SruSat02-170, SruSat03-170, and SruSat08-172. Interestingly, those two exclusive satDNAs in S9 also are abundant in the B chromosome. This means that these repeats were massively amplified covering almost the entire length of those two chromosomes. The SruSat01-194 that is present in the pair M6 is also highly abundant in the B chromosome. We ruled out the possibility of B origin from M6 due to the absence of other three satDNAs that are present in the B chromosome, including those pericentromeric satDNA. Furthermore, if the pair M6 is involved in B chromosome origin it has a secondary contribution in comparison to the pair S9. It should be noted that SruSat01-194 corresponds to the most abundant satDNA in the *S. rubiginosa* genome, visible in the B chromosome as a large block likely due to amplification after its origin. It might be possible that the presence of this repeat in other A chromosomes (including pair S9), but arranged non-tandemly, makes it difficult to reach the FISH threshold resolution.

The satDNA content and distribution in the B chromosome of *X. d. angulatus* indicate a more complex evolution than in *R. brasiliensis* and *S. rubiginosa*, with additional chromosomal rearrangements after the B chromosome origin followed by accumulation/deletion involving repeats, as suggested by the previous analyses [35,36] (see below). Even though there are 11 satDNAs clustered on the A chromosomes of *X. d. angulatus*, only three of them are present in the B chromosome. There is no satDNA exclusively shared between the B chromosome and one chromosome of A complement. However, the pair S10 shares the most satDNAs with B chromosome (three satDNAs families), and it seems to be the ancestral pair involved in the B chromosome origin. The three satDNAs shared between B chromosome and the pair S10 are located at pericentromeric or interstitial regions (not far from the centromere), highlighting the origin of the B chromosome from about the half proximal part of the pair S10. Recently, it was suggested that pericentromeric and proximal regions enriched of repetitive DNAs were involved with the B chromosome origin in *X. d. angulatus*, followed by repetitive DNA amplification and rearrangements, like inversions [36].

Although the origin of the B chromosome in *X. d. angulatus* from the proximal part of the pair S10 is supported by current data, the presence of two other satDNAs in the pericentromeric region of pair S10 (XanSat02-21 and XanSat12-246), not shared with the B chromosome, is contrary to this hypothesis. The difference between the satDNA content in B and chromosome S10 can be explained by the changes of satDNAs amounts in the B chromosome during its evolution. In that way, the satDNA XanSat03-10 was amplified in the pericentromeric region of the B chromosome, while the other ones were completely deleted or conserved in small copy number, not detected by FISH. Interestingly, XanSat03-10 is a unique satDNA exclusively located in the pericentromeric region of all A chromosomes, likely involved in centromeric function. This could be the explanation for its amplification in the centromere of B chromosome, giving more stability through cell divisions. Besides amplification/deletion of satDNAs, the distribution of repeats in the B chromosome suggests the possibility of putative events of duplication and inversion that gave origin to the terminal region. The amplification of satDNAs after its origin and the changing satDNA repeat abundance was postulated in *E. monticola* [7]. Moreover, the putative duplication and inversion on the B chromosome

of *X. d. angulatus* highlights how dynamic the repetitive DNAs are on this element, leading to the emergence of distinct morphotypes.

5. Conclusions

The present data expands the knowledge about the B chromosomes composition and their origin in grasshoppers. Our results provide support for the intraspecific origin of the B chromosome in the three species, like in the other species of grasshoppers [7,16]. Although the B chromosomes share some meiotic peculiarities with the X chromosomes that suggested origin from this chromosome, the current knowledge indicates a more common origin from autosomes in grasshoppers [7,8,16,47]. Furthermore, the species studied here and other grasshopper species with B chromosome ancestry [7,8,47] support the recurrent involvement of small chromosomes in the B chromosome origin. This could be due to the fewer number of genes and the enrichment of repetitive DNAs in small autosomes [7,31,48]. The analysis of other populations employing the repetitive DNA markers used here will shed light on the evolution of B chromosome polymorphism in the species.

Supplementary Materials: The following are available online at http://www.mdpi.com/2073-4425/9/11/523/s1, Table S1. Primers designed in this work and used for PCR amplification of satellite DNAs in the three species of grasshoppers.

Author Contributions: D.C.C.-d.-M., D.M., V.L., R.C.M., H.S. conceived and designed the experiments; D.M., A.B.S.M.F., V.B.B., O.M.P.-G., A.S.M., performed the experiments; all authors analyzed the data and wrote the paper.

Funding: Fundação de Amparo à Pesquisa do Estado de São Paulo-FAPESP (process number 2015/16661-1) and Conselho Nacional de Desenvolvimento Científico e Tecnológico-CNPq (process number 305300/2017-2).

Conflicts of Interest: The authors declare no conflicts of interest.

References

1. Charlesworth, B.; Sniegowski, P.; Stephan, W. The evolutionary dynamics of repetitive DNA in eukaryotes. *Nature* **1994**, *371*, 215–220. [CrossRef] [PubMed]
2. Garrido-Ramos, M.A. Satellite DNA: An evolving topic. *Genes* **2017**, *8*, 230. [CrossRef] [PubMed]
3. Lower, S.S.; McGurk, M.P.; Clark, A.G.; Barbash, D.A. Satellite DNA evolution: Old ideas, new approaches. *Curr. Opin. Genet. Dev.* **2018**, *49*, 70–78. [CrossRef] [PubMed]
4. Camacho, J.P.M. B chromosomes. In *The Evolution of the Genome*; Gregory, T.R., Ed.; Elsevier: San Diego, CA, USA, 2005; pp. 223–286.
5. Houben, A. B chromosomes—A matter of chromosome drive. *Front. Plant Sci.* **2017**, *8*, 210. [CrossRef] [PubMed]
6. Wilson, E.B. The supernumerary chromosomes of Hemiptera. *Science* **1907**, *26*, 870–871.
7. Ruiz-Ruano, F.J.; Cabrero, J.; López-León, M.D.; Camacho, J.P.M. Satellite DNA content illuminates the ancestry of a supernumerary (B) chromosome. *Chromosoma* **2017**, *126*, 487–500. [CrossRef] [PubMed]
8. Ruiz-Ruano, F.J.; Cabrero, J.; López-León, M.D.; Sánchez, A.; Camacho, J.P.M. Quantitative sequence characterization for repetitive DNA content in the supernumerary chromosome of the migratory locust. *Chromosoma* **2018**, *127*, 45–57. [CrossRef] [PubMed]
9. McAllister, B.F.; Werren, J.H. Hybrid origin of a B chromosome (PSR) in the parasitic wasp *Nasonia vitripennis*. *Chromosoma* **1997**, *106*, 243–253. [CrossRef] [PubMed]
10. Silva, D.M.Z.A.; Utsunomia, R.; Ruiz-Ruano, F.J.; Daniel, S.N.; Porto-Foresti, F.; Hashimoto, D.T.; Oliveira, C.; Camacho, J.P.M.; Foresti, F. High-throughput analysis unveils a highly shared satellite DNA library among three species of fish genus *Astyanax*. *Sci. Rep.* **2017**, *7*, 12726. [CrossRef] [PubMed]
11. Kumke, K.; Macas, J.; Fuchs, J.; Altschmied, L.; Kour, J.; Dhar, M.K.; Houben, A. *Plantago lagopus* B chromosome is enriched in 5S rDNA-derived satellite DNA. *Cytogenet. Genome Res.* **2016**, *148*, 68–73. [CrossRef] [PubMed]
12. Palestis, B.G.; Cabrero, J.; Trivers, R.; Camacho, J.P.M. Prevalence of B chromosomes in Orthoptera is associated with shape and number of A chromosomes. *Genetica* **2010**, *138*, 1181–1189. [CrossRef] [PubMed]

13. López-León, M.D.; Neves, N.; Schwarzacher, T.; Heslop-Harrison, J.S.; Hewitt, G.M.; Camacho, J.P.M. Possible origin of a B chromosome deduced from its DNA composition using double FISH technique. *Chromosom. Res.* **1994**, *2*, 87–92. [CrossRef]
14. Oliveira, N.L.; Cabral-de-Mello, D.C.; Rocha, M.F.; Loreto, V.; Martins, C. Chromosomal mapping of rDNAs and H3 histone sequences in the grasshopper *Rhammatocerus brasiliensis* (acrididae, gomphocerinae): Extensive chromosomal dispersion and co-localization of 5S rDNA/H3 histone clusters in the A complement and B chromosome. *Mol. Cytogenet.* **2011**, *4*, 24. [CrossRef] [PubMed]
15. Teruel, M.; Cabrero, J.; Perfectti, F.; Camacho, J.P.M. B chromosome ancestry revealed by histone genes in the migratory locust. *Chromosoma* **2010**, *119*, 217–225. [CrossRef] [PubMed]
16. Bueno, D.; Palacios-Gimenez, O.M.; Cabral-de-Mello, D.C. Chromosomal mapping of repetitive DNAs in *Abracris flavolineata* reveal possible ancestry for the B chromosome and surprisingly H3 histone spreading. *PLoS ONE* **2013**, *8*, e66532. [CrossRef] [PubMed]
17. Montiel, E.E.; Cabrero, J.; Camacho, J.P.M.; López-león, M.D. Gypsy, RTE and Mariner transposable elements populate *Eyprepocnemis plorans* genome. *Genetica* **2012**, *140*, 365–374. [CrossRef] [PubMed]
18. Palacios-Gimenez, O.M.; Bueno, D.; Cabral-de-Mello, D.C. Chromosomal mapping of two Mariner-like elements in the grasshopper *Abracris flavolineata* (orthoptera: Acrididae) reveals enrichment in euchromatin. *Eur. J. Entomol.* **2014**, *111*, 329–334. [CrossRef]
19. Milani, D.; Cabral-de-Mello, D.C. Microsatellite organization in the grasshopper *Abracris flavolineata* (Orthoptera: Acrididae) revealed by FISH mapping: Remarkable spreading in the A and B chromosomes. *PLoS ONE* **2014**, *9*, e97956. [CrossRef] [PubMed]
20. Milani, D.; Ramos, E.; Loreto, V.; Martí, D.A.; Cardoso, A.L.; Moraes, K.C.M.; Martins, C.; Cabral-de-Mello, D.C. The satellite DNA AflaSAT-1 in the A and B chromosomes of the grasshopper *Abracris flavolineata*. *BMC Genet.* **2017**, *18*, 81. [CrossRef] [PubMed]
21. Novák, P.; Neumann, P.; Pech, J.; Steinhaisl, J.; Macas, J. RepeatExplorer: A Galaxy-based web server for genome-wide characterization of eukaryotic repetitive elements from next generation sequence reads. *Bioinformatics* **2013**, *29*, 792–793. [CrossRef] [PubMed]
22. Utsunomia, R.; Silva, D.M.Z.A.; Ruiz-Ruano, F.J.; Araya-Jayme, C.; Pansonato-Alves, J.C.; Scacchetti, P.C.; Hashimoto, D.T.; Oliveira, C.; Trifonov, V.A.; Porto-Foresti, F.; et al. Uncovering the ancestry of B chromosomes in *Moenkhausia sanctaefilomenae* (Teleostei, Characidae). *PLoS ONE* **2016**, *11*, e0150573. [CrossRef] [PubMed]
23. Song, H.; Mariño-Pérez, R.; Woller, D.A.; Cigliano, M.M. Evolution, diversification, and biogeography of grasshoppers (Orthoptera: Acrididae). *Insect Sys. Div.* **2018**, *2*, 1–25. [CrossRef]
24. Song, H.; Foquet, B.; Mariño-Pérez, R.; Woller, D. Phylogeny of locusts and grasshoppers reveals complex evolution of density-dependent phenotypic plasticity. *Sci. Rep.* **2017**, *7*, 1–13. [CrossRef] [PubMed]
25. Sambrook, J.; Russell, D.W. *Molecular Cloning, a Laboratory Manual*, 3rd ed.; Cold Spring Harbor: New York, NY, USA, 2001.
26. Sumner, A.T. A simple technique for demonstrating centromeric heterochromatin. *Exp. Cell. Res.* **1972**, *75*, 304–306. [CrossRef]
27. *FastQC*, Version 0.10.1; A Quality Control Tool for High throughput Sequence Data; Babraham Bioinformatics: Cambridge, UK, 2012.
28. Novák, P.; Neumann, P.; Macas, J. Graph-based clustering and characterization of repetitive sequences in next-generation sequencing data. *BMC Bioinform.* **2010**, *11*, 378. [CrossRef] [PubMed]
29. *Geneious*, Version 4.8.5; Biomatters Ltd.: Aukland, New Zealand, 2009.
30. *RepeatMasker Open*, Version 4.0; Institute for Systems Biology: Seattle, WA, USA, 2013.
31. Ruiz-Ruano, F.J.; López-León, M.D.; Cabrero, J.; Camacho, J.P.M. High-throughput analysis of the satellitome illuminates satellite DNA evolution. *Sci. Rep.* **2016**, *6*, 28333. [CrossRef] [PubMed]
32. Rozen, S.; Skaletsky, H. Primer3 on the WWW for general users and for biologist programmers in Bioinformatics. *Methods Mol. Biol* **2000**, *132*, 365–386. [CrossRef] [PubMed]
33. Pinkel, D.; Lanlegent, J.; Collins, C.; Fuscoe, J.; Segraves, R.; Lucas, J.; Gray, J. Fluorescence in situ hybridization with human chromosome-specific libraries: Detection of trisomy 21 and translocations of chromosome 4. *Proc. Natl. Acad. Sci. USA* **1986**, *85*, 9138–9142. [CrossRef]

34. Camacho, J.P.M.; Cabrero, J.; López-León, M.D.; Cabral-de-Mello, D.C.; Ruiz-Ruano, F.J. Grasshoppers (Orthoptera). In *Protocols for Cytogenetic Mapping of Arthropod Genomes*, 1st ed.; Sharakhov, I.V., Ed.; CRC Press: Boca Raton, FL, USA, 2015; pp. 381–438.
35. Loreto, V.; Cabrero, J.; López-León, M.D.; Camacho, J.P.M. Possible autosomal origin of macro B chromosomes in two grasshopper species. *Chromosom. Res.* **2008**, *16*, 233–241. [CrossRef] [PubMed]
36. Bernardino, A.C.S.; Cabral-de-Mello, D.C.; Machado, C.B.; Palacios-Gimenez, O.M.; Santos, N.; Loreto, V. B chromosome variants of the Grasshopper *Xyleus discoideus angulatus* are potentially derived from pericentromeric DNA. *Cytogenet. Genome Res.* **2017**, *152*, 213–221. [CrossRef] [PubMed]
37. Camacho, J.P.M.; Shaw, M.W.; Cabrero, J.; Bakkali, M.; Ruíz-Estévez, M.; Ruiz-Ruano, F.J.; Martín-Blázquez, R.; López-León, M.D. Transient microgeographic clines during B chromosome invasion. *Am. Nat.* **2015**, *186*, 675–681. [CrossRef] [PubMed]
38. Souza, M.J.; Melo, N.F. Chromosome study in Schistocerca (Orthoptera-Acrididae-Cyrtacanthacridinae): Karyotypes and distribution patterns of constitutive heterochromatin and nucleolus organizer regions (NORs). *Genet. Mol. Biol.* **2007**, *30*, 54–59. [CrossRef]
39. Ruiz-Ruano, F.J.; Castillo-Martínez, J.; Cabrero, J.; Gómez, R.; Camacho, J.P.M.; López-León, M.D. High-throughput analysis of satellite DNA in the grasshopper *Pyrgomorpha conica* reveals abundance of homologous and heterologous higher-order repeats. *Chromosoma* **2018**, *127*, 3. [CrossRef] [PubMed]
40. Palacios-Gimenez, O.M.; Dias, G.B.; de Lima, L.G.; Kuhn, G.C.E.S.; Ramos, E.; Martins, C.; Cabral-de-Mello, D.C. High-throughput analysis of the satellitome revealed enormous diversity of satellite DNAs in the neo-Y chromosome of the cricket *Eneoptera surinamensis*. *Sci. Rep.* **2017**, *7*, 6422. [CrossRef] [PubMed]
41. Palacios-Gimenez, O.M.; Milani, D.; Lemos, B.; Castillo, E.R.; Martí, D.A.; Ramos, E.; Martins, C.; Cabral-de-Mello, D.C. Uncovering the evolutionary history of neo-XY sex chromosomes in the grasshopper *Ronderosia bergii* (Orthoptera, Melanoplinae) through satellite DNA analysis. *BMC Evol. Biol.* **2018**, *18*, 2. [CrossRef] [PubMed]
42. Palacios-Gimenez, O.M.; Bardella, V.B.; Lemos, B.; Cabral-de-Mello, D.C. Satellite DNAs are conserved and differentially transcribed among Gryllus cricket species. *DNA Res.* **2018**, *25*, 137–147. [CrossRef] [PubMed]
43. Marques, A.; Klemme, S.; Guerra, M.; Houben, A. Cytomolecular characterization of de novo formed rye B chromosome variants. *Mol. Cytogenet.* **2012**, *5*, 34. [CrossRef] [PubMed]
44. Cabrero, J.; López-León, M.D.; Ruíz-Estévez, M.; Gómez, R.; Petitpierre, E.; Rufas, J.S.; Massa, B.; Kamel Ben Halima, M.; Camacho, J.P.M. B1 was the ancestor B chromosome variant in the western Mediterranean area in the grasshopper *Eyprepocnemis plorans*. *Cytogenet. Genome Res.* **2014**, *142*, 54–58. [CrossRef] [PubMed]
45. Melo, A.S.; Moura, R.C. (Universidade de Pernambuco, Recife, Pernambuco, BR). Personal communication, 2018.
46. Martis, M.M.; Klemme, S.; Banaei-Moghaddam, A.M.; Blattner, F.R.; Macas, J.; Schmutzer, T.; Scholz, U.; Gundlach, H.; Wicker, T.; Simkova, H.; et al. Selfish supernumerary chromosome reveals its origin as a mosaic of host genome and organellar sequences. *Proc. Natl. Acad. Sci. USA* **2012**, *109*, 13343–13346. [CrossRef] [PubMed]
47. Teruel, M.; Ruiz-Ruano, F.J.; Marchal, J.A.; Sánchez, A.; Cabrero, J.; Camacho, J.P.M.; Perfectti, F. Disparate molecular evolution of two types of repetitive DNAs in the genome of the grasshopper *Eyprepocnemis plorans*. *Heredity* **2014**, *112*, 531–542. [CrossRef] [PubMed]
48. Hewitt, G.M. The integration of supernumerary chromosomes into the orthopteran genome. *Cold Spring Harb. Symp. Quant. Biol.* **1974**, *38*, 183–194. [CrossRef] [PubMed]

4.2. Chapter 2

Out of patterns, the euchromatic B chromosome of the grasshopper Abracris flavolineata is not enriched in high-copy repeats

Diogo Milani, Francisco J. Ruiz-Ruano, Juan Pedro M. Camacho and Diogo C. Cabral-de-Mello

Published in *Heredity* (2021), 127,475–483.

the geneticssociety

www.nature.com/hdy

ARTICLE

Check for updates

Out of patterns, the euchromatic B chromosome of the grasshopper *Abracris flavolineata* is not enriched in high-copy repeats

Diogo Milani[1], Francisco J. Ruiz-Ruano[2,3], Juan Pedro M. Camacho[4] and Diogo C. Cabral-de-Mello[1]✉

In addition to the normal set of standard (A) chromosomes, some eukaryote species harbor supernumerary (B) chromosomes. In most cases, B chromosomes show differential condensation with respect to A chromosomes and display dark C-bands of heterochromatin, and some of them are highly enriched in repetitive DNA. Here we perform a comprehensive NGS (next-generation sequencing) analysis of the repeatome in the grasshopper *Abracris flavolineata* aimed at uncovering the molecular composition and origin of its B chromosome. Our results have revealed that this B chromosome shows a DNA repeat content highly similar to the DNA repeat content observed for euchromatic (non-C-banded) regions of A chromosomes. Moreover, this B chromosome shows little enrichment for high-copy repeats, with only a few elements showing overabundance in B-carrying individuals compared to the 0B individuals. Consequently, the few satellite DNAs (satDNAs) mapping on the B chromosome were mostly restricted to its centromeric and telomeric regions, and they displayed much smaller bands than those observed on the A chromosomes. Our data support the intraspecific origin of the B chromosome from the longest autosome by misdivision, isochromosome formation, and additional restructuring, with accumulation of specific repeats in one or both B chromosome arms, yielding a submetacentric B. Finally, the absence of B-specific satDNAs, which are frequent in other species, along with its euchromatic nature, suggest that this B chromosome arose recently and might still be starting a heterochromatinization process. On this basis, it could be a good model to investigate the initial steps of B chromosome evolution.

Heredity; https://doi.org/10.1038/s41437-021-00470-5

INTRODUCTION

B chromosomes are dispensable genomic elements reported in many plant, animal, and fungal species (Jones and Rees 1982; Camacho 2005; Houben et al. 2014; Jones 2017). B chromosomes were discovered more than a century ago (Wilson 1907) and, for many years, only repetitive DNA had been found on them (for review, see Camacho 2005). However, it is now known that B chromosomes also contain protein-coding genes (Martis et al. 2012; Valente et al. 2014; Navarro-Dominguez et al. 2017). A common characteristic of most B chromosomes is the accumulation of repetitive DNA, which accounts for its evolution and differentiation from A chromosomes (Camacho 2005; Houben et al. 2014). These accumulated repeats include microsatellites and satellite DNAs (satDNAs), multiple classes of transposable elements (TEs), and multigene families (see for example Nur et al. 1988; Ziegler et al. 2003; Coleman et al. 2009; Poletto et al. 2010; Peng and Cheng 2011; Bueno et al. 2013; Klemme et al. 2013; Milani and Cabral-de-Mello 2014; Silva et al. 2014; Coan and Martins 2018; Hanlon et al. 2018; Malimpensa et al. 2018; Marques et al. 2018; Ruiz-Ruano et al. 2018; Felicetti et al. 2021; Stornioli et al. 2021).

In grasshoppers, cytological and molecular analysis in multiple species revealed that most B chromosomes show C-banded heterochromatin and plenty of DNA repeats (for instance, see Ruiz-Ruano et al. 2016a, 2018; Milani et al. 2017a, 2018). For example, most B chromosome variants found in *Eyprepocnemis plorans* are mostly made of rDNA and a satDNA family (Cabrero et al. 1999; 2014; López-León et al. 2008) and they are enriched in R2 retrotransposons (Montiel et al. 2014). The most complete quantification of the repeatome in a grasshopper was recently performed in *Locusta migratoria* and showed that the B chromosome contains 94.9% of repetitive DNA, with a single satDNA comprising 55% of the B chromosome (Ruiz-Ruano et al. 2018). In addition, this B chromosome showed a 17 kb region, including 29 different TEs, which was apparent as a FISH band on the B chromosome. Similarly, heterochromatic B chromosomes rich in a variety of repetitive DNAs have been reported in other grasshopper species, such as *Eumigus monticola*, *Rhammatocerus brasiliensis*, *Xyleus* (*discoideus*) *angulatus, Schistocerca rubiginosa, Podisma sapporensis* and *Dichroplus pratensis* (Bidau et al. 2004; Loreto et al. 2008; Oliveira et al. 2011; Ruiz-Ruano et al. 2016a; Jetybayev et al. 2018; Milani et al. 2018).

[1]Departamento de Biologia Geral e Aplicada, UNESP - Univ Estadual Paulista, Instituto de Biociências/IB, Rio Claro, São Paulo, Brazil. [2]Evolutionary Biology Centre, Department of Organismal Biology – Systematic Biology, Uppsala University, Uppsala, Sweden. [3]Norwich Research Park, School of Biological Sciences, University of East Anglia, Norwich, UK. [4]Departamento de Genética, Facultad de Ciencias, UGR - Univ de Granada, Granada, Spain. ✉email: cabral.mello@unesp.br

Received: 28 April 2021 Revised: 24 August 2021 Accepted: 25 August 2021
Published online: 04 September 2021

An exception to this general pattern is the South American grasshopper *Abracris flavolineata* (2n = 22 + X0♂/XX♀) where a submetacentric B chromosome failed to show heterochromatin defined by the C-banding technique, i.e., C-positive blocks (Cella and Ferreira 1991; Bueno et al. 2013). This B chromosome is mitotically stable thus showing the same number in all cells from the same individual and occurring in one or two copies in a natural population sampled at Rio Claro, São Paulo, Brazil (Milani et al. 2017b). Current evidence supports the origin of this B chromosome from the longest chromosome pair (L1), based on the U2 snDNA being only visualized by FISH on these two chromosomes (Bueno et al. 2013). In addition, we detected other repeats on this B chromosome, a satDNA family (Milani et al. 2017a), some microsatellite repeats (Milani and Cabral-de-Mello 2014), and two TEs (Palacios-Gimenez et al. 2014), which were shared with many A chromosomes. Intrigued by the absence of C-positive heterochromatin on the B chromosome of *A. flavolineata*, we decided to perform high-throughput complementary bioinformatic and cytogenetic analyses to characterize its repetitive DNA content. Repeatome analysis including 1744 TEs, 53 satDNAs, and 9 multigene families revealed that, consistent with its C-heterochromatin scarcity, this B chromosome is not enriched in high-copy repetitive DNAs, which makes it unusual among B chromosomes in general. Exceptionally, we found a few repetitive DNAs present on the euchromatic (C-negative) regions of the A chromosomes, which also decorate the interstitial regions of the B chromosome. In contrast, other repetitive DNAs that were enriched in heterochromatic regions (C-bands) of the A complement were mostly restricted to centromeric and distal regions of the B chromosome. In addition, satellitome analysis revealed that the B chromosome shared one satDNA family in exclusivity with the L1 autosome thus supporting B ancestry from this A chromosome. We finally suggest that this B chromosome could be a young element currently being in an initial step of heterochromatinization.

MATERIALS AND METHODS

Biological materials, genomic DNA extraction, and chromosome preparations

For molecular and bioinformatic analysis, we used the same seven male individuals of *Abracris flavolineata* (three 0B, two 1B, and two 2B) previously studied by Bueno et al. (2013), Milani et al. (2017b), and Ahmad et al. (2020). The hind legs of these animals, previously stored in 100% ethanol at −20 °C, were used for genomic DNA (gDNA) extraction following the phenol/chloroform-based protocol (Sambrook and Russell 2001), which was used for genomic sequencing and PCR assays (see next topics).

For chromosomal mapping we collected five gravid females, which were maintained alive in cages at the laboratory until oviposition, allowing embryos to be obtained. Mitotic embryo chromosome spreads were prepared according to the protocol proposed by Webb et al. (1978). Chromosome spreads were performed by maceration and spreading of portions of embryos on a slide within a drop of 50% acetic acid, under a hot plate at 45 °C.

Genome sequencing and identification of repetitive DNA sequences being overabundant in B-carrying individuals

Genomic DNA sequencing was performed by the Illumina HiSeq 4000 platform using the Macrogen Inc. service (Seoul, Republic of Korea). Sequencing yielded 27–41 Gb DNA (per sample) of 151 bp paired reads. The genomes from seven individuals are deposited in the Sequence Read Archive (SRA) under the accession numbers SRX7784770–SRX7784772. Repetitive sequences making up the repeatome of *A. flavolineata* were recovered and characterized using different approaches, including a thorough search for the satDNA families making up the satellitome, multigene families, and TEs (see details below).

To find and characterize the maximum number of different satDNA families, we applied the satMiner protocol (Ruiz-Ruano et al. 2016b). For this purpose, we randomly selected 2 × 5,000,000 reads from each individual using SeqTK (https://github.com/lh3/seqtk) and pooled those belonging to the same type of genome (0B, 1B, or 2B) by concatenating them. We then performed sequence preprocessing for each group of reads using the "rexp_prepare_normaltag.py" script (https://github.com/fjruizruano/ngs-protocols), which uses Trimmomatic (Bolger et al. 2014) to remove adapters and low-quality nucleotides ($Q < 20$), and finally selected only completely paired reads after trimming, i.e., those read pairs with 151 bp in both members. The script then interleaves forward and reverse reads and converts them to fasta format. We obtained 100,000 read pairs for each of the three libraries (0B, 1B, and 2B) and concatenated them into a single file. We then applied the satMiner protocol (Ruiz-Ruano et al. 2016b) consisting of several rounds of clustering with RepeatExplorer (RE) software (Novák et al. 2013) alternated with the DeconSeq filtering tool (Schmieder and Edwards 2011) to remove those satDNA sequences identified in previous RE rounds and added 100,000 of these cleaned read pairs from each pool sample (0B, 1B, and 2B) prior to each new RE round (again summing up 300,000 read pairs).

RE clusters putatively containing satDNAs were selected by visual graph inspection to identify those showing spherical or ring shapes, which are characteristic of this type of DNA sequence. Then, we performed manual curation of the selected contigs by Geneious v4.8 software (Drummond et al. 2009), checked their tandem structure by dotplot graphic inspection, and recovered the consensus sequence for repeat units of each satDNA family or subfamily. To search for homology between different satDNA families we first compared their consensus sequences using multiple sequence alignments with Muscle (Edgar 2004) implemented in Geneious v4.8 software (Drummond et al. 2009), and second, we ran a homology test based on RepeatMasker (Smit et al. 2017) with "rm_homology.py" (https://github.com/fjruizruano/ngs-protocols). The results of these analyses were used to classify the satDNA collection into superfamilies, families or subfamilies according to the identity criterion proposed in Ruiz-Ruano et al. (2016b).

For TE identification, we randomly selected 100,000 read pairs from each pool of genomes (0B, 1B, and 2B), for a total of 600,000 reads, which were used as input for a single RE round followed by a reclustering-specific tool available in the Galaxy platform (https://repeatexplorer-elixir.cerit-sc.cz/galaxy/). This tool was used for merging clusters showing homology into larger contigs, which are prone to improve TE assembly. Then, we analyzed all the cluster contigs for sequence extraction with Geneious v4.8 software (Drummond et al. 2009). Since this method allowed the recovery of fewer than 200 different TE families, we also used the dnaPipeTE pipeline (Goubert et al. 2015), which uses Trinity (Grabherr et al. 2011) as an assembler, followed by recurrent TE annotation and quantification in the raw reads compared with a custom database previously built by Ruiz-Ruano et al. (2018) from B-carrying genomes of *Locusta migratoria*. This analysis was performed using only forward reads and default parameters recommended for dnaPipeTE. Next, by means of a custom script (https://github.com/fjruizruano/ngs-protocols/blob/master/dnapipete_createdb.py) we used dnaPipeTE assembly and annotation to generate a fasta file with annotated contigs in the RepeatMasker format (Smit et al. 2017) for further analysis.

Finally, the multigene families (H3 histone gene, 18S, 28S, 5.8S, and 5S rDNAs, U1, U2, and U6 snDNAs) and full mitochondrial DNA (mtDNA) were recovered using MITObim (Hahn et al. 2013) with the seed sequences used for *Locusta migratoria* in Ruiz-Ruano et al. (2018).

All the repeats obtained by these different methods were later concatenated, and redundancy was removed by CD-HIT-EST clustering (Li and Godzik 2006) using an 80% sequence identity level, implying that those repeats showing at least 80% identity were considered the same family.

Estimation of repetitive DNA sequence abundances and divergences in the *A. flavolineata* genome

Sequence abundance and divergence of each repetitive DNA family were determined in each of the seven genomes analyzed by means of RepeatMasker (Smit et al. 2017) using the Cross_match search engine on 5,000,000 read pairs from each library. SatDNA families were named in decreasing order of abundance in 0B genomes, following Ruiz-Ruano et al. (2016b). Sequence divergence was estimated by the Kimura 2-parameter (K2P) model using the calcDivergenceFromAlign.pl script within RepeatMasker software (Smit et al. 2017). Abundance for a given repetitive DNA family was calculated as a genome proportion, represented by the sum of all mapped nucleotides belonging to it (including all subfamilies) with respect to the total number of nucleotides in the selected reads from each

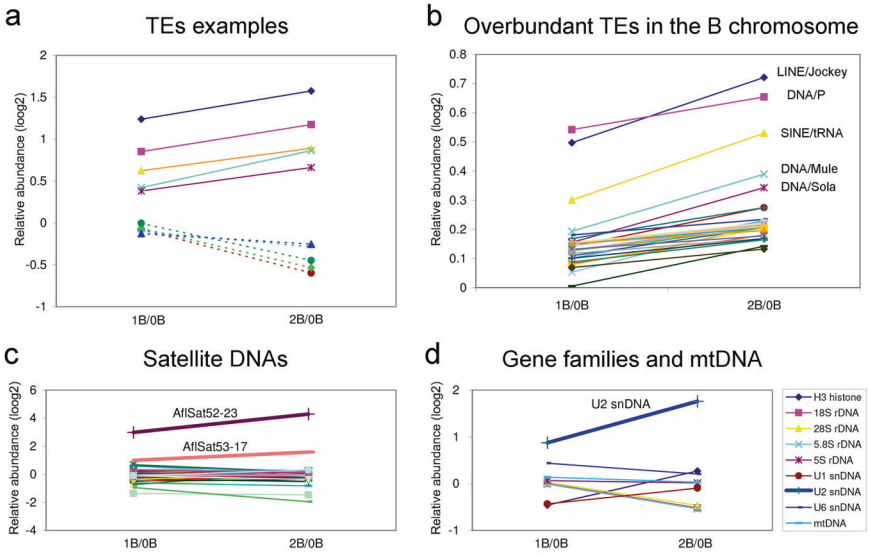

Fig. 1 Relative abundance of several types of repetitive DNA in *A. flavolineata* genomes carrying 1B and 2B, in comparison with the B-lacking genome, measured by the log2 transformed 1B/0B and 2B/0B quotients. a Five examples of TEs showing overabundance in the B chromosome (solid lines), and five others showing the dilution effect (dotted lines) with negative values for both quotients. **b** Overabundant TEs in the B chromosome, indicating TE type for the five showing the highest quotients. **c** Only two satDNA families were overabundant in the B chromosome. Note the dilution effect for many other satDNAs. **d** Only the U2 snDNA showed clear overabundance in the B-carrying genomes, whereas the other families showed the dilution effect or quotients close to zero, suggesting their scarcity in the B chromosome.

Illumina library. Abundance and divergence for each family were separately estimated for each individual and later averaged for 0B (three individuals), 1B (two individuals), and 2B (two individuals) genomes. We then calculated two sequence abundance quotients, 1B/0B and 2B/0B, to search for repeats being overabundant in the B-carrying genomes so that those repeats showing both quotients clearly higher than 1 and that 2B/0B was higher than 1B/0B were considered overabundant in B-carrying individuals and thus enriched in the B chromosome. However, those repeats showing quotients lower than 1 are considered less abundant (or absent) in the B chromosome rather than in the average A chromosome. All satDNA families and some TEs showing overabundance in B-carrying genomes were selected for subsequent chromosomal mapping (see below).

DNA amplification and chromosomal mapping of repetitive DNAs

We designed primers for PCR amplification either manually or else using Primer3 software (Untergasser et al. 2012) (Supplementary Table 1), and PCR conditions followed the same protocol described in Milani et al. (2018). For satDNA sequences, the monomeric bands were isolated and purified using the Zymoclean™ Gel DNA Recovery Kit (Zymo Research Corp., The Epigenetics Company, CA, USA) according to the manufacturer's recommendations. The same method was applied for TE isolation, taking care of isolating fragments showing the size expected from computational annealing of primers. These products were used for reamplification using the same PCR conditions. All amplified sequences were sequenced by the Sanger method using Macrogen Inc. (Seoul, Republic of Korea) service to confirm the actual amplification of the target sequence.

We performed fluorescence in situ hybridization (FISH) on mitotic chromosome spreads from embryos using one or two probes simultaneously, according to Cabral-de-Mello and Marec (2021). Probes were labeled by digoxigenin-11-dUTP (Roche, Mannheim, Germany) or biotin-14-dATP (Invitrogen) and detected by antidigoxigenin-rhodamine (Roche) and streptavidin, Alexa Fluor 488-conjugated (Invitrogen), respectively. The chromosomes were counterstained using 4′,6-diamidine-20-phenylindole dihydrochloride (DAPI) and slides were mounted in VECTASHIELD (Vector, Burlingame, CA, USA). The preparations were observed and images were captured using a BX61 Olympus microscope equipped with a fluorescence lamp and appropriate filters and a DP70 cooled digital camera. All images were processed and optimized using Adobe Photoshop CS6. According to the results observed, we classified the satDNA families into three types: (i) visible FISH bands covering the whole chromosome width (B-pattern), (ii) occurrence of dot-like scattered signals across the chromosome (D-pattern), and (iii) no FISH signal at all (NS-pattern).

Statistical methods

We compared repeat abundance between the 0B, 1B, and 2B genomic libraries by means of nonparametric Friedman ANOVA and the Wilcoxon matched pairs test.

RESULTS

Comparative genomic abundance reveals little enrichment for high-copy repeats in the B chromosome

The overall mean repetitive DNA abundance in *A. flavolineata* genomes from the Rio Claro, São Paulo, Brazil population was 52.94% in 0B individuals, 52.59% in 1B individuals, and 52.00% in 2B individuals; this figure thus decreased with an increasing number of B chromosomes (Friedman ANOVA: $\chi^2 = 8.08$, $N = 1806$, df$= 2$, $P < 0.018$). This result suggests that this B chromosome shows lower repetitive DNA content than the A chromosomes, on average, so that when a given repetitive element is scarce in the B chromosome, its genomic proportion will decrease as the number of Bs grows. This "dilution effect" was significant for TEs ($\chi^2 = 10.12$, $N = 1744$, df $= 2$, $P < 0.0064$), marginally significant for satDNA ($\chi^2 = 4.57$, $N = 53$, df $= 2$, $P > 0.10$), and not significant for multigene families ($\chi^2 = 1.56$, $N = 9$, df $= 2$, $P > 0.45$) (Fig. 1). However, a few repeats showed the reverse pattern, i.e., their abundance increased with increasing numbers of B chromosomes. This pattern suggested the presence of these repeats in the B chromosome. For quantitative application of this criterion, we calculated the 1B/0B and 2B/0B quotients and selected those elements showing 1B/0B > 1 and 2B/0B > 1B/0B, as the two conditions, as a whole, allowed selection for repeats showing increasing abundance with B number.

We found 53 satDNA families in *A. flavolineata*, all of which were present in the three genome libraries analyzed (Supplementary Table 2), thus revealing the absence of B-specific satDNAs. The dilution effect was also apparent for satDNA, as its genomic content decreased in the presence of B chromosomes (4.52% in 0B, 4.03% in 1B, and 3.99% in 2B) (see Supplementary Table 2 and Fig. 1c) (Wilcoxon matched pairs test: 0B vs. 1B: $z = 3.27$, $P = 0.001$; 0B vs. 2B: $z = 2.19$, $P = 0.028$). However, we found no significant difference in satDNA content between the 1B and 2B libraries ($z = 0.27$, $P = 0.79$), perhaps due to some degree of B chromosome heterogeneity. Consistent with the general dilution effect for satDNA, abundance

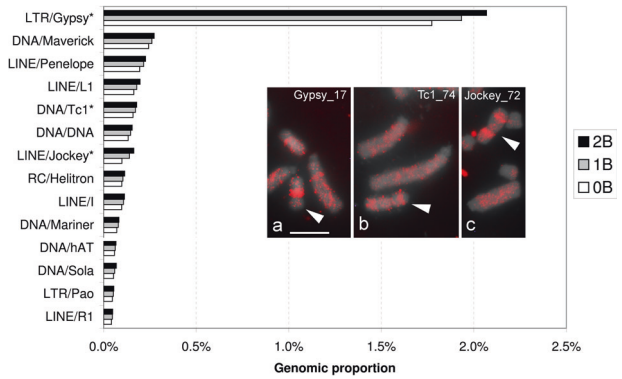

Fig. 2 Comparative genomic proportion between the 0B, 1B, and 2B genomes for the most abundant TEs in *Abracris flavolineata*. The asterisks indicate the superfamilies in which one representative was selected for FISH mapping on chromosomes (**a**–**c**). Note the spread distribution on long arms and absence of signals on pericentromeric C-heterochromatic region of A chromosomes. In the B chromosome (arrowheads) observe the differential distribution of TEs, i.e., first interstitial half of long arm (**a**), spread signal along the entire extension of the B chromosome, except distal regions (**b**) and enrichment on interstitial areas of both arms, and faint signals in proximal half of long arm (**c**). This last repeat was also absent in the terminal regions. Bar = 10 μm.

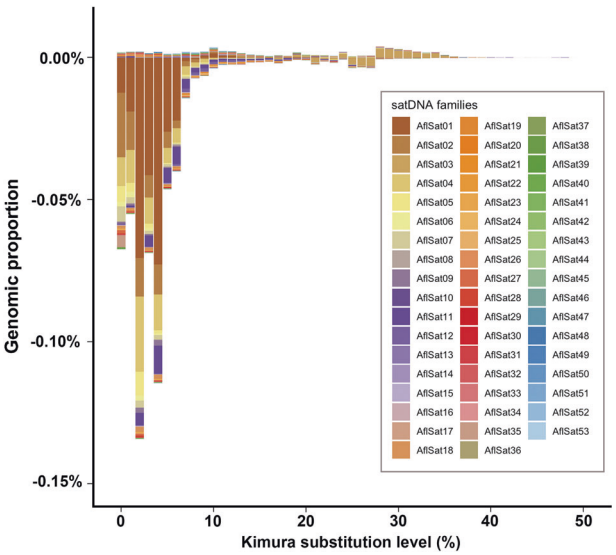

Fig. 3 Subtractive repetitive landscape (genome proportion versus sequence divergence based on Kimura substitution level) obtained from average counts for satDNAs in two males with 2B chromosomes and three with no B chromosome of *Abracris flavolineata*. Abundance values show the difference between the 2B minus the 0B genomes. Thus, positive values indicate overabundance in the 2B genomes, and negative values indicate overabundance in the 0B genomes. Note the occurrence of mainly negative values indicating the low enrichment of satDNAs in 2B-carrying genomes.

comparisons between libraries revealed that only two satDNA families (AflSat52-23 and AflSat53-17) were overabundant in the B-carrying genomes (see Table S2 and Fig. 1c).

The analysis of coding tandem repeats (including rRNA, U snRNA, and H3 histone multigene families) revealed that only the U2 snRNA family showed overabundance in the B-carrying genomes (Fig. 1d). The presence of U2 snDNA on the *A. flavolineata* B chromosome was previously shown by FISH analyses (Bueno et al. 2013; Menezes-de-Carvalho et al. 2015; Milani et al. 2017b). The remaining gene families and mtDNA failed to show differences in relative abundance between B-carrying and B-lacking genomes, but some of them displayed the dilution effect (Fig. 1d).

In the case of TEs, we found 212 elements (out of the 1744 analyzed) meeting the 1B/0B > 1 and 2B/0B > 1B/0B criteria. These elements belonged to 28 families (Supplementary Table 3), the most abundant being LTR/Gypsy elements (Fig. 2). To test whether these results actually reflect overabundance in the B chromosome, we performed FISH for one element belonging to three distinct superfamilies, LTR/Gypsy (Gypsy_17), DNA/Tc1 (Tc1_74), and LINE/Jockey (Jockey_72). This analysis revealed their concentration on certain B chromosome regions with the appearance of chromosome bands (Fig. 2). As these three families were among the seven most abundant, additional FISH work would reveal whether the observed pattern critically depends on abundance, a highly feasible possibility (see also Supplementary Figure 1).

High-throughput analysis of the satellitome reveals that satDNA is scarce on the B chromosome

One of the 53 satDNA families found (named here as AflSat02-391) had previously been described as AflaSAT-1 (Milani et al. 2017a). The repeat unit length (RUL) of the 53 families ranged from 7 to 832 bp (mean = 224, SD = 167.6), and the total A + T content ranged from 30.43% to 76.50% (mean = 57.1%, SD = 8%). Homology tests between all satDNA families revealed the occurrence of only two superfamilies (SFs), with AflSat15-299, AflSat16-298, and AflSat26-296 comprising SF1, and AflSat20-233 and AflSat28-247 constituting SF2. As expected, the families belonging to each SF showed highly similar sequence properties (RUL and A + T content) (Supplementary Table 2).

A subtractive landscape (2B/0B) revealed a clear dilution effect for satDNA abundance, as the 2B genome showed a high deficit for most satDNA families, especially for the most abundant ones (Fig. 3). To analyze whether these genomic results are reflected at the cytogenetic level, we performed the physical mapping by FISH on A and B chromosomes of *A. flavolineata* for all 53 satDNA families identified by bioinformatic analysis. Similar to other grasshopper species (for instance, see Ruiz-Ruano et al. 2016a, 2018), we observed three different patterns, with 44 families showing bands on chromosomes (B-pattern), three families showing many small dots scattered on chromosomes (D-pattern), and the six remainder showing no FISH signals (NS-pattern) (Table 1 and Supplementary Figure 2).

A summary of chromosome locations for the 53 satDNA families (Table 1) indicated that 47% of the 205 FISH bands found on A chromosomes were located on pericentromeric regions involving the centromere and the short chromosomal arm. The location of these satDNAs thus coincided with the heterochromatin location in this species, as revealed by C-banding (Bueno et al. 2013). However, the other half of the satDNA bands were found on euchromatic regions at proximal (5%), interstitial (30%), or distal (18%) locations of the long A chromosome arms (Table 1 and Supplementary Figure 2a-x). Notwithstanding, it is clear that the pericentric heterochromatic regions were enriched in satDNA as they contained the five most abundant families representing 81% of all satDNA content in the 0B genome (Supplementary Table 2) (i.e., 3.67% out of the total 4.52%) (Fig. 4, Supplementary Figure 2a, b, Table 1). Remarkably, of these five satDNAs, only the satDNA showing the highest abundance (AflSat01-179) was present on all A chromosomes (Fig. 4a, Table 1), thus most likely playing a centromeric function (Melters et al. 2013). However, the least abundant satDNA families tended to show FISH bands on a single chromosome pair (Fig. 4b, Supplementary Figure 2), as 15 of the 20 families with this condition showed abundance under the median value of all 53 families, and only 5 showed abundance above the median (Table 1). X was the A chromosome showing more satDNA FISH bands in exclusivity (three interstitially and three distally located), followed by S10 (4), M6 (3), L2 and M8 (2),

Table 1. Chromosome location of the 53 satDNA families found in *Abracris flavolineata*.

SatDNA family	Pattern	Chromosome pair and location												
		L1	L2	L3	M4	M5	M6	M7	M8	S9	S10	S11	X	B
AflSat01-179	B	p	p	p	p	p	p	p	p	p	p	p	p	p
AflSat02-391	B	p	p	p	p	p	p	p	p	p	p		p	p
AflSat03-17	B	p	p	p	p	p	p	p	p	p		p	p	p
AflSat04-161	B		p*	p		p	p	p		p		p		
AflSat05-437	B	p	p	p	p	p	p	p	p	p		p	p	
AflSat06-265	B	d	d	d	d	d	d	d	d	d			d	
AflSat07-36	B	i	i	i	i	i	i+d	i+d	i	p			i	p+d
AflSat08-184	D													
AflSat09-187	B			d	d	d	d				d		d	
AflSat10-297	B	p	p	p	p	p	p	p	p	p	p		p	
AflSat11-407	NS													
AflSat12-237	B					pr	pr				p	p		
AflSat13-177	D													
AflSat14-110	B	i		i	i			d*					i	
AflSat15-299/SF1	B	pr		pr										
AflSat16-298/SF1	B						pr							
AflSat17-231	B		i											
AflSat18-7	B	d	d	d	d	d	d	d					i	
AflSat19-17	NS													
AflSat20-233/SF2	B							pr	pr					
AflSat21-260	NS													
AflSat22-135	B	i	i	i	i	i		i		d		d	i	
AflSat23-286	B							p						
AflSat24-308	B								p					
AflSat25-40	B	p+i*	p+i	p+i	p+i	p+i	p+i	p+i	p+i+d	p	p		p+i	p+d
AflSat26-296/SF1	B						pr							
AflSat27-609	B			i										
AflSat28-247/SF2	B		i					i	i					
AflSat29-616	B										p			
AflSat30-197	B					d							d	
AflSat31-226	B						d							
AflSat32-429	B									d	p			
AflSat33-295	B						pr						i	
AflSat34-30	B		i*	i										
AflSat35-362	B										i			
AflSat36-41	NS													
AflSat37-134	B	i	i	i	i		i	i					pr	
AflSat38-377	B										p			
AflSat39-832	B		i											
AflSat40-218	B										d		i	p+i
AflSat41-186	B								p					
AflSat42-75	D													
AflSat43-131	B												i	
AflSat44-254	B										d			
AflSat45-414	NS													
AflSat46-153	B	p												p+d
AflSat47-75	B												d	
AflSat48-167	B												d	
AflSat49-138	B												d	
AflSat50-102	B												i	

Table 1 continued

SatDNA family	Pattern	Chromosome pair and location												
		L1	L2	L3	M4	M5	M6	M7	M8	S9	S10	S11	X	B
AflSat51-30	B												i	
AflSat52-23	B	p+i	p+i	p+i	p+i	p+i	p+i	p+i	p+i	p+i	p+i	p+i	p+i	p+d
AflSat53-17	NS													
Total (p)		8	8	8	7	8	8	9	9	9	9	6	7	8
Total (pr)		1	0	1	0	1	4	1	1	0	0	0	1	0
Total (i)		6	9	8	6	4	4	6	4	1	2	1	11	1
Total (d)		2	2	3	3	4	4	4	2	3	3	1	6	4
Total		17	19	20	16	17	20	20	16	13	14	8	25	13
Shared with B		7	6	6	6	6	6	6	6	6	5	3	7	–

SF = superfamily, L1–L3 = three long autosomes, M4–M8 = five medium autosomes, S9–S11 = three short autosomes, X = X chromosome, B = B chromosome, p = pericentromeric (centromere plus short chromosomal arms), pr = proximal (near to centromere), i = interstitial, d = distal. B = banded pattern, D = dotted pattern, and NS = no signal. Repeats with dotted patterns occurred on all chromosomes, including the B chromosome (see text for details). Asterisks (*) indicate the occurrence of heteromorphisms for the presence/absence of bands in homologous chromosomes.

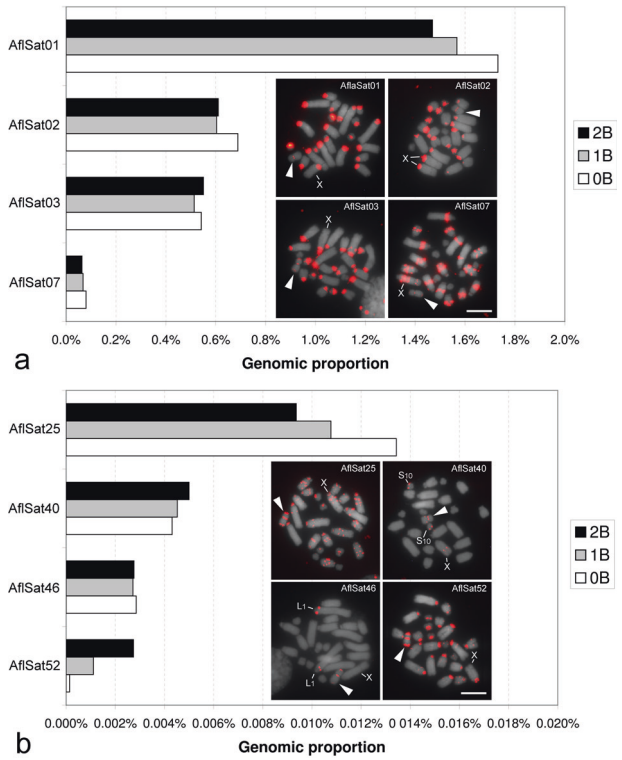

Fig. 4 Comparative genomic proportion and FISH mapping for eight satDNAs occurring in the B chromosomes with a banded pattern. SatDNAs showing high (**a**) or low (**b**) abundance (expressed as genome proportion). Repeat names are indicated on the left. Some A chromosomes are indicated on each embryo mitotic metaphase plate, and the B chromosome is indicated by arrowheads. The differential satDNA distribution on the B chromosome was observed, with pericentromeric signals for AflSat01 and AflSat02, pericentromeric plus distal signals for AflSat03, AflSat07, AflSat25, AflSat46, and AflSat52, and pericentromeric plus interstitial (on the long arm) signals for AfSat40. In addition, note the exclusive presence of AflSat46 bands on the B chromosome and the L1 pair. Bar = 10 µm.

and L3 and M7 (1). The X chromosome harbored the highest number of satDNA families (25) and it was the A chromosome showing the highest number of interstitial and distal satDNA bands (Table 1).

We noticed a clear-cut difference in chromosome location between the two superfamilies existing in the genome of *A. flavolineata*, as the three families belonging to SF1 always showed proximal locations on one (AflSat16-298 and AflSat26-296) or two (AflSat15-299) A chromosome pairs (Table 1, Supplementary Figure 2g,i,n), whereas the two SF2 family members showed either proximal (AflSat20-233) or interstitial (AflSat28-247) locations (Table 1, Supplementary Figure 2m,w).

Finally, there were nine other satDNA families where the location on A chromosomes was not in the form of FISH bands, three of which showed the dotted pattern (D) (Table 1, Supplementary Figure 3), and the six remaining showed no FISH signal at all (NS) (Table 1, Supplementary Figures 2y, 4).

Regarding the B chromosome, we observed that eight of the 44 satDNA families showing the B-pattern on A chromosomes (AflSat01-179, AflSat02-391, AflSat03-17, AflSat07-36, AflSat025-40, AflSat40-218, AflSat46-153, and AflSat52-23), were also present on the B chromosome, whereas the three families showing the D-pattern also showed multiple small dots on the B chromosome (Table 1 and Fig. 4, Supplementary Figure 3). Among the 13 satDNA bands observed on the B chromosome, eight were pericentromeric, one was interstitial and four were distal. Most of the eight satDNA families showing FISH bands on the B chromosome showed multichromosomal locations on A chromosomes, except two showing locations on only one (AflSat46-153 on L1) or two (AflSat40-218 on S10 and X) A chromosomes (Table 1 and Fig. 4b). Among all A chromosomes, L1 and X were the A chromosomes sharing the highest number of satDNA families with the B chromosome (seven each; see Table 1). Bearing in mind that L1 also shares the U2 snDNA in exclusivity with the B chromosome (Milani et al. 2017b), we consider that, with the available data (repetitive DNA only), L1 is the best candidate to be the ancestor of this B chromosome.

The satDNA families with dotted patterns occupied virtually the entire extension of the B chromosome, but AflSat08-184 and AflSat42-75 were less abundant on pericentromeric and terminal regions (Supplementary Figure 3a,c) whereas AflSat13-177 was less evident on the proximal region of the short arm (Supplementary Figure 3b). They also showed FISH signals on the euchromatic (non-C-banded) regions of the long arm of all A chromosomes, but they were absent in their C-banded regions located on the pericentromeric region and the short arm (Supplementary Figure 3).

A comparative analysis of abundance for the eight satDNA families displaying the B FISH pattern on the B chromosome revealed why the global abundance of satDNA in the 0B, 1B, and 2B genomes showed a dilution effect. For this purpose, we separately represented the most and the least abundant families

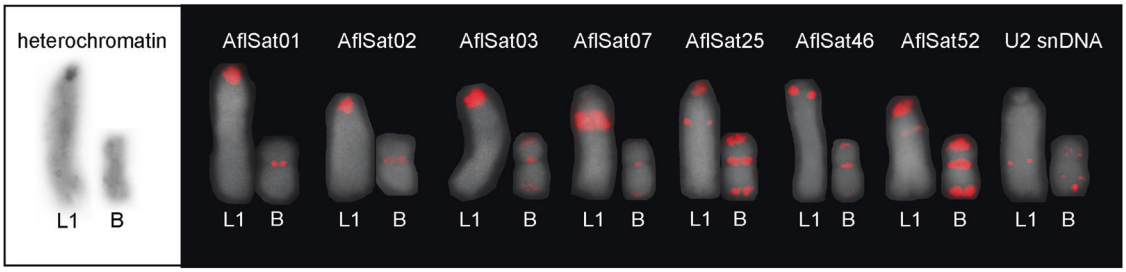

Fig. 5 Comparative C-banding and FISH for repeat location between the L1 and B chromosomes of *A. flavolineata*. The L1 autosome showed, like the remaining A chromosomes, a large pericentromeric C-band including the pericentromeric region and the short arm. The FISH analysis for seven satDNA families and the U2 snDNA repeat showed pericentromeric and telomeric locations on the B chromosome whereas they were located on the pericentromeric region and the short arm of L1 (AflSat01, AflSat02, AflSat03, the pericentromeric region (AflSat46), interstitial (AflSat07), interstitial region and the short arm (AflSat25 and AflSat52). satDNAs thus might suggest that B originates from the proximal third of L1, including the interstitial region containing several satDNAs. However, the U2 snDNA is located on an L1 region outside the former proximal region, so the presence of U2 on B is not explained by a single rearrangement event.

(Fig. 4), thus revealing that three families (AflSat01-179, AflSat07-36, and AflSat25-40) showed a clear decrease in abundance with an increasing number of B chromosomes, whereas only two (AflSat40-218 and AflSat52-23) showed the reverse pattern, due to B-enrichment, but these two satDNA families were among the least abundant in the genome.

DISCUSSION

Genome low-pass sequencing combined with computational and chromosomal analysis provides a comprehensive understanding of the organization and evolution of DNA repeats on B chromosomes (Kumke et al. 2016; Ruiz-Ruano et al. 2018; Milani et al. 2018; Ebrahimzadegan et al. 2019; Serrano-Freitas et al. 2019). Through this approach, we found that the B chromosome of the grasshopper *A. flavolineata* is poorly enriched in repetitive DNA. Only three of the 53 satDNA families found in this species (AflSat40-218, AflSat52-23, and AflSat53-17), which are among the less abundant in the 0B genome, were overabundant in B-carrying genomes. Likewise, only 28 TE families, containing 212 elements, representing only 12% of the 1744 TEs found, showed over-abundance in B-carrying genomes. This scenario contrasts with the general idea that B chromosomes are enriched in repetitive DNA (Camacho 2005; Houben et al. 2014; Marques et al. 2018). Consistently, repeat-enriched B chromosomes have been reported in fish (Ziegler et al. 2003; Coan and Martins 2018; Stornioli et al. 2021), reptiles (Kichigin et al. 2019), plants (Martis et al. 2012; Kumke et al. 2016; Ebrahimzadegan et al. 2019), and insects (Hanlon et al. 2018; Ruiz-Ruano et al. 2018). Among the repeats found in B chromosomes, satDNA is the most frequent component (McAllister 1995; Klemme et al. 2013; Hanlon et al. 2018; Ruiz-Ruano et al. 2018; Ebrahimzadegan et al. 2019; Langdon et al. 2000; Stornioli et al. 2021).

This accumulation of repetitive DNAs on B chromosomes is commonly assumed to be due to their genetic isolation from A chromosomes, with which they do not recombine (Camacho 2005; Houben et al. 2014). In this way, the nonenrichment in repetitive DNA, the absence of C-heterochromatin blocks, and the absence of B-specific satDNA families would be consistent with the hypothesis that this B is a young element, resembling the composition of the A chromosome from which it derived (most likely L1, see below). The high similarity between B and A chromosomes is also supported also by B chromosome micro-dissection of *A. flavolineata* followed by chromosome painting, as all C-negative A chromosome regions and the B chromosome were similarly labeled (Menezes-de-Carvalho et al. 2015).

Based on FISH mapping of the U2 snDNA, the B chromosome in *A. flavolineata* was suggested to have derived from the L1 autosome, as only these two chromosomes harbor this sequence (Bueno et al. 2013). Here, chromosomal mapping of the full satellitome of this species has provided additional clues about B chromosome ancestry and evolution. We observed that the L1 autosome and the X chromosome both share the highest number of satDNA families with the B chromosome, i.e., seven families. However, the absence of U2 on the X chromosome and the fact that the L1 autosome is the only A chromosome sharing AflaSat46-153 with the B chromosome, reinforce the conclusion that L1 is the most likely B ancestor. Although our data support the possible derivation of the B chromosome from the L1 autosome, with possible subsequent restructuring of the B chromosome, additional research is necessary to obtain accurate information on the possible synteny of the repeats shared by these chromosomes, as it would help to unveil the precise origin of the B chromosome. In addition, some repeats present on the L1 autosome were not found on the B chromosome, indicating some additional degree of B differentiation attributed to the intense dynamism of repetitive DNAs. Among grasshoppers, the origin of B chromosomes from large A chromosomes, as the current results suggest in *A. flavolineata* appears to be uncommon, as the few cases where B chromosome ancestry was claimed involved medium (M) or small (S) A chromosomes, such as S11 in *E. plorans* (Teruel et al. 2014), S8 in *E. monticola* (Ruiz-Ruano et al. 2016a), M8 and S9 in *L. migratoria* (Ruiz-Ruano et al. 2018), S9 in *S. rubiginosa*, S11 in *R. brasiliensis*, and S10 in *X. d. angulatus* (Milani et al. 2018). These medium- or small-sized A chromosomes are enriched in repetitive DNAs because their pericentromeric C-banded regions are the same size as the pericentromeric C-banded regions in long A chromosomes, but their non-C-banded regions are much smaller. Therefore, M and S chromosomes are more prone to be involved in chromosome rearrangements, which might be an initial step for B chromosome origin (Hewitt 1974; Perfectti and Werren 2001; Camacho 2005; Raskina et al. 2008; Houben et al. 2014; Ruiz-Ruano et al. 2016a; Milani et al. 2018). In *A. flavolineata*, the low amount of repeats on the B chromosome would be consistent with the low proportion of the C-banded region in L1 (see Fig. 5) and the loss of most of the C-banded chromatin in the B. In contrast, B derivation from medium or small A chromosomes with a lower proportion of non-C-banded chromatin should most likely render heterochromatic Bs, likewise in cases with B chromosome ancestry related to highly heterochromatic chromosomes, such as sex chromosomes (Sharbel et al. 1998; Pansonato-Alves et al. 2014; Ventura et al. 2015; Serrano-Freitas et al. 2019).

Remarkably, satDNAs displaying FISH bands on the *A. flavolineata* B chromosome frequently showed a symmetrical pattern for the FISH bands located on pericentromeric and distal regions, such as the U2 snDNA in both B chromosome arms (Fig. 5, Table 1), suggesting the isochromosome nature of this B chromosome and the involvement of centromeric misdivision in its origin. The small size of the FISH bands observed on the B chromosome for most

satDNA families (e.g., AflSat01-179, AflSat02-391, and AflSat03-17), would be consistent with the loss of the L1 short arm (which contains the largest amount of C-heterochromatin and satDNA families) during the B-forming misdivision. Isochromosomes arising from misdivision have been reported in grasshoppers such as *Eyprepocnemis plorans* (López-León et al. 1993), *Omocestus burri* (Del Cerro et al. 1994) and *Metaleptea brevicornis adspersa* (Grieco and Bidau 2000), plants such as *Zea mays* (Carlson and Phillips 1986), *Crepis capillaris* (Leach et al. 2005) and *S. cereale* (Marques et al. 2012), the fish *Astyanax scabripinnis* (Mestriner et al. 2000) and *Drosophila melanogaster* (Hanlon et al. 2018). Against the isochromosome hypothesis in *A. flavolineata* would be the B chromosome being not perfectly metacentric, as this would require additional events of inversion or differential duplications or deletions between B arms. More intense amplification of DNA repeats on one of the B chromosome arms has been noticed for TEs such as Gypsy_17, Tc1_74, and *Afmar2* (Palacios-Gimenez et al. 2014), and two satDNAs analyzed here (AflaSat07-36 and AflaSat40-218). This kind of event could have contributed to the emergence of the submetacentric B chromosome, which is currently prevalent in *A. flavolineata*. Notwithstanding, the evidence for L1 derivation of the B chromosome is still preliminary, as we all are still in the initial steps to disentangle the conundrum of B chromosome origin.

Altogether our results indicate that the B chromosome in *A. flavolineata* is unusually little enriched in repetitive DNAs, presumably because this B chromosome arose from the longest A chromosome, with a low proportion of C-heterochromatin, the most part of which was lost during the misdivision that yielded the B chromosome from the L1 autosome. The B chromosome is enriched in only a few repetitive elements, to a low extent, and the absence of B-specific satDNAs suggests that this B chromosome is young. This fact might be helpful in testing the L1-derivation hypothesis of the B chromosome, as a putatively young element could still conserve high similarity in gene content with its ancestor chromosome.

Data archiving

Genomes have been deposited at the Sequence Read Archive (SRA) under accession numbers SRX7784770–SRX7784772.

REFERENCES

Ahmad SF, Jehangir M, Cardoso AL, Wolf IR, Margarido VP, Cabral-de-Mello DC et al. (2020) B chromosomes of multiple species have intense evolutionary dynamics and accumulated genes related to important biological processes. BMC Genomics 21:656

Bidau CJ, Rosato M, Marti DA (2004) FISH detection of ribosomal cistrons and assortment-distortion for X and B chromosomes in *Dichroplus pratensis* (Acrididae). Cytogenet Genome Res 106:295–301

Bolger AM, Lohse M, Usadel B (2014) Trimmomatic: a flexible trimmer for Illumina sequence data. Bioinformatics 30:2114–2120

Bueno D, Palacios-Gimenez OM, Cabral-de-Mello DC (2013) Chromosomal mapping of repetitive DNAs in the grasshopper *Abracris flavolineata* reveal possible ancestry of the B chromosome and H3 histone spreading. PLoS ONE 8:e66532

Cabral-de-Mello DC, Marec F (2021) Universal fluorescence in situ hybridization (FISH) protocol for mapping repetitive DNAs in insects and other arthropods. Mol Genet Genomics 296:513–526

Cabrero J, López-León MD, Bakkali M, Camacho JPM (1999) Common origin of B chromosome variants in the grasshopper *Eyprepocnemis plorans*. Heredity 83:435–439

Cabrero J, López-León MD, Ruíz-Estévez M, Gómez R, Petitpierre E, Rufas JS et al. (2014) B1 was the ancestor B chromosome variant in the western Mediterranean area in the grasshopper *Eyprepocnemis plorans*. Cytogenet Genome Res 142:54–58

Camacho JPM (2005) B chromosomes. In: Gregory TR (ed) The evolution of the genome. Elsevier, San Diego, p 223–286

Carlson WR, Phillips RL (1986) The B chromosome of maize. Crit Rev Plant Sci 3:201–226

Cella MD, Ferreira A (1991) The cytogenetics of *Abracris flavolineata* (Orthoptera, Caelifera, Ommatolampinae, Abracrini). Rev Brasileira Genética 14:315–329

Coan RL, Martins C (2018) Landscape of transposable elements focusing on the B chromosome of the cichlid fish *Astatotilapia latifasciata*. Genes 9:269

Coleman JJ, Rounsley SD, Rodriguez-Carres M, Kuo A, Wasmann CC, Grimwood J et al. (2009) The genome of *Nectria haematococca*: contribution of supernumerary chromosomes to gene expansion. PLoS Genet 5:e1000618

Del Cerro AD, Fernández A, Santos JL (1994) Spreading synaptonemal complexes of B isochromosomes in the grasshopper *Omocestus burri*. Genome 37:1035–1040

Drummond AJ, Ashton B, Cheung M, Heled J, Kearse M (2009) Geneious v.4.8.5. Biomatters Ltd, Aukland, New Zealand

Ebrahimzadegan R, Houben A, Mirzaghaderi G (2019) Repetitive DNA landscape in essential A and supernumerary B chromosomes of *Festuca pratensis* Huds. Sci Rep. 9:1–11

Edgar RC (2004) MUSCLE: multiple sequence alignment with high accuracy and high throughput. Nucleic Acids Res 32:1792–1797

Felicetti D, Haerter CA, Baumgärtner L, Paiz LM, Takagui FH, Margarido VP et al. (2021) A new variant B chromosome in auchenipteridae: the role of $(GATA)_n$ and $(TTAGGG)_n$ sequences in understanding the evolution of supernumeraries in *Trachelyopterus*. Cytogenet Genome Res 161:70–81

Goubert C, Modolo L, Vieira C, ValienteMoro C, Mavingui P, Boulesteix M (2015) De novo assembly and annotation of the Asian tiger mosquito (*Aedes albopictus*) repeatome with dnaPipeTE from raw genomic reads and comparative analysis with the yellow fever mosquito (*Aedes aegypti*). Genome Biol Evol 7:1192–1205

Grabherr MG, Haas BJ, Yassour M, Levin JZ, Thompson DA, Amit I et al. (2011) Trinity: reconstructing a full-length transcriptome without a genome from RNA-Seq data. Nat Biotechnol 29:644

Grieco ML, Bidau CJ (2000) The dicentric nature of the metacentric B chromosome of *Metaleptea brevicornis adspersa* (Acridinae, acrididae). Heredity 84:639–646

Hahn C, Bachmann L, Chevreux B (2013) Reconstructing mitochondrial genomes directly from genomic next-generation sequencing reads—a baiting and iterative mapping approach. Nucleic Acids Res 41:e129–e129

Hanlon SL, Miller DE, Eche S, Hawley RS (2018) Origin, composition, and structure of the supernumerary B chromosome of *Drosophila melanogaster*. Genetics 210:1197–1212

Hewitt GM (1974) The integration of supernumerary chromosomes into the orthopteran genome. Cold Spring Harb symposia Quant Biol 38:183–194. Cold Spring Harbor Laboratory Press

Houben A, Banaei-Moghaddam AM, Klemme S, Timmis JN (2014) Evolution and biology of supernumerary B chromosomes. Cell Mol Life Sci 71:467–478

Jetybayev IY, Bugrov AG, Dzuybenko VV, Rubtsov NB (2018) B chromosomes in grasshoppers: different origins and pathways to the modern Bs. Genes 9:509

Jones RN (2017) New species with B chromosomes discovered since 1980. Nucleus 60:263–281

Jones RN, Rees H (1982) B chromosomes. Academic press

Kichigin IG, Lisachov AP, Giovannotti M, Makunin AI, Kabilov MR, O'Brien PC et al. (2019) First report on B chromosome content in a reptilian species: the case of *Anolis carolinensis*. Mol Genet Genomics 294:13–21

Klemme S, Banaei-Moghaddam AM, Macas J, Wicker T, Novák P, Houben A (2013) High-copy sequences reveal distinct evolution of the rye B chromosome. N. Phytol 199:550–558

Kumke K, Macas J, Fuchs J, Altschmied L, Kour J, Dhar MK et al. (2016) Plantago lagopus B chromosome is enriched in 5S rDNA-derived satellite DNA. Cytogenet Genome Res 148:68–73

Langdon T, Seago C, Jones RN, Ougham H, Thomas H, Forster JW, Jenkins G (2000) De novo evolution of satellite DNA on the rye B chromosome. Genetics 154:869–884

Leach CR, Houben A, Field B, Pistrick K, Demidov D, Timmis JN (2005) Molecular evidence for transcription of genes on a B chromosome in *Crepis capillaris*. Genetics 171:269–278

Li W, Godzik A (2006) Cd-hit: a fast program for clustering and comparing large sets of protein or nucleotide sequences. Bioinformatics 22:1658–1659

López-León MD, Cabrero J, Dzyubenko VV, Bugrov AG, Karamysheva TV, Rubtsov NB, Camacho JPM (2008) Differences in ribosomal DNA distribution on A and B chromosomes between eastern and western populations of the grasshopper *Eyprepocnemis plorans* plorans. Cytogenet Genome Res 121:260–265

López-León MD, Cabrero J, Pardo MC, Viseras E, Camacho JPM, Santos JL (1993) Generating high variability of B chromosomes in *Eyprepocnemis plorans* (grasshopper). Heredity 71:352–362

Loreto V, Cabrero J, López-León MD, Camacho JPM, Souza MJ (2008) Possible autosomal origin of macro B chromosomes in two grasshopper species. Chromosome Res 16:233–241

Malimpensa GC, Traldi JB, Toyama D, Henrique-Silva F, Vicari MR, Moreira-Filho O (2018) Chromosomal mapping of repeat DNA in *Bergiaria westermanni* (Pimelodidae, Siluriformes): localization of 45S rDNA in B chromosomes. Cytogenet Genome Res 154:99–106

Marques A, Klemme S, Guerra M, Houben A (2012) Cytomolecular characterization of de novo formed rye B chromosome variants. Mol Cytogenet 5:34

Marques A, Klemme S, Houben A (2018) Evolution of plant B chromosome enriched sequences. Genes 9:515

Martis MM, Klemme S, Banaei-Moghaddam AM, Blattner FR, Macas J, Schmutzer T et al. (2012) Selfish supernumerary chromosome reveals its origin as a mosaic of host genome and organellar sequences. Proc Natl Acad Sci USA 109:13343–13346

McAllister BF (1995) Isolation and characterization of a retroelement from B chromosome (PSR) in the parasitic wasp *Nasonia vitripennis*. Insect Mol Biol 4:253–262
Melters DP, Bradnam KR, Young HA, Telis N, May MR, Ruby JG et al. (2013) Comparative analysis of tandem repeats from hundreds of species reveals unique insights into centromere evolution. Genome Biol 14:R10
Menezes-de-Carvalho NZ, Palacios-Gimenez OM, Milani D, Cabral-de-Mello DC (2015) High similarity of U2 snDNA sequence between A and B chromosomes in the grasshopper *Abracris flavolineata*. Mol Genet Genomics 290:1787–1792
Mestriner CA, Galetti PM, Valentini SR, Ruiz IR, Abel LD, Moreira-Filho O, Camacho JPM (2000) Structural and functional evidence that a B chromosome in the characid fish *Astyanax scabripinnis* is an isochromosome. Heredity 85:1–9
Milani D, Bardella VB, Ferretti AB, Palacios-Gimenez OM, Melo ADS, Moura RC et al. (2018) Satellite DNAs unveil clues about the ancestry and composition of B chromosomes in three grasshopper species. Genes 9:523
Milani D, Cabral-de-Mello DC (2014) Microsatellite organization in the grasshopper *Abracris flavolineata* (Orthoptera: Acrididae) revealed by FISH mapping: remarkable spreading in the A and B chromosomes. PLoS ONE 9:e97956
Milani D, Palacios-Gimenez OM, Cabral-de-Mello DC (2017b) The U2 snDNA is a useful marker for B chromosome detection and frequency estimation in the grasshopper *Abracris flavolineata*. Cytogenet Genome Res 151:36–40
Milani D, Ramos É, Loreto V, Martí DA, Cardoso AL, de Moraes KCM et al. (2017a) The satellite DNA AflaSAT-1 in the A and B chromosomes of the grasshopper *Abracris flavolineata*. BMC Genet 18:81
Montiel EE, Cabrero J, Ruiz-Estévez M, Burke WD, Eickbush TH, Camacho JPM, López-León MD (2014) Preferential occupancy of R2 retroelements on the B chromosomes of the grasshopper *Eyprepocnemis plorans*. PLoS ONE 9:e91820
Navarro-Dominguez B, Ruiz-Ruano FJ, Cabrero J, Corral JM, LópezLeón MD, Sharbel TF, Camacho JPM (2017) Protein-coding genes in B chromosomes of the grasshopper *Eyprepocnemis plorans*. Sci Rep. 7:45200
Novák P, Neumann P, Pech J, Steinhaisl J, Macas J (2013) RepeatExplorer: a galaxy-based web server for genome-wide characterization of eukaryotic repetitive elements from next-generation sequence reads. Bioinformatics 29:792–793
Nur U, Werren JH, Eickbush DG, Burke WD, Eickbush TH (1988) A "selfish" B chromosome that enhances its transmission by eliminating the paternal genome. Science 240:512–514
Oliveira NL, Cabral-de-Mello DC, Rocha MF, Loreto V, Martins C, Moura RC (2011) Chromosomal mapping of rDNAs and H3 histone sequences in the grasshopper *Rhammatocerus brasiliensis* (Acrididae, Gomphocerinae): extensive chromosomal dispersion and co-localization of 5S rDNA/H3 histone clusters in the A complement and B chromosome. Mol Cytogenet 4:24
Palacios-Gimenez OM, Bueno D, Cabral-De-Mello DC (2014) Chromosomal mapping of two Mariner-like elements in the grasshopper *Abracris flavolineata* (Orthoptera: Acrididae) reveals enrichment in euchromatin. Eur J Entomol 111:329–334
Pansonato-Alves JC, Serrano ÉA, Utsunomia R, Camacho JPM, da Costa Silva GJ, Vicari MR et al. (2014) Single origin of sex chromosomes and multiple origins of B chromosomes in fish genus *Characidium*. PLoS ONE 9:e107169
Peng SF, Cheng YM (2011) Characterization of satellite CentC repeats from heterochromatic regions on the long arm of maize B-chromosome. Chromosome Res 19:183–191
Perfectti F, Werren JH (2001) The interspecific origin of B chromosomes: experimental evidence. Evolution 55:1069–1073
Poletto AB, Ferreira IA, Martins C (2010) The B chromosomes of the African cichlid fish *Haplochromis obliquidens* harbour 18S rRNA gene copies. BMC Genet 11:1
Raskina O, Barber JC, Nevo E, Belyayev A (2008) Repetitive DNA and chromosomal rearrangements: speciation-related events in plant genomes. Cytogenet Genome Res 120:351–357
Ruiz-Ruano FJ, Cabrero J, López-León MD, Camacho JPM (2016a) Satellite DNA content illuminates the ancestry of a supernumerary (B) chromosome. Chromosoma 126:487–500
Ruiz-Ruano FJ, Cabrero J, López-León MD, Sánchez A, Camacho JPM (2018) Quantitative sequence characterization for repetitive DNA content in the supernumerary chromosome of the migratory locust. Chromosoma 127:45–57
Ruiz-Ruano FJ, López-León MD, Cabrero J, Camacho JPM (2016b) High-throughput analysis of the satellitome illuminates satellite DNA evolution. Sci Rep 6:28333
Sambrook J, Russell DW (2001) Molecular cloning. Sambrook Russe 1(2):3. Cold Springs Harbour Laboratory Press
Schmieder R, Edwards R (2011) Fast identification and removal of sequence contamination from genomic and metagenomic datasets. PLoS ONE 6:e17288
Serrano-Freitas ÉA, Silva DM, Ruiz-Ruano FJ, Utsunomia R, Araya-Jaime C, Oliveira C et al. (2019) Satellite DNA content of B chromosomes in the characid fish *Characidium gomesi* supports their origin from sex chromosomes. Mol Genet Genomics 295:195–207
Sharbel TF, Green DM, Houben A (1998) B-chromosome origin in the endemic New Zealand frog *Leiopelma hochstetteri* through sex chromosome devolution. Genome 41:14–22
Silva DMDA, Pansonato-Alves JC, Utsunomia R, Araya-Jaime C, Ruiz-Ruano FJ, Daniel SN et al. (2014) Delimiting the origin of a B chromosome by FISH mapping, chromosome painting and DNA sequence analysis in *Astyanax paranae* (Teleostei, Characiformes). PLoS ONE 9:e94896
Smit AFA, Hubley R, Green P (2017) RepeatMasker Open-4.0. http://www.repeatmasker.org
Stornioli JHF, Goes CAG, Calegari RM, dos Santos RZ, Giglio LM, Foresti F et al. (2021) The B chromosomes of *Prochilodus lineatus* (Teleostei, Characiformes) are highly enriched in satellite DNAs. Cells 10:1527
Teruel M, Ruiz-Ruano FJ, Marchal JA, Sánchez A, Cabrero J, Camacho JPM, Perfectti F (2014) Disparate molecular evolution of two types of repetitive DNAs in the genome of the grasshopper *Eyprepocnemis plorans*. Heredity 112:531–542
Untergasser A, Cutcutache I, Koressaar T, Ye J, Faircloth BC, Remm M, Rozen SG (2012) Primer3—new capabilities and interfaces. Nucleic Acids Res 40:e115–e115
Valente GT, Conte MA, Fantinatti BEA, Cabral-de-Mello DC, Carvalho RF, Vicari MR, Kocher TD, Martins C (2014) Origin and evolution of B chromosomes in the cichlid fish *Astatotilapia latifasciata* based on integrated genomic analyses. Mol Biol Evol 31:2061–2072
Ventura K, O'Brien PCM, do Nascimento Moreira C, Yonenaga-Yassuda Y, Ferguson-Smith MA (2015) On the origin and evolution of the extant system of B chromosomes in *Oryzomyini* radiation (Rodentia, Sigmodontinae). PLoS ONE 10: e0136663
Webb GC, White MJD, Contreras N, Cheney J (1978) Cytogenetics of the parthenogenetic grasshopper *Warramaba* (formely *Moraba*) *virgo* and its bisexual relatives. IV. Chromosome banding studies. Chromosoma 67:309–339
Wilson EB (1907) The supernumerary chromosomes of Hemiptera. Sci NY 26:870–871
Ziegler CG, Lamatsch DK, Steinlein C, Engel W, Schartl M, Schmid M (2003) The giant B chromosome of the cyprinid fish *Alburnus alburnus* harbours a retrotransposon-derived repetitive DNA sequence. Chromosome Res 11:23–35

ACKNOWLEDGEMENTS

We acknowledge the three anonymous reviewers for helpful comments that contributed significantly to improve the manuscript. This study was financed in part by the Coordenação de Aperfeiçoamento de Pessoal de Nível Superior—Brasil (CAPES), by Fundação de Amparo à Pesquisa do Estado de São Paulo (FAPESP) (process numbers 2014/11763-8 and 2015/16661-1), and Conselho Nacional de Desenvolvimento Científico e Tecnológico (CNPq). DCC-d-M is a recipient of a research productivity fellowship from the Conselho Nacional de Desenvolvimento Científico e Tecnológico-CNPq (process number 308290/2020-8). FJRR hold posdoctoral fellowships from Junta de Andalucía fellowship (Spain), Sven och Lilly Lawskis fond (Sweden), and a Marie Skłodowska-Curie Individual Fellowship (grant agreement 875732, European Commission).

AUTHOR CONTRIBUTIONS

DM and DCC-d-M conceived the study; DM and FJRR performed the bioinformatic analysis; DM performed the chromosomal analysis; DM, FJRR, JPMC, and DCC-d-M performed formal data analysis and wrote the paper; DCC-d-M led the project management. All authors read and approved the manuscript..

COMPETING INTERESTS

The authors declare no competing interests.

ADDITIONAL INFORMATION

Supplementary information The online version contains supplementary material available at https://doi.org/10.1038/s41437-021-00470-5.

Correspondence and requests for materials should be addressed to Diogo C. Cabral-de-Mello.

4.3. Chapter 3

Single origin and high molecular differentiation of the B chromosome in the grasshopper Abracris flavolineata revealed by cytogenomic population analysis

Diogo Milani, Ana Elisa Gasparotto, Vilma Loreto, Dardo A. Martí and Diogo C. Cabral-de-Mello

Manuscript under review in *Gene*

Gene

Single origin and high molecular differentiation of the B chromosome in the grasshopper Abracris flavolineata revealed by cytogenomic population analysis

--Manuscript Draft--

Manuscript Number:	GENEJOURNAL-D-21-03383
Article Type:	Research paper
Keywords:	FISH; genome; population; repetitive DNAs; supernumerary chromosome
Corresponding Author:	Diogo Cavalcanti Cabral-de-Mello, PhD Sao Paulo State University Julio de Mesquita Filho: Universidade Estadual Paulista Julio de Mesquita Filho Rio Claro, São Paulo BRAZIL
First Author:	Diogo Milani
Order of Authors:	Diogo Milani
	Ana Elisa Gasparotto
	Vilma Loreto
	Dardo A Martí
	Diogo Cavalcanti Cabral-de-Mello
Manuscript Region of Origin:	BRAZIL
Abstract:	Additional supernumerary chromosomes (B) have been an interesting subject of study since the past century. However, our understanding of the molecular differentiation of B chromosomes from an interpopulation point of view is poor, and in most cases, analysis is limited to chromosome banding and mapping of few sequences. To gather novel information regarding the molecular composition, origin, and evolution of B chromosome polymorphisms, we performed an integrative cytogenetic and next-generation sequencing (NGS) analysis of the repeatome in the grasshopper Abracris flavolineata from different populations. Our results revealed the occurrence of B chromosomes in two newly studied populations and the description of new satDNAs in A. flavolineata. Although we observed low geographical differentiation among the populations of A. flavolineata, our comparative analysis of B-lacking and B-carrying genomes provides evidence of two new variants of B chromosomes, presenting different compositions of distinct classes of repeats (TEs, satDNAs, and multigene families), as a consequence of the high dynamics of the B chromosomes. Based on some shared repeats, their chromosomal location and C-positive heterochromatin content on the B chromosome, these variants putatively have a single origin followed by distinct molecular differentiation, presenting distinct stages of heterochromatinization. Our data provides a detailed example of how dynamic and differentiated could be the molecular content of the B chromosomes at interpopulation level, even when they have a single origin.
Suggested Reviewers:	Eva Satovic, Dr Ruder Boskovic Institute Eva.Satovic@irb.hr Specialist in invertebrate molecular cytogenetics, specially on satellite DNAs
	Eugenia Montiel, Dr Universidad de Jaen Campus de las Lagunillas: Universidad de Jaen emontiel@ujaen.es Specialist on B chromosomes and molecular cytogenetics of grasshoppers
	Vladimir Trifonov, Dr Institute of Molecular and Cellular Biology SB RAS vlad@mcb.nsc.ru Specialist on evolution of B chromosomes
	Andreas Houben, Dr Leibniz Institute of Plant Genetics and Crop Plant Research (IPK)

	houben@ipk-gatersleben.de Specialist on evolution of B chromosomes
	Alexandr Sember, Dr Institute of Animal Physiology and Genetics, Academy of Sciences of the Czech Republic (ASCR) sember@iapg.cas.cz specialist on repetitive DNA evolution
Opposed Reviewers:	

unesp
UNIVERSIDADE ESTADUAL PAULISTA
"JÚLIO DE MESQUITA FILHO"
Instituto de Biociências - Câmpus de Rio Claro

Rio Claro, October 18, 2021

Dear Dr. Andre Van Wijnen:

We hope you will consider our manuscript entitled "Single origin and high molecular differentiation of the B chromosome in the grasshopper *Abracris flavolineata* revealed by cytogenomic population analysis" for publication in *GENE*. The study is transformational, makes novel discoveries, and reports findings about molecular population dynamics of B chromosomes that will be of interest to the broad scientific readership of the journal as well as the general public that is interested in B chromosome evolution. Recently, with the approaches of genomic era the studies of B chromosome gained high visibility in literature as this genomic element was reported across almost all eukaryotes and could influence the structure/evolution of genomes.

Each of the authors confirms that this manuscript has not been previously published and is not currently under consideration by any other journal. Additionally, all of the authors have approved the contents of this paper and have agreed to the journal's submission policies. If you feel that the manuscript is appropriate for your journal, we suggest the following associate editors to handle the submission:

Editor 1: Dr. David Ray
Editor 2: Dr. Miroslav Plohl

To the best of our knowledge, none of the above-suggested persons have any conflict of interest, financial or otherwise.

Sincerely yours,

Diogo C. Cabral-De-Mello (on behalf of all authors)

Dr. Diogo C. Cabral-de-Mello
Associated professor
São Paulo State University
São Paulo/Brazil

Single origin and high molecular differentiation of the B chromosome in the grasshopper *Abracris flavolineata* revealed by cytogenomic analysis

Diogo Milani[1], Ana Elisa Gasparotto[1], Vilma Loreto[2], Dardo A Martí[3], Diogo C Cabral-de-Mello[1,*]

[1]UNESP - Univ Estadual Paulista, Instituto de Biociências/IB, Departamento de Biologia Geral e Aplicada, Rio Claro, São Paulo, Brazil

[2]Departamento de Genética, UFPE - Univ Federal de Pernambuco, Centro de Biociências/CB, Recife, Pernambuco, Brazil

[3]IBS - UNaM – CONICET, Posadas, Misiones, Argentina

*_Corresponding author:_ UNESP - Univ Estadual Paulista, Instituto de Biociências/IB, Departamento de Biologia Geral e Aplicada, 13506-900 Rio Claro, SP, Brazil Phone/Fax: 55 19 35264152. E-mail: cabral.mello@unesp.br

Abstract

Additional supernumerary chromosomes (B) have been an interesting subject of study since the past century. However, our understanding of the molecular differentiation of B chromosomes from an interpopulation point of view is poor, and in most cases, analysis is limited to chromosome banding and mapping of few sequences. To gather novel information regarding the molecular composition, origin, and evolution of B chromosome polymorphisms, we performed an integrative cytogenetic and next-generation sequencing (NGS) analysis of the repeatome in the grasshopper *Abracris flavolineata* from different populations. Our results revealed the occurrence of B chromosomes in two newly studied populations and the description of new satDNAs in *A. flavolineata*. Although we observed low geographical differentiation among the populations of *A. flavolineata,* our comparative analysis of B-lacking and B-carrying genomes provides evidence of two new variants of B chromosomes, presenting different compositions of distinct classes of repeats (TEs, satDNAs, and multigene families), as a consequence of the high dynamics of the B chromosomes. Based on some shared repeats, their chromosomal location and C-positive heterochromatin content on the B chromosome, these variants putatively have a single origin followed by distinct molecular differentiation, presenting distinct stages of heterochromatinization. Our data provides a detailed example of how dynamic and differentiated could be the molecular content of the B chromosomes at interpopulation level, even when they have a single origin.

Keywords: FISH, genome, population, repetitive DNAs, supernumerary chromosome

Introduction

Supernumerary chromosomes (B) are extra and dispensable elements in the karyotype of some eukaryote species, which, in most cases, do not confer any advantage and in low number do not interfere with the normal development of the individuals (Camacho et al., 2000; Houben et al., 2014; Jones, 2017). A curious aspect of many B chromosomes is their higher rates of transmission in comparison to A chromosomes, not obeying the Mendelian law of segregation, which causes accumulation (Houben et al., 2014; Jones, 1995). Moreover, the B chromosomes do not recombine with A chromosomes, following their own evolutionary pathway with the accumulation of specific mutations and distinct sequences, such as repetitive DNA, ultimately resulting in their molecular differentiation (Beukeboom, 1994; Camacho, 2005; Trifonov et al., 2013; Houben et al., 2014; Valente et al., 2014).

At the population level, B chromosomes are highly variable in frequency among individuals, number per individual, morphology, size, and composition. Different types of B chromosomes can coexist in the same species, as observed in the plants *Brachycome dichromosomatica* (Houben et al., 1999) and *Secale cereale* (Marques et al., 2012), the fish *Prochilodus lineatus* (Cavallaro et al., 2000), the deer *Mazama nana* (Abril et al., 2008), and the frog *Gastrotheca espeletia* (Schmid et al., 2002). One case of extreme B chromosome polymorphism, i.e. occurrence of B variants, has been described in the grasshopper *E. plorans*, in which more than 50 variants were observed, presenting different sizes and banding patterns in multiple populations (López-León et al., 1993; Bakkali et al., 1999).

Although variations of B chromosomes among populations have been well documented in some species, the specific molecular composition of Bs among

populations is not well known, with the polymorphism described mostly by classical cytogenetic and chromosome banding. Moreover, some studies have applied DNA sequencing and/or molecular analysis of B chromosomes to obtain information about the origin, composition, and evolution of B variants based on few chromosomal markers (Jin et al., 2005; Martis et al., 2012; Valente et al., 2014; Ruiz-Ruano et al., 2016a; Milani et al., 2021). In the *Moenkhausia sanctaefilomenae* fish, two B chromosome variants differed in their C-banding patterns, frequency, and abundance of repeats (Utsunomia et al., 2016). For the *Xyleus discoideus angulatus* grasshopper, at least three variants have been reported in different populations (Bernardino et al., 2017) and a comparative analysis of micro B and macro B in the Korean field mouse *Apodemus peninsulae* from different populations revealed different DNA compositions based on chromosome painting experiments (Rubtsov et al., 2014). Although DNA sequence-based studies have helped to elucidate the origin and evolution of B chromosomes, a detailed understanding of the molecular differentiation of B chromosomes at the population level has yet to be obtained.

The grasshopper *Abracris flavolineata* from Rio Claro/São Paulo, Brazil population harbors an intriguing C-negative B chromosome not enriched in highly copy repeats (Milani et al., 2021). This differs from most B chromosomes, which are generally repeated-enriched (Camacho, 2005; Houben et al., 2014). These findings suggest that the B chromosome of *A. flavolineata* is young and is in an early stage of heterochromatinization. To improve our understanding of the molecular composition, origin, and evolution of the B chromosome of *A. flavolineata*, and the patterns of molecular differentiation of B chromosomes at interpopulation level, we studied this polymorphism in three additional geographically distant populations, focusing mainly on the analysis of repeats on this element and their differentiation. In this way, we

101 studied B chromosome frequency and characterized the repeatome of B chromosomes
102 using a combination of bioinformatic and cytogenetic approaches. We observed the
103 occurrence of B chromosomes in two newly studied populations and observed the
104 occurrence of undescribed satDNA in *A. flavolineata* genome. Our comparative analysis
105 provides evidence of two new variants of B chromosomes in *A. flavolineata*, presenting
106 different compositions of distinct classes of repeats (TEs, satDNA, and multigene
107 families). Some shared repetitive DNAs, their chromosomal locations and C-positive
108 heterochromatin content, suggests that these variants were putatively have a single
109 origin, followed by distinct intense molecular differentiation, presenting distinct stages
110 of heterochromatinization and accumulation of repeats.
111
112 **Materials and Methods**
113 ***Biological material, chromosome preparations, and classical cytogenetic techniques***
114 Adult animals of *A. flavolineata* were collected at three distinct localities in Brazil (BR),
115 including Rio Claro/São Paulo (SP) at 22°24'45"S; 47°31'28"W (37 individuals), Cabo
116 de Santo Agostinho/Pernambuco (PE) at 8°17’15’’S; 35°2’7’’W (19 individuals), and
117 Santa Bárbara do Pará/Pará (PA) at 1°13’27’’S; 48°17’38’’W (76 individuals), as well
118 as in Argentine, at Posadas/Misiones (ARG) at 27°25’S; 55°56’W (14 individuals). The
119 testes were dissected from anesthetized animals, fixed in 3:1 absolute ethanol:glacial
120 acetic acid, and stored at −20°C for chromosomal analysis. Entire animals were
121 immersed in absolute ethanol and stored at −20°C for genomic DNA (gDNA)
122 extraction.
123 Chromosome spreads were performed by maceration and spreading of testis
124 follicles in a drop of 50% acetic acid on a slide under a hot plate at 45°C. For
125 conventional analysis and counting of B chromosome presence, the chromosomes were

stained with Giemsa 5%. Individuals harboring B chromosomes were selected for subsequent classic and molecular cytogenetic assays. Heterochromatin distribution was analyzed by C-banding, as described by Sumner (1972). Genomic DNA was extracted from the hind legs using the Wizard Genomic DNA Purification Kit (Promega, WI, USA), according to the manufacturer's instructions.

Genome sequencing and obtaining the repetitive DNA library

For genome sequencing, we selected individuals from populations that presented B chromosomes, which included PE, ARG, and SP. For the SP population, we used sequenced genomes available in Sequence Read Achieve (SRA) under accession numbers SRR11148657 (B-lacking, 0B) and SRR11148656 (B-carrying, +1B). These genomes were sequenced by our group using the Illumina HiSeq 4000 platform (Macrogen Inc., Seoul, Republic of Korea) with a read length of 151 bp (Ahmad et al., 2020; Milani et al., 2021). For the other two populations, that is, PE and ARG, we sequenced one male individual lacking the B chromosome and one male individual carrying one B chromosome of each population. Sequencing was performed using the Illumina HiSeq 4000 platform in Macrogen, with a read length of 101 bp. These raw data were deposited on SRA under the accession numbers SAMN23009930-SAMN23009933.

The repetitive DNA library of *A. flavolineata* used in our analysis was previously characterized by Milani et al. (2021), including 53 satDNA families, 1,744 TE elements, and some multigene families (H3 histone gene, 18S, 28S, 5.8S, and 5S rDNAs, U1, U2, and U6 snDNAs). To recover possible satDNA families from PE and ARG that were not detected before the SP population by Milani et al. (2021), we also applied the satMiner protocol (Ruiz-Ruano et al., 2016b) using both genomes mixed

(0B and +1B) from these populations separately. In this way, we pre-processed the reads following the same steps as Milani et al. (2021), resulting in trimmed, completed, high-quality filtered (Q < 20) paired reads in fasta format, ready for use as an input in the RepeatExplorer round series of satMiner protocol. As previously mentioned, the two populations (PE and ARG) were analyzed separately, consisting of 100,000 read pairs of each genome (0B and +1B), resulting in 200,000 read pairs. Consecutive rounds were prepared by adding 100,000 more read pairs of each genome (0B and +1B) in each round until no satDNA families were found (Ruiz-Ruano et al., 2016b). The identified families of tandem repeats, specifically satDNAs in the RepeatExplorer report in both populations were analyzed using Geneious v4.8 software (Drummond et al., 2009), checking if they presented a tandem structure by dotplot analysis. Next, we ran a homology test based on RepeatMasker (Smit et al., 2017) with "rm_homology.py" (https://github.com/fjruizruano/ngs-protocols) to ensure that these satDNA families were not the same as previously reported (Milani et al., 2021).

Estimating the B chromosome repetitive DNA content of* A. flavolineata *among the different populations

The sequence abundance of each repetitive DNA family was determined in each B-lacking and B-carrying genome of each population using RepeatMasker software (Smit et al., 2017). Likewise, with RepeatMasker, the divergence of each of these repeats was estimated using the Kimura 2-parameter (K2P) model, which is generally applied for this estimation (Ruiz-Ruano et al., 2016b, 2018; Coan and Martins, 2018; Milani et al., 2021). Since a set of satDNA families were already described in *A. flavolineata* by Milani et al. (2021) and named according to Ruiz-Ruano et al. (2016b), following the decreasing order of abundance in the genome of individuals with standard karyotype, i.e. 0B, the new satDNA families found in the other two populations (PE and

ARG) were named separately with a new list order, considering decreasing in abundance. All satDNA families, including the previously described in SP population, were tagged with the initials belonging to the respective population where the satDNA was firstly discovered (for example, Afl_SPSat, Afl_PESat, and Afl_ARGSat). For the SP population that was obtained from tree B-lacking genomes (0B) and two 1B-carrying genomes (+1B), the abundance and divergence for each repetitive family were separately averaged for 0B (three individuals) and +1B (two individuals) genomes using the same number of reads as described by Milani et al. (2021) (5,000,000 read pairs from each library). Finally, the abundance of a given repetitive DNA family in each genome library was calculated as a genome proportion, represented by the sum of all nucleotides belonging to it with respect to the total number of nucleotides in the selected reads. To check for possible overabundance of repeats in the genomes harboring B chromosomes and to compare these results between the populations, we calculated the sequence abundance quotients between +1B/0B genomes from individuals belonging to the same population. Repeats with proportion +1B/0B > 1 were considered overabundant in the +1B genomes.

PCR amplification and chromosomal mapping of repetitive DNAs

For polymerase chain reaction (PCR) amplification, we used the primer sets described by Milani et al. (2021). Primers for sequences described for the first time here were designed manually or using Primer3 software (Untergasser et al., 2012) (Supplementary Table 1). PCR amplification was conducted following the conditions described by Milani et al. (2018). PCR products were visualized on a 1% agarose gel and bands were isolated and purified using the Zymoclean™ Gel DNA Recovery Kit (Zymo Research Corp., The Epigenetics Company, CA, USA) according to the

manufacturer's instructions, taking care to isolate fragments with the expected size by computational analysis. For satDNA, monomeric bands were isolated using the same purification kit. All products were re-amplified using the same PCR conditions for subsequent fluorescence *in situ* hybridization (FISH) experiments.

We used five previously described repeats in *A. flavolineata*, including the U2 snDNA gene, two satDNA families AflSat01-179 and AflSat52-23, and two TEs LINE/Jockey_72 and LTR/Gypsy_17. The two satDNAs Afl_SPSat01-179 and Afl_SPSat52-23 were chosen because one is the most abundant in the species and the other is the lowest abundant with FISH banded pattern, occurring in all A chromosomes, and in addition to the B chromosome with evident blocks (see Milani et al., 2021). The U2 snDNA is a B chromosome marker for the SP population, occurring in four clusters in the B chromosome (Bueno et al., 2013). Both the LINE/Jockey_72 and LTR/Gypsy_17 showed evident signals on the B chromosome of individuals from SP, presenting different banding patterns (Milani et al., 2021). In addition, we mapped five other repeats to check their organization by chromosomal mapping of the B chromosome between populations. Among the five repeats chosen, two were satDNAs and three were TEs. For the TEs, we selected the three highest elements that presented abundance quotients 1B/0B > 1 in each of the three populations, and we selected families from PE and ARG populations based on the same criteria of overabundance in +1B genomes, one satDNA per population. In this way, we were able to map highly overabundant repeats on +B genomes with a high chance of obtaining B chromosome candidate markers, allowing evolutionary tracking of this element.

We mapped the ten repeats by FISH on meiotic metaphase chromosome spreads, using one or two probes simultaneously, following the protocol described by Cabral-de-Mello and Marec (2021). All probes were labeled with digoxigenin-11-dUTP (Roche,

227 Mannheim, Germany) or biotin-14-dATP (Invitrogen) and detected using anti-
228 digoxigenin-rhodamine (Roche) and streptavidin and Alexa Fluor 488-conjugated
229 (Invitrogen), respectively. After probe detection, the slides were counterstained using
230 4',6-diamidino-20-phenylindole (DAPI) and mounted in VECTASHIELD (Vector,
231 Burlingame, CA, USA). The images were captured using a BX61 Olympus microscope
232 equipped with a fluorescence lamp, appropriate filters, and a DP70 cooled digital
233 camera. The images were edited using Adobe Photoshop CS6.
234
235 ***mtDNA haplotype network***
236 To understand the genetic connection between the populations, we reconstructed
237 a haplotype network based on a fragment of the cytochrome c oxidase subunit I (COI)
238 gene from 54 individuals, 13 from SP, 13 from PE, 15 from PA, and 13 from ARG. COI
239 was amplified using primers A2442 and S1718 (Normark, 1996). The PCR products
240 were sequenced by the Sanger method using the service of Macrogen Inc. and analyzed
241 using Geneious v4.8.5 software (Drummond et al., 2009). Then, DNA polymorphism
242 and haplotype recognition were analyzed using the DnaSP v.5.10.01 tool (Librado and
243 Rozas, 2009), and a graphical haplotype network was constructed employing Network
244 4.6.1.2 software (http://www.fluxus-engineering.com). All amplified sequences were
245 deposited in the NCBI database under accession numbers OL415778-OL415831.
246
247 **Results**
248 ***Genetic connectivity and B chromosome population frequency***
249 We constructed a COI based haplotype network to understand the possible genetic
250 connectivity between the four studied populations. The average length of the COI
251 sequences was 619 bp, with 33 polymorphic sites, resulting in a total of 19 haplotypes.

Haplotype diversity was 0.834 (SD = 0.044), and nucleotide diversity was 0.00496 (Pi). The haplotype network suggests a certain degree of connectivity between populations with some shared haplotypes. The probable ancestor haplotype grouped the majority of the sequences (21 of 54 sequences) occurring in all four populations. In general, the haplotypes differed among them in a single mutational step. The only noticeable exception was two haplotypes from the ARG population, which differed by 16 mutations with regard to the putative ancestral haplotype (Supplementary Figure 1).

For B chromosome frequency estimation, we studied only males, observing the presence of B chromosomes in individuals from PE with a frequency of 21.05%, and in ARG the frequency was 7.14%. Our previous study in Rio Claro/SP, considering only B chromosome estimation in males, revealed variable B chromosome frequency, depending on the year of collection (31.5%) (Bueno et al., 2013) and 13.5% (Milani et al., 2017). No B chromosomes were observed in the PA population. For PE and ARG, one B chromosome per individual was noticed, differing from previous estimations in SP that reported one or two B chromosomes per individual (Bueno et al., 2013; Milani et al., 2017).

Comparative genomic abundance reveals the distinct repetitive DNA composition of B chromosomes

Using satMiner analysis, we identified nine new satDNAs in the *A. flavolineata* genome, which were not previously recovered from the SP population (Milani et al., 2021). Among them, seven were recovered from individuals from PE and two from ARG. All satDNAs, considering the three populations (PE, SP, and ARG), resulted in a library composed of 62 families. All these satDNAs were shared among all populations. Concerning the TEs, through DNAPipeTE analysis we observed the same 1,744

277 elements (Supplementary Table 2) in all genomes previously identified in SP population
278 (Milani et al., 2021).

279 The general abundance of the repeats was similar between B-lacking genomes,
280 as follows: 52.53% in SP, 50.05% in PE, and 51.33% in ARG. Among these repeats, the
281 satDNAs represented 4.63% in SP, 5.19% in PE, and 5.20% in ARG. The TE
282 abundance was 47.28% in SP, 44.51% in PE, and 45.79% in ARG. Multigene families,
283 including rDNAs, histone genes, and snDNAs, corresponded to 0.63% in SP, 0.34% PE,
284 and 0.33% ARG (Supplementary Table 2).

285 As a general trend, we noticed that repetitive DNA abundance decreased in +1B
286 genomes compared to that in 0B genomes. In SP, the abundance of repeats in +1B
287 genomes was 52.13%, 48.99% in PE, and 50.56% in ARG (Supplementary Table 2).
288 This general panorama reinforces the dilution effect of repeat abundance in B
289 chromosomes in comparison to A chromosomes, previously observed in SP (Milani et
290 al., 2021). In contrast to this general picture, we observed the enrichment of specific
291 repeats in the +1B genomes among the three populations, suggesting their abundance in
292 B chromosomes. Overabundance was observed by comparing the abundance between
293 +1B and 0B genomes, considering the ratio 1B/0B > 1.

294 The dilution effect, due to the low number of repeats on the B chromosome, was
295 observed in the SP (4.63% in 0B, 4.13% in +1B) and PE (5.19% in 0B, 5.05% in +1B)
296 populations. In contrast, the total satDNA content in the +1B genome (7.60%) from
297 ARG was higher than that of the 0B genome (5.21%), suggesting the amplification of
298 satDNAs in its B chromosome (Figure 1a and Supplementary Table 2). Subtractive
299 landscapes (1B/0B) exposed different scenarios of satDNA occurrence on the B
300 chromosome for each population. The SP population revealed a clear impoverished
301 content indicating the dilution effect for satDNA abundance, including the most

abundant ones (Figure 1b) (Milani et al., 2021). Slight differences were observed in the population from PE, which clearly showed overabundance for some satDNA families for the +1B genome in comparison to 0B (Figure 1b). The population from ARG showed the opposite of SP, with an intense amplification of the majority of satDNA families (Figure 1b). In particular, one satDNA family recovered from the ARG population (Afl_ARGSat02-72) showed an extreme amplification in the +1B genome from ARG, reaching more than 500-fold higher than that in the 0B genome. This repeat was very scarce in all of the other genomes analyzed (Supplementary Table 2).

Among the multigene families, only the +1B genomes from SP population showed overabundance for U2 snDNA gene in comparison to the 0B genomes, as reported in Milani et al. (2021). Additionally, we noticed +1B genome overabundances for H3 histone in PE and 5S rDNA plus U1 snDNA in ARG (Figure 1c and Supplementary Table 2).

The general abundance of TEs was similar between the 0B and +1B genomes (Figure 1d). For a more accurate abundance comparison of TEs between the +1B and 0B genomes, we selected the ten highest abundant families of each population, meeting the 1B/0B > 1 criteria out of the 1,744 elements analyzed. For SP, the total abundance of these ten families reached 0.91% in 0B and 1.03% in +1B genomes. The LINE/Jockey family was the most abundant, with over 2-fold higher (0.47%) compared to the second abundant element, that is, DNA/Kolobok (0.21%) (Supplementary Figure 2a). For PE, the total TE abundance was slightly lower than that of SP, with 0.68% for 0B and 0.74% for +1B genomes. For this population, one family LINE/L1 represented the major component of B chromosome TE overabundance (Supplementary Figure 2b). In contrast, the population of ARG showed low values of abundance for the top ten

abundant TEs with 0.20% for 0B and 0.27% for +1B genomes, with two families as the major components, SINE/tRNA and DNA/Sola (Supplementary Figure 2c).

Finally, for a better comparative analysis of the molecular composition of the B chromosomes between populations, we selected the 15 most abundant repeats in the +B genome per population considering the ratio 1B/0B > 1 and compared them with the other two populations. The SP population was overabundant in the +B genome of the U2 snDNA, four satDNAs, and ten TEs, mostly LINE/Jockey. For the population of PE, TEs from distinct families and two satDNAs were among the most abundant repeats. In contrast, the ARG population presented among the most abundant repeats ten satDNAs, differing from the other two populations that presented more TEs overabundant on the +1B genome. Among these 15 overabundant repeats on the +1B genome in each population, the repeat Afl_SPSat52 was the unique among the most abundant in all populations (Figure 2).

***Chromosome distribution of repeats in the populations of* A. flavolineata**

We observed C-heterochromatin located in the pericentromeric regions, extending to the short chromosomal arms in all A chromosomes in all populations. The B chromosome of the SP (Bueno et al., 2013) and PE populations were C-negative. In contrast, the B chromosome from the ARG population was fully heterochromatic (Supplementary Figure 3).

FISH analysis confirmed the enrichment of selected repeats on the B chromosome and their specific organization on the A and B chromosomes. We mapped a total of ten repetitive DNAs sequences, including four satDNAs (Afl_SPSat01, Afl_SPSat52, Afl_PESat01, and Afl_ARGSat02), one multigene family (U2 snDNA), and five TEs (LINE/Jockey_72, LTR/Gypsy_17, DNA/Tc1_275, LINE/L1_100, and

LINE/Jockey_110). Details of the selection of these repeats are provided in the Materials and Methods.

Depending on the satDNA, we observed variations in the distribution of A chromosomes between populations. Remarkably, Afl_SPSat01 presented signals in the pericentromeric regions of all A chromosomes in the three populations (Supplementary Figure 4a-c). On the other hand, the other three satDNAs varied in the number of clusters between populations. Afl_SPSat52 occurred in 11 A chromosomes, including the X in SP, whereas in PE and ARG, it was restricted to one autosome (Supplementary Figure 4d-f). Afl_ARGSat02 did not form clusters on A chromosomes, and Afl_PESat01 formed blocks exclusively in five A chromosomes (including X) only in the PE population (Supplementary Figure 4g-l). With regards to the B chromosomes, variable patterns for Afl_SPSat01, Afl_SPSat52, and Afl_ARGSat02 were observed between populations. Afl_SPSat01 was exclusively observed on the centromere of B chromosome in SP, in centromeres and telomeres in PE, and spread throughout the entire B chromosome of ARG. Afl_SPSat52 was located in the centromere and telomeres of the B chromosomes from SP and PE, whereas in ARG it was pericentromeric as a large block. Afl_ARGSat02 was exclusive to the B chromosome of the ARG population and was located in the pericentromeric region. Finally, Afl_PESat01 was absent from the B chromosome in all the populations (Figure 3).

The U2 snDNA was on the largest autosome in all of the populations studied, interstitially located (Supplementary Figure 4m-o). The B chromosome formed four interstitial blocks (Figure 3).

Because of their general spread as dot signals of these repeats on the A chromosomes of *A. flavolineata* (Palacios-Gimenez et al., 2014; Milani et al., 2021), the resolution of signals in meiotic cells was hampered. On the contrary, TE signals could

be easily observed for mitotic chromosomes. As the B chromosome was more compact and for some TEs, and they were enriched in specific regions, it was possible to clearly observe the signals (Supplementary Figure 5). As good mitotic metaphases were only found in the SP population obtained from embryos, and the material from other localities were testis, only meiotic cells were obtained in large numbers for confident analysis. In this way, we describe only the organization of TEs on B chromosomes in a comparative manner. LINE/Jockey_72 presented prominent bands in the interstitial regions of both arms in SP and PE, while it was enriched in ARG in the pericentromeric region, extending to the long arm. LTR/Gypsy_17 was enriched on the long arm of the B chromosome in SP and PE and absent on the B chromosome from ARG (Figure 3). The other three TEs mapped, DNA/Tc1_275, LINE/L1_100, and LINE/Jockey_110, were not on the B chromosomes.

Discussion

Numerous studies describing B chromosome polymorphisms in multiple species have helped in the understanding of its biology and evolution. However, the available data regarding the physical chromosome mapping and molecular composition of B chromosome population variants remain scarce and based on a few chromosomal markers (Cabrero et al., 1999; Marques et al., 2013; Bernardino et al., 2017; Felicetti et al., 2021). Here, our first comprehensive analysis of the repeatome in distinct populations of a species with B chromosome, that is, the grasshopper *A. flavolineata*, provides evidence of a unique origin and intense turnover in repeat composition, resulting in the establishment of distinct variants at the interpopulation level.

Although the COI-based haplotype network indicated a low spatial degree of genetic differentiation among the populations, distinct variants of the B chromosome

401 were established with respect to molecular composition, presenting different
402 frequencies. This interpopulation variation of B chromosome frequency and B variants,
403 as observed in *A. flavolineata,* has been reported in a range of groups, including
404 grasshoppers (Palestis et al., 2010; Manrique-Poyato et al., 2020), fish (Cavallaro et al.,
405 2000; de Marco-Ferro et al., 2003), reptiles (Bertolotto et al., 2004), mammals
406 (Vujošević et al., 2018), and plants (Bougourd and Parker, 1979; Parker et al., 1991;
407 Houben et al., 1999; Belyayev and Raskina, 2013), among others. The variation in
408 frequency and prevalence of B chromosomes could be dependent on diverse
409 evolutionary factors, including accumulation by drive, phenotypic selection, and genetic
410 drift (Camacho et al., 2000). Thus, the accumulation of new emerging repeated
411 sequences on the B chromosome acting simultaneously with all the other evolutionary
412 forces mentioned above could explain the molecular differentiation of the B
413 chromosomes among populations of *A. flavolineata*, causing variation in B chromosome
414 frequency and the fixation of B variants.

415 Although highly differentiated among populations, we observed evidence of a
416 single origin of the B chromosome in *A. flavolineata* by the sharing of multiple
417 elements in the B chromosome among the populations. The clusters of U2 snDNA were
418 observed using FISH in all B chromosomes occupying a similar position, that is,
419 interstitially. This sequence was restricted to the large chromosome L1 in all
420 populations, reinforcing the origin of the B chromosome from this element in the SP
421 population (Milani et al., 2021). In addition, the sharing of others repeats Afl_SPSat01
422 and LINE/Jockey_72 between all B chromosomes was also observed. Afl_SPSat52
423 shared large blocks for all Bs and was present in the top 15 most abundant repeats in the
424 three B-carrying genomes. Similar to *A. flavolineata*, the origin of the B chromosome
425 from *S. cereale* was also monophyletic, but in this case, the B chromosome presented a

conserved structure (Marques et al. 2013). In the grasshopper *E. plorans* and the plant *Brachycome dichromosomatica*, a unique origin of the B chromosome was observed (Houben et al., 1999; Muñoz-Pajares et al., 2011). The unique origin of B chromosomes among populations from a species could occur more frequently than previously reported, simply because this knowledge is hampered due to the high dynamism of repeats present in the B chromosome.

The B chromosome variants observed in *A. flavolineata* differed significantly in repetitive DNA content, that is, satDNAs, TEs, and multigene families. However, as observed for the SP B chromosome variant (Milani et al., 2021) in the other two variants of B chromosomes from PE and ARG, we did not observe an enrichment of the global genome content in repeats on B chromosomes, evidencing the resemblance of each B chromosome variant with the normal A complement. This resemblance reinforces the hypothesis that the B chromosome of *A. flavolineata* is a young element (Milani et al., 2021). The low abundance of repeats on B chromosomes contrasts with other B systems from multiple species, which generally accumulate in repetitive DNA, such as in rye, maize, and other plants (Marques et al., 2018), *Drosophila melanogaster* (Hanlon et al., 2018), *L. migratoria* (Ruiz-Ruano et al., 2018), *Astatotilapia latifasciata* (Valente et al., 2014), and *Apodemus peninsulae* (Matsubara et al., 2008).

The genomic and chromosomal data clearly suggest that the B chromosome from the ARG population was more differentiated in comparison to PE and SP, which were more similar to each other. Despite not being highly enriched in general repeats, the B chromosome from ARG revealed a higher abundance of satDNAs in comparison to the B chromosomes of SP and PE populations, which were more enriched in TEs, generally specific LINEs. It is evident from chromosomal mapping that some satDNAs colonized the whole B chromosome of the ARG population, for example, Afl_SPSat01,

but was restricted to specific areas in other populations. Moreover, the B chromosome from ARG had some satDNAs that were not present in the PE and SP populations, such as the new satDNA identified in this population, that is, Afl_ARGSat02. Finally, we observed a high homogenization (K2P level) of abundant satDNAs in the B genome of the ARG population, which is a pattern that is commonly observed in repeats that pass through the amplification process. This was not observed in the other populations. The enrichment in satDNAs could be the reason for the heterochromatinization of the B chromosome from ARG, as evidenced by C-positive blocks along its entire extension, in contrast to evidence in PE and SP that the B chromosomes are C-negative and poor in satDNAs. The expansion of specific satDNAs, occupying long extensions of B chromosomes, is a common fate for some B chromosomes (Hanlon et al., 2018, Ruiz-Ruano et al., 2016a, 2018; Benetta et al., 2020; Stornioli et al., 2021). This pattern is a consequence of non-recombination with A chromosomes (Camacho, 2005; Houben et al., 2014), which could lead to the accumulation of repetitive DNA on B chromosomes, including B-specific repeats during its evolution. Highly heterochromatic B chromosomes with B-specific repeats, not detected as clusters in A complement, have been observed, for example, in the fish *P. lineatus* (Stornioli et al., 2021), the grasshopper *Eumigus monticola* (Ruiz-Ruano et al., 2016a), and the plant *S. cereale* (Martis et al., 2012), indicating a certain degree of differentiation to a complement, as the B chromosome of the ARG population in *A. flavolineata*.

Our findings support a single origin of the B chromosome in *A. flavolineata*, followed by posterior modifications among populations. The B variants from SP and PE are more similar in general repetitive content, frequency, and heterochromatin pattern (C-negative); however, divergences were also observed with respect to specific repetitive family composition, suggesting independent and fast evolution. The B variant

from the ARG population was found to be in a more advanced step of heterochromatinization, presenting a higher abundance of satDNAs, lower molecular divergence, and an extremely amplified satDNA family, specifically visualized by FISH as a potential marker. This data provides a detailed example of the dynamics of the repeats on the B chromosome at the population level, resulting in its intense molecular differentiation.

Acknowledgements

This study was financed in part by the Coordenação de Aperfeiçoamento de Pessoal de Nível Superior—Brasil (CAPES), by Fundação de Amparo à Pesquisa do Estado de São Paulo (FAPESP) (process numbers 2014/11763-8 and 2015/16661-1), and Conselho Nacional de Desenvolvimento Científico e Tecnológico (CNPq). DCC-d-M is a recipient of a research productivity fellowship from the Conselho Nacional de Desenvolvimento Científico e Tecnológico-CNPq (process number 308290/2020-8).

References

Abril, V.V., Duarte, J.M.B., 2008. Chromosome polymorphism in the Brazilian dwarf brocket deer, *Mazama nana* (Mammalia, Cervidae). Genet. Mol. Biol. 31, 53-57. https://doi.org/10.1590/s1415-47572008000100011.

Ahmad, S.F., Jehangir, M., Cardoso, A.L., Wolf, I.R., Margarido, V.P., Cabral-de-Mello, D.C., et al., 2020. B chromosomes of multiple species have intense evolutionary dynamics and accumulated genes related to important biological processes. BMC Genomics 21, 656. https://doi.org/10.1186/s12864-020-07072-1.

500 Bakkali, M., Cabrero, J., López-León, M.D., Perfectti, F., Camacho, J.P.M., 1999. The
501 B chromosome polymorphism of the grasshopper *Eyprepocnemis plorans* in
502 North Africa. I. B variants and frequency. Heredity 83, 428-434.
503 https://doi.org/10.1038/sj.hdy.6800002.
504 Belyayev, A., Raskina, O., 2013. Chromosome evolution in marginal populations of
505 *Aegilops speltoides*: causes and consequences. Ann. Bot. 111, 531-
506 538. https://doi.org/10.1093/aob/mct023.
507 Benetta, D.E., Antoshechkin, I., Yang, T., Nguyen, H.Q.M., Ferree, P.M., Akbari, O.S.,
508 2020. Genome elimination mediated by gene expression from a selfish
509 chromosome. Sci .Adv. 6, eaaz9808. https://doi.org/10.1101/793273.
510 Bernardino, A.C., Cabral-de-Mello, D.C., Machado, C.B., Palacios-Gimenez, O.M.,
511 Santos, N., Loreto, V., 2017. B Chromosome variants of the grasshopper *Xyleus*
512 *discoideus angulatus* are potentially derived from pericentromeric
513 DNA. Cytogenet. Genome Res. 152, 213-
514 221. https://doi.org/10.1159/000480036.
515 Bertolotto, C.E.V., Pellegrino, K.C.M., Yonenaga-Yassuda, Y., 2004. Occurrence of B
516 chromosomes in lizards: a review. Cytogenet. Genome Res. 106, 243-
517 246. https://doi.org/10.1159/000079294.
518 Beukeboom, L.W., 1994. Bewildering Bs: an impression of the 1st B-Chromosome
519 Conference. Heredity 73, 328-335. https://doi.org/10.1038/hdy.1994.140.
520 Bougourd, S.M., Parker, J.S., 1979. The B-chromosome system of *Allium*
521 *schoenoprasum*. Chromosoma 75, 369-383. https://doi.org/10.1007/bf00329177.
522 Bueno, D., Palacios-Gimenez, O.M., Cabral-de-Mello, D.C., 2013. Chromosomal
523 mapping of repetitive DNAs in the grasshopper *Abracris flavolineata* reveal

524 possible ancestry of the B chromosome and H3 histone spreading. PLoS One 8,
525 e66532. https://doi.org/10.1371/journal.pone.0066532.
526 Cabral-de-Mello, D.C., Marec, F., 2021. Universal fluorescence in situ hybridization
527 (FISH) protocol for mapping repetitive DNAs in insects and other arthropods.
528 Mol. Genet. Genomics 296, 513–526. https://doi.org/10.1007/s00438-021-
529 01765-2.
530 Cabrero, J., López-León, M.D., Bakkali, M., Camacho, J.P.M., 1999. Common origin of
531 B chromosome variants in the grasshopper *Eyprepocnemis plorans*. Heredity 83,
532 435–439. https://doi.org/10.1038/sj.hdy.6885960.
533 Camacho, J.P.M., 2005. B chromosomes. In: Gregory TR (ed) The evolution of the
534 genome. Elsevier San Diego 223–286. https://doi.org/10.1016/b978-012301463-
535 4/50003-6.
536 Camacho, J.P.M., Sharbel, T.F., Beukeboom, L.W., 2000. B-chromosome
537 evolution. Philos. Trans. R. Soc. Series B: Biological Sciences 355, 163-178.
538 https://doi.org/10.1098/rstb.2000.0556.
539 Cavallaro, Z.I., Bertollo, L.A.C., Perfectti, F., Camacho, J.P.M., 2000. Frequency
540 increase and mitotic stabilization of a B chromosome in the fish *Prochilodus*
541 *lineatus*. Chromosome Res. 8, 627-634.
542 https://doi.org/10.1023/A:1009242209375.
543
544 Coan, R.L., Martins, C., 2018. Landscape of transposable elements focusing on the B
545 chromosome of the cichlid fish *Astatotilapia latifasciata*. Genes 9, 269.
546 https://doi.org/10.3390/genes9060269.

547 de Marco-Ferro, D.A., Moreira-Filho, O., Bertollo, L.A.C., 2003. B chromosome
548 polymorphism in the fish, *Astyanax scabripinnis*. Genetica 119, 147-153.
549 https://doi.org/10.1023/A:1026086501252.
550 Drummond, A.J., Ashton, B., Cheung, M., Heled, J., Kearse, M., 2009. Geneious
551 v.4.8.5, biomatters ltd. Aukland, New Zealand. http://www.geneious.com.
552 Felicetti, D., Haerter, C.A., Baumgärtner, L., Paiz, L.M., Takagui, F.H., Margarido,
553 V.P., et al., 2021. A New Variant B Chromosome in Auchenipteridae: The Role
554 of (GATA) n and (TTAGGG) n Sequences in Understanding the Evolution of
555 Supernumeraries in *Trachelyopterus*. Cytogenet. Genome Res. 161, 70-81.
556 https://doi.org/10.1159/000513107.
557 Hanlon, S.L., Miller, D.E., Eche, S., Hawley, R.S., 2018. Origin, composition, and
558 structure of the supernumerary B chromosome of *Drosophila*
559 *melanogaster*. Genetics 210, 1197-1212.
560 https://doi.org/10.1534/genetics.118.301478.
561 Houben, A., Banaei-Moghaddam, A.M., Klemme, S,. Timmis, J.N., 2014. Evolution
562 and biology of supernumerary B chromosomes. Cell Mol. Life Sci. 71, 467–478.
563 https://doi.org/10.1007/s00018-013-1437-7.
564 Houben, A., Thompson, N., Ahne, R., Leach, C.R., Verlin, D., Timmis, J.N., 1999. A
565 monophyletic origin of the B chromosomes of *Brachycome dichromosomatica*
566 (Asteraceae). Plant Syst. Evol. 219, 127-
567 135. https://doi.org/10.1007/bf01090304.
568 Jin, W., Lamb, J.C., Vega, J.M., Dawe, R.K., Birchler, J.A., Jiang, J., 2005. Molecular
569 and functional dissection of the maize B chromosome centromere. The Plant
570 Cell 17, 1412-1423. https://doi.org/10.1105/tpc.104.030643.

571 Jones, R.N., 1995. B chromosomes in plants. New Phytologist 131, 411-434.
572 https://doi.org/10.1111/j.1469-8137.1995.tb03079.x.
573 Jones, R.N., 2017. New species with B chromosomes discovered since 1980. Nucleus
574 60, 263–281. https://doi.org/10.1007/s13237-017-0215-6.
575 Librado, P., Rozas, J., 2009. DnaSP v5: a software for comprehensive analysis of DNA
576 polymorphism data. Bioinformatics 25, 1451-1452.
577 https://doi.org/10.1093/bioinformatics/btp187.
578 López-León, M.D., Cabrero, J., Pardo, M.C., Viseras, E., Camacho, J.P.M., Santos, J.L.,
579 1993. Generating high variability of B chromosomes in *Eyprepocnemis plorans*
580 (grasshopper). Heredity 71, 352-362. https://doi.org/10.1038/hdy.1993.149.
581 Manrique-Poyato, M.I., Cabrero, J., López-León, M.D., Perfectti, F., Gómez, R.,
582 Camacho, J.P.M., 2020. Interpopulation spread of a parasitic B chromosome is
583 unlikely through males in the grasshopper *Eyprepocnemis*
584 *plorans*. Heredity 124, 197-206. https://doi.org/10.1038/s41437-019-0248-5.
585 Marques, A., Banaei-Moghaddam, A.M., Klemme, S., Blattner, F.R., Niwa, K., Guerra,
586 M., et al., 2013. B chromosomes of rye are highly conserved and accompanied
587 the development of early agriculture. Ann. Bot. 112, 527-534.
588 https://doi.org/10.1093/aob/mct121.
589 Marques, A., Klemme, S., Guerra, M., Houben, A., 2012. Cytomolecular
590 characterization of de novo formed rye B chromosome variants. Molecular
591 Cytogenet. 5, 1-4. https://doi.org/10.1186/1755-8166-5-34.
592 Marques, A., Klemme, S., Houben, A., 2018. Evolution of plant B chromosome
593 enriched sequences. Genes 9, 515. https://doi.org/10.3390/genes9100515.
594 Martis, M.M., Klemme, S., Banaei-Moghaddam, A.M., Blattner, F.R., Macas, J.,
595 Schmutzer, T., et al., 2012. Selfish supernumerary chromosome reveals its

origin as a mosaic of host genome and organellar sequences. Proc. Natl. Acad. Sci. 109, 13343-13346. https://doi.org/10.1073/pnas.1204237109.

Matsubara, K., Yamada, K., Umemoto, S., Tsuchiya, K., Ikeda, N., Nishida, C., et al., 2008. Molecular cloning and characterization of the repetitive DNA sequences that comprise the constitutive heterochromatin of the A and B chromosomes of the Korean field mouse (*Apodemus peninsulae*, Muridae, Rodentia). Chromosome Res. 16, 1013-1026. https://doi.org/10.1007/s10577-008-1259-x.

Milani, D., Bardella, V.B., Ferretti, A.B., Palacios-Gimenez, O.M., Melo, A.D.S., Moura, R.C., et al., 2018. Satellite DNAs unveil clues about the ancestry and composition of B chromosomes in three grasshopper species. Genes 9, 523. https://doi.org/10.3390/genes9110523.

Milani, D., Palacios-Gimenez, O.M., Cabral-de-Mello, D.C., 2017. The U2 snDNA is a useful marker for B chromosome detection and frequency estimation in the grasshopper *Abracris flavolineata*. Cytogenet. Genome Res. 151, 36–40. https://doi.org/10.1159/000458468.

Milani, D., Ruiz-Ruano, F.J., Camacho, J.P.M., Cabral-de-Mello, D.C., 2021. Out of patterns, the euchromatic B chromosome of the grasshopper *Abracris flavolineata* is not enriched in high-copy repeats. Heredity 1-9. https://doi.org/10.1038/s41437-021-00470-5.

Munoz-Pajares, A.J., Martínez-Rodríguez, L., Teruel, M., Cabrero, J., Camacho, J.P.M., Perfectti, F., 2011. A single, recent origin of the accessory B chromosome of the grasshopper *Eyprepocnemis plorans*. Genetics 187, 853-863. https://doi.org/10.1534/genetics.110.122713.

620 Normark, B.B., 1996. Phylogeny and evolution of parthenogenetic weevils of the
621 *Aramigus tessellates* species complex (Coleoptera: Curculionidae:
622 Naupactini): Evidence form mitochondrial DNA sequences. Evolution 50, 734-
623 745. https://doi.org/10.2307/2410846.
624 Palacios-Gimenez, O.M., Bueno, D., Cabral-De-Mello, D.C., 2014. Chromosomal
625 mapping of two Mariner-like elements in the grasshopper *Abracris flavolineata*
626 (Orthoptera: Acrididae) reveals enrichment in euchromatin. Eur. J. Entomol.
627 111, 329–334. https://doi.org/10.14411/eje.2014.052.
628 Palestis, B.G., Cabrero, J., Trivers, R., Camacho, J.P.M., 2010. Prevalence of B
629 chromosomes in Orthoptera is associated with shape and number of A
630 chromosomes. Genetica 138, 1181-1189. https://doi.org/10.1007/s10709-010-
631 9509-1.
632 Parker, J.S., Jones, G.H., Edgar, L.A., Whitehouse, C., 1991. The population
633 cytogenetics of *Crepis capillaris* IV. The distribution of B-chromosomes in
634 British populations. Heredity 66, 211-218. https://doi.org/10.1038/hdy.1991.27.
635 Rubtsov, N.B., Kartavtseva, I.V., Roslik, G.V., Karamysheva, T.V., Pavlenko, M.V.,
636 Iwasa, M.A., et al., 2015. Features of the B chromosome in Korean field mouse
637 *Apodemus peninsulae* (Thomas, 1906) from Transbaikalia and the Far East
638 identified by the FISH method. Russ. J. Genet. 51, 278-
639 288. https://doi.org/10.1134/s1022795415030114.
640 Ruiz-Ruano, F.J., Cabrero, J., López-León, M.D., Camacho, J.P.M., 2016a. Satellite
641 DNA content illuminates the ancestry of a supernumerary (B) chromosome.
642 Chromosoma 126, 487–500. https://doi.org/10.1007/s00412-016-0611-8.
643 Ruiz-Ruano, F.J., Cabrero, J., López-León, M.D., Sánchez, A., Camacho, J.P.M., 2018.
644 Quantitative sequence characterization for repetitive DNA content in the

supernumerary chromosome of the migratory locust. Chromosoma 127, 45–57. https://doi.org/10.1007/s00412-017-0644-7.

Ruiz-Ruano, F.J., López-León, M.D., Cabrero, J., Camacho, J.P.M., 2016b. High-throughput analysis of the satellitome illuminates satellite DNA evolution. Sci. Rep. 6, 28333. https://doi.org/10.1038/srep28333.

Schmid, M., Ziegler, C.G., Steinlein, C., Nanda, I., Haaf, T., 2002. Chromosome banding in Amphibia: XXIV. The B chromosomes of *Gastrotheca espeletia* (Anura, Hylidae). Cytogenet. Genome Res. 97, 205. https://doi.org/10.1159/000066615.

Smit, A.F.A., Hubley, R., Green, P., 2017. RepeatMasker Open-4.0. http:// www.repeatmasker.org.

Stornioli, J.H.F., Goes, C.A.G., Calegari, R.M., dos Santos, R.Z., Giglio, L.M., Foresti, F., et al., 2021. The B Chromosomes of *Prochilodus lineatus* (Teleostei, Characiformes) Are Highly Enriched in Satellite DNAs. Cells 10, 1527. https://doi.org/10.3390/cells10061527.

Sumner, A.T., 1972. A simple technique for demonstrating centromeric heterochromatin. Exp. Cell Res. 75, 304-306. https://doi.org/10.1016/0014-4827(72)90558-7.

Trifonov, V.A., Dementyeva, P.V., Larkin, D.M., O'Brien, P.C., Perelman, P.L., Yang, F., et al., 2013. Transcription of a protein-coding gene on B chromosomes of the Siberian roe deer (*Capreolus pygargus*). BMC Biology 11, 1-11. https://doi.org/10.1186/1741-7007-11-90.

Untergasser, A., Cutcutache, I., Koressaar, T., Ye, J., Faircloth, B.C., Remm, M., Rozen, S.G., 2012. Primer3—new capabilities and interfaces. Nucleic Acids Res. 40, e115– e115. https://doi.org/10.1093/nar/gks596.

Utsunomia, R., Silva, D.M.Z.D.A., Ruiz-Ruano, F.J., Araya-Jaime, C., Pansonato-Alves, J.C., Scacchetti, P.C., et al., 2016. Uncovering the ancestry of B chromosomes in *Moenkhausia sanctaefilomenae* (Teleostei, Characidae). PLoS One 11, e0150573. https://doi.org/10.1371/journal.pone.0150573.

Valente, G.T., Conte, M.A., Fantinatti, B.E.A., Cabral-de-Mello, D.C., Carvalho, R.F., Vicari, M.R., Kocher, T.D., Martins, C. 2014. Origin and evolution of B chromosomes in the cichlid fish *Astatotilapia latifasciata* based on integrated genomic analyses. Mol. Biol. Evol. 31, 2061–2072. https://doi.org/10.1093/molbev/msu148.

Vujošević, M., Rajičić, M., Blagojević, J., 2018. B chromosomes in populations of mammals revisited. Genes 9, 487. https://doi.org/10.3390/genes9100487.

Figures

Figure 1. Comparative genomic proportion between the 0B and 1B genomes for different classes of repetitive DNAs in *Abracris flavolineata* populations. (a) Total satDNA genome proportion. (b) Subtractive satDNA landscapes (genome proportion versus sequence divergence based on Kimura substitution level) obtained from average counts for satDNAs in males with 1B chromosome and with no B chromosome. (c) Genome proportion of the multigene families H3, U1 and U2 snDNAs, 28S, 18S, 5.8S and 5S rDNAs. (d) Genome proportion of different subclasses of transposable elements. It is worth noting the overabundance of satDNAs in ARG population with B chromosome and U2 snDNA for SP population.

Figure 2. Relative genome proportion of the 15 most overabundant repeat sequences of B-carrying genomes from each of population studied of *Abracris flavolineata*. The x-axis represents how many times more the sequence is more abundant in 1B genomes than 0B genomes estimated based in the coefficient 1B/0B > 1. Asterisks (*) denotes sequences that were selected for FISH experiments. Note that some repeats presents at least 10-fold higher abundance in 1B genome in relation to 0B for a specific population. Highlighted, only the Afl_SPSat52 are shared between the three populations. Dashed lines separate distinct classes of sequences.

Figure 3. Frequency in percentage, morphology, heterochromatin distribution, and location of some repetitive DNAs in the B chromosomes of *Abracris flavolineata* from distinct populations that are showed in its geographical location. Yellow (SP), green (PE), purple (PA), and red (ARG). It is worth noting that B chromosomes from SP and PE share similar composition in the B chromosomes, as ARG are the only C-positive B chromosome and presenting the satDNA (Afl_ARGSat02), the absence of Gypsy_17 signal and the satDNA Afl_SPSat01 distributed along the whole B chromosome.

Supplementary Material

Supplementary Table 1. List of primers used for the amplification of repetitive DNAs mapped on chromosome spreads of *Abracris flavolineata* populations through FISH.

Supplementary Table 2. Repeatome data features in *Abracris flavolineata* individuals with and without one B chromosome in the three populations. Asterisks (*) denote

718 sequences selected for FISH experiments. Abund (abundance), SF (superfamily), K2P
719 (Kimura 2-parameter divergence).
720
721 **Supplementary Figure 1.** Haplotype network for COI-1 gene obtained from different
722 populations showing the 19 haplotypes and their relationships. Hairlines correspond to
723 mutational steps, and the haplotype circle size is proportional to abundance of each
724 haplotype. The different populations are represented in different colors. Note that two
725 haplotypes from ARG presented higher genetic distance in relation to the others, with
726 16 mutational steps.
727
728 **Supplementary Figure 2.** Comparative genomic proportion between the 0B and 1B
729 genomes for the B chromosome overabundant TE families in *Abracris flavolineata*
730 populations. SP (a), PE (b), and ARG (c).
731
732 **Supplementary Figure 3.** C-banding revealing the heterochromatin location in
733 metaphase I chromosomes of *Abracris flavolineata* populations from SP, PE, and ARG.
734 Note the pericentromeric location (extending to the short arms) of C-positive blocks on
735 A chromosomes and the intense C-positive pattern for the B chromosome of ARG
736 population, while in PE and SP the B chromosome is C-negative. Arrowheads indicate
737 B chromosomes. Scale bar, 5 μm.
738
739 **Supplementary Figure 4.** FISH data of the satDNAs and U2 snDNA mapped in the
740 chromosomes of each population that presented a B chromosome, i.e. SP, PE, and ARG.
741 X chromosomes are identified in each image and arrowheads indicate B chromosomes.
742 It is worth noting the specific signal for the Afl_ARGSat02 in ARG B chromosome and

743 Afl_PESat01 population-specific satDNA. Highlighted, the U2 snDNA gene shared
744 signals between the B chromosome and pair L1 for the three populations.
745
746 **Supplementary Figure 5.** Comparative TEs FISH results on B chromosome of
747 *Abracris flavolineata* SP population obtained from mitotic metaphases (a–b and e–f)
748 and meiotic metaphases I (c–d and g–h). DAPI (a, c, e, g); Gypsy_17 (b, d); and
749 Jockey_72 (f, h) signals. Arrowheads indicate the B chromosomes.

List of abbreviations

ARG: Argentine

bp: base pair

COI: cytochrome c oxidase subunit I

DAPI: 4′,6-Diamidino-2-phenylindole

FISH: fluorescence *in situ* hybridization

gDNA: genomic DNA

K2P: Kimura 2-parameter

mtDNA: mitochondrial DNA

PA: Pará

PCR: Polymerase chain reaction

PE: Pernambuco

rDNA: Ribosomal DNA

SF: superfamily

SP: São Paulo

SSC: Saline–sodium citrate buffer

satDNA: satellite DNA

snDNA: small nucleolar DNA

TE: transposable element

declaration

Declaration of interests

☒ The authors declare that they have no known competing financial interests or personal relationships that could have appeared to influence the work reported in this paper.

☐The authors declare the following financial interests/personal relationships which may be considered as potential competing interests:

Single origin and high molecular differentiation of the B chromosome in the grasshopper *Abracris flavolineata* revealed by cytogenomic population analysis

Diogo Milani[1], Ana Elisa Gasparotto[1], Vilma Loreto[2], Dardo A Martí[3], Diogo C Cabral-de-Mello[1,*]

[1]UNESP - Univ Estadual Paulista, Instituto de Biociências/IB, Departamento de Biologia Geral e Aplicada, Rio Claro, São Paulo, Brazil

[2]Departamento de Genética, UFPE - Univ Federal de Pernambuco, Centro de Biociências/CB, Recife, Pernambuco, Brazil

[3]IBS - UNaM – CONICET, Posadas, Misiones, Argentina

*_Corresponding author:_ UNESP - Univ Estadual Paulista, Instituto de Biociências/IB, Departamento de Biologia Geral e Aplicada, 13506-900 Rio Claro, SP, Brazil Phone/Fax: 55 19 35264152. E-mail: cabral.mello@unesp.br

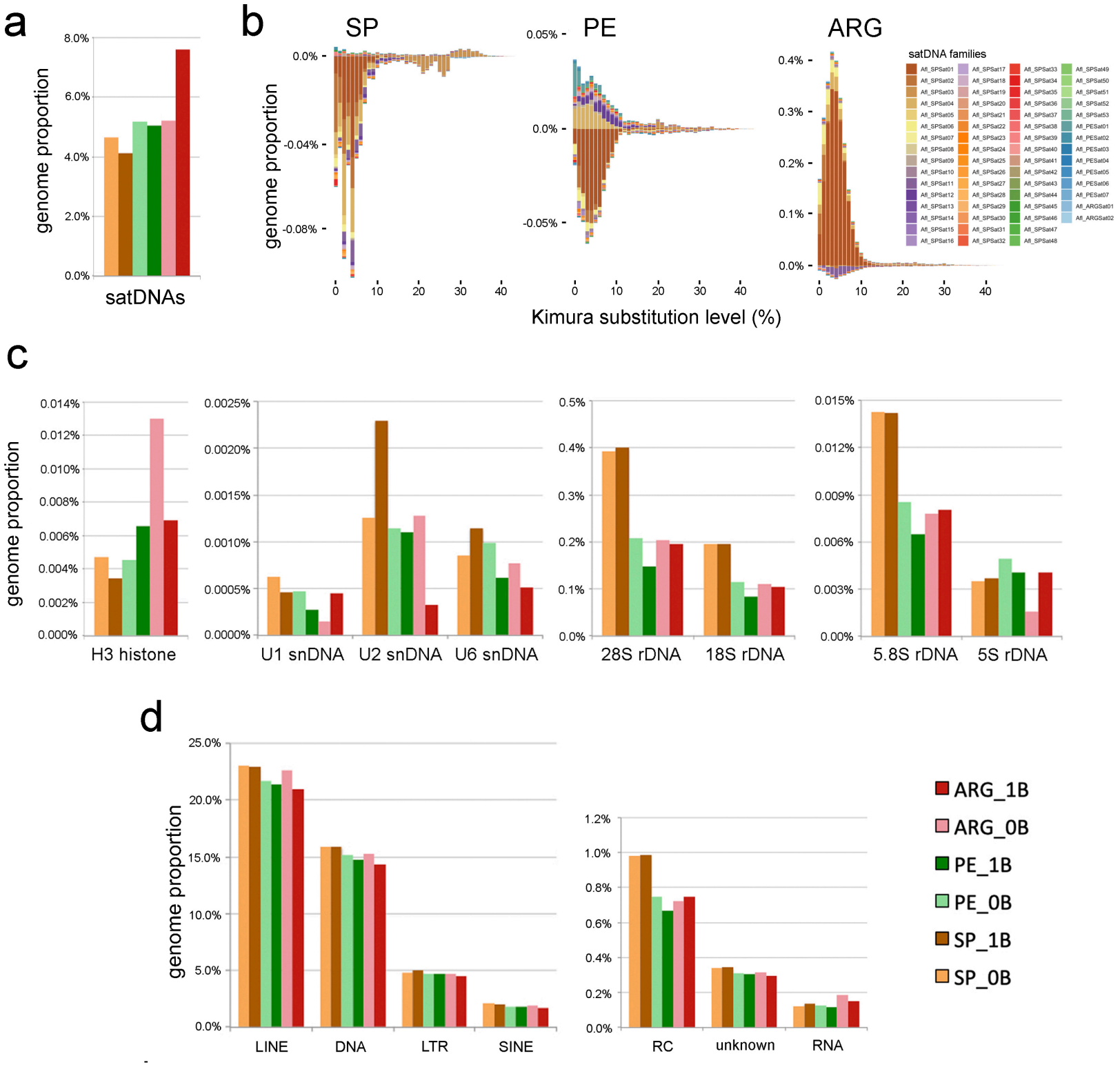
a
genome proportion
satDNAs
b
SP
PE
ARG
genome proportion
Kimura substitution level (%)
satDNA families
c
genome proportion
H3 histone
U1 snDNA
U2 snDNA
U6 snDNA
28S rDNA
18S rDNA
5.8S rDNA
5S rDNA
d
genome proportion
LINE
DNA
LTR
SINE
RC
unknown
RNA
ARG_1B
ARG_0B
PE_1B
PE_0B
SP_1B
SP_0B

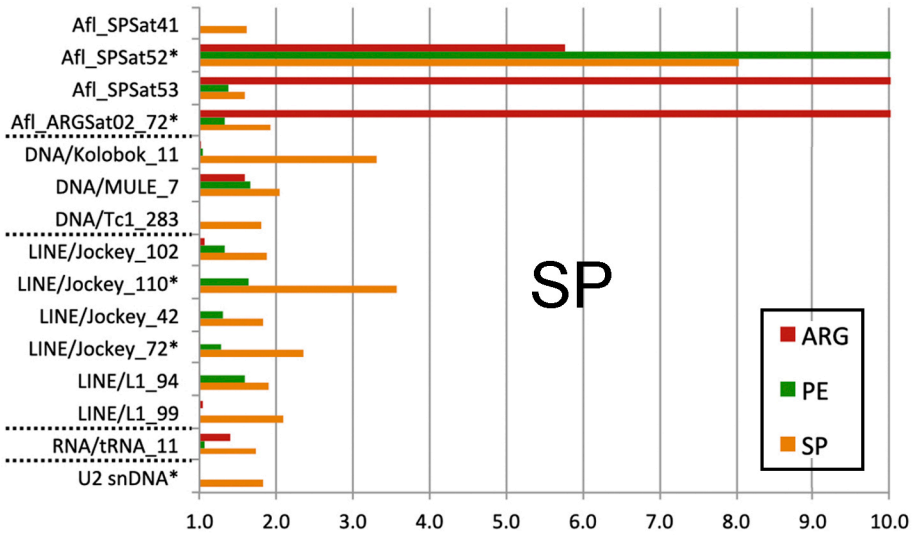
Afl_SPSat41
Afl_SPSat52*
Afl_SPSat53
Afl_ARGSat02_72*
DNA/Kolobok_11
DNA/MULE_7
DNA/Tc1_283
LINE/Jockey_102
LINE/Jockey_110*
LINE/Jockey_42
LINE/Jockey_72*
LINE/L1_94
LINE/L1_99
RNA/tRNA_11
U2 snDNA*
SP
ARG
PE
SP
1.0
2.0
3.0
4.0
5.0
6.0
7.0
8.0
9.0
10.0

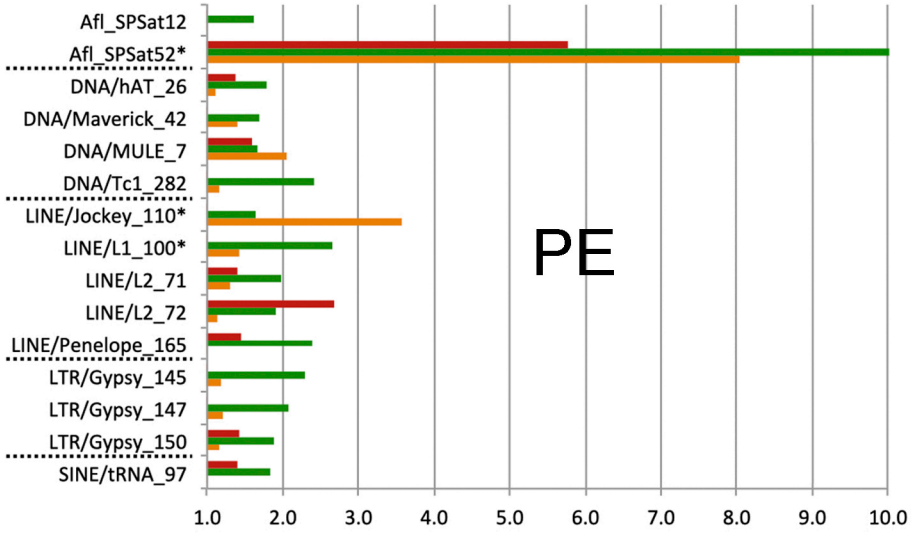
Afl_SPSat12
Afl_SPSat52*
DNA/hAT_26
DNA/Maverick_42
DNA/MULE_7
DNA/Tc1_282
LINE/Jockey_110*
LINE/L1_100*
LINE/L2_71
LINE/L2_72
LINE/Penelope_165
LTR/Gypsy_145
LTR/Gypsy_147
LTR/Gypsy_150
SINE/tRNA_97
PE
1.0
2.0
3.0
4.0
5.0
6.0
7.0
8.0
9.0
10.0

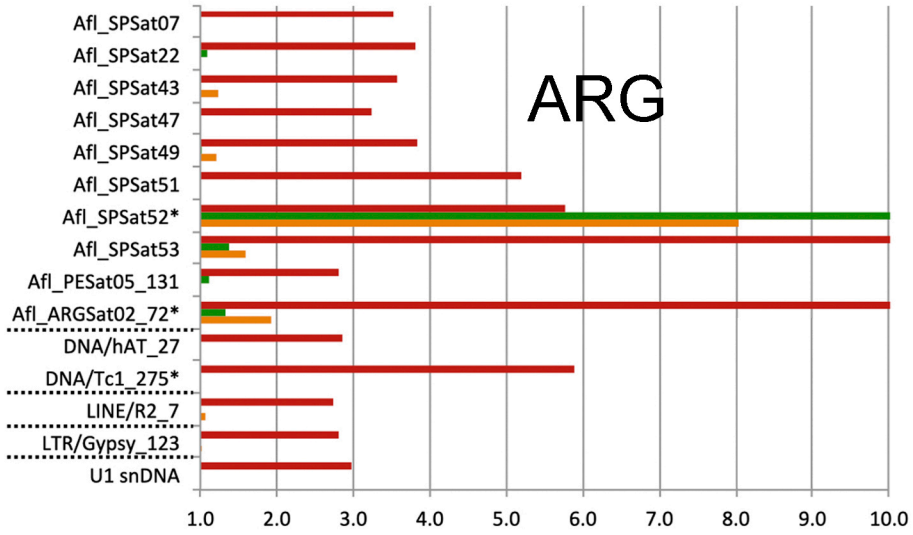
Afl_SPSat07
Afl_SPSat22
Afl_SPSat43
Afl_SPSat47
Afl_SPSat49
Afl_SPSat51
Afl_SPSat52*
Afl_SPSat53
Afl_PESat05_131
Afl_ARGSat02_72*
DNA/hAT_27
DNA/Tc1_275*
LINE/R2_7
LTR/Gypsy_123
U1 snDNA
ARG
1.0
2.0
3.0
4.0
5.0
6.0
7.0
8.0
9.0
10.0

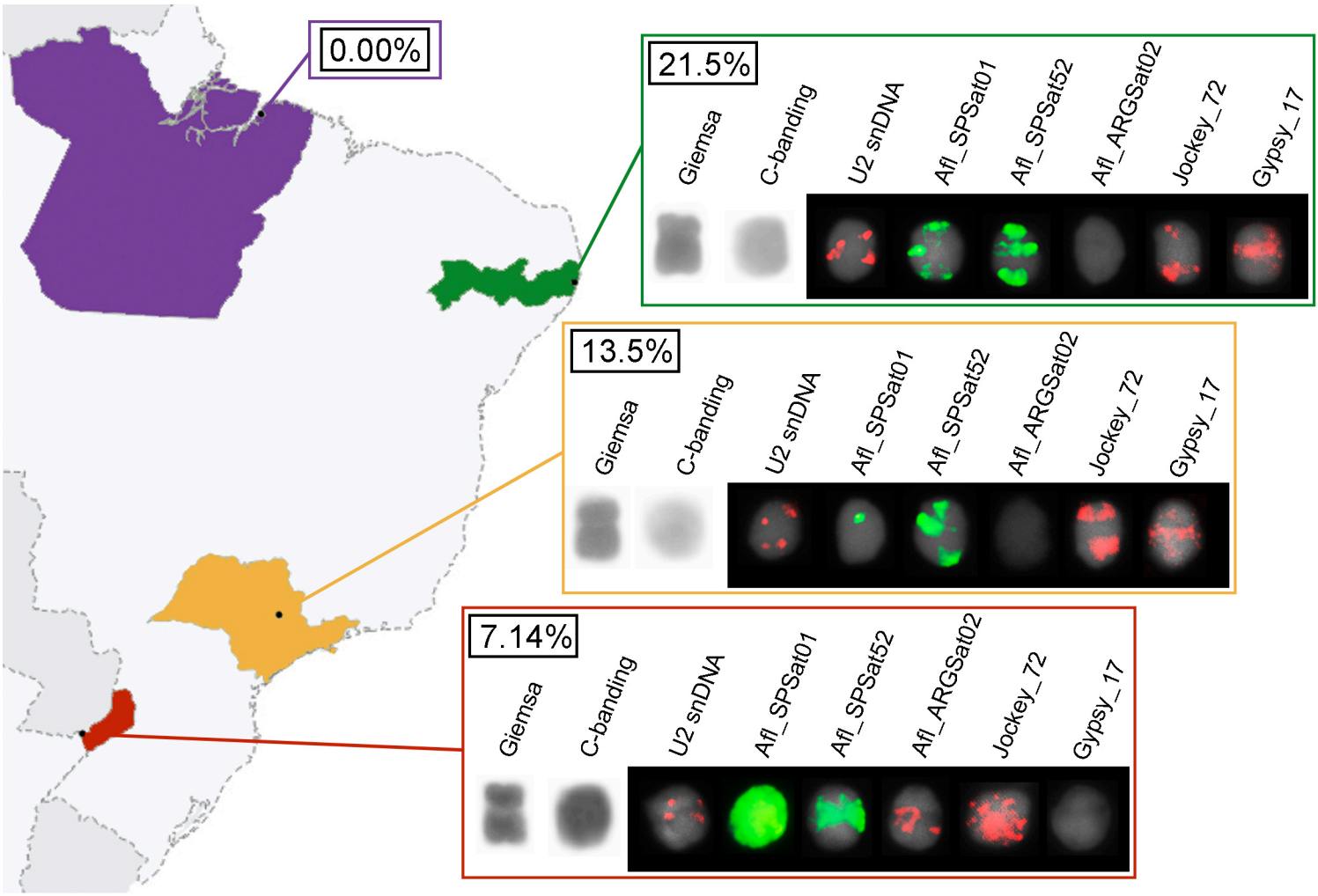
0.00%
21.5%
Giemsa
C-banding
U2 snDNA
Afl_SPSat01
Afl_SPSat52
Afl_ARGSat02
Jockey_72
Gypsy_17
13.5%
Giemsa
C-banding
U2 snDNA
Afl_SPSat01
Afl_SPSat52
Afl_ARGSat02
Jockey_72
Gypsy_17
7.14%
Giemsa
C-banding
U2 snDNA
Afl_SPSat01
Afl_SPSat52
Afl_ARGSat02
Jockey_72
Gypsy_17

Sequence name	Primer forward	Primer reverse
Afl_SPSat01-179	CTCAGACCACTGGGCCATAT	AGACGCTAGTTATAATGAAAAACTGT
Afl_SPSat52-23	GTGCAACCCCCTTGGCTCGG	CGAGCCAAGGGGGTTGCACG
Afl_PESat01-7	GCAACTTGCAACTTGCAACTT	AAGTTGCAAGTTGCAAGTTGC
Afl_ARGSat02-72	GTCTGTACGGAACGCACCT	TCATCGTTTAAGGCATGTGCT
LINE/Jockey-72	GGGTCTTGGTCGGGTTGAA	TGGCATGGAAACATGCTGAG
LTR/Gypsy_17	GTACCTGAAACAGATAGGCC	CCTCCAACTCTGTTATCGAG
LINE/Jockey_110	AGCTGGATGACCACCGGAA	GGGTCGCTCGGATCTTCG
LINE/L1_100	GGGTCCAGGTGATTTATTGTT	ACGACATCAAAGAAGCCATAC
DNA/Tc1_275	GTTGTCTCATATTTGGTGAAAGT	TTTGTCAGATGACAGTCGCC
U2 snDNA	ATCGCTTCTCGGCCTTATG	TCCCGGCGGTACTGCAATA

Supplementary Table 2. Repeatome data features in *Abracris flavolineata* individuals with and without one B chromosome in three populations. The asterisks (*) mark sequences that were selected for FISH experimen
Abund (Abundance), SF (superfamily), K2P (Kimura 2-parameter divergence).

	Rio Claro / SP				Cabo / PE				Posadas / ARG				Coefficient 1B/0B		
Repeats	0B Abund mean (3 ind)	0B K2P% mean (3 ind)	1B Abund mean (2 ind)	1B K2P% mean (2 ind)	0B Abund	0B K2P%	1B Abund	1B K2P%	0B Abund	0B K2P%	1B Abund	1B K2P%	SP	PE	ARG
DNA/Academ_1	0.00445%	5.30	0.00345%	6.80	0.00308%	5.3	0.00309%	5.16	0.00152%	7.49	0.00198%	7.52	0.77	1.00	1.31
DNA/CMC_1	0.04033%	14.29	0.03998%	14.64	0.03298%	13.31	0.03204%	13.15	0.02666%	13.17	0.03224%	13.49	0.99	0.97	1.21
DNA/CMC_2	0.02427%	6.38	0.02569%	6.61	0.02584%	7.17	0.02410%	6.4	0.02823%	6.24	0.02522%	6.35	1.06	0.93	0.89
DNA/CMC_3	0.02299%	14.76	0.02333%	15.57	0.02412%	13.24	0.02171%	13.97	0.01652%	14.99	0.02184%	14.41	1.01	0.90	1.32
DNA/CMC_4	0.01013%	12.09	0.01056%	12.64	0.01001%	11.49	0.01022%	12.05	0.00822%	12.44	0.00924%	11.17	1.04	1.02	1.12
DNA/CMC_5	0.00862%	18.43	0.00911%	18.84	0.01074%	13.92	0.01011%	14.57	0.00653%	19.63	0.00703%	17.88	1.06	0.94	1.08
DNA/CMC_6	0.00431%	6.72	0.00429%	5.86	0.00405%	6.99	0.00448%	5.43	0.00540%	8.9	0.00366%	5.67	1.00	1.10	0.68
DNA/CMC_7	0.00164%	6.43	0.00190%	9.01	0.00151%	8.36	0.00166%	7.16	0.00175%	7.8	0.00173%	7.18	1.16	1.10	0.99
DNA/Crypton_1	0.02037%	6.83	0.02069%	7.01	0.01923%	6.6	0.02055%	6.55	0.01955%	6.8	0.01520%	6.91	1.02	1.07	0.78
DNA/DNA_1	0.15191%	10.37	0.15587%	10.35	0.15599%	9.62	0.16315%	9.64	0.14957%	10.38	0.14157%	10.25	1.03	1.05	0.95
DNA/DNA_10	0.02957%	8.28	0.02807%	8.25	0.02929%	7.3	0.02751%	6.88	0.02600%	6.81	0.02607%	6.83	0.95	0.94	1.00
DNA/DNA_11	0.02632%	21.21	0.02869%	21.31	0.02188%	18.72	0.02208%	18.93	0.02300%	18.92	0.02209%	18.88	1.09	1.01	0.96
DNA/DNA_12	0.02213%	12.76	0.02237%	13.10	0.02290%	10.02	0.02278%	10.19	0.02277%	11.19	0.02050%	11.38	1.01	0.99	0.90
DNA/DNA_13	0.02211%	10.40	0.02303%	10.32	0.02311%	9.26	0.02168%	9.37	0.01973%	9.5	0.02198%	9.41	1.04	0.94	1.11
DNA/DNA_14	0.02181%	10.38	0.02192%	10.59	0.02259%	10.36	0.02125%	10.37	0.01916%	11.1	0.02074%	10.46	1.01	0.94	1.08
DNA/DNA_15	0.02179%	11.21	0.02401%	11.17	0.02273%	10.87	0.02196%	11.11	0.02396%	10.42	0.02165%	10.55	1.10	0.97	0.90
DNA/DNA_16	0.02077%	15.11	0.02129%	15.33	0.01897%	13.03	0.01871%	12.69	0.01971%	13.14	0.01949%	13.37	1.03	0.99	0.99
DNA/DNA_17	0.02008%	19.71	0.02292%	21.07	0.01958%	15.75	0.01897%	16.33	0.01361%	22.68	0.01461%	20.51	1.14	0.97	1.07
DNA/DNA_18	0.01874%	13.32	0.01959%	13.61	0.01830%	12.26	0.01630%	12.26	0.01832%	11.92	0.01818%	12.7	1.05	0.89	0.99
DNA/DNA_19	0.01849%	17.03	0.02060%	17.06	0.01887%	16.5	0.01828%	16.26	0.02135%	16.02	0.01996%	16.21	1.11	0.97	0.93
DNA/DNA_2	0.07712%	13.88	0.07702%	14.56	0.06919%	12.98	0.07134%	13.25	0.06981%	12.97	0.07335%	12.95	1.00	1.03	1.05
DNA/DNA_20	0.01790%	17.81	0.02082%	19.09	0.01875%	16	0.01956%	15.56	0.01196%	22.85	0.01460%	19.16	1.16	1.04	1.22
DNA/DNA_21	0.01671%	8.27	0.01731%	8.41	0.01675%	8.26	0.01681%	7.83	0.01699%	8.39	0.01558%	8.31	1.04	1.00	0.92
DNA/DNA_22	0.01644%	13.72	0.01627%	13.94	0.01769%	9.8	0.01544%	11.38	0.01240%	13.85	0.01271%	13.59	0.99	0.87	1.02
DNA/DNA_23	0.01530%	13.23	0.01616%	13.30	0.01446%	12.83	0.01402%	11.58	0.01477%	12.23	0.01491%	12.2	1.06	0.97	1.01

DNA/DNA_24	0.01490%	20.49	0.01726%	20.27	0.01278%	19.09	0.01496%	18.49	0.01431%	18.53	0.01380%	18.72	1.16	1.17	0.96
DNA/DNA_25	0.01416%	11.27	0.01570%	11.87	0.01391%	11.11	0.01374%	10.57	0.01468%	10.71	0.01430%	10.9	1.11	0.99	0.97
DNA/DNA_26	0.01272%	13.47	0.01308%	14.69	0.01029%	13.62	0.00972%	13.41	0.01011%	13.97	0.00924%	14.36	1.03	0.94	0.91
DNA/DNA_27	0.01254%	8.15	0.01331%	8.05	0.01394%	7.55	0.01434%	7.4	0.01238%	7.9	0.01374%	7.55	1.06	1.03	1.11
DNA/DNA_28	0.01201%	9.94	0.01135%	11.22	0.01033%	9.79	0.00994%	10.68	0.00791%	12.49	0.00755%	11.58	0.95	0.96	0.95
DNA/DNA_29	0.01179%	13.07	0.01163%	13.34	0.01121%	12.05	0.01055%	12.43	0.01053%	12.47	0.01017%	12.15	0.99	0.94	0.97
DNA/DNA_3	0.05566%	10.86	0.05730%	11.22	0.05680%	10.24	0.05543%	10.18	0.05149%	10.5	0.05563%	10.56	1.03	0.98	1.08
DNA/DNA_30	0.01150%	13.64	0.01196%	13.43	0.01003%	12.75	0.01042%	12.12	0.01008%	12.25	0.01051%	12.48	1.04	1.04	1.04
DNA/DNA_31	0.01136%	17.64	0.01183%	17.38	0.01318%	15.72	0.01305%	16.29	0.01295%	16.02	0.01320%	16.05	1.04	0.99	1.02
DNA/DNA_32	0.01132%	19.71	0.01002%	20.68	0.01299%	19.32	0.01243%	19.75	0.01141%	21.68	0.01220%	21.18	0.89	0.96	1.07
DNA/DNA_33	0.01019%	12.79	0.01059%	12.63	0.00861%	11.34	0.00854%	10.83	0.00887%	10.67	0.00899%	11.19	1.04	0.99	1.01
DNA/DNA_34	0.00992%	13.34	0.01000%	13.65	0.01110%	12.01	0.01094%	12.2	0.01058%	12.1	0.01042%	11.97	1.01	0.99	0.98
DNA/DNA_35	0.00890%	17.41	0.00257%	20.46	0.00160%	19.49	0.00182%	16.12	0.01522%	10.55	0.00171%	18.27	0.29	1.14	0.11
DNA/DNA_36	0.00889%	10.17	0.01062%	11.74	0.00891%	11.39	0.00858%	11.26	0.00872%	11.07	0.00816%	11.27	1.19	0.96	0.94
DNA/DNA_37	0.00867%	17.74	0.00800%	17.09	0.00717%	15.42	0.00756%	16.9	0.00576%	19.06	0.00625%	18.9	0.92	1.05	1.09
DNA/DNA_38	0.00818%	17.02	0.00792%	17.62	0.00764%	14.73	0.00728%	15.16	0.00676%	14.14	0.00786%	15.29	0.97	0.95	1.16
DNA/DNA_39	0.00801%	8.83	0.00717%	10.37	0.00667%	6.83	0.00638%	7.34	0.00178%	12.62	0.00357%	9.73	0.89	0.96	2.00
DNA/DNA_4	0.05434%	12.04	0.02121%	12.65	0.01898%	11.31	0.02138%	11.42	0.08784%	9.4	0.02202%	11.54	0.39	1.13	0.25
DNA/DNA_40	0.00768%	13.34	0.00759%	13.41	0.00182%	13.41	0.00185%	13.46	0.00212%	13.03	0.00183%	12.6	0.99	1.02	0.86
DNA/DNA_41	0.00760%	12.74	0.00748%	11.40	0.00878%	7.88	0.00806%	8.51	0.00650%	9.52	0.00798%	8.03	0.98	0.92	1.23
DNA/DNA_42	0.00757%	19.83	0.00827%	20.19	0.00620%	17.25	0.00676%	18.52	0.00647%	17.31	0.00690%	18.6	1.09	1.09	1.07
DNA/DNA_43	0.00754%	8.74	0.00687%	9.89	0.00435%	6.98	0.00479%	8.26	0.00233%	12.2	0.00328%	10.68	0.91	1.10	1.41
DNA/DNA_44	0.00749%	12.39	0.00676%	11.78	0.00692%	8.95	0.00730%	9.19	0.00782%	9.1	0.00616%	9.41	0.90	1.05	0.79
DNA/DNA_45	0.00735%	11.26	0.00690%	11.84	0.00585%	11.22	0.00683%	12.26	0.00471%	16.55	0.00529%	13.78	0.94	1.17	1.12
DNA/DNA_46	0.00734%	15.39	0.00807%	15.17	0.00874%	16.62	0.00933%	15.51	0.00933%	15.6	0.00912%	16.15	1.10	1.07	0.98
DNA/DNA_47	0.00701%	21.20	0.00555%	21.96	0.00878%	20.13	0.00834%	20	0.00795%	21.78	0.00903%	21.26	0.79	0.95	1.14
DNA/DNA_48	0.00688%	10.75	0.00600%	11.15	0.00483%	10.16	0.00490%	10.42	0.00345%	15.26	0.00374%	12.75	0.87	1.01	1.09
DNA/DNA_49	0.00631%	15.26	0.00707%	15.07	0.00670%	14.66	0.00656%	13.8	0.00507%	15.14	0.00628%	14.55	1.12	0.98	1.24
DNA/DNA_5	0.03791%	16.51	0.04191%	18.19	0.03698%	14.92	0.03905%	15.28	0.03030%	18.41	0.03407%	17.42	1.11	1.06	1.12
DNA/DNA_50	0.00579%	17.51	0.00524%	17.94	0.00473%	15.46	0.00470%	15.51	0.00500%	16.57	0.00446%	15.75	0.90	0.99	0.89
DNA/DNA_51	0.00542%	21.13	0.00574%	23.07	0.00493%	20.54	0.00466%	20.19	0.00430%	21.89	0.00524%	21.53	1.06	0.94	1.22

DNA/DNA_52	0.00540%	29.42	0.00509%	29.35	0.00558%	27.38	0.00650%	26.74	0.00500%	27.69	0.00578%	27.55	0.94	1.16	1.16
DNA/DNA_53	0.00531%	12.76	0.00440%	13.87	0.00392%	11.94	0.00367%	10.96	0.00218%	15.49	0.00286%	14.95	0.83	0.94	1.31
DNA/DNA_54	0.00501%	18.47	0.00462%	19.52	0.00396%	19.19	0.00429%	18.34	0.00362%	20.94	0.00368%	20.65	0.92	1.08	1.02
DNA/DNA_55	0.00500%	9.21	0.00503%	8.37	0.00483%	5.62	0.00543%	6.08	0.00174%	15.78	0.00277%	11.62	1.01	1.12	1.59
DNA/DNA_56	0.00482%	22.23	0.00414%	21.59	0.01738%	16.17	0.01659%	16.03	0.01848%	15.7	0.01658%	16.13	0.86	0.95	0.90
DNA/DNA_57	0.00470%	14.43	0.00507%	14.44	0.00436%	12.34	0.00466%	12.35	0.00316%	15.33	0.00432%	13.11	1.08	1.07	1.37
DNA/DNA_58	0.00454%	17.72	0.00347%	15.70	0.00361%	12.38	0.00390%	13.64	0.00237%	23.17	0.00280%	17.77	0.76	1.08	1.18
DNA/DNA_59	0.00436%	4.91	0.00366%	5.83	0.00290%	4.65	0.00313%	4.93	0.00157%	6.05	0.00171%	6.47	0.84	1.08	1.09
DNA/DNA_6	0.03642%	2.08	0.03488%	1.82	0.01844%	2.57	0.01392%	3.7	0.01630%	3.44	0.01897%	3.12	0.96	0.75	1.16
DNA/DNA_60	0.00431%	11.50	0.00454%	11.47	0.00566%	9.56	0.00509%	10.38	0.00534%	10.32	0.00535%	10.39	1.05	0.90	1.00
DNA/DNA_61	0.00421%	12.32	0.00365%	13.04	0.00360%	13.22	0.00329%	13.16	0.00210%	21.28	0.00250%	17.1	0.87	0.91	1.19
DNA/DNA_62	0.00413%	12.34	0.00440%	13.48	0.00436%	11.2	0.00485%	13.3	0.00262%	19.98	0.00330%	16.05	1.07	1.11	1.26
DNA/DNA_63	0.00406%	14.59	0.00341%	13.83	0.00409%	10.59	0.00357%	10.61	0.00282%	16.11	0.00258%	14.43	0.84	0.87	0.92
DNA/DNA_64	0.00384%	14.67	0.00304%	16.40	0.00387%	17.52	0.00410%	17.99	0.00339%	19.35	0.00333%	19.66	0.79	1.06	0.98
DNA/DNA_65	0.00358%	16.48	0.00358%	17.95	0.00283%	17.59	0.00283%	17.23	0.00213%	20.12	0.00263%	19.39	1.00	1.00	1.24
DNA/DNA_66	0.00352%	10.99	0.00384%	10.74	0.00445%	10.94	0.00555%	10.25	0.00506%	11.02	0.00458%	10.79	1.09	1.25	0.90
DNA/DNA_67	0.00344%	17.14	0.00360%	17.40	0.00269%	17.01	0.00234%	17.67	0.00301%	18.44	0.00271%	17.81	1.05	0.87	0.90
DNA/DNA_68	0.00334%	21.16	0.00308%	21.04	0.00211%	19.31	0.00262%	19.7	0.00252%	20.37	0.00249%	19.12	0.92	1.24	0.99
DNA/DNA_69	0.00317%	15.93	0.00290%	16.70	0.00336%	15.48	0.00348%	15.69	0.00329%	14.77	0.00349%	15	0.92	1.04	1.06
DNA/DNA_7	0.03462%	10.17	0.03625%	9.96	0.03196%	9.55	0.03238%	9.08	0.03108%	9.19	0.02976%	9.51	1.05	1.01	0.96
DNA/DNA_70	0.00302%	12.10	0.00060%	14.07	0.00034%	11.46	0.00049%	12.41	0.00645%	8.74	0.00039%	12.09	0.20	1.45	0.06
DNA/DNA_71	0.00299%	16.58	0.00301%	16.64	0.00232%	15.29	0.00273%	12.88	0.00200%	16.91	0.00215%	15.43	1.01	1.18	1.08
DNA/DNA_72	0.00286%	16.62	0.00288%	16.87	0.00290%	15.77	0.00253%	15.04	0.00238%	16.12	0.00277%	16	1.01	0.87	1.17
DNA/DNA_73	0.00272%	19.53	0.00230%	19.28	0.00187%	17.14	0.00192%	20.12	0.00152%	20.86	0.00156%	20.95	0.85	1.02	1.03
DNA/DNA_74	0.00256%	11.01	0.00243%	11.10	0.00237%	11	0.00198%	10.89	0.00233%	10.54	0.00231%	10.58	0.95	0.84	0.99
DNA/DNA_75	0.00254%	22.41	0.00328%	24.62	0.00286%	24.26	0.00295%	23.68	0.00235%	26.51	0.00257%	26.12	1.29	1.03	1.10
DNA/DNA_76	0.00231%	14.87	0.00221%	16.56	0.00317%	15.71	0.00280%	14.77	0.00272%	16.43	0.00251%	16.7	0.96	0.88	0.92
DNA/DNA_77	0.00201%	10.92	0.00186%	11.49	0.00190%	9.97	0.00176%	8.55	0.00109%	17.33	0.00128%	13.27	0.92	0.93	1.17
DNA/DNA_78	0.00196%	5.03	0.00167%	5.38	0.00201%	5.03	0.00217%	4.46	0.00144%	5.25	0.00156%	4.56	0.85	1.08	1.08
DNA/DNA_79	0.00195%	16.24	0.00135%	15.67	0.00142%	15.87	0.00113%	14.39	0.00090%	22.92	0.00104%	19	0.69	0.79	1.16
DNA/DNA_8	0.03209%	11.23	0.03268%	11.18	0.02715%	11.49	0.02651%	11.49	0.02517%	12.55	0.02535%	12.22	1.02	0.98	1.01

DNA/DNA_80	0.00182%	25.74	0.00151%	25.51	0.00285%	23.77	0.00260%	23.68	0.00229%	23.62	0.00259%	24.32	0.83	0.91	1.13
DNA/DNA_81	0.00170%	4.28	0.00153%	3.99	0.00205%	3.86	0.00208%	3.99	0.00180%	3.56	0.00194%	3.82	0.90	1.02	1.08
DNA/DNA_82	0.00170%	11.83	0.00153%	10.68	0.00188%	11.26	0.00200%	11.79	0.00173%	13.43	0.00155%	12.52	0.90	1.06	0.90
DNA/DNA_83	0.00159%	14.49	0.00156%	17.90	0.00172%	16.48	0.00160%	16.14	0.00144%	17.91	0.00137%	18.68	0.98	0.93	0.95
DNA/DNA_84	0.00158%	9.99	0.00133%	10.55	0.00188%	13.71	0.00199%	11.97	0.00115%	21.13	0.00142%	18.47	0.84	1.06	1.24
DNA/DNA_85	0.00147%	24.39	0.00106%	24.79	0.00153%	23.51	0.00152%	22.57	0.00160%	21.36	0.00169%	21.59	0.72	0.99	1.06
DNA/DNA_86	0.00053%	9.56	0.00061%	6.84	0.00062%	7.66	0.00062%	4.9	0.00045%	6.85	0.00047%	10.77	1.16	1.00	1.05
DNA/DNA_87	0.00020%	0.69	0.00020%	0.20	0.00023%	0.07	0.00020%	0.07	0.00019%	0.66	0.00024%	0.57	1.01	0.86	1.28
DNA/DNA_9	0.02970%	12.33	0.02911%	12.53	0.03893%	12.35	0.03815%	11.79	0.04029%	11.93	0.03848%	12.23	0.98	0.98	0.95
DNA/Fot1_1	0.00416%	17.01	0.00383%	17.17	0.00398%	15.58	0.00350%	15.04	0.00269%	15.98	0.00483%	17.14	0.92	0.88	1.80
DNA/Ginger_1	0.21557%	15.12	0.19720%	15.08	0.19627%	14.92	0.19630%	14.88	0.18948%	14.97	0.21067%	14.91	0.91	1.00	1.11
DNA/Ginger_2	0.04561%	2.38	0.03131%	3.42	0.12150%	2.81	0.06489%	3.34	0.04728%	3.01	0.07003%	2.54	0.69	0.53	1.48
DNA/Ginger_3	0.00162%	2.04	0.00163%	3.17	0.00184%	2.82	0.00162%	2.88	0.00138%	2.13	0.00185%	2.17	1.00	0.88	1.34
DNA/Ginger_4	0.00124%	10.87	0.00105%	11.60	0.00123%	10.69	0.00075%	10.49	0.00079%	12.04	0.00111%	11.24	0.85	0.61	1.40
DNA/hAT_1	0.09210%	18.65	0.09689%	19.29	0.08501%	17.48	0.08447%	17.46	0.08297%	19.43	0.08019%	18.78	1.05	0.99	0.97
DNA/hAT_10	0.01300%	15.18	0.01327%	16.86	0.01044%	15.06	0.01067%	14.93	0.00982%	17.61	0.00935%	16.69	1.02	1.02	0.95
DNA/hAT_11	0.00893%	4.60	0.00954%	4.44	0.00608%	4.22	0.00591%	3.84	0.00649%	4.5	0.00620%	4.52	1.07	0.97	0.96
DNA/hAT_12	0.00883%	9.92	0.00802%	11.47	0.00619%	11.5	0.00749%	11.42	0.00484%	13.52	0.00554%	13.59	0.91	1.21	1.15
DNA/hAT_13	0.00869%	18.08	0.00885%	20.03	0.00788%	17.04	0.00715%	17.85	0.00569%	21.68	0.00564%	20.3	1.02	0.91	0.99
DNA/hAT_14	0.00858%	12.94	0.00807%	12.97	0.01989%	7.68	0.02086%	7.75	0.02311%	7.89	0.01861%	8.3	0.94	1.05	0.81
DNA/hAT_15	0.00857%	9.38	0.00802%	10.16	0.00667%	9.84	0.00615%	9.84	0.00430%	12.97	0.00492%	12.06	0.94	0.92	1.14
DNA/hAT_16	0.00757%	18.46	0.00590%	17.59	0.01207%	20.11	0.01154%	18.79	0.00924%	23.86	0.01039%	21.31	0.78	0.96	1.12
DNA/hAT_17	0.00596%	20.21	0.00629%	20.77	0.00534%	15.76	0.00566%	15.62	0.00356%	21.54	0.00385%	20.16	1.06	1.06	1.08
DNA/hAT_18	0.00520%	14.44	0.00539%	14.13	0.00496%	13.46	0.00494%	13.09	0.00511%	13.75	0.00536%	14.09	1.04	1.00	1.05
DNA/hAT_19	0.00518%	10.03	0.00526%	10.20	0.00939%	7.06	0.00833%	7.21	0.00301%	14.55	0.00349%	12.64	1.02	0.89	1.16
DNA/hAT_2	0.04172%	22.67	0.04425%	24.67	0.03023%	22.26	0.03198%	21.81	0.02812%	25.9	0.02765%	23.66	1.06	1.06	0.98
DNA/hAT_20	0.00513%	8.42	0.00586%	8.66	0.01073%	5.54	0.00954%	5.83	0.00282%	12.83	0.00357%	11.24	1.14	0.89	1.26
DNA/hAT_21	0.00460%	13.65	0.00494%	13.96	0.00526%	13.05	0.00437%	12.91	0.00518%	12.49	0.00487%	12.75	1.08	0.83	0.94
DNA/hAT_22	0.00375%	12.19	0.00383%	12.50	0.00428%	11.24	0.00368%	11.38	0.00161%	18.01	0.00241%	15.44	1.02	0.86	1.49
DNA/hAT_23	0.00349%	17.51	0.00350%	18.26	0.00208%	13.95	0.00174%	13.63	0.00162%	16.43	0.00194%	16.62	1.00	0.84	1.20
DNA/hAT_24	0.00317%	6.07	0.00332%	7.11	0.00315%	6.21	0.00260%	6.78	0.00325%	3.81	0.00357%	5.91	1.05	0.83	1.10

DNA/hAT_25	0.00280%	11.03	0.00294%	10.71	0.00268%	11.31	0.00266%	11.37	0.00246%	10.89	0.00245%	10.34	1.05	0.99	1.00
DNA/hAT_26	0.00252%	12.98	0.00277%	12.00	0.00176%	11.47	0.00313%	8.92	0.00171%	13.51	0.00236%	13.21	1.10	1.78	1.38
DNA/hAT_27	0.00202%	1.91	0.00171%	2.02	0.00278%	1.47	0.00172%	0.89	0.00036%	4.08	0.00102%	2.82	0.84	0.62	2.86
DNA/hAT_28	0.00197%	9.77	0.00173%	10.42	0.00221%	11.24	0.00221%	10	0.00235%	10.25	0.00206%	10.97	0.88	1.00	0.88
DNA/hAT_29	0.00172%	4.49	0.00177%	5.91	0.00170%	3.03	0.00147%	4.02	0.00196%	3.13	0.00201%	2.87	1.03	0.86	1.02
DNA/hAT_3	0.04015%	24.66	0.04137%	25.27	0.03558%	22.11	0.03440%	22.4	0.03211%	24.84	0.03231%	24.14	1.03	0.97	1.01
DNA/hAT_30	0.00157%	1.62	0.00133%	2.45	0.00154%	1.32	0.00136%	1.1	0.00131%	1.5	0.00124%	1.32	0.85	0.88	0.94
DNA/hAT_31	0.00134%	13.07	0.00098%	8.90	0.00091%	7.67	0.00082%	8	0.00102%	8.21	0.00063%	10.04	0.73	0.90	0.61
DNA/hAT_32	0.00132%	16.44	0.00128%	17.02	0.00133%	15.6	0.00121%	15.77	0.00136%	17.44	0.00116%	15.57	0.97	0.92	0.85
DNA/hAT_33	0.00120%	8.49	0.00113%	9.97	0.00083%	7.4	0.00105%	7.85	0.00064%	10.49	0.00071%	11.06	0.94	1.27	1.11
DNA/hAT_4	0.03461%	26.60	0.03727%	27.38	0.03180%	25.35	0.02925%	25.22	0.02864%	26.63	0.02955%	26.21	1.08	0.92	1.03
DNA/hAT_5	0.03263%	16.38	0.03312%	16.54	0.03181%	15.84	0.03076%	15.62	0.02971%	16.29	0.03038%	16.22	1.02	0.97	1.02
DNA/hAT_6	0.02983%	17.42	0.03196%	18.40	0.02757%	17.41	0.02867%	17.47	0.02465%	18	0.02665%	17.94	1.07	1.04	1.08
DNA/hAT_7	0.01837%	4.49	0.01897%	4.51	0.01555%	4.57	0.01534%	4.61	0.01539%	4.63	0.01624%	4.71	1.03	0.99	1.06
DNA/hAT_8	0.01774%	12.41	0.01905%	12.33	0.01641%	11.56	0.01716%	11.41	0.01464%	11.74	0.01562%	11.82	1.07	1.05	1.07
DNA/hAT_9	0.01641%	20.27	0.01727%	20.77	0.01421%	20.17	0.01441%	20.01	0.01244%	20.63	0.01228%	20.28	1.05	1.01	0.99
DNA/hAT-Charlie_1	0.12100%	2.76	0.12173%	2.77	0.12168%	2.72	0.11673%	2.71	0.12231%	2.75	0.12711%	2.77	1.01	0.96	1.04
DNA/hAT-Charlie_2	0.01576%	20.07	0.01001%	23.03	0.00803%	21.53	0.00694%	20.57	0.01848%	13.12	0.00798%	22.04	0.64	0.86	0.43
DNA/hAT-Tip100_1	0.04228%	6.10	0.03088%	7.90	0.05948%	4.41	0.06363%	3.71	0.02046%	10.71	0.01327%	14.32	0.73	1.07	0.65
DNA/IS3EU_1	0.01563%	12.33	0.01532%	12.56	0.01453%	11.65	0.01530%	11.39	0.01746%	11.76	0.01472%	11.99	0.98	1.05	0.84
DNA/ISRm11_1	0.05219%	4.05	0.04439%	4.33	0.05361%	3.75	0.05425%	3.89	0.01011%	8.06	0.02065%	5.37	0.85	1.01	2.04
DNA/Kolobok_1	0.05349%	2.18	0.05198%	2.23	0.04941%	2.4	0.05213%	2.23	0.05031%	2.1	0.05320%	2.09	0.97	1.05	1.06
DNA/Kolobok_10	0.00640%	5.68	0.00642%	5.62	0.00585%	5.33	0.00531%	5.46	0.00580%	5.46	0.00591%	5.29	1.00	0.91	1.02
DNA/Kolobok_11	0.00473%	16.85	0.01563%	29.28	0.00832%	22.77	0.00877%	23.66	0.00961%	22.41	0.00980%	22.11	3.30	1.05	1.02
DNA/Kolobok_12	0.00369%	19.30	0.00428%	20.26	0.00294%	21.62	0.00260%	19.41	0.00261%	21.37	0.00347%	21.45	1.16	0.88	1.33
DNA/Kolobok_13	0.00359%	6.03	0.00373%	5.95	0.00415%	5.2	0.00409%	5.24	0.00285%	6.02	0.00357%	5.48	1.04	0.99	1.25
DNA/Kolobok_14	0.00304%	18.99	0.00391%	23.37	0.00317%	18.03	0.00359%	15.88	0.00305%	16.44	0.00332%	19.27	1.29	1.13	1.09
DNA/Kolobok_15	0.00236%	22.72	0.00238%	23.50	0.00150%	23.4	0.00167%	23.36	0.00167%	23.77	0.00174%	22.91	1.01	1.11	1.04
DNA/Kolobok_16	0.00220%	13.55	0.00273%	19.05	0.00194%	10.3	0.00182%	10.99	0.00294%	6.47	0.00253%	9.17	1.24	0.94	0.86
DNA/Kolobok_17	0.00210%	4.96	0.00228%	4.98	0.00196%	5.33	0.00204%	5.78	0.00223%	5.63	0.00196%	5.54	1.08	1.04	0.88
DNA/Kolobok_18	0.00206%	7.86	0.00215%	7.65	0.00221%	6.84	0.00186%	7.1	0.00190%	7.32	0.00199%	7.2	1.04	0.84	1.05

DNA/Kolobok_19	0.00115%	9.99	0.00114%	10.89	0.00134%	8.1	0.00129%	6.8	0.00197%	7.06	0.00257%	5.42	0.99	0.97	1.31
DNA/Kolobok_2	0.04829%	6.26	0.04851%	5.87	0.04463%	5.26	0.04412%	5.04	0.03497%	6.23	0.04368%	5.46	1.00	0.99	1.25
DNA/Kolobok_20	0.00080%	13.58	0.00092%	14.08	0.00061%	16.35	0.00057%	15.24	0.00079%	15.39	0.00110%	15.01	1.14	0.93	1.40
DNA/Kolobok_3	0.03400%	2.32	0.03541%	1.50	0.03167%	2.23	0.03281%	2.03	0.03080%	2.61	0.03185%	2.53	1.04	1.04	1.03
DNA/Kolobok_4	0.03358%	3.43	0.03346%	3.91	0.02952%	3.21	0.03002%	3.1	0.02952%	3.29	0.02857%	3.35	1.00	1.02	0.97
DNA/Kolobok_5	0.02588%	1.95	0.02582%	2.07	0.02349%	2.52	0.02393%	2.5	0.02500%	2.23	0.02401%	2.37	1.00	1.02	0.96
DNA/Kolobok_6	0.01639%	15.92	0.01782%	16.20	0.01163%	14.2	0.01367%	12.92	0.01445%	11.64	0.01587%	11.46	1.09	1.17	1.10
DNA/Kolobok_7	0.01118%	3.90	0.01103%	3.69	0.00983%	3.04	0.01027%	3.09	0.01073%	3.21	0.01010%	2.94	0.99	1.04	0.94
DNA/Kolobok_8	0.00959%	23.51	0.01121%	24.50	0.00992%	25.61	0.01054%	25.07	0.01059%	24.98	0.01056%	24.51	1.17	1.06	1.00
DNA/Kolobok_9	0.00744%	20.48	0.00768%	20.45	0.00634%	18.98	0.00698%	19.08	0.00739%	17.42	0.00764%	18.06	1.03	1.10	1.03
DNA/m44_1	0.01066%	16.41	0.01250%	16.78	0.00987%	15.81	0.01004%	15.22	0.00978%	15.2	0.01039%	15.86	1.17	1.02	1.06
DNA/m44_2	0.01055%	10.19	0.00885%	11.48	0.00665%	9.95	0.00715%	10.16	0.00381%	12.55	0.00444%	11.74	0.84	1.07	1.17
DNA/m44_3	0.00901%	17.42	0.00954%	17.77	0.00840%	16.56	0.00815%	16	0.00883%	15.59	0.00806%	15.82	1.06	0.97	0.91
DNA/m44_4	0.00765%	10.47	0.00814%	12.68	0.00830%	7.74	0.00724%	8.67	0.00700%	8.78	0.00650%	8.23	1.06	0.87	0.93
DNA/m44_5	0.00729%	14.11	0.00798%	15.37	0.00709%	11.98	0.00656%	12.02	0.00710%	13.21	0.00645%	13.43	1.10	0.93	0.91
DNA/m44_6	0.00319%	12.46	0.00324%	15.16	0.00303%	10.02	0.00291%	10.8	0.00261%	11.44	0.00269%	9.93	1.02	0.96	1.03
DNA/m44_7	0.00116%	5.12	0.00098%	6.68	0.00069%	5.39	0.00085%	5.95	0.00047%	8.63	0.00070%	6.29	0.84	1.23	1.50
DNA/Mariner_1	0.16825%	7.31	0.17147%	7.42	0.15585%	6.87	0.15496%	6.9	0.16981%	6.85	0.14817%	6.95	1.02	0.99	0.87
DNA/Mariner_10	0.06267%	6.80	0.06442%	6.73	0.06147%	6.57	0.05984%	6.59	0.06447%	6.48	0.06220%	6.59	1.03	0.97	0.96
DNA/Mariner_100	0.00197%	9.03	0.00183%	8.99	0.00555%	8.4	0.00550%	8.56	0.00573%	8.17	0.00553%	8.38	0.93	0.99	0.97
DNA/Mariner_101	0.00193%	11.11	0.00209%	10.72	0.00329%	8.1	0.00246%	8.36	0.00106%	14.47	0.00123%	15.16	1.08	0.75	1.17
DNA/Mariner_102	0.00148%	14.35	0.00151%	15.80	0.00125%	11.65	0.00149%	12.51	0.00171%	11.9	0.00128%	12.46	1.02	1.19	0.75
DNA/Mariner_103	0.00135%	7.78	0.00150%	10.66	0.00096%	6.62	0.00135%	6.29	0.00111%	7.48	0.00096%	6.89	1.12	1.40	0.87
DNA/Mariner_104	0.00112%	15.41	0.00095%	15.37	0.00074%	14.58	0.00083%	13.59	0.00104%	13.83	0.00090%	15.43	0.84	1.12	0.86
DNA/Mariner_105	0.00102%	5.10	0.00083%	5.68	0.00126%	5.56	0.00111%	5.68	0.00039%	4.95	0.00054%	4.85	0.81	0.88	1.36
DNA/Mariner_106	0.00083%	9.51	0.00086%	11.08	0.00069%	8.3	0.00071%	11.63	0.00030%	16.46	0.00042%	11.85	1.04	1.03	1.39
DNA/Mariner_107	0.00081%	10.24	0.00080%	10.64	0.00056%	7.62	0.00061%	9.85	0.00037%	13	0.00036%	11.16	0.98	1.10	0.95
DNA/Mariner_108	0.00077%	18.38	0.00075%	22.04	0.00076%	12.42	0.00109%	11.57	0.00093%	17.67	0.00064%	17.48	0.98	1.44	0.68
DNA/Mariner_109	0.00063%	19.80	0.00064%	18.07	0.00063%	20.01	0.00057%	12.29	0.00074%	14.26	0.00056%	14.9	1.01	0.91	0.76
DNA/Mariner_11	0.06113%	8.14	0.06042%	8.36	0.04605%	8.05	0.04698%	8.01	0.04472%	8.4	0.04374%	8.43	0.99	1.02	0.98
DNA/Mariner_110	0.00029%	19.25	0.00024%	17.22	0.00038%	11.15	0.00026%	13.07	0.00040%	11.49	0.00041%	11.14	0.81	0.68	1.02

DNA/Mariner_12	0.05563%	6.70	0.05807%	6.75	0.05310%	5.84	0.05143%	5.93	0.05413%	5.88	0.05237%	5.96	1.04	0.97	0.97
DNA/Mariner_13	0.05278%	7.87	0.04654%	7.87	0.04425%	7.76	0.04231%	7.63	0.05829%	7.75	0.04304%	7.61	0.88	0.96	0.74
DNA/Mariner_14	0.05141%	6.21	0.05292%	6.37	0.03798%	5.98	0.03393%	6.05	0.04137%	6.24	0.03748%	6.14	1.03	0.89	0.91
DNA/Mariner_15	0.04970%	1.68	0.05004%	1.49	0.05185%	1.47	0.05211%	1.5	0.05335%	1.43	0.05180%	1.5	1.01	1.01	0.97
DNA/Mariner_16	0.04901%	10.35	0.04932%	10.36	0.04351%	9.21	0.04150%	9.29	0.04526%	9.15	0.04341%	9.23	1.01	0.95	0.96
DNA/Mariner_17	0.04863%	6.08	0.04663%	6.14	0.05828%	5.62	0.05629%	5.76	0.06704%	5.67	0.05857%	5.82	0.96	0.97	0.87
DNA/Mariner_18	0.04427%	20.58	0.04771%	20.53	0.05511%	19.55	0.05351%	19.92	0.04613%	19.56	0.03806%	19.16	1.08	0.97	0.83
DNA/Mariner_19	0.04240%	12.45	0.04246%	12.43	0.03898%	10.54	0.03678%	11.02	0.03574%	11.72	0.03470%	11.58	1.00	0.94	0.97
DNA/Mariner_2	0.16271%	3.57	0.16150%	3.83	0.14763%	3.47	0.14583%	3.54	0.15359%	3.43	0.14486%	3.57	0.99	0.99	0.94
DNA/Mariner_20	0.04220%	16.07	0.04304%	16.43	0.03669%	16.31	0.03592%	16.31	0.03438%	16.83	0.03562%	16.53	1.02	0.98	1.04
DNA/Mariner_21	0.04220%	4.60	0.04417%	4.67	0.04091%	4.72	0.04011%	4.65	0.04121%	4.73	0.03798%	4.7	1.05	0.98	0.92
DNA/Mariner_22	0.03796%	3.94	0.03536%	4.13	0.04374%	3.59	0.04138%	3.78	0.04562%	3.7	0.04096%	3.75	0.93	0.95	0.90
DNA/Mariner_23	0.03589%	6.83	0.03763%	6.93	0.03586%	4.75	0.03196%	4.59	0.03560%	4.6	0.03327%	4.61	1.05	0.89	0.93
DNA/Mariner_24	0.03253%	8.53	0.03122%	8.58	0.02168%	8.15	0.01934%	8.15	0.02153%	7.96	0.02049%	7.88	0.96	0.89	0.95
DNA/Mariner_25	0.03166%	15.79	0.03183%	15.85	0.03153%	15.36	0.03011%	15.21	0.03183%	15.45	0.02935%	15.28	1.01	0.96	0.92
DNA/Mariner_26	0.03018%	10.89	0.02858%	11.11	0.02724%	11.21	0.02545%	11.12	0.02777%	11.28	0.02663%	11.19	0.95	0.93	0.96
DNA/Mariner_27	0.02941%	9.92	0.02896%	9.91	0.02735%	8.27	0.02510%	9.21	0.02682%	8.09	0.02599%	8.5	0.98	0.92	0.97
DNA/Mariner_28	0.02897%	7.20	0.03273%	7.71	0.02784%	6.22	0.02926%	6.62	0.02767%	6.28	0.02938%	6.33	1.13	1.05	1.06
DNA/Mariner_29	0.02629%	15.33	0.03138%	17.61	0.02284%	12.87	0.02211%	12.24	0.02213%	11.74	0.02228%	11.68	1.19	0.97	1.01
DNA/Mariner_3	0.09817%	5.37	0.10322%	5.51	0.09463%	4.68	0.09306%	4.76	0.09645%	4.71	0.09513%	4.86	1.05	0.98	0.99
DNA/Mariner_30	0.02480%	5.89	0.02529%	5.85	0.02187%	5.62	0.02041%	5.53	0.02226%	5.66	0.01937%	5.77	1.02	0.93	0.87
DNA/Mariner_31	0.02328%	16.10	0.02435%	15.80	0.02345%	15.9	0.02177%	15.6	0.02441%	16.05	0.02282%	15.98	1.05	0.93	0.94
DNA/Mariner_32	0.02325%	14.93	0.02430%	14.90	0.02177%	14.61	0.02041%	14.74	0.02253%	14.68	0.02056%	14.62	1.05	0.94	0.91
DNA/Mariner_33	0.02274%	7.81	0.02220%	7.82	0.02374%	6.39	0.02214%	6.28	0.02453%	6.49	0.02195%	6.4	0.98	0.93	0.89
DNA/Mariner_34	0.02257%	10.19	0.02288%	10.58	0.01972%	9.66	0.01990%	10.29	0.02194%	9.64	0.01899%	10.09	1.01	1.01	0.87
DNA/Mariner_35	0.02016%	11.41	0.02155%	11.53	0.01725%	10.06	0.01769%	9.35	0.01683%	10.29	0.01764%	9.71	1.07	1.03	1.05
DNA/Mariner_36	0.02013%	12.19	0.02199%	14.12	0.01790%	10.53	0.01689%	10.19	0.01794%	10.26	0.01765%	10.03	1.09	0.94	0.98
DNA/Mariner_37	0.02013%	11.03	0.02361%	13.32	0.01733%	10.12	0.01574%	9.37	0.01695%	9.53	0.01762%	9.46	1.17	0.91	1.04
DNA/Mariner_38	0.01956%	15.22	0.01964%	16.34	0.01691%	15.37	0.01828%	14.74	0.01505%	18.18	0.01516%	16.86	1.00	1.08	1.01
DNA/Mariner_39	0.01850%	22.59	0.01575%	23.14	0.01402%	20.94	0.01412%	20.36	0.01288%	23.62	0.01261%	23.37	0.85	1.01	0.98
DNA/Mariner_4	0.08590%	2.85	0.05943%	4.33	0.12386%	2.32	0.13774%	1.97	0.03354%	4.92	0.01945%	6	0.69	1.11	0.58

DNA/Mariner_40	0.01743%	8.43	0.01821%	8.46	0.01642%	7.58	0.01612%	7.72	0.01613%	8.1	0.01614%	7.88	1.04	0.98	1.00
DNA/Mariner_41	0.01740%	3.22	0.01695%	3.36	0.01607%	3.38	0.01527%	3.42	0.01657%	3.55	0.01571%	3.7	0.97	0.95	0.95
DNA/Mariner_42	0.01725%	18.14	0.01825%	18.80	0.01563%	17.3	0.01747%	16.13	0.00967%	19.55	0.00986%	18.51	1.06	1.12	1.02
DNA/Mariner_43	0.01647%	11.43	0.01634%	12.33	0.01487%	11.29	0.01546%	11.39	0.01486%	10.89	0.01557%	10.84	0.99	1.04	1.05
DNA/Mariner_44	0.01632%	14.70	0.01583%	15.45	0.01397%	14.58	0.01363%	14.05	0.01335%	13.89	0.01437%	14.08	0.97	0.98	1.08
DNA/Mariner_45	0.01625%	11.09	0.01532%	11.52	0.01408%	8.77	0.01555%	8.33	0.01304%	8.36	0.01315%	8.94	0.94	1.10	1.01
DNA/Mariner_46	0.01616%	6.17	0.01793%	6.88	0.01689%	4.86	0.01566%	5.21	0.01785%	5.49	0.01570%	5.42	1.11	0.93	0.88
DNA/Mariner_47	0.01484%	26.31	0.01529%	26.72	0.01031%	22.48	0.00963%	23.12	0.00771%	21.95	0.00814%	22.19	1.03	0.93	1.06
DNA/Mariner_48	0.01456%	10.47	0.01599%	10.95	0.01413%	9.63	0.01434%	9.98	0.01276%	9.91	0.01422%	9.35	1.10	1.01	1.11
DNA/Mariner_49	0.01449%	15.98	0.01535%	16.18	0.01331%	15.96	0.01290%	15.97	0.01382%	15.94	0.01307%	15.83	1.06	0.97	0.95
DNA/Mariner_5	0.07945%	7.44	0.08098%	7.62	0.08488%	7.2	0.08550%	7.15	0.09101%	7.1	0.08549%	7.14	1.02	1.01	0.94
DNA/Mariner_50	0.01392%	10.38	0.01485%	10.60	0.01163%	10.33	0.01033%	10.19	0.01195%	10.5	0.01064%	10.4	1.07	0.89	0.89
DNA/Mariner_51	0.01374%	11.18	0.01526%	11.49	0.01333%	10.69	0.01331%	9.54	0.01296%	9.7	0.01397%	9.72	1.11	1.00	1.08
DNA/Mariner_52	0.01356%	27.46	0.01611%	28.31	0.01008%	26.27	0.01002%	25.71	0.01007%	27.39	0.00958%	27.27	1.19	0.99	0.95
DNA/Mariner_53	0.01350%	3.76	0.01399%	3.75	0.01483%	3.99	0.01368%	3.89	0.01485%	3.82	0.01471%	3.95	1.04	0.92	0.99
DNA/Mariner_54	0.01302%	9.82	0.01311%	9.98	0.01337%	9.56	0.01340%	8.97	0.01359%	9.31	0.01311%	9.52	1.01	1.00	0.96
DNA/Mariner_55	0.01278%	17.36	0.01321%	18.15	0.02429%	13.37	0.02417%	13.51	0.02308%	14	0.02355%	14.05	1.03	0.99	1.02
DNA/Mariner_56	0.01224%	15.08	0.01337%	16.35	0.01124%	13.44	0.01162%	13.22	0.01131%	13.62	0.01097%	13.61	1.09	1.03	0.97
DNA/Mariner_57	0.01199%	14.68	0.01264%	15.69	0.00963%	13.09	0.01068%	13.93	0.01034%	13.14	0.01054%	13.7	1.05	1.11	1.02
DNA/Mariner_58	0.01168%	8.54	0.01297%	9.20	0.00961%	7.93	0.00936%	8.2	0.00896%	8.19	0.00947%	8.05	1.11	0.97	1.06
DNA/Mariner_59	0.01145%	11.54	0.01383%	14.57	0.00916%	10.76	0.01122%	9.15	0.00846%	10.54	0.00853%	10.82	1.21	1.22	1.01
DNA/Mariner_6	0.07439%	10.83	0.07586%	10.72	0.07269%	10.9	0.06929%	10.56	0.07497%	10.65	0.07156%	10.67	1.02	0.95	0.95
DNA/Mariner_60	0.01100%	12.94	0.01067%	13.35	0.01076%	9.83	0.00863%	10.03	0.00951%	10.13	0.01039%	10.42	0.97	0.80	1.09
DNA/Mariner_61	0.01089%	13.03	0.01123%	13.88	0.01004%	11.58	0.00904%	11.87	0.01042%	12.67	0.00906%	12.65	1.03	0.90	0.87
DNA/Mariner_62	0.01052%	9.46	0.01128%	9.52	0.00985%	8.6	0.00967%	7.94	0.00906%	8.37	0.00916%	8.52	1.07	0.98	1.01
DNA/Mariner_63	0.01013%	7.78	0.01058%	9.24	0.00956%	6.98	0.01043%	6.59	0.00957%	6.86	0.00960%	6.89	1.04	1.09	1.00
DNA/Mariner_64	0.00996%	8.51	0.00982%	8.33	0.01167%	7.68	0.01131%	8.34	0.01208%	8.22	0.01091%	8.1	0.99	0.97	0.90
DNA/Mariner_65	0.00989%	18.60	0.01125%	19.99	0.00902%	16.35	0.00908%	15.77	0.00874%	17.08	0.00879%	16	1.14	1.01	1.01
DNA/Mariner_66	0.00945%	13.80	0.01058%	17.31	0.00982%	12.35	0.00865%	14.52	0.00499%	18.32	0.00593%	15.79	1.12	0.88	1.19
DNA/Mariner_67	0.00922%	9.92	0.00924%	10.26	0.01008%	8.42	0.00866%	9.59	0.00932%	9.45	0.00937%	9.12	1.00	0.86	1.01
DNA/Mariner_68	0.00921%	11.33	0.00918%	11.60	0.00746%	10.61	0.00767%	10.76	0.00753%	10.86	0.00778%	11.01	1.00	1.03	1.03

DNA/Mariner_69	0.00895%	8.71	0.00983%	9.50	0.00967%	6.68	0.00971%	7.22	0.00711%	9.93	0.00800%	9.29	1.10	1.00	1.13
DNA/Mariner_7	0.07128%	10.38	0.07573%	11.42	0.06169%	9.35	0.06160%	8.75	0.05889%	9.81	0.05594%	9.84	1.06	1.00	0.95
DNA/Mariner_70	0.00879%	16.15	0.00853%	16.10	0.00796%	15.88	0.00916%	16.07	0.00860%	16.03	0.00862%	16.63	0.97	1.15	1.00
DNA/Mariner_71	0.00765%	26.07	0.00818%	26.38	0.00593%	23.78	0.00515%	24.47	0.00568%	26.82	0.00484%	26.53	1.07	0.87	0.85
DNA/Mariner_72	0.00757%	14.05	0.00770%	14.32	0.00651%	12.9	0.00673%	12.42	0.00645%	12.96	0.00691%	12.73	1.02	1.03	1.07
DNA/Mariner_73	0.00737%	14.76	0.00745%	15.60	0.00644%	15.35	0.00551%	15.02	0.00465%	16.44	0.00456%	16.51	1.01	0.86	0.98
DNA/Mariner_74	0.00733%	21.96	0.00751%	22.05	0.00625%	21.38	0.00571%	21.51	0.00662%	21.32	0.00577%	21.52	1.02	0.91	0.87
DNA/Mariner_75	0.00715%	8.45	0.00610%	10.80	0.00494%	10.09	0.00516%	9.94	0.00198%	14.66	0.00292%	12.86	0.85	1.04	1.47
DNA/Mariner_76	0.00701%	10.73	0.00729%	11.77	0.00643%	11.52	0.00619%	10.46	0.00639%	9.99	0.00600%	10.48	1.04	0.96	0.94
DNA/Mariner_77	0.00675%	14.46	0.00697%	14.65	0.00614%	11.15	0.00516%	11.97	0.00519%	12.17	0.00527%	11.41	1.03	0.84	1.02
DNA/Mariner_78	0.00590%	15.73	0.00639%	16.55	0.00481%	13.98	0.00467%	12.64	0.00485%	12.92	0.00508%	14.08	1.08	0.97	1.05
DNA/Mariner_79	0.00542%	11.13	0.00504%	11.30	0.00484%	11.9	0.00440%	10.97	0.00290%	15.92	0.00298%	14.93	0.93	0.91	1.03
DNA/Mariner_8	0.06963%	2.61	0.07107%	2.75	0.06617%	2	0.06361%	2	0.06743%	2.03	0.06370%	2.09	1.02	0.96	0.94
DNA/Mariner_80	0.00512%	16.43	0.00507%	18.75	0.00514%	11.89	0.00442%	13.18	0.00473%	12.56	0.00399%	14.78	0.99	0.86	0.84
DNA/Mariner_81	0.00509%	12.13	0.00536%	13.13	0.00471%	11.64	0.00441%	10.92	0.00466%	11.87	0.00526%	10.83	1.05	0.94	1.13
DNA/Mariner_82	0.00507%	4.85	0.00512%	5.69	0.00550%	4.89	0.00534%	5.25	0.00376%	6.14	0.00467%	5.68	1.01	0.97	1.24
DNA/Mariner_83	0.00432%	8.75	0.00471%	8.85	0.00229%	9.65	0.00323%	9.63	0.00333%	10.05	0.00244%	9.99	1.09	1.41	0.73
DNA/Mariner_84	0.00413%	12.29	0.00505%	12.06	0.00514%	8.7	0.00514%	8.28	0.00230%	14.46	0.00253%	13.53	1.22	1.00	1.10
DNA/Mariner_85	0.00406%	23.71	0.00414%	24.68	0.00278%	18.84	0.00263%	19.62	0.00220%	22.77	0.00208%	21.93	1.02	0.95	0.94
DNA/Mariner_86	0.00405%	13.37	0.00423%	13.59	0.00464%	12.81	0.00483%	11.82	0.00401%	12.43	0.00373%	13.22	1.05	1.04	0.93
DNA/Mariner_87	0.00389%	6.50	0.00474%	5.95	0.00418%	6.47	0.00404%	6.29	0.00347%	6.56	0.00413%	6.5	1.22	0.97	1.19
DNA/Mariner_88	0.00383%	5.48	0.00401%	5.51	0.00438%	4.65	0.00376%	5.03	0.00486%	4.9	0.00402%	4.87	1.05	0.86	0.83
DNA/Mariner_89	0.00366%	7.42	0.00399%	7.29	0.00323%	7.4	0.00300%	7.27	0.00306%	6.6	0.00334%	6.96	1.09	0.93	1.09
DNA/Mariner_9	0.06946%	5.36	0.06976%	5.41	0.07117%	5.24	0.07077%	5.14	0.07468%	5.14	0.06882%	5.13	1.00	0.99	0.92
DNA/Mariner_90	0.00318%	10.23	0.00286%	12.28	0.00219%	13.42	0.00193%	12.42	0.00140%	16.97	0.00162%	14.04	0.90	0.88	1.16
DNA/Mariner_91	0.00316%	23.28	0.00014%	27.21	0.00014%	19.64	0.00005%	28.64	0.00645%	8.4	0.00007%	19.03	0.04	0.35	0.01
DNA/Mariner_92	0.00284%	19.38	0.00274%	19.31	0.00252%	19.63	0.00257%	18.09	0.00269%	19.08	0.00263%	18.67	0.96	1.02	0.98
DNA/Mariner_93	0.00279%	9.28	0.00226%	7.11	0.00161%	5.22	0.00203%	4.92	0.00183%	5.64	0.00193%	5.94	0.81	1.26	1.06
DNA/Mariner_94	0.00253%	22.59	0.00275%	24.69	0.00151%	22.58	0.00137%	20.44	0.00117%	22.97	0.00127%	21.35	1.09	0.90	1.08
DNA/Mariner_95	0.00224%	15.41	0.00217%	14.17	0.00199%	12	0.00247%	10.23	0.00256%	11.59	0.00256%	11.51	0.97	1.24	1.00
DNA/Mariner_96	0.00223%	8.89	0.00230%	8.35	0.00232%	6.36	0.00211%	6.66	0.00243%	6.47	0.00186%	7.26	1.03	0.91	0.76

DNA/Mariner_97	0.00212%	12.11	0.00234%	12.35	0.00175%	10.85	0.00183%	11.67	0.00159%	11.79	0.00176%	11.35	1.10	1.04	1.10
DNA/Mariner_98	0.00203%	11.07	0.00195%	11.22	0.00172%	12.62	0.00147%	11.9	0.00145%	12.29	0.00141%	12.58	0.96	0.85	0.97
DNA/Mariner_99	0.00202%	11.23	0.00196%	11.71	0.00124%	11.75	0.00120%	10.55	0.00145%	10.97	0.00141%	10.61	0.97	0.97	0.98
DNA/Maverick_1	1.69682%	1.04	1.62599%	1.08	1.46931%	1.04	1.40493%	1	1.74331%	0.99	1.39048%	1.07	0.96	0.96	0.80
DNA/Maverick_10	0.04681%	8.23	0.04421%	8.39	0.04016%	8.49	0.04067%	8.86	0.04658%	8.23	0.03941%	8.42	0.94	1.01	0.85
DNA/Maverick_11	0.03914%	3.79	0.03965%	3.82	0.04093%	3.69	0.03976%	3.78	0.04501%	3.32	0.04253%	3.53	1.01	0.97	0.94
DNA/Maverick_12	0.03875%	5.85	0.03889%	6.43	0.03985%	6.31	0.04008%	6.16	0.04250%	5.07	0.04171%	5.89	1.00	1.01	0.98
DNA/Maverick_13	0.03685%	4.80	0.03774%	4.66	0.03739%	4.71	0.03470%	4.36	0.03947%	4.71	0.03734%	4.79	1.02	0.93	0.95
DNA/Maverick_14	0.03641%	5.75	0.03837%	5.69	0.03198%	5.5	0.03262%	5.62	0.03385%	5.52	0.03338%	5.69	1.05	1.02	0.99
DNA/Maverick_15	0.03408%	11.56	0.03735%	11.93	0.03403%	11.45	0.03348%	11.38	0.04063%	11.07	0.03448%	11.25	1.10	0.98	0.85
DNA/Maverick_16	0.03275%	4.87	0.03232%	4.99	0.03207%	4.83	0.03113%	5.27	0.03835%	4.81	0.03307%	5.17	0.99	0.97	0.86
DNA/Maverick_17	0.03237%	7.56	0.03553%	7.42	0.02924%	7.92	0.02802%	7.03	0.03062%	7.19	0.02768%	7.4	1.10	0.96	0.90
DNA/Maverick_18	0.02949%	2.09	0.02872%	2.16	0.02511%	2.29	0.02351%	2.27	0.02891%	2.21	0.02575%	2.21	0.97	0.94	0.89
DNA/Maverick_19	0.02846%	7.73	0.02828%	8.71	0.03030%	5.83	0.02980%	6.06	0.01359%	12.61	0.01866%	10.35	0.99	0.98	1.37
DNA/Maverick_2	0.37211%	4.99	0.37657%	4.95	0.37791%	4.69	0.36332%	4.57	0.38603%	4.46	0.36951%	4.67	1.01	0.96	0.96
DNA/Maverick_20	0.02728%	0.45	0.01721%	0.71	0.07524%	0.87	0.03645%	1.05	0.02692%	0.94	0.04241%	0.68	0.63	0.48	1.58
DNA/Maverick_21	0.02689%	6.04	0.02647%	6.37	0.02686%	5.63	0.02744%	5.39	0.02936%	5.22	0.02914%	5.51	0.98	1.02	0.99
DNA/Maverick_22	0.02603%	4.37	0.02653%	4.54	0.02355%	4.07	0.02409%	4.16	0.02903%	4.24	0.02429%	4.23	1.02	1.02	0.84
DNA/Maverick_23	0.02011%	6.35	0.01927%	6.48	0.01914%	6.27	0.02009%	6.07	0.02258%	6.16	0.02079%	6.2	0.96	1.05	0.92
DNA/Maverick_24	0.01958%	4.49	0.02132%	4.43	0.01739%	3.95	0.01855%	3.89	0.01952%	3.82	0.01757%	4.29	1.09	1.07	0.90
DNA/Maverick_25	0.01706%	6.89	0.01620%	6.88	0.01586%	5.43	0.01558%	5.53	0.01852%	5.24	0.01580%	5.69	0.95	0.98	0.85
DNA/Maverick_26	0.01360%	8.48	0.01319%	9.65	0.01548%	6.52	0.01347%	7.32	0.00747%	14.21	0.00855%	12.35	0.97	0.87	1.14
DNA/Maverick_27	0.00991%	10.24	0.00963%	10.50	0.01188%	9.31	0.01071%	9.71	0.00714%	16.39	0.00738%	14	0.97	0.90	1.03
DNA/Maverick_28	0.00951%	3.97	0.00993%	3.97	0.00853%	4.77	0.00924%	4.24	0.00917%	4.45	0.00931%	4.29	1.04	1.08	1.02
DNA/Maverick_29	0.00937%	3.63	0.00913%	3.79	0.01023%	3.89	0.01022%	3.64	0.01060%	4	0.01002%	3.85	0.97	1.00	0.94
DNA/Maverick_3	0.27634%	7.72	0.28600%	7.78	0.26397%	7.06	0.25998%	7.14	0.27275%	7.06	0.26261%	7.08	1.03	0.98	0.96
DNA/Maverick_30	0.00878%	5.05	0.00875%	4.89	0.00839%	6.45	0.00730%	6.32	0.00884%	6.04	0.00813%	6.3	1.00	0.87	0.92
DNA/Maverick_31	0.00850%	9.98	0.00875%	10.92	0.00894%	7.1	0.00847%	7.43	0.00441%	14.74	0.00550%	11.5	1.03	0.95	1.25
DNA/Maverick_32	0.00556%	7.28	0.00566%	7.35	0.00397%	7.63	0.00466%	7.63	0.00503%	7.78	0.00467%	8.31	1.02	1.18	0.93
DNA/Maverick_33	0.00513%	13.99	0.00486%	14.72	0.00472%	12.49	0.00489%	11.68	0.00502%	12.24	0.00482%	12.22	0.95	1.04	0.96
DNA/Maverick_34	0.00330%	7.79	0.00316%	7.46	0.00392%	7.75	0.00384%	7.9	0.00417%	7.13	0.00379%	7.44	0.96	0.98	0.91

DNA/Maverick_35	0.00283%	16.82	0.00304%	16.31	0.00184%	17.13	0.00218%	14	0.00228%	11.24	0.00246%	13.56	1.08	1.19	1.08
DNA/Maverick_36	0.00206%	5.61	0.00189%	6.13	0.00255%	4.92	0.00196%	5.33	0.00107%	11.09	0.00124%	5.94	0.92	0.77	1.16
DNA/Maverick_37	0.00184%	4.52	0.00167%	4.01	0.00233%	4.72	0.00206%	5.1	0.00093%	8.61	0.00108%	7.4	0.90	0.88	1.16
DNA/Maverick_38	0.00103%	14.06	0.00104%	14.20	0.00079%	15.7	0.00096%	13.74	0.00083%	12.41	0.00106%	12.15	1.00	1.21	1.28
DNA/Maverick_39	0.00103%	17.09	0.00112%	14.69	0.00097%	19.95	0.00060%	14.81	0.00087%	17.7	0.00103%	17.41	1.09	0.62	1.17
DNA/Maverick_4	0.13192%	4.13	0.13954%	4.13	0.11886%	3.66	0.12312%	3.62	0.12500%	3.82	0.11931%	3.84	1.06	1.04	0.95
DNA/Maverick_40	0.00076%	15.17	0.00079%	14.03	0.00058%	13.09	0.00042%	12.2	0.00061%	10.92	0.00057%	10.62	1.04	0.73	0.95
DNA/Maverick_41	0.00054%	9.64	0.00062%	9.15	0.00047%	7.77	0.00046%	5.99	0.00067%	8.96	0.00054%	7.72	1.16	0.98	0.81
DNA/Maverick_42	0.00029%	11.52	0.00041%	8.40	0.00017%	12.25	0.00029%	7.74	0.00027%	7.98	0.00020%	10.34	1.40	1.69	0.76
DNA/Maverick_5	0.07464%	19.14	0.06069%	18.49	0.07449%	16.85	0.07133%	17.22	0.07342%	17.75	0.06751%	17.51	0.81	0.96	0.92
DNA/Maverick_6	0.06509%	4.33	0.06431%	4.40	0.04431%	4.59	0.04314%	4.42	0.04459%	4.27	0.04412%	4.61	0.99	0.97	0.99
DNA/Maverick_7	0.05852%	5.15	0.06354%	5.28	0.06450%	4.78	0.06524%	4.6	0.06594%	4.4	0.06489%	4.76	1.09	1.01	0.98
DNA/Maverick_8	0.05263%	5.87	0.05284%	6.03	0.05177%	5.96	0.05509%	5.75	0.05183%	5.86	0.05778%	6.03	1.00	1.06	1.11
DNA/Maverick_9	0.05058%	6.19	0.05131%	6.27	0.04045%	6.61	0.04073%	6.67	0.05391%	5.71	0.04733%	6.1	1.01	1.01	0.88
DNA/MULE_1	0.05198%	14.85	0.05505%	15.46	0.05255%	13.9	0.05180%	14.23	0.05046%	14.44	0.05311%	14.25	1.06	0.99	1.05
DNA/MULE_2	0.00568%	13.26	0.00589%	13.77	0.00579%	10.94	0.00500%	10.76	0.00484%	10.71	0.00527%	11.05	1.04	0.86	1.09
DNA/MULE_3	0.00495%	9.96	0.00645%	9.21	0.00456%	10.27	0.00527%	9.48	0.00405%	9.5	0.00573%	9.41	1.30	1.16	1.41
DNA/MULE_4	0.00383%	10.20	0.00425%	10.71	0.00541%	10.02	0.00559%	10.89	0.00434%	11.61	0.00497%	11.99	1.11	1.03	1.14
DNA/MULE_5	0.00202%	6.15	0.00205%	7.35	0.00187%	6.23	0.00207%	5.76	0.00126%	6.6	0.00197%	5.82	1.01	1.11	1.57
DNA/MULE_6	0.00068%	11.04	0.00071%	11.81	0.00068%	9.44	0.00086%	12.47	0.00034%	11.18	0.00063%	10.24	1.05	1.28	1.86
DNA/MULE_7	0.00044%	21.83	0.00090%	22.84	0.00037%	18.19	0.00062%	17.24	0.00035%	17.49	0.00056%	18.21	2.05	1.66	1.58
DNA/MULE_8	0.00034%	5.62	0.00035%	6.74	0.00053%	3.73	0.00049%	5.52	0.00033%	5.77	0.00046%	7.03	1.02	0.92	1.39
DNA/P_1	0.00014%	6.69	0.00020%	4.96	0.00029%	2.42	0.00019%	3.23	0.00020%	1.95	0.00028%	4.3	1.46	0.65	1.35
DNA/PIF_1	0.02068%	6.93	0.02240%	7.16	0.01925%	6.42	0.01915%	6.05	0.01734%	6.72	0.01977%	6.59	1.08	0.99	1.14
DNA/PIF_2	0.00720%	13.46	0.00733%	13.40	0.00634%	12.89	0.00633%	12.95	0.00553%	12.84	0.00616%	13.42	1.02	1.00	1.11
DNA/PIF_3	0.00306%	12.96	0.00361%	13.40	0.00298%	12.16	0.00301%	12.6	0.00302%	13.51	0.00318%	12.74	1.18	1.01	1.05
DNA/PIF_4	0.00194%	7.58	0.00195%	7.39	0.00171%	6.9	0.00217%	5.16	0.00140%	8.36	0.00159%	7.9	1.00	1.27	1.13
DNA/PiggyBac_1	0.05335%	15.87	0.05315%	16.53	0.04675%	14.34	0.04488%	14.38	0.03912%	15.2	0.04791%	15.08	1.00	0.96	1.22
DNA/PiggyBac_2	0.00619%	15.81	0.00733%	16.66	0.00619%	16.02	0.00602%	15.79	0.00624%	15.36	0.00674%	15.42	1.18	0.97	1.08
DNA/PiggyBac_3	0.00511%	16.65	0.00536%	17.34	0.00420%	13.96	0.00395%	14.22	0.00454%	13.61	0.00419%	14.28	1.05	0.94	0.92
DNA/PiggyBac_4	0.00506%	19.16	0.00571%	20.04	0.00438%	18.87	0.00458%	18.7	0.00503%	18.11	0.00490%	17.39	1.13	1.05	0.97

DNA/Pogo_1	0.00153%	6.86	0.00142%	7.73	0.00186%	5.83	0.00178%	6.01	0.00153%	6.65	0.00157%	7.11	0.93	0.96	1.03
DNA/Sola_1	0.02671%	5.14	0.03161%	5.13	0.02738%	5.04	0.02841%	4.71	0.01919%	4.93	0.02749%	4.83	1.18	1.04	1.43
DNA/Sola_10	0.00274%	14.51	0.00268%	14.69	0.00255%	14.28	0.00196%	15.47	0.00179%	16.79	0.00236%	15.85	0.98	0.77	1.32
DNA/Sola_11	0.00269%	9.19	0.00282%	9.10	0.00244%	8.86	0.00228%	8.6	0.00239%	9.73	0.00259%	9.16	1.05	0.93	1.08
DNA/Sola_12	0.00194%	3.06	0.00152%	2.97	0.00186%	3.11	0.00150%	2.65	0.00043%	2.41	0.00093%	3.8	0.78	0.81	2.18
DNA/Sola_13	0.00187%	4.25	0.00168%	4.48	0.00168%	4.76	0.00147%	4.37	0.00059%	6.11	0.00079%	6.69	0.90	0.88	1.35
DNA/Sola_14	0.00168%	9.28	0.00162%	10.29	0.00138%	10.59	0.00172%	10.38	0.00095%	11.63	0.00126%	10.83	0.96	1.25	1.33
DNA/Sola_15	0.00033%	6.09	0.00050%	5.46	0.00047%	3.7	0.00050%	3.73	0.00017%	3.74	0.00033%	4.76	1.54	1.07	1.89
DNA/Sola_2	0.02228%	7.56	0.02250%	8.81	0.01939%	7.48	0.02396%	7.5	0.01126%	9.03	0.01660%	8.41	1.01	1.24	1.47
DNA/Sola_3	0.01133%	14.01	0.01064%	14.53	0.01788%	12.01	0.01873%	12.25	0.01768%	11.98	0.01784%	12.02	0.94	1.05	1.01
DNA/Sola_4	0.01023%	13.90	0.00983%	16.04	0.00819%	15.81	0.00935%	15.83	0.00583%	17.06	0.00780%	16.74	0.96	1.14	1.34
DNA/Sola_5	0.00612%	5.40	0.00607%	5.83	0.00431%	5.31	0.00456%	5.46	0.00363%	5.95	0.00440%	5.41	0.99	1.06	1.21
DNA/Sola_6	0.00551%	17.53	0.00547%	18.25	0.00429%	18.34	0.00393%	17.48	0.00370%	19.52	0.00431%	18.91	0.99	0.92	1.17
DNA/Sola_7	0.00527%	13.04	0.00472%	13.55	0.00385%	12.07	0.00389%	11.3	0.00290%	17.05	0.00371%	15.01	0.90	1.01	1.28
DNA/Sola_8	0.00441%	7.34	0.00521%	6.74	0.00505%	7.39	0.00470%	6.55	0.00362%	7.38	0.00445%	7	1.18	0.93	1.23
DNA/Sola_9	0.00401%	4.49	0.00386%	4.96	0.00321%	4.86	0.00400%	4.77	0.00262%	5.1	0.00296%	5.16	0.96	1.25	1.13
DNA/Tc1_1	0.35109%	7.56	0.35503%	7.74	0.33803%	6.94	0.32710%	6.89	0.36075%	6.91	0.32423%	7.01	1.01	0.97	0.90
DNA/Tc1_10	0.13955%	1.68	0.14882%	1.58	0.14148%	1.46	0.14026%	1.43	0.16240%	1.31	0.14467%	1.46	1.07	0.99	0.89
DNA/Tc1_100	0.01579%	5.94	0.01630%	6.13	0.01519%	3.96	0.01338%	4.44	0.01376%	4.37	0.01453%	4.76	1.03	0.88	1.06
DNA/Tc1_101	0.01553%	6.35	0.01517%	6.99	0.01758%	4.69	0.01600%	4.85	0.00555%	14.56	0.00796%	9.85	0.98	0.91	1.43
DNA/Tc1_102	0.01500%	25.64	0.01550%	26.04	0.01373%	24.71	0.01193%	24.29	0.01435%	24.64	0.01297%	24.87	1.03	0.87	0.90
DNA/Tc1_103	0.01495%	7.27	0.01334%	8.03	0.01098%	7.45	0.01204%	7.26	0.00910%	8.83	0.00975%	8.23	0.89	1.10	1.07
DNA/Tc1_104	0.01487%	6.48	0.01363%	6.83	0.01263%	5.22	0.01160%	5.33	0.01400%	5.26	0.01209%	5.44	0.92	0.92	0.86
DNA/Tc1_105	0.01447%	22.19	0.01465%	22.86	0.01274%	22.89	0.01287%	22.15	0.01321%	22.16	0.01211%	22.21	1.01	1.01	0.92
DNA/Tc1_106	0.01433%	12.34	0.01340%	13.97	0.01253%	12.58	0.01295%	11.31	0.00834%	17.29	0.00894%	16.28	0.94	1.03	1.07
DNA/Tc1_107	0.01427%	15.50	0.01545%	15.58	0.01401%	14.75	0.01475%	14.42	0.01294%	14.94	0.01407%	14.74	1.08	1.05	1.09
DNA/Tc1_108	0.01396%	5.36	0.01331%	6.32	0.01295%	4.65	0.01384%	4.58	0.00975%	6.32	0.01161%	4.93	0.95	1.07	1.19
DNA/Tc1_109	0.01395%	6.54	0.01385%	6.62	0.01300%	6.36	0.01183%	6.38	0.01239%	6.57	0.01298%	6.53	0.99	0.91	1.05
DNA/Tc1_11	0.13597%	10.56	0.13640%	10.66	0.13834%	10.41	0.13535%	10.29	0.14364%	10.4	0.13531%	10.44	1.00	0.98	0.94
DNA/Tc1_110	0.01312%	11.41	0.01260%	11.81	0.01384%	10.7	0.01348%	10.42	0.00970%	14.21	0.01062%	13.1	0.96	0.97	1.09
DNA/Tc1_111	0.01252%	22.58	0.01337%	23.08	0.00983%	21.46	0.00963%	20.75	0.00950%	22.42	0.00905%	21.95	1.07	0.98	0.95

DNA/Tc1_112	0.01214%	23.70	0.01350%	24.40	0.00847%	20.28	0.00858%	20.34	0.00899%	19.27	0.00767%	20.34	1.11	1.01	0.85
DNA/Tc1_113	0.01201%	18.36	0.01227%	19.55	0.00967%	17.16	0.00921%	17.9	0.00909%	19.38	0.00908%	18.45	1.02	0.95	1.00
DNA/Tc1_114	0.01185%	8.10	0.01187%	8.05	0.00932%	7.99	0.00838%	8.28	0.00949%	8.38	0.00867%	8.69	1.00	0.90	0.91
DNA/Tc1_115	0.01176%	6.37	0.01189%	6.39	0.01123%	5.8	0.01004%	5.93	0.01143%	5.67	0.01113%	5.96	1.01	0.89	0.97
DNA/Tc1_116	0.01166%	5.81	0.01144%	5.92	0.01209%	5.87	0.01169%	5.86	0.01113%	6.08	0.01173%	6.05	0.98	0.97	1.05
DNA/Tc1_117	0.01148%	13.23	0.01103%	14.00	0.00844%	13.07	0.00869%	13.12	0.00645%	16.62	0.00754%	15	0.96	1.03	1.17
DNA/Tc1_118	0.01145%	9.27	0.01095%	9.34	0.01057%	7.7	0.01032%	8.32	0.00931%	9.57	0.00885%	8.71	0.96	0.98	0.95
DNA/Tc1_119	0.01129%	10.63	0.01152%	11.08	0.00975%	10.38	0.00972%	10.35	0.00926%	11.33	0.00892%	11.19	1.02	1.00	0.96
DNA/Tc1_12	0.12823%	10.95	0.12120%	11.06	0.10619%	10.81	0.10677%	10.62	0.13709%	11.05	0.10987%	10.62	0.95	1.01	0.80
DNA/Tc1_120	0.01128%	8.14	0.01154%	8.32	0.01248%	7.5	0.01092%	7.08	0.01270%	7.25	0.01242%	7.54	1.02	0.87	0.98
DNA/Tc1_121	0.01126%	10.34	0.01119%	11.50	0.00851%	11.31	0.00781%	11.22	0.00561%	14.09	0.00697%	13.15	0.99	0.92	1.24
DNA/Tc1_122	0.01125%	12.63	0.01054%	13.52	0.01026%	12.07	0.01024%	11.79	0.01005%	12.52	0.00943%	12.38	0.94	1.00	0.94
DNA/Tc1_123	0.01112%	13.45	0.01055%	14.82	0.01301%	13.13	0.01280%	13.31	0.01119%	14.49	0.01207%	14.68	0.95	0.98	1.08
DNA/Tc1_124	0.01071%	10.37	0.01170%	10.11	0.00994%	9.15	0.00929%	9.65	0.01124%	9.58	0.01040%	9.96	1.09	0.93	0.93
DNA/Tc1_125	0.01050%	7.89	0.01092%	7.58	0.00925%	6.33	0.01071%	6.25	0.01132%	5.93	0.00992%	6.35	1.04	1.16	0.88
DNA/Tc1_126	0.01031%	17.57	0.01026%	16.94	0.00937%	17.53	0.00907%	18.18	0.00843%	20.36	0.00816%	19.73	0.99	0.97	0.97
DNA/Tc1_127	0.01029%	10.57	0.01058%	10.77	0.00907%	10.56	0.00764%	10.23	0.00910%	10.65	0.00892%	10.68	1.03	0.84	0.98
DNA/Tc1_128	0.00990%	12.49	0.01047%	14.31	0.00874%	13.32	0.00833%	13.23	0.00562%	17.58	0.00665%	15.97	1.06	0.95	1.18
DNA/Tc1_129	0.00988%	14.76	0.01384%	20.06	0.01107%	12.41	0.01128%	12.52	0.01210%	12.71	0.01091%	12.95	1.40	1.02	0.90
DNA/Tc1_13	0.12061%	2.06	0.12479%	2.18	0.11210%	1.8	0.11098%	1.72	0.13674%	1.55	0.11864%	1.74	1.03	0.99	0.87
DNA/Tc1_130	0.00983%	24.29	0.01223%	25.93	0.00758%	23.91	0.00850%	24.7	0.00825%	26.47	0.00738%	25.46	1.25	1.12	0.89
DNA/Tc1_131	0.00973%	8.97	0.00995%	8.88	0.00982%	8.28	0.01027%	8.35	0.01115%	8.38	0.01007%	8.45	1.02	1.05	0.90
DNA/Tc1_132	0.00961%	10.89	0.01003%	11.09	0.00974%	9.36	0.01037%	9.44	0.01058%	9.62	0.00989%	9.81	1.04	1.07	0.93
DNA/Tc1_133	0.00959%	5.47	0.00988%	5.31	0.00889%	5.18	0.00942%	5.02	0.00853%	5.43	0.00862%	5.37	1.03	1.06	1.01
DNA/Tc1_134	0.00958%	7.19	0.00996%	7.43	0.01187%	6.76	0.01111%	6.76	0.01223%	6.95	0.01070%	6.9	1.04	0.94	0.87
DNA/Tc1_135	0.00952%	13.02	0.00957%	12.87	0.00857%	11.75	0.00850%	11.6	0.00966%	11.71	0.00905%	11.94	1.01	0.99	0.94
DNA/Tc1_136	0.00933%	22.06	0.00932%	21.23	0.00713%	17.58	0.00680%	16.54	0.00698%	16.77	0.00706%	17.46	1.00	0.95	1.01
DNA/Tc1_137	0.00930%	14.69	0.01020%	14.33	0.00839%	13.68	0.00922%	13.26	0.00948%	13.38	0.00843%	13.71	1.10	1.10	0.89
DNA/Tc1_138	0.00911%	14.73	0.00894%	15.63	0.00762%	12.51	0.00870%	11.73	0.00435%	17.11	0.00594%	15.87	0.98	1.14	1.37
DNA/Tc1_139	0.00907%	17.20	0.01054%	16.91	0.00868%	14.13	0.00920%	14.25	0.00922%	13.05	0.00821%	14.4	1.16	1.06	0.89
DNA/Tc1_14	0.11764%	9.07	0.11680%	9.32	0.11955%	8.61	0.11496%	8.6	0.11159%	8.64	0.11495%	8.73	0.99	0.96	1.03

DNA/Tc1_140	0.00889%	11.23	0.00814%	11.30	0.00697%	10.13	0.00728%	9.95	0.00762%	10.75	0.00718%	10.16	0.92	1.04	0.94
DNA/Tc1_141	0.00885%	13.77	0.00935%	14.70	0.00827%	13.17	0.00794%	12.46	0.00521%	18.3	0.00581%	16.01	1.06	0.96	1.12
DNA/Tc1_142	0.00867%	10.62	0.00827%	10.46	0.00785%	10.42	0.00818%	10.55	0.00809%	10.55	0.00830%	10.64	0.95	1.04	1.03
DNA/Tc1_143	0.00856%	13.44	0.00892%	15.06	0.00666%	11.57	0.00735%	10.88	0.00703%	11.94	0.00689%	12.11	1.04	1.10	0.98
DNA/Tc1_144	0.00849%	11.40	0.00870%	11.45	0.00683%	10.68	0.00731%	10.62	0.00769%	10.61	0.00694%	10.55	1.02	1.07	0.90
DNA/Tc1_145	0.00844%	10.13	0.00869%	10.12	0.00678%	9.64	0.00653%	10.23	0.00687%	9.92	0.00641%	10.08	1.03	0.96	0.93
DNA/Tc1_146	0.00836%	17.59	0.00777%	17.89	0.00777%	14.36	0.00678%	14.48	0.00679%	16.53	0.00683%	16.09	0.93	0.87	1.01
DNA/Tc1_147	0.00816%	14.84	0.00834%	14.43	0.00899%	11.15	0.00798%	9.82	0.00859%	12.17	0.00788%	12.75	1.02	0.89	0.92
DNA/Tc1_148	0.00805%	7.79	0.00811%	7.57	0.01094%	7.53	0.01105%	7.19	0.01129%	7.81	0.01130%	7.45	1.01	1.01	1.00
DNA/Tc1_149	0.00801%	8.28	0.00868%	8.60	0.00796%	7.38	0.00692%	6.83	0.00816%	7.82	0.00717%	7.49	1.08	0.87	0.88
DNA/Tc1_15	0.11751%	13.24	0.11903%	13.25	0.09892%	12.07	0.09607%	11.91	0.10507%	12.06	0.10060%	12.09	1.01	0.97	0.96
DNA/Tc1_150	0.00796%	15.83	0.00801%	15.64	0.00654%	13.21	0.00595%	13.57	0.00554%	15.57	0.00495%	15.08	1.01	0.91	0.89
DNA/Tc1_151	0.00782%	9.26	0.00830%	9.31	0.00784%	8.7	0.00807%	8.54	0.00848%	8.17	0.00840%	8.43	1.06	1.03	0.99
DNA/Tc1_152	0.00770%	10.50	0.00635%	10.16	0.00343%	11.66	0.00323%	11.4	0.00911%	10.4	0.00308%	11.97	0.82	0.94	0.34
DNA/Tc1_153	0.00759%	19.97	0.00734%	20.39	0.00557%	18.93	0.00555%	18.18	0.00548%	17.63	0.00558%	18.61	0.97	1.00	1.02
DNA/Tc1_154	0.00712%	30.77	0.00919%	31.50	0.00595%	28.89	0.00620%	28.46	0.00631%	29.11	0.00519%	28.95	1.29	1.04	0.82
DNA/Tc1_155	0.00693%	16.38	0.00744%	15.55	0.00508%	11.73	0.00513%	11.33	0.00453%	17.73	0.00402%	15.38	1.07	1.01	0.89
DNA/Tc1_156	0.00689%	16.78	0.00667%	17.49	0.00512%	17.74	0.00540%	17.97	0.00431%	21.68	0.00468%	19.48	0.97	1.05	1.09
DNA/Tc1_157	0.00686%	11.78	0.00734%	12.15	0.00744%	11.26	0.00703%	11.31	0.00905%	10.82	0.00790%	10.59	1.07	0.94	0.87
DNA/Tc1_158	0.00671%	13.79	0.00627%	13.17	0.00555%	11.67	0.00521%	12.21	0.00434%	14.5	0.00421%	13.43	0.93	0.94	0.97
DNA/Tc1_159	0.00670%	12.94	0.00696%	13.48	0.00834%	10.41	0.00784%	9.69	0.00618%	12.8	0.00694%	11.81	1.04	0.94	1.12
DNA/Tc1_16	0.11617%	11.08	0.11502%	11.08	0.11644%	10.74	0.11034%	10.69	0.10943%	11.11	0.09958%	11.11	0.99	0.95	0.91
DNA/Tc1_160	0.00654%	2.90	0.00664%	2.45	0.00625%	1.47	0.00572%	1.48	0.00219%	4.05	0.00345%	2.95	1.02	0.92	1.58
DNA/Tc1_161	0.00641%	8.83	0.00642%	8.90	0.00704%	9.14	0.00642%	8.84	0.00671%	8.83	0.00697%	9.15	1.00	0.91	1.04
DNA/Tc1_162	0.00638%	19.53	0.00660%	20.43	0.00382%	18.31	0.00459%	17.42	0.00322%	20.78	0.00363%	19.53	1.03	1.20	1.13
DNA/Tc1_163	0.00635%	14.49	0.00658%	15.25	0.00478%	16	0.00494%	15.02	0.00466%	16.81	0.00443%	16.41	1.04	1.03	0.95
DNA/Tc1_164	0.00628%	8.56	0.00553%	10.40	0.00420%	9.53	0.00443%	8.76	0.00244%	14.01	0.00239%	10.44	0.88	1.06	0.98
DNA/Tc1_165	0.00628%	4.05	0.00490%	5.24	0.00332%	6.97	0.00411%	5.86	0.00229%	8.05	0.00313%	6.65	0.78	1.24	1.37
DNA/Tc1_166	0.00628%	10.82	0.00680%	11.36	0.00626%	10.09	0.00595%	10.63	0.00695%	10.22	0.00649%	10.52	1.08	0.95	0.93
DNA/Tc1_167	0.00599%	16.03	0.00573%	15.79	0.00424%	14.91	0.00452%	15.25	0.00411%	14.88	0.00430%	15.23	0.96	1.06	1.05
DNA/Tc1_168	0.00596%	18.67	0.00439%	18.00	0.00289%	16.9	0.00324%	16.44	0.00347%	17.07	0.00299%	17.17	0.74	1.12	0.86

DNA/Tc1_169	0.00596%	8.27	0.00619%	8.28	0.00568%	7.81	0.00530%	7.87	0.00597%	7.87	0.00566%	7.77	1.04	0.93	0.95
DNA/Tc1_17	0.11348%	7.61	0.11669%	7.61	0.10888%	7.26	0.10885%	7.14	0.11824%	7.14	0.11271%	7.25	1.03	1.00	0.95
DNA/Tc1_170	0.00591%	9.88	0.00503%	10.40	0.00395%	9.87	0.00378%	9.24	0.00878%	6.79	0.00404%	8.52	0.85	0.96	0.46
DNA/Tc1_171	0.00575%	9.85	0.00576%	10.44	0.00504%	9	0.00516%	9.28	0.00569%	9.24	0.00549%	9.3	1.00	1.02	0.96
DNA/Tc1_172	0.00555%	15.21	0.00503%	15.09	0.00511%	13.97	0.00503%	13.15	0.00447%	14.88	0.00491%	15.36	0.91	0.98	1.10
DNA/Tc1_173	0.00553%	9.30	0.00547%	9.32	0.00492%	8.72	0.00481%	9.02	0.00396%	10.83	0.00463%	10.49	0.99	0.98	1.17
DNA/Tc1_174	0.00548%	12.87	0.00525%	13.05	0.00548%	10.05	0.00518%	10.74	0.00592%	10.68	0.00453%	10.36	0.96	0.95	0.76
DNA/Tc1_175	0.00543%	5.96	0.00560%	6.91	0.00668%	4.51	0.00626%	5.11	0.00361%	7.73	0.00396%	6.46	1.03	0.94	1.09
DNA/Tc1_176	0.00542%	13.74	0.00558%	13.57	0.00439%	12.48	0.00516%	12.63	0.00597%	11.41	0.00478%	13.34	1.03	1.18	0.80
DNA/Tc1_177	0.00536%	11.74	0.00566%	12.96	0.00404%	12.58	0.00400%	11.33	0.00311%	15.01	0.00336%	13.99	1.06	0.99	1.08
DNA/Tc1_178	0.00535%	11.86	0.00485%	12.27	0.00521%	12.2	0.00418%	12.77	0.00332%	15.25	0.00334%	14.79	0.91	0.80	1.01
DNA/Tc1_179	0.00535%	23.54	0.00545%	23.91	0.00434%	20.27	0.00442%	21.74	0.00479%	21.41	0.00413%	22.44	1.02	1.02	0.86
DNA/Tc1_18	0.11291%	7.93	0.11635%	7.95	0.10968%	7.76	0.10656%	7.8	0.11079%	7.78	0.10712%	7.84	1.03	0.97	0.97
DNA/Tc1_180	0.00528%	6.88	0.00488%	6.43	0.00605%	6.94	0.00567%	6.59	0.00611%	6.11	0.00548%	6.34	0.92	0.94	0.90
DNA/Tc1_181	0.00508%	13.80	0.00442%	12.62	0.00452%	13.1	0.00446%	13.21	0.00356%	14.06	0.00385%	13.14	0.87	0.99	1.08
DNA/Tc1_182	0.00502%	12.72	0.00525%	13.64	0.00440%	12.53	0.00400%	12.19	0.00402%	13.13	0.00409%	13.04	1.05	0.91	1.02
DNA/Tc1_183	0.00488%	14.69	0.00444%	14.66	0.00366%	13.36	0.00354%	13.12	0.00454%	13.41	0.00350%	12.8	0.91	0.97	0.77
DNA/Tc1_184	0.00487%	11.92	0.00433%	12.42	0.00363%	9.51	0.00390%	9.28	0.00410%	11.37	0.00361%	11.38	0.89	1.07	0.88
DNA/Tc1_185	0.00485%	7.33	0.00471%	7.22	0.00441%	6.53	0.00440%	6.45	0.00448%	6.79	0.00405%	6.95	0.97	1.00	0.90
DNA/Tc1_186	0.00468%	5.99	0.00430%	5.72	0.00408%	5.6	0.00403%	5.91	0.00353%	5.85	0.00397%	5.84	0.92	0.99	1.12
DNA/Tc1_187	0.00466%	10.88	0.00490%	11.46	0.00362%	12.67	0.00355%	12.62	0.00288%	15.49	0.00328%	14.63	1.05	0.98	1.14
DNA/Tc1_188	0.00463%	7.77	0.00471%	8.24	0.00544%	5.76	0.00465%	6.01	0.00533%	5.38	0.00530%	4.91	1.02	0.86	0.99
DNA/Tc1_189	0.00455%	16.64	0.00510%	19.16	0.00390%	17.48	0.00384%	17.19	0.00315%	19.67	0.00338%	18.62	1.12	0.98	1.07
DNA/Tc1_19	0.10972%	5.52	0.11046%	5.61	0.11049%	5.18	0.10614%	5.08	0.11674%	5.13	0.10594%	5.18	1.01	0.96	0.91
DNA/Tc1_190	0.00445%	6.81	0.00382%	7.58	0.00313%	7.15	0.00293%	5.55	0.00120%	11.64	0.00202%	8.06	0.86	0.94	1.67
DNA/Tc1_191	0.00425%	16.65	0.00416%	16.57	0.00377%	15.27	0.00316%	14.34	0.00368%	14.68	0.00346%	14.74	0.98	0.84	0.94
DNA/Tc1_192	0.00424%	9.97	0.00447%	10.00	0.00391%	9.3	0.00374%	9.49	0.00392%	9.33	0.00385%	9.52	1.06	0.96	0.98
DNA/Tc1_193	0.00406%	16.70	0.00424%	18.80	0.00350%	17.63	0.00309%	16.56	0.00280%	19.38	0.00254%	19.36	1.04	0.88	0.91
DNA/Tc1_194	0.00406%	8.51	0.00398%	9.79	0.00242%	11.95	0.00246%	12.37	0.00157%	14.8	0.00220%	13.7	0.98	1.02	1.40
DNA/Tc1_195	0.00406%	12.35	0.00351%	13.39	0.00232%	12.22	0.00264%	11.02	0.00220%	13.32	0.00203%	13.48	0.87	1.14	0.92
DNA/Tc1_196	0.00403%	6.77	0.00434%	7.21	0.00239%	6.92	0.00325%	6.7	0.00314%	6.15	0.00316%	7.23	1.08	1.36	1.01

DNA/Tc1_197	0.00402%	5.78	0.00343%	6.79	0.00363%	4.2	0.00393%	3.64	0.00090%	14.52	0.00151%	8.63	0.85	1.08	1.69
DNA/Tc1_198	0.00397%	3.14	0.00370%	3.36	0.00074%	5.33	0.00092%	9.73	0.00138%	5.92	0.00093%	5.6	0.93	1.25	0.68
DNA/Tc1_199	0.00394%	11.16	0.00408%	11.55	0.00389%	10.85	0.00414%	11.39	0.00294%	13.08	0.00346%	12.4	1.04	1.07	1.18
DNA/Tc1_2	0.29743%	6.53	0.29963%	6.54	0.30158%	6.34	0.29021%	6.42	0.30130%	6.43	0.28522%	6.42	1.01	0.96	0.95
DNA/Tc1_20	0.09889%	6.44	0.09960%	6.58	0.09336%	6.2	0.08934%	6.16	0.09826%	6.1	0.08806%	6.32	1.01	0.96	0.90
DNA/Tc1_200	0.00394%	10.40	0.00358%	12.05	0.00286%	12.55	0.00324%	9.66	0.00149%	14.18	0.00180%	11.56	0.91	1.13	1.20
DNA/Tc1_201	0.00388%	7.87	0.00408%	7.45	0.00319%	6.78	0.00325%	6.77	0.00326%	6.61	0.00310%	7.02	1.05	1.02	0.95
DNA/Tc1_202	0.00382%	17.82	0.00366%	18.39	0.00328%	14.92	0.00313%	15.66	0.00244%	17.94	0.00260%	16.72	0.96	0.96	1.06
DNA/Tc1_203	0.00381%	7.91	0.00402%	7.96	0.00321%	7.56	0.00348%	6.94	0.00359%	7.95	0.00282%	7.79	1.06	1.09	0.79
DNA/Tc1_204	0.00367%	13.04	0.00380%	14.87	0.00305%	14.78	0.00297%	13.97	0.00308%	15.7	0.00289%	15.71	1.03	0.97	0.94
DNA/Tc1_205	0.00363%	15.34	0.00353%	17.58	0.00334%	14.21	0.00319%	14.89	0.00292%	17.54	0.00296%	15.06	0.97	0.96	1.01
DNA/Tc1_206	0.00360%	7.62	0.00339%	7.75	0.00349%	7.18	0.00307%	6.54	0.00243%	8.61	0.00252%	8.64	0.94	0.88	1.04
DNA/Tc1_207	0.00356%	10.29	0.00380%	10.30	0.00330%	9.16	0.00347%	9.73	0.00390%	9.5	0.00375%	9.47	1.07	1.05	0.96
DNA/Tc1_208	0.00351%	18.22	0.00450%	21.24	0.00384%	17.1	0.00388%	16.6	0.00263%	21.91	0.00299%	20.89	1.28	1.01	1.14
DNA/Tc1_209	0.00345%	6.76	0.00304%	7.35	0.00251%	6.95	0.00272%	7.08	0.00211%	7.95	0.00248%	7.31	0.88	1.09	1.18
DNA/Tc1_21	0.08720%	10.86	0.07541%	11.07	0.08739%	10.2	0.08460%	10.08	0.11232%	10.34	0.08668%	10.25	0.86	0.97	0.77
DNA/Tc1_210	0.00322%	21.54	0.00371%	20.66	0.00267%	19.18	0.00242%	21.21	0.00224%	23.96	0.00209%	21.41	1.15	0.90	0.93
DNA/Tc1_211	0.00322%	11.67	0.00292%	12.12	0.00558%	8.84	0.00613%	8.76	0.00668%	9.12	0.00518%	8.68	0.91	1.10	0.78
DNA/Tc1_212	0.00310%	14.74	0.00040%	13.42	0.00026%	19.47	0.00031%	12.6	0.00576%	9.36	0.00038%	12.8	0.13	1.17	0.07
DNA/Tc1_213	0.00310%	15.11	0.00368%	15.31	0.00319%	14.62	0.00364%	15.49	0.00304%	15.1	0.00336%	14.48	1.19	1.14	1.10
DNA/Tc1_214	0.00303%	6.87	0.00245%	7.45	0.00185%	7.9	0.00156%	7.37	0.00071%	9.31	0.00095%	10.15	0.81	0.84	1.32
DNA/Tc1_215	0.00302%	22.30	0.00382%	23.99	0.00263%	16.93	0.00238%	17.6	0.00210%	18.63	0.00222%	19.84	1.26	0.91	1.06
DNA/Tc1_216	0.00302%	8.08	0.00247%	7.93	0.00360%	8.68	0.00385%	8.44	0.00430%	8.32	0.00304%	8.78	0.82	1.07	0.71
DNA/Tc1_217	0.00291%	14.54	0.00295%	16.70	0.00243%	14.78	0.00191%	15.33	0.00200%	16.65	0.00186%	16.88	1.01	0.79	0.93
DNA/Tc1_218	0.00290%	11.68	0.00262%	10.57	0.00431%	10.15	0.00417%	10.33	0.00264%	17.72	0.00330%	14.22	0.90	0.97	1.25
DNA/Tc1_219	0.00286%	10.37	0.00314%	10.11	0.00311%	9.18	0.00313%	9.25	0.00361%	9.51	0.00308%	9.88	1.10	1.01	0.85
DNA/Tc1_22	0.08175%	10.65	0.08497%	10.61	0.07626%	8.7	0.07155%	8.39	0.07504%	8.27	0.07473%	8.61	1.04	0.94	1.00
DNA/Tc1_220	0.00282%	6.13	0.00247%	9.50	0.00192%	7.67	0.00169%	7.9	0.00117%	11.54	0.00114%	9.52	0.88	0.88	0.98
DNA/Tc1_221	0.00278%	17.75	0.00272%	18.23	0.00209%	19.43	0.00222%	16.16	0.00223%	17	0.00250%	15.54	0.98	1.06	1.12
DNA/Tc1_222	0.00276%	11.49	0.00271%	11.60	0.00127%	10.64	0.00121%	10.66	0.00121%	11.39	0.00134%	10.49	0.98	0.95	1.10
DNA/Tc1_223	0.00273%	12.67	0.00290%	14.07	0.00266%	14.27	0.00216%	12.71	0.00205%	16.32	0.00184%	17.97	1.06	0.81	0.89

DNA/Tc1_224	0.00268%	12.18	0.00267%	11.89	0.00271%	11.83	0.00273%	11.47	0.00278%	11.14	0.00257%	11.46	1.00	1.01	0.92
DNA/Tc1_225	0.00253%	11.86	0.00230%	10.76	0.00231%	10.42	0.00225%	11.58	0.00229%	11.57	0.00213%	11.91	0.91	0.97	0.93
DNA/Tc1_226	0.00232%	9.85	0.00192%	8.84	0.00230%	7.26	0.00198%	9.26	0.00200%	10.64	0.00190%	7.84	0.83	0.86	0.95
DNA/Tc1_227	0.00232%	1.70	0.00216%	2.37	0.00335%	2.35	0.00295%	1.41	0.00082%	3.98	0.00122%	2.85	0.93	0.88	1.49
DNA/Tc1_228	0.00229%	10.32	0.00214%	10.30	0.00272%	9.48	0.00227%	10.18	0.00202%	11.07	0.00223%	10.62	0.93	0.83	1.10
DNA/Tc1_229	0.00229%	9.95	0.00252%	9.61	0.00239%	10.58	0.00225%	10.56	0.00232%	11.35	0.00180%	10.58	1.10	0.94	0.78
DNA/Tc1_23	0.07761%	6.43	0.07914%	6.48	0.07662%	5.72	0.07716%	5.55	0.08462%	5.3	0.07500%	5.73	1.02	1.01	0.89
DNA/Tc1_230	0.00227%	8.39	0.00251%	8.46	0.00238%	7.75	0.00271%	8.05	0.00280%	7.2	0.00233%	7.68	1.10	1.14	0.83
DNA/Tc1_231	0.00223%	14.30	0.00227%	13.93	0.00161%	13.81	0.00151%	15.14	0.00165%	14.5	0.00179%	14.4	1.02	0.94	1.08
DNA/Tc1_232	0.00214%	13.89	0.00224%	14.37	0.00274%	13.95	0.00270%	13.09	0.00278%	12.33	0.00246%	13.35	1.05	0.98	0.88
DNA/Tc1_233	0.00214%	14.23	0.00224%	12.82	0.00188%	8.5	0.00173%	10.34	0.00075%	19.13	0.00110%	13.8	1.05	0.92	1.47
DNA/Tc1_234	0.00211%	8.60	0.00214%	9.73	0.00118%	8.14	0.00163%	6.49	0.00163%	6.49	0.00184%	5.8	1.01	1.38	1.13
DNA/Tc1_235	0.00210%	12.18	0.00189%	11.28	0.00163%	10.2	0.00159%	10.62	0.00119%	13.94	0.00111%	12.7	0.90	0.98	0.94
DNA/Tc1_236	0.00205%	17.83	0.00241%	22.07	0.00166%	15.95	0.00158%	15.97	0.00168%	15.85	0.00146%	14.84	1.17	0.95	0.87
DNA/Tc1_237	0.00203%	9.15	0.00221%	9.72	0.00211%	10.37	0.00190%	10.62	0.00197%	7.78	0.00173%	9.16	1.09	0.90	0.88
DNA/Tc1_238	0.00191%	5.08	0.00190%	5.13	0.00107%	5.26	0.00111%	5.22	0.00139%	4.66	0.00102%	5.3	1.00	1.04	0.73
DNA/Tc1_239	0.00188%	9.86	0.00180%	10.97	0.00208%	8.32	0.00201%	9.35	0.00158%	9.56	0.00146%	10.43	0.95	0.97	0.92
DNA/Tc1_24	0.06900%	19.04	0.07159%	19.13	0.06256%	17.71	0.06188%	17.84	0.06747%	17.83	0.06199%	17.82	1.04	0.99	0.92
DNA/Tc1_240	0.00186%	6.38	0.00193%	6.34	0.00213%	6.54	0.00166%	6.51	0.00177%	6.61	0.00187%	6.64	1.03	0.78	1.06
DNA/Tc1_241	0.00184%	7.85	0.00180%	8.55	0.00136%	6.54	0.00148%	9.31	0.00069%	16.95	0.00080%	10.93	0.98	1.09	1.15
DNA/Tc1_242	0.00178%	13.86	0.00161%	14.68	0.00138%	14.16	0.00153%	15.61	0.00086%	16.89	0.00097%	19.14	0.91	1.11	1.12
DNA/Tc1_243	0.00175%	9.46	0.00163%	9.30	0.00500%	15.12	0.00472%	16.57	0.00366%	19.8	0.00401%	18.09	0.93	0.94	1.10
DNA/Tc1_244	0.00172%	6.79	0.00166%	7.00	0.00207%	5.57	0.00185%	5.97	0.00234%	5.3	0.00167%	5.41	0.96	0.89	0.72
DNA/Tc1_245	0.00167%	8.42	0.00166%	8.17	0.00183%	8.44	0.00154%	7.64	0.00193%	8.58	0.00156%	8.45	0.99	0.84	0.81
DNA/Tc1_246	0.00157%	9.67	0.00139%	11.00	0.00211%	9.25	0.00212%	9.23	0.00135%	14.47	0.00162%	13.86	0.89	1.00	1.20
DNA/Tc1_247	0.00149%	14.69	0.00128%	14.86	0.00093%	14.28	0.00111%	14.49	0.00104%	14.03	0.00103%	13.01	0.86	1.19	0.99
DNA/Tc1_248	0.00142%	15.16	0.00132%	14.97	0.00124%	13.97	0.00108%	14.51	0.00137%	16.47	0.00118%	15.88	0.93	0.87	0.86
DNA/Tc1_249	0.00142%	9.51	0.00134%	10.17	0.00136%	8.3	0.00109%	10.78	0.00090%	10.58	0.00094%	9.6	0.95	0.80	1.04
DNA/Tc1_25	0.06320%	7.83	0.06116%	8.08	0.06172%	7.14	0.05917%	7.17	0.05641%	7.36	0.05731%	7.33	0.97	0.96	1.02
DNA/Tc1_250	0.00139%	4.86	0.00137%	4.45	0.00206%	1.79	0.00187%	3.05	0.00034%	10.65	0.00091%	3.9	0.99	0.91	2.69
DNA/Tc1_251	0.00135%	4.04	0.00137%	4.24	0.00117%	3.56	0.00101%	3.99	0.00138%	3.97	0.00125%	3.98	1.01	0.86	0.90

DNA/Tc1_252	0.00133%	22.92	0.00123%	20.96	0.00083%	20.66	0.00094%	20.92	0.00105%	17.69	0.00132%	18.99	0.92	1.13	1.26
DNA/Tc1_253	0.00131%	3.46	0.00141%	3.32	0.00133%	3.56	0.00141%	3.91	0.00150%	3.31	0.00153%	3.55	1.08	1.06	1.02
DNA/Tc1_254	0.00131%	17.03	0.00023%	21.44	0.00031%	19.83	0.00014%	17.3	0.00493%	5.19	0.00031%	19.83	0.17	0.45	0.06
DNA/Tc1_255	0.00130%	25.00	0.00144%	25.44	0.00078%	22.07	0.00075%	23.42	0.00101%	24.24	0.00096%	22.72	1.11	0.96	0.95
DNA/Tc1_256	0.00126%	8.94	0.00111%	8.87	0.00109%	6.99	0.00102%	8.73	0.00094%	7.75	0.00103%	7.89	0.88	0.93	1.09
DNA/Tc1_257	0.00125%	8.75	0.00102%	9.51	0.00115%	3.62	0.00110%	3.01	0.00127%	2.84	0.00032%	5.92	0.82	0.96	0.25
DNA/Tc1_258	0.00123%	12.89	0.00122%	12.49	0.00110%	9.37	0.00105%	11.08	0.00113%	11.38	0.00123%	10.35	0.99	0.95	1.08
DNA/Tc1_259	0.00118%	16.09	0.00115%	15.54	0.00342%	10.71	0.00338%	10.51	0.00415%	10.26	0.00355%	10.62	0.97	0.99	0.86
DNA/Tc1_26	0.06289%	8.62	0.06782%	8.86	0.06194%	8.21	0.05975%	8.14	0.06466%	8.22	0.06239%	8.3	1.08	0.96	0.96
DNA/Tc1_260	0.00117%	14.43	0.00113%	14.76	0.00132%	11.43	0.00111%	12.33	0.00131%	14.01	0.00115%	13.61	0.96	0.84	0.88
DNA/Tc1_261	0.00116%	17.60	0.00119%	16.80	0.00080%	13.48	0.00087%	12.65	0.00099%	13.19	0.00087%	13.15	1.03	1.09	0.88
DNA/Tc1_262	0.00114%	17.68	0.00103%	17.83	0.00104%	16.43	0.00093%	17.36	0.00121%	16.18	0.00106%	15.82	0.91	0.90	0.88
DNA/Tc1_263	0.00112%	12.25	0.00117%	12.66	0.00091%	9.72	0.00085%	11.4	0.00110%	12.15	0.00123%	9.82	1.04	0.93	1.12
DNA/Tc1_264	0.00112%	5.92	0.00101%	5.45	0.00120%	5.39	0.00122%	3.44	0.00148%	4.74	0.00142%	3.78	0.90	1.02	0.96
DNA/Tc1_265	0.00105%	16.48	0.00094%	16.82	0.00159%	13.67	0.00151%	14.78	0.00122%	14.58	0.00134%	14.76	0.90	0.95	1.10
DNA/Tc1_266	0.00104%	15.33	0.00104%	15.81	0.00098%	15.2	0.00072%	16.35	0.00092%	15.62	0.00075%	15.55	1.00	0.73	0.82
DNA/Tc1_267	0.00099%	15.83	0.00105%	14.91	0.00073%	12.74	0.00077%	12.7	0.00095%	13.59	0.00090%	14.07	1.06	1.05	0.94
DNA/Tc1_268	0.00094%	6.11	0.00110%	6.03	0.00081%	7.16	0.00094%	4.88	0.00118%	5.16	0.00083%	5.63	1.16	1.15	0.70
DNA/Tc1_269	0.00084%	13.51	0.00070%	13.44	0.00076%	12.73	0.00081%	12.73	0.00073%	12.86	0.00060%	13.78	0.84	1.05	0.81
DNA/Tc1_27	0.06227%	2.94	0.06581%	3.16	0.06167%	2.25	0.06359%	2.14	0.06308%	2.27	0.06271%	2.25	1.06	1.03	0.99
DNA/Tc1_270	0.00081%	16.59	0.00096%	14.40	0.00048%	16.1	0.00061%	13.2	0.00086%	12.3	0.00059%	16.07	1.19	1.28	0.68
DNA/Tc1_271	0.00078%	10.60	0.00063%	11.04	0.00085%	8.64	0.00088%	9.88	0.00057%	13.48	0.00059%	10.06	0.81	1.03	1.04
DNA/Tc1_272	0.00077%	5.12	0.00080%	5.30	0.00017%	22.51	0.00019%	22.62	0.00149%	4.78	0.00162%	4.34	1.04	1.08	1.09
DNA/Tc1_273	0.00073%	11.93	0.00064%	12.69	0.00074%	6.87	0.00050%	7.99	0.00050%	14.19	0.00038%	10.33	0.88	0.68	0.77
DNA/Tc1_274	0.00072%	6.24	0.00063%	7.15	0.00046%	7.7	0.00067%	7.11	0.00053%	7.69	0.00058%	7.54	0.88	1.47	1.09
*DNA/Tc1_275	0.00070%	2.83	0.00065%	2.29	0.00083%	1.06	0.00079%	1.03	0.00006%	5.08	0.00037%	2.44	0.92	0.96	5.90
DNA/Tc1_276	0.00066%	4.08	0.00055%	4.96	0.00040%	2.49	0.00038%	4.93	0.00018%	6.73	0.00025%	4.4	0.84	0.96	1.40
DNA/Tc1_277	0.00057%	19.55	0.00043%	19.06	0.00050%	13.4	0.00045%	13.55	0.00038%	19.04	0.00038%	18.62	0.75	0.90	1.01
DNA/Tc1_278	0.00051%	7.78	0.00043%	9.27	0.00059%	6.95	0.00075%	4.36	0.00032%	12.45	0.00025%	14.56	0.85	1.27	0.79
DNA/Tc1_279	0.00045%	6.95	0.00051%	5.94	0.00046%	7.55	0.00054%	7.08	0.00020%	11.28	0.00022%	6.71	1.15	1.17	1.15
DNA/Tc1_28	0.06061%	12.13	0.06593%	12.69	0.06018%	10.77	0.05589%	10.96	0.06247%	10.76	0.06006%	10.59	1.09	0.93	0.96

DNA/Tc1_280	0.00042%	16.04	0.00031%	18.30	0.00058%	17.22	0.00046%	17.81	0.00040%	20.38	0.00031%	19.69	0.74	0.80	0.77
DNA/Tc1_281	0.00038%	16.05	0.00027%	15.03	0.00015%	14.33	0.00022%	17.82	0.00021%	14.87	0.00017%	17.19	0.70	1.44	0.78
DNA/Tc1_282	0.00011%	14.14	0.00013%	16.05	0.00011%	12.02	0.00026%	15.18	0.00015%	13.95	0.00012%	15.01	1.15	2.42	0.76
DNA/Tc1_283	0.00004%	15.02	0.00008%	7.53	0.00026%	4.8	0.00022%	4.91	0.00023%	5.77	0.00011%	5	1.80	0.84	0.46
DNA/Tc1_29	0.05896%	7.71	0.06153%	7.75	0.05679%	7.6	0.05615%	7.66	0.05778%	7.63	0.05828%	7.61	1.04	0.99	1.01
DNA/Tc1_3	0.25431%	7.58	0.26788%	7.56	0.26540%	7.14	0.25743%	7.23	0.27999%	7.19	0.25680%	7.26	1.05	0.97	0.92
DNA/Tc1_30	0.05755%	9.46	0.05650%	9.49	0.05409%	8.84	0.05176%	8.9	0.04601%	10.39	0.04769%	9.84	0.98	0.96	1.04
DNA/Tc1_31	0.05343%	0.95	0.05370%	0.95	0.05373%	0.84	0.05054%	0.83	0.05631%	0.86	0.05141%	0.88	1.00	0.94	0.91
DNA/Tc1_32	0.05302%	16.36	0.05364%	16.30	0.05482%	15.42	0.05260%	15.52	0.05636%	15.34	0.05423%	15.59	1.01	0.96	0.96
DNA/Tc1_33	0.05253%	8.41	0.05593%	8.77	0.05038%	7.52	0.04910%	7.2	0.05228%	7.29	0.04710%	7.57	1.06	0.97	0.90
DNA/Tc1_34	0.05145%	5.65	0.04529%	5.53	0.04088%	5.15	0.04184%	4.84	0.05698%	5.41	0.04053%	5.27	0.88	1.02	0.71
DNA/Tc1_35	0.05138%	21.54	0.05655%	22.13	0.04123%	18.62	0.03878%	18.93	0.04164%	19	0.03933%	18.92	1.10	0.94	0.94
DNA/Tc1_36	0.05070%	18.43	0.05284%	18.28	0.05593%	16.6	0.05161%	17.19	0.05096%	18.7	0.04715%	18.48	1.04	0.92	0.93
DNA/Tc1_37	0.05032%	11.23	0.05368%	11.98	0.04967%	10.41	0.04819%	11	0.05401%	10.58	0.04930%	10.59	1.07	0.97	0.91
DNA/Tc1_38	0.04950%	15.63	0.05361%	16.34	0.04837%	14.5	0.04835%	14.56	0.04878%	14.79	0.04879%	14.82	1.08	1.00	1.00
DNA/Tc1_39	0.04878%	5.17	0.05329%	5.06	0.05543%	3.95	0.05730%	3.92	0.05289%	4	0.04985%	4.4	1.09	1.03	0.94
DNA/Tc1_4	0.23885%	10.61	0.25460%	10.73	0.24008%	10.09	0.23364%	10.14	0.24784%	10.11	0.22865%	10.12	1.07	0.97	0.92
DNA/Tc1_40	0.04876%	19.09	0.05635%	20.56	0.04793%	19.04	0.04920%	18.83	0.04656%	19.63	0.04564%	19.56	1.16	1.03	0.98
DNA/Tc1_41	0.04875%	3.18	0.04993%	3.31	0.04349%	3.41	0.04280%	3.38	0.04373%	3.27	0.04333%	3.15	1.02	0.98	0.99
DNA/Tc1_42	0.04785%	13.61	0.05049%	13.72	0.04393%	12.95	0.04221%	13.02	0.04716%	12.95	0.04392%	13.06	1.06	0.96	0.93
DNA/Tc1_43	0.04578%	8.87	0.04594%	8.97	0.03930%	8.2	0.03983%	7.96	0.04191%	7.89	0.03954%	8.25	1.00	1.01	0.94
DNA/Tc1_44	0.04436%	20.64	0.04624%	20.75	0.04263%	19.92	0.04071%	19.85	0.04470%	19.72	0.04108%	19.84	1.04	0.96	0.92
DNA/Tc1_45	0.04288%	7.17	0.04362%	7.36	0.03871%	6.98	0.03797%	6.9	0.03930%	6.92	0.04052%	7	1.02	0.98	1.03
DNA/Tc1_46	0.04087%	18.91	0.04307%	19.15	0.04292%	18.59	0.04029%	18.54	0.04116%	18.13	0.04104%	18.01	1.05	0.94	1.00
DNA/Tc1_47	0.04085%	6.06	0.04503%	6.58	0.03782%	5.45	0.03832%	5.02	0.04553%	4.48	0.04238%	4.79	1.10	1.01	0.93
DNA/Tc1_48	0.03950%	16.13	0.03998%	16.26	0.03879%	14.74	0.03721%	14.51	0.03491%	17.25	0.03132%	16.36	1.01	0.96	0.90
DNA/Tc1_49	0.03890%	4.95	0.04166%	5.28	0.03946%	4.25	0.03679%	4.02	0.03691%	4.61	0.03537%	4.6	1.07	0.93	0.96
DNA/Tc1_5	0.19206%	8.19	0.19490%	8.15	0.19812%	8	0.18799%	8.05	0.20700%	8.07	0.18727%	8.12	1.01	0.95	0.90
DNA/Tc1_50	0.03879%	22.71	0.04138%	23.10	0.03589%	20.91	0.03602%	20.98	0.03025%	23.86	0.03167%	23.17	1.07	1.00	1.05
DNA/Tc1_51	0.03772%	8.70	0.03823%	8.51	0.03574%	8.16	0.03525%	8.08	0.03511%	8.15	0.03558%	8.31	1.01	0.99	1.01
DNA/Tc1_52	0.03766%	6.41	0.03844%	6.55	0.03646%	5.86	0.03477%	6	0.03867%	6.08	0.03438%	6.08	1.02	0.95	0.89

DNA/Tc1_53	0.03502%	11.74	0.03650%	11.84	0.03093%	11.7	0.02957%	11.58	0.02884%	11.7	0.03320%	11.7	1.04	0.96	1.15
DNA/Tc1_54	0.03446%	7.76	0.03644%	8.03	0.03532%	6.68	0.03208%	7.02	0.03319%	6.92	0.03235%	6.94	1.06	0.91	0.97
DNA/Tc1_55	0.03310%	16.11	0.03272%	15.97	0.02588%	14.87	0.02540%	14.92	0.02620%	15.41	0.02475%	15.28	0.99	0.98	0.94
DNA/Tc1_56	0.03130%	6.16	0.03109%	6.06	0.03118%	5.96	0.03112%	6.05	0.03466%	6.17	0.02858%	6.06	0.99	1.00	0.82
DNA/Tc1_57	0.03110%	15.76	0.03117%	15.92	0.03157%	15.41	0.02840%	15.07	0.03154%	15.36	0.02962%	15.24	1.00	0.90	0.94
DNA/Tc1_58	0.03104%	9.06	0.03235%	8.95	0.03026%	8.59	0.03004%	8.79	0.03235%	8.64	0.03127%	8.68	1.04	0.99	0.97
DNA/Tc1_59	0.02975%	6.61	0.02924%	6.49	0.02915%	6.16	0.02897%	6.2	0.02758%	6.4	0.02729%	6.69	0.98	0.99	0.99
DNA/Tc1_6	0.19159%	6.96	0.19382%	7.00	0.18782%	6.78	0.17786%	6.8	0.20094%	6.83	0.17713%	6.88	1.01	0.95	0.88
DNA/Tc1_60	0.02967%	7.04	0.03000%	7.20	0.03405%	6.94	0.03528%	6.98	0.03823%	6.93	0.03604%	6.93	1.01	1.04	0.94
DNA/Tc1_61	0.02902%	20.60	0.03008%	20.73	0.02757%	20.24	0.02693%	20.05	0.02924%	20	0.02570%	19.97	1.04	0.98	0.88
DNA/Tc1_62	0.02881%	7.17	0.02978%	7.73	0.01176%	14.3	0.01333%	15.18	0.01684%	11.14	0.01456%	12.61	1.03	1.13	0.86
DNA/Tc1_63	0.02865%	7.50	0.02966%	7.59	0.02950%	7.42	0.02866%	7.3	0.02974%	7.28	0.03071%	7.29	1.04	0.97	1.03
DNA/Tc1_64	0.02838%	9.58	0.02957%	9.90	0.02937%	8.65	0.02765%	8.21	0.03020%	8.5	0.02810%	8.4	1.04	0.94	0.93
DNA/Tc1_65	0.02791%	11.21	0.02856%	11.34	0.02384%	10.03	0.02322%	9.92	0.02549%	10.1	0.02435%	10.36	1.02	0.97	0.96
DNA/Tc1_66	0.02787%	13.15	0.03152%	12.94	0.02897%	12.56	0.02961%	12.37	0.02788%	12.66	0.03021%	12.46	1.13	1.02	1.08
DNA/Tc1_67	0.02760%	6.76	0.02821%	6.76	0.02613%	6.53	0.02401%	6.6	0.02533%	6.4	0.02526%	6.58	1.02	0.92	1.00
DNA/Tc1_68	0.02743%	7.17	0.02673%	7.12	0.02560%	6.59	0.02574%	6.79	0.02801%	6.6	0.02621%	6.62	0.97	1.01	0.94
DNA/Tc1_69	0.02738%	21.79	0.02768%	22.10	0.02545%	20.35	0.02558%	20.22	0.02372%	22.55	0.02316%	21.65	1.01	1.01	0.98
DNA/Tc1_7	0.15762%	9.27	0.15669%	9.30	0.15216%	9.06	0.14530%	8.97	0.16175%	8.92	0.15015%	8.99	0.99	0.95	0.93
DNA/Tc1_70	0.02720%	5.15	0.02861%	5.39	0.02593%	3.65	0.02700%	3.32	0.02479%	4.1	0.02524%	3.81	1.05	1.04	1.02
DNA/Tc1_71	0.02580%	7.76	0.02604%	7.94	0.02884%	7.12	0.02710%	7.22	0.03006%	7.11	0.02879%	7.18	1.01	0.94	0.96
DNA/Tc1_72	0.02487%	13.45	0.02413%	13.27	0.02763%	11.95	0.02763%	12.06	0.02745%	11.7	0.02521%	12.22	0.97	1.00	0.92
DNA/Tc1_73	0.02339%	6.35	0.02383%	6.47	0.01889%	6.04	0.01823%	6.31	0.02015%	6.09	0.01838%	6.21	1.02	0.96	0.91
DNA/Tc1_74	0.02288%	5.27	0.02438%	4.46	0.02754%	1.87	0.02876%	1.58	0.02597%	2.08	0.02312%	2.72	1.07	1.04	0.89
DNA/Tc1_75	0.02281%	3.49	0.02193%	4.25	0.00678%	9.95	0.00694%	10.27	0.01155%	6.87	0.00849%	7.84	0.96	1.02	0.73
DNA/Tc1_76	0.02269%	9.65	0.02249%	9.56	0.01993%	9.68	0.01980%	9.91	0.02024%	9.53	0.02041%	9.64	0.99	0.99	1.01
DNA/Tc1_77	0.02260%	6.50	0.02192%	6.55	0.01975%	5.77	0.01988%	5.99	0.02022%	6.12	0.02017%	6.07	0.97	1.01	1.00
DNA/Tc1_78	0.02230%	21.29	0.02282%	21.48	0.02154%	19.98	0.02095%	19.87	0.02011%	20.8	0.01969%	20.45	1.02	0.97	0.98
DNA/Tc1_79	0.02218%	13.18	0.02262%	13.17	0.02012%	11.99	0.01820%	11.71	0.02125%	11.86	0.01951%	11.96	1.02	0.90	0.92
DNA/Tc1_8	0.15456%	6.33	0.15457%	6.49	0.14981%	6.13	0.14733%	6.1	0.15564%	6.03	0.14821%	6.14	1.00	0.98	0.95
DNA/Tc1_80	0.02144%	17.65	0.02129%	17.76	0.02428%	16.33	0.02294%	16.48	0.02497%	16.36	0.02340%	16.34	0.99	0.94	0.94

DNA/Tc1_81	0.02108%	15.33	0.02189%	15.36	0.01848%	13.43	0.01889%	13.43	0.01855%	14.08	0.01943%	13.8	1.04	1.02	1.05
DNA/Tc1_82	0.02047%	12.49	0.01975%	12.69	0.01504%	11.8	0.01482%	11.68	0.01492%	11.71	0.01501%	11.71	0.96	0.99	1.01
DNA/Tc1_83	0.01982%	8.48	0.01891%	8.50	0.02109%	7.97	0.01930%	7.89	0.01407%	10.3	0.01485%	9.6	0.95	0.92	1.06
DNA/Tc1_84	0.01852%	8.42	0.01915%	8.10	0.01629%	7.75	0.01683%	7.61	0.01508%	8.5	0.01447%	8.76	1.03	1.03	0.96
DNA/Tc1_85	0.01816%	7.02	0.01884%	7.14	0.01778%	6.35	0.01886%	6.6	0.01893%	6.76	0.01812%	6.88	1.04	1.06	0.96
DNA/Tc1_86	0.01789%	7.41	0.01692%	7.45	0.02193%	6.88	0.02151%	6.9	0.02281%	6.7	0.02246%	6.9	0.95	0.98	0.98
DNA/Tc1_87	0.01768%	13.53	0.01790%	13.40	0.01714%	12.01	0.01564%	11.93	0.01755%	12.15	0.01706%	11.99	1.01	0.91	0.97
DNA/Tc1_88	0.01757%	21.52	0.01946%	22.01	0.01681%	16.36	0.01547%	18.06	0.01221%	23.06	0.01194%	22.04	1.11	0.92	0.98
DNA/Tc1_89	0.01752%	13.01	0.01800%	13.12	0.01770%	12.71	0.01619%	12.22	0.01755%	12.71	0.01737%	12.46	1.03	0.91	0.99
DNA/Tc1_9	0.14407%	11.64	0.14453%	11.76	0.14267%	11.27	0.13631%	11.31	0.14406%	11.34	0.13954%	11.35	1.00	0.96	0.97
DNA/Tc1_90	0.01744%	11.66	0.01718%	11.48	0.01700%	11.16	0.01653%	10.85	0.01851%	10.88	0.01680%	11.01	0.98	0.97	0.91
DNA/Tc1_91	0.01719%	5.09	0.01711%	5.19	0.01767%	4.63	0.01663%	4.82	0.01606%	5.23	0.01744%	5.12	1.00	0.94	1.09
DNA/Tc1_92	0.01717%	10.86	0.01698%	11.22	0.01439%	10.34	0.01327%	10.47	0.01238%	11.83	0.01335%	11.4	0.99	0.92	1.08
DNA/Tc1_93	0.01711%	14.49	0.01804%	14.92	0.01633%	10.17	0.01689%	10.25	0.00966%	17.55	0.01087%	14.56	1.05	1.03	1.13
DNA/Tc1_94	0.01677%	4.59	0.01785%	4.37	0.01253%	4.31	0.01236%	4.34	0.01238%	4.24	0.01181%	4.43	1.06	0.99	0.95
DNA/Tc1_95	0.01672%	8.70	0.01627%	8.93	0.01465%	8.75	0.01481%	8.78	0.01518%	8.78	0.01511%	8.78	0.97	1.01	1.00
DNA/Tc1_96	0.01654%	10.59	0.01596%	10.81	0.01491%	9.55	0.01529%	9.69	0.01627%	9.91	0.01381%	10.24	0.96	1.03	0.85
DNA/Tc1_97	0.01637%	19.43	0.01592%	19.64	0.01393%	19.41	0.01424%	19.21	0.01438%	19.8	0.01398%	19.46	0.97	1.02	0.97
DNA/Tc1_98	0.01633%	24.03	0.01801%	24.44	0.01310%	18.97	0.01209%	19.49	0.01098%	24.24	0.01067%	22.58	1.10	0.92	0.97
DNA/Tc1_99	0.01615%	15.45	0.01596%	15.25	0.01451%	14.93	0.01312%	14.89	0.01437%	14.83	0.01466%	14.97	0.99	0.90	1.02
DNA/Tc2_1	0.00754%	6.43	0.00847%	6.18	0.00746%	5.69	0.00738%	5.67	0.00667%	6.21	0.00724%	6.02	1.12	0.99	1.09
DNA/Tc2_2	0.00196%	15.82	0.00213%	15.29	0.00164%	15.59	0.00182%	14.52	0.00156%	15.62	0.00185%	15.88	1.09	1.11	1.18
DNA/Tc2_3	0.00174%	6.49	0.00188%	6.72	0.00104%	6.43	0.00141%	6.17	0.00104%	6.38	0.00154%	5.81	1.08	1.35	1.48
DNA/Tc2_4	0.00111%	12.75	0.00113%	12.48	0.00088%	14.9	0.00099%	10.67	0.00060%	10.2	0.00109%	9.9	1.02	1.12	1.81
DNA/Tc2_5	0.00109%	23.22	0.00152%	25.47	0.00124%	21.8	0.00115%	20.9	0.00111%	21.93	0.00118%	22.87	1.39	0.93	1.06
DNA/Tc4_1	0.01438%	13.98	0.01466%	14.04	0.01440%	13.77	0.01502%	13.5	0.01487%	13.58	0.01325%	13.67	1.02	1.04	0.89
DNA/Tc4_2	0.00852%	11.85	0.00853%	12.63	0.00885%	10.21	0.00893%	9.07	0.00533%	16.9	0.00593%	13.69	1.00	1.01	1.11
DNA/Tc4_3	0.00574%	21.53	0.00584%	22.23	0.00466%	21.1	0.00386%	21.62	0.00389%	23.32	0.00438%	22.25	1.02	0.83	1.13
DNA/Tc4_4	0.00446%	15.16	0.00506%	15.75	0.00380%	13.51	0.00464%	14.15	0.00448%	14.31	0.00421%	13.8	1.13	1.22	0.94
DNA/Tc4_5	0.00364%	18.99	0.00366%	21.89	0.00280%	17.94	0.00238%	17.65	0.00205%	23.22	0.00217%	21.04	1.01	0.85	1.06
DNA/Tc4_6	0.00363%	15.02	0.00367%	16.80	0.00290%	15.9	0.00267%	13.96	0.00225%	18.97	0.00198%	17.13	1.01	0.92	0.88

DNA/Tc4_7	0.00270%	8.75	0.00238%	8.17	0.00260%	5.08	0.00245%	4.55	0.00115%	12.99	0.00146%	9.88	0.88	0.94	1.27
DNA/Tigger_1	0.00903%	10.61	0.00863%	10.40	0.00794%	9.92	0.00824%	8.9	0.00650%	9.31	0.00780%	9.72	0.96	1.04	1.20
DNA/Tigger_2	0.00613%	8.56	0.00617%	9.67	0.00532%	9.77	0.00500%	7.39	0.00560%	8.04	0.00551%	7.93	1.01	0.94	0.98
DNA/Tigger_3	0.00209%	5.55	0.00183%	5.26	0.00225%	5.91	0.00234%	5.29	0.00047%	7.51	0.00092%	5.32	0.88	1.04	1.96
DNA/Tigger_4	0.00134%	8.73	0.00131%	8.72	0.00170%	5.96	0.00151%	7.82	0.00060%	15.07	0.00086%	10.52	0.98	0.88	1.43
LINE/CR1_1	3.51395%	10.11	3.44970%	10.36	3.37200%	9.6	3.28593%	9.54	3.39825%	9.38	3.29348%	9.6	0.98	0.97	0.97
LINE/CR1_10	0.05778%	8.53	0.05561%	8.31	0.05605%	7.36	0.05677%	7.17	0.06261%	7.26	0.05913%	7.3	0.96	1.01	0.94
LINE/CR1_100	0.00342%	18.94	0.00162%	24.34	0.00143%	21.55	0.00105%	21.36	0.00497%	11.04	0.00122%	21.26	0.48	0.73	0.24
LINE/CR1_101	0.00341%	6.90	0.00308%	7.17	0.00297%	4.8	0.00321%	4.97	0.00112%	12.77	0.00152%	7.62	0.90	1.08	1.36
LINE/CR1_102	0.00337%	11.14	0.00255%	10.94	0.00314%	12.18	0.00300%	11.99	0.00382%	14.94	0.00283%	13.82	0.76	0.96	0.74
LINE/CR1_103	0.00322%	7.94	0.00314%	7.87	0.00464%	5.73	0.00395%	6.25	0.00149%	12.19	0.00195%	9.39	0.97	0.85	1.31
LINE/CR1_104	0.00314%	16.32	0.00276%	13.92	0.00301%	16.44	0.00259%	18.82	0.00205%	23.6	0.00212%	18.36	0.88	0.86	1.04
LINE/CR1_105	0.00307%	24.24	0.00251%	25.05	0.00439%	26.62	0.00436%	26.12	0.00413%	27.47	0.00414%	26.47	0.82	0.99	1.00
LINE/CR1_106	0.00289%	18.25	0.00246%	16.17	0.00296%	15.45	0.00246%	14.3	0.00209%	19.03	0.00233%	17.89	0.85	0.83	1.12
LINE/CR1_107	0.00283%	8.84	0.00282%	9.02	0.00301%	9.8	0.00290%	9.31	0.00379%	8.59	0.00315%	9.36	1.00	0.96	0.83
LINE/CR1_108	0.00283%	13.29	0.00279%	12.64	0.00342%	9.19	0.00326%	10.56	0.00194%	17.36	0.00240%	17.5	0.99	0.95	1.24
LINE/CR1_109	0.00271%	19.36	0.00225%	16.42	0.00188%	22.75	0.00193%	19.57	0.00173%	22.48	0.00176%	21.45	0.83	1.03	1.02
LINE/CR1_11	0.05184%	12.53	0.05397%	12.76	0.05019%	11.73	0.04585%	11.71	0.05198%	11.68	0.04663%	11.76	1.04	0.91	0.90
LINE/CR1_110	0.00268%	12.32	0.00211%	10.27	0.00213%	13.57	0.00246%	12.16	0.00146%	18.28	0.00191%	14.5	0.79	1.16	1.31
LINE/CR1_111	0.00261%	17.44	0.00204%	17.73	0.00131%	17.28	0.00169%	16.79	0.00128%	16.52	0.00139%	19.97	0.78	1.29	1.08
LINE/CR1_112	0.00260%	11.17	0.00240%	10.92	0.00338%	11.67	0.00295%	12.59	0.00331%	13.24	0.00321%	12.96	0.92	0.87	0.97
LINE/CR1_113	0.00260%	19.44	0.00250%	19.86	0.00230%	20.17	0.00205%	19.13	0.00225%	22.54	0.00262%	21.07	0.96	0.89	1.16
LINE/CR1_114	0.00254%	15.07	0.00192%	14.86	0.00348%	14.22	0.00342%	13.41	0.00359%	15.9	0.00269%	14.52	0.76	0.98	0.75
LINE/CR1_115	0.00247%	15.57	0.00226%	17.00	0.00173%	15.3	0.00182%	14.61	0.00158%	18.75	0.00140%	17.49	0.92	1.05	0.89
LINE/CR1_116	0.00245%	26.55	0.00302%	28.37	0.00189%	23.02	0.00189%	24.48	0.00207%	24.03	0.00191%	23.4	1.23	1.00	0.93
LINE/CR1_117	0.00241%	8.33	0.00222%	11.55	0.00172%	9.82	0.00196%	8.74	0.00122%	14.41	0.00115%	11.38	0.92	1.14	0.94
LINE/CR1_118	0.00222%	5.04	0.00193%	5.11	0.00194%	5.41	0.00199%	4.72	0.00098%	7.55	0.00114%	8.8	0.87	1.03	1.16
LINE/CR1_119	0.00220%	18.13	0.00209%	17.72	0.00484%	18.17	0.00455%	18.9	0.00473%	19.61	0.00459%	19.81	0.95	0.94	0.97
LINE/CR1_12	0.05146%	13.81	0.05210%	13.84	0.06354%	9.92	0.05802%	10.02	0.02781%	19.26	0.03346%	16.75	1.01	0.91	1.20
LINE/CR1_120	0.00216%	20.62	0.00102%	16.90	0.00152%	15.82	0.00178%	13.67	0.00133%	19.83	0.00149%	19.79	0.47	1.18	1.12
LINE/CR1_121	0.00207%	14.48	0.00045%	17.70	0.00063%	15.04	0.00048%	17.47	0.00433%	7.09	0.00055%	16.41	0.22	0.75	0.13

LINE/CR1_122	0.00205%	15.43	0.00171%	14.07	0.00228%	10.41	0.00203%	10.05	0.00152%	17.21	0.00157%	16.83	0.83	0.89	1.03
LINE/CR1_123	0.00198%	11.62	0.00163%	11.75	0.00129%	11.8	0.00136%	10.45	0.00100%	14.5	0.00100%	13.53	0.82	1.05	1.00
LINE/CR1_124	0.00194%	7.76	0.00156%	7.70	0.00168%	8.78	0.00164%	8.62	0.00071%	9.58	0.00100%	9.87	0.81	0.98	1.42
LINE/CR1_125	0.00186%	19.89	0.00171%	18.44	0.00494%	18.16	0.00483%	18.02	0.00435%	18.05	0.00463%	17.98	0.92	0.98	1.06
LINE/CR1_126	0.00169%	24.82	0.00154%	24.81	0.00219%	22.89	0.00178%	22.47	0.00234%	23.86	0.00212%	24.03	0.91	0.81	0.90
LINE/CR1_127	0.00168%	14.64	0.00148%	14.11	0.00179%	13.46	0.00186%	13.67	0.00196%	12.75	0.00182%	14.09	0.88	1.04	0.93
LINE/CR1_128	0.00161%	9.50	0.00162%	9.18	0.00379%	9.07	0.00335%	9.28	0.00375%	9.43	0.00349%	9.36	1.01	0.89	0.93
LINE/CR1_129	0.00104%	21.34	0.00080%	20.46	0.00116%	19.91	0.00115%	19.91	0.00129%	19.7	0.00130%	20.52	0.77	1.00	1.00
LINE/CR1_13	0.04782%	9.73	0.04953%	9.63	0.04366%	9.17	0.04816%	9.09	0.05117%	9.15	0.04950%	9.21	1.04	1.10	0.97
LINE/CR1_130	0.00085%	19.23	0.00103%	19.52	0.00092%	18.42	0.00087%	15.04	0.00098%	21.64	0.00101%	21.29	1.21	0.94	1.03
LINE/CR1_131	0.00054%	17.28	0.00043%	15.53	0.00015%	13.71	0.00019%	9.56	0.00024%	13.15	0.00024%	19.97	0.79	1.33	1.03
LINE/CR1_132	0.00053%	18.69	0.00045%	18.53	0.00043%	21.31	0.00037%	18.66	0.00044%	17.16	0.00041%	17.46	0.85	0.87	0.93
LINE/CR1_133	0.00043%	15.13	0.00029%	17.35	0.00033%	16.91	0.00040%	16.02	0.00052%	12.44	0.00031%	14.62	0.68	1.21	0.59
LINE/CR1_134	0.00016%	23.80	0.00008%	18.25	0.00008%	15.92	0.00007%	21.11	0.00013%	23.23	0.00009%	17.27	0.47	0.87	0.75
LINE/CR1_14	0.04538%	18.96	0.04464%	19.33	0.05805%	17.88	0.05600%	17.7	0.06037%	17.57	0.05772%	17.79	0.98	0.96	0.96
LINE/CR1_15	0.04405%	21.06	0.04042%	21.00	0.03765%	19.28	0.03692%	19.95	0.03977%	20.93	0.03526%	20.78	0.92	0.98	0.89
LINE/CR1_16	0.04181%	10.81	0.04100%	10.90	0.03997%	10.63	0.04060%	10.25	0.04648%	10.24	0.04077%	10.47	0.98	1.02	0.88
LINE/CR1_17	0.03959%	14.68	0.03974%	15.51	0.04711%	13.09	0.04313%	12.82	0.05038%	12.85	0.04321%	13.05	1.00	0.92	0.86
LINE/CR1_18	0.03828%	15.16	0.03630%	15.97	0.03404%	13.71	0.03160%	13.44	0.02450%	16.59	0.02562%	16.56	0.95	0.93	1.05
LINE/CR1_19	0.03226%	12.03	0.02760%	10.50	0.03943%	10.58	0.03933%	10.29	0.04362%	10.84	0.03627%	10.65	0.86	1.00	0.83
LINE/CR1_2	1.45670%	8.98	1.43338%	9.29	1.36725%	8.57	1.32334%	8.51	1.53705%	8.23	1.35767%	8.49	0.98	0.97	0.88
LINE/CR1_20	0.03148%	15.23	0.03128%	15.62	0.03010%	12.67	0.02895%	12.8	0.02233%	17.87	0.02294%	15.78	0.99	0.96	1.03
LINE/CR1_21	0.02951%	21.30	0.02160%	19.61	0.02867%	19.09	0.02761%	18.45	0.02221%	23.77	0.02372%	22.88	0.73	0.96	1.07
LINE/CR1_22	0.02921%	15.61	0.02757%	16.61	0.03016%	13.58	0.03218%	13.97	0.02566%	16.01	0.02589%	16.4	0.94	1.07	1.01
LINE/CR1_23	0.02921%	11.95	0.02662%	12.47	0.02148%	11.13	0.02300%	10.49	0.01503%	14.82	0.01767%	13.83	0.91	1.07	1.18
LINE/CR1_24	0.02675%	17.35	0.02411%	18.19	0.01949%	17.68	0.01881%	17.3	0.01653%	20.34	0.01608%	19.88	0.90	0.96	0.97
LINE/CR1_25	0.02509%	5.40	0.01939%	7.26	0.03132%	4.88	0.03479%	4.39	0.01396%	10.46	0.00975%	13.02	0.77	1.11	0.70
LINE/CR1_26	0.02479%	20.78	0.02526%	21.49	0.02311%	20.88	0.02159%	20.54	0.02167%	22.02	0.02131%	21.59	1.02	0.93	0.98
LINE/CR1_27	0.02281%	9.95	0.02307%	10.66	0.02835%	9.8	0.02675%	9.7	0.03132%	9.53	0.02606%	9.81	1.01	0.94	0.83
LINE/CR1_28	0.02233%	16.33	0.02337%	16.61	0.02186%	15.65	0.02195%	15.98	0.02092%	15.91	0.02094%	15.62	1.05	1.00	1.00
LINE/CR1_29	0.02175%	6.70	0.02102%	6.04	0.02102%	5.35	0.02099%	5.35	0.02311%	5.4	0.02110%	5.3	0.97	1.00	0.91

LINE/CR1_3	0.88415%	10.02	0.87683%	10.37	0.76843%	9.81	0.75347%	9.8	0.87571%	9.78	0.75125%	9.88	0.99	0.98	0.86
LINE/CR1_30	0.02141%	14.60	0.01815%	14.89	0.01644%	14.61	0.01545%	14.39	0.01396%	17.05	0.01454%	16.1	0.85	0.94	1.04
LINE/CR1_31	0.01986%	22.83	0.01977%	23.53	0.01729%	21.23	0.01660%	20.88	0.01587%	23.92	0.01423%	23.49	1.00	0.96	0.90
LINE/CR1_32	0.01980%	20.65	0.02016%	22.58	0.01382%	18.55	0.01422%	18.55	0.01153%	22.67	0.01199%	21.78	1.02	1.03	1.04
LINE/CR1_33	0.01977%	10.26	0.02009%	10.44	0.01961%	9.47	0.02085%	9.52	0.02181%	9.45	0.02089%	9.88	1.02	1.06	0.96
LINE/CR1_34	0.01957%	16.65	0.02013%	16.80	0.01884%	16.46	0.01751%	15.87	0.01834%	16.09	0.01828%	16.05	1.03	0.93	1.00
LINE/CR1_35	0.01947%	11.66	0.01665%	12.09	0.01504%	12.47	0.01593%	11.76	0.01055%	15.96	0.01059%	16.04	0.85	1.06	1.00
LINE/CR1_36	0.01877%	16.84	0.01959%	16.93	0.01892%	16.09	0.01839%	15.8	0.01988%	16.07	0.01932%	16.34	1.04	0.97	0.97
LINE/CR1_37	0.01680%	9.51	0.01646%	9.19	0.02234%	8.5	0.02046%	8.9	0.02225%	8.82	0.02090%	8.95	0.98	0.92	0.94
LINE/CR1_38	0.01667%	15.90	0.01525%	15.39	0.03420%	13.68	0.03234%	13.77	0.03557%	14.37	0.03107%	14.18	0.91	0.95	0.87
LINE/CR1_39	0.01635%	17.02	0.01577%	17.35	0.01477%	16.38	0.01373%	16.23	0.01281%	18.01	0.01293%	17.58	0.96	0.93	1.01
LINE/CR1_4	0.18593%	17.01	0.19618%	17.59	0.19395%	15.99	0.18331%	15.95	0.19510%	16.27	0.18972%	16.13	1.06	0.95	0.97
LINE/CR1_40	0.01620%	17.13	0.01565%	17.05	0.01620%	15.85	0.01539%	15.82	0.01651%	16.46	0.01568%	16.42	0.97	0.95	0.95
LINE/CR1_41	0.01557%	6.30	0.01506%	7.39	0.01359%	5.82	0.01270%	5.72	0.01473%	5.94	0.01268%	6.27	0.97	0.93	0.86
LINE/CR1_42	0.01491%	15.58	0.01460%	16.14	0.01768%	15.31	0.01774%	15.34	0.01614%	15.23	0.01815%	15.29	0.98	1.00	1.12
LINE/CR1_43	0.01478%	14.22	0.01422%	14.20	0.01716%	12.85	0.01456%	13.5	0.01151%	19.19	0.01245%	17.17	0.96	0.85	1.08
LINE/CR1_44	0.01464%	21.81	0.01378%	21.94	0.01380%	22.06	0.01441%	21.59	0.01461%	22.36	0.01441%	21.77	0.94	1.04	0.99
LINE/CR1_45	0.01361%	15.72	0.01448%	16.19	0.01303%	14.89	0.01333%	15.87	0.01261%	15.19	0.01317%	15.17	1.06	1.02	1.04
LINE/CR1_46	0.01241%	13.97	0.01197%	15.07	0.01094%	13.65	0.01053%	14.01	0.00897%	15.59	0.00920%	15.94	0.97	0.96	1.03
LINE/CR1_47	0.01209%	9.35	0.01144%	9.31	0.01007%	10.12	0.01011%	9.21	0.00610%	13.28	0.00731%	11.9	0.95	1.00	1.20
LINE/CR1_48	0.01199%	12.11	0.01147%	12.81	0.00846%	11.33	0.00926%	10.91	0.01028%	10.13	0.00823%	10.15	0.96	1.10	0.80
LINE/CR1_49	0.01166%	15.36	0.01129%	16.02	0.01162%	12.72	0.01087%	12.71	0.01267%	12.72	0.01105%	13.25	0.97	0.94	0.87
LINE/CR1_5	0.11117%	12.01	0.11215%	12.12	0.09994%	11.07	0.09737%	10.93	0.10531%	11.28	0.09557%	11.15	1.01	0.97	0.91
LINE/CR1_50	0.01137%	15.23	0.01296%	16.84	0.01024%	11.89	0.01066%	10.96	0.01061%	11.97	0.01055%	11.67	1.14	1.04	0.99
LINE/CR1_51	0.01050%	17.10	0.00603%	20.64	0.00555%	18.92	0.00482%	18.98	0.01722%	11.83	0.00544%	18.91	0.57	0.87	0.32
LINE/CR1_52	0.01036%	5.43	0.00983%	4.90	0.00934%	4.3	0.00886%	4.31	0.00890%	4.76	0.00942%	4.09	0.95	0.95	1.06
LINE/CR1_53	0.01020%	16.25	0.00899%	16.21	0.01037%	16.16	0.00945%	15.85	0.00735%	21.23	0.00813%	19.2	0.88	0.91	1.11
LINE/CR1_54	0.01002%	19.35	0.01054%	20.83	0.00968%	17.01	0.00911%	17.47	0.00688%	21.76	0.00709%	21.14	1.05	0.94	1.03
LINE/CR1_55	0.00955%	11.05	0.00856%	11.39	0.00763%	10.99	0.00729%	10.53	0.00470%	14.89	0.00473%	14.69	0.90	0.95	1.01
LINE/CR1_56	0.00954%	8.14	0.00962%	8.60	0.01046%	7.45	0.01022%	7.73	0.01096%	7.76	0.01009%	7.09	1.01	0.98	0.92
LINE/CR1_57	0.00941%	8.37	0.00834%	9.16	0.00653%	9.14	0.00679%	7.17	0.00450%	11.92	0.00496%	11.48	0.89	1.04	1.10

LINE/CR1_58	0.00878%	15.33	0.00839%	16.41	0.00608%	16.04	0.00594%	14.62	0.00540%	17.62	0.00555%	16.86	0.96	0.98	1.03
LINE/CR1_59	0.00862%	10.62	0.00777%	8.79	0.00812%	5.66	0.00691%	6.16	0.00558%	10.14	0.00519%	9	0.90	0.85	0.93
LINE/CR1_6	0.08747%	16.45	0.09124%	16.77	0.07544%	15.66	0.06978%	15.46	0.07458%	15.52	0.07331%	15.53	1.04	0.92	0.98
LINE/CR1_60	0.00836%	14.88	0.00746%	14.60	0.01939%	10.85	0.01963%	10.69	0.02153%	10.9	0.01876%	11.07	0.89	1.01	0.87
LINE/CR1_61	0.00833%	19.57	0.00685%	20.11	0.01206%	18.69	0.01282%	18.76	0.01502%	17.47	0.01212%	18.41	0.82	1.06	0.81
LINE/CR1_62	0.00818%	23.87	0.00735%	22.99	0.01607%	20.46	0.01494%	20.61	0.01433%	23.19	0.01407%	22.43	0.90	0.93	0.98
LINE/CR1_63	0.00800%	13.47	0.00670%	14.24	0.00708%	13.69	0.00651%	13.41	0.00528%	16.46	0.00616%	15.58	0.84	0.92	1.17
LINE/CR1_64	0.00764%	12.80	0.00676%	11.84	0.01115%	10.83	0.01231%	11.14	0.01309%	11.49	0.01180%	11.11	0.89	1.10	0.90
LINE/CR1_65	0.00752%	13.70	0.00724%	13.71	0.00980%	12.03	0.00950%	12.19	0.01032%	12.15	0.00932%	12.12	0.96	0.97	0.90
LINE/CR1_66	0.00723%	10.94	0.00581%	11.53	0.00826%	9.46	0.00743%	10.05	0.00339%	18.52	0.00473%	15.04	0.80	0.90	1.40
LINE/CR1_67	0.00719%	10.70	0.00709%	11.09	0.00687%	10.64	0.00707%	9.91	0.00673%	9.98	0.00650%	10.24	0.99	1.03	0.97
LINE/CR1_68	0.00716%	14.93	0.00827%	14.66	0.00622%	15.35	0.00608%	14.1	0.00775%	13.98	0.00698%	14.41	1.16	0.98	0.90
LINE/CR1_69	0.00713%	24.18	0.00549%	24.00	0.00808%	23.46	0.00840%	23.45	0.00827%	23.97	0.00724%	23.87	0.77	1.04	0.88
LINE/CR1_7	0.07817%	20.88	0.08097%	21.84	0.06514%	19.73	0.06216%	19.76	0.06278%	20.92	0.06196%	20.68	1.04	0.95	0.99
LINE/CR1_70	0.00677%	14.25	0.00699%	15.44	0.00562%	11.81	0.00526%	12.75	0.00423%	16.89	0.00380%	16.07	1.03	0.94	0.90
LINE/CR1_71	0.00675%	7.46	0.00586%	6.41	0.00710%	5.5	0.00611%	4.95	0.00236%	13.04	0.00334%	9.8	0.87	0.86	1.42
LINE/CR1_72	0.00670%	12.08	0.00588%	11.59	0.00710%	11.41	0.00696%	11.03	0.00685%	10.93	0.00631%	11.89	0.88	0.98	0.92
LINE/CR1_73	0.00622%	24.68	0.00467%	24.81	0.00409%	22.71	0.00458%	23.39	0.00404%	25.64	0.00427%	24.38	0.75	1.12	1.06
LINE/CR1_74	0.00612%	21.90	0.00591%	22.77	0.00549%	22	0.00519%	23.27	0.00580%	24.97	0.00518%	23.63	0.97	0.94	0.89
LINE/CR1_75	0.00586%	14.37	0.00640%	14.55	0.00602%	14.15	0.00565%	14.27	0.00676%	14.8	0.00528%	13.74	1.09	0.94	0.78
LINE/CR1_76	0.00579%	19.47	0.00536%	20.85	0.00579%	18.2	0.00583%	17.88	0.00551%	19.56	0.00525%	20.17	0.93	1.01	0.95
LINE/CR1_77	0.00567%	12.75	0.00583%	12.94	0.00606%	9.95	0.00660%	11.38	0.00350%	18.91	0.00415%	15.04	1.03	1.09	1.19
LINE/CR1_78	0.00560%	15.07	0.00510%	14.70	0.00541%	11.81	0.00513%	11.86	0.00548%	11.82	0.00495%	11.69	0.91	0.95	0.90
LINE/CR1_79	0.00560%	19.76	0.00422%	19.28	0.00541%	20.56	0.00573%	20.7	0.00610%	21.38	0.00553%	20.83	0.75	1.06	0.91
LINE/CR1_8	0.06838%	1.52	0.06711%	1.12	0.04087%	2.3	0.02922%	3.03	0.04339%	2.44	0.04239%	2.07	0.98	0.71	0.98
LINE/CR1_80	0.00548%	17.26	0.00510%	17.28	0.00485%	15.59	0.00500%	14.95	0.00544%	14.75	0.00493%	15.34	0.93	1.03	0.91
LINE/CR1_81	0.00542%	17.93	0.00537%	18.20	0.00588%	14.86	0.00581%	15.32	0.00612%	15.34	0.00577%	15.74	0.99	0.99	0.94
LINE/CR1_82	0.00539%	15.60	0.00558%	16.21	0.00542%	14.9	0.00535%	14.91	0.00599%	14.65	0.00541%	14.57	1.03	0.99	0.90
LINE/CR1_83	0.00528%	16.74	0.00482%	17.19	0.00657%	16.89	0.00572%	15.95	0.00560%	18.82	0.00576%	17.93	0.91	0.87	1.03
LINE/CR1_84	0.00505%	14.13	0.00472%	12.32	0.00283%	16.34	0.00230%	15.17	0.00284%	13.28	0.00382%	12.64	0.93	0.81	1.35
LINE/CR1_85	0.00491%	23.87	0.00508%	24.70	0.00333%	26.05	0.00351%	22.84	0.00337%	25.79	0.00307%	24.86	1.03	1.05	0.91

LINE/CR1_86	0.00481%	17.41	0.00468%	18.36	0.00295%	15.5	0.00291%	16.92	0.00266%	20.16	0.00255%	18.83	0.97	0.99	0.96
LINE/CR1_87	0.00463%	18.04	0.00135%	21.16	0.00149%	20.67	0.00165%	20.18	0.00859%	11.22	0.00193%	19.83	0.29	1.11	0.23
LINE/CR1_88	0.00451%	19.48	0.00388%	19.08	0.00636%	15.9	0.00648%	15.79	0.00564%	18.72	0.00577%	18.38	0.86	1.02	1.02
LINE/CR1_89	0.00450%	12.73	0.00309%	13.82	0.00274%	12.63	0.00251%	12.8	0.00524%	10.59	0.00297%	12.71	0.69	0.92	0.57
LINE/CR1_9	0.05915%	22.67	0.06129%	23.64	0.04798%	21.29	0.04487%	21.54	0.04508%	22.89	0.04258%	22.57	1.04	0.94	0.94
LINE/CR1_90	0.00441%	8.18	0.00392%	8.75	0.00475%	14.03	0.00436%	13.67	0.00382%	16.22	0.00366%	15.78	0.89	0.92	0.96
LINE/CR1_91	0.00430%	12.45	0.00444%	12.68	0.00510%	12.35	0.00476%	12.15	0.00503%	11.16	0.00422%	11.87	1.03	0.93	0.84
LINE/CR1_92	0.00408%	11.15	0.00405%	11.20	0.00521%	10.91	0.00485%	10.74	0.00497%	11.89	0.00447%	11.21	0.99	0.93	0.90
LINE/CR1_93	0.00405%	16.26	0.00351%	15.02	0.00594%	15.02	0.00607%	15.92	0.00377%	20.73	0.00516%	18.61	0.87	1.02	1.37
LINE/CR1_94	0.00391%	18.06	0.00388%	16.74	0.00385%	18.76	0.00371%	18.49	0.00409%	17.21	0.00394%	18.25	0.99	0.96	0.96
LINE/CR1_95	0.00389%	24.79	0.00328%	25.32	0.00483%	22.01	0.00441%	20.9	0.00502%	21.33	0.00458%	20.51	0.84	0.91	0.91
LINE/CR1_96	0.00364%	20.70	0.00213%	21.70	0.00509%	20.24	0.00509%	19.42	0.00168%	22.85	0.00113%	22.26	0.59	1.00	0.67
LINE/CR1_97	0.00363%	12.35	0.00359%	11.96	0.00373%	11.82	0.00354%	12.09	0.00435%	12.61	0.00322%	11.54	0.99	0.95	0.74
LINE/CR1_98	0.00359%	17.86	0.00335%	19.35	0.00310%	17.78	0.00260%	18.11	0.00254%	20.8	0.00264%	20.57	0.93	0.84	1.04
LINE/CR1_99	0.00354%	10.23	0.00363%	10.76	0.00506%	10.81	0.00483%	10.52	0.00271%	16.82	0.00351%	14.19	1.03	0.95	1.29
LINE/I_1	0.08220%	14.71	0.08593%	14.82	0.07041%	13.07	0.07272%	13.05	0.07946%	12.98	0.07619%	13.05	1.05	1.03	0.96
LINE/I_10	0.01586%	12.89	0.01752%	12.97	0.01430%	11.39	0.01508%	12.59	0.01589%	11.48	0.01327%	11.83	1.10	1.05	0.84
LINE/I_11	0.01399%	14.02	0.01331%	14.72	0.01385%	11.38	0.01481%	11.96	0.00629%	17.27	0.01021%	15.64	0.95	1.07	1.62
LINE/I_12	0.01357%	11.17	0.01418%	11.04	0.01213%	10.33	0.01275%	11.2	0.01392%	10.75	0.01079%	10.74	1.05	1.05	0.78
LINE/I_13	0.01280%	14.75	0.01315%	14.95	0.00977%	15.16	0.00902%	15.46	0.00955%	16.16	0.00860%	15.78	1.03	0.92	0.90
LINE/I_14	0.01257%	16.45	0.01364%	17.19	0.01141%	15.26	0.01094%	15.17	0.01192%	15.51	0.01092%	15.49	1.09	0.96	0.92
LINE/I_15	0.01219%	18.26	0.01324%	18.44	0.01064%	16.69	0.01209%	16.58	0.01198%	16.88	0.01100%	17.39	1.09	1.14	0.92
LINE/I_16	0.01200%	18.06	0.01227%	17.95	0.01112%	17.37	0.01037%	17.1	0.01165%	17.29	0.01126%	17.57	1.02	0.93	0.97
LINE/I_17	0.01160%	16.15	0.01213%	16.62	0.01089%	14.02	0.01048%	14.36	0.00792%	20.29	0.00839%	17.45	1.05	0.96	1.06
LINE/I_18	0.01003%	14.68	0.01071%	15.37	0.01072%	13.93	0.01089%	14.31	0.00890%	13.94	0.00965%	13.95	1.07	1.02	1.08
LINE/I_19	0.00976%	18.23	0.00984%	19.49	0.00997%	15.84	0.00951%	16.17	0.00931%	16.99	0.00956%	15.9	1.01	0.95	1.03
LINE/I_2	0.05614%	14.59	0.05903%	15.15	0.04954%	12.34	0.05106%	12.13	0.05063%	13	0.04603%	12.95	1.05	1.03	0.91
LINE/I_20	0.00891%	15.68	0.00968%	16.74	0.00883%	14.78	0.00826%	14.49	0.00794%	15.01	0.00836%	14.51	1.09	0.94	1.05
LINE/I_21	0.00883%	13.11	0.00974%	13.87	0.00850%	11.43	0.00815%	12.35	0.00556%	16.65	0.00579%	16.25	1.10	0.96	1.04
LINE/I_22	0.00846%	13.16	0.00889%	13.22	0.01071%	11.01	0.01112%	11.86	0.00999%	11.9	0.00846%	11.34	1.05	1.04	0.85
LINE/I_23	0.00824%	11.27	0.00829%	11.45	0.00845%	9.76	0.00844%	9.16	0.00791%	10.47	0.00648%	10.65	1.01	1.00	0.82

LINE/I_24	0.00800%	8.81	0.00888%	8.57	0.00747%	7.71	0.00898%	7.16	0.00892%	7.39	0.00798%	7.48	1.11	1.20	0.89
LINE/I_25	0.00779%	16.72	0.00860%	18.05	0.00746%	15.36	0.00766%	15.71	0.00776%	15.65	0.00717%	15.58	1.10	1.03	0.92
LINE/I_26	0.00694%	24.28	0.00755%	24.99	0.00531%	22.31	0.00546%	22.17	0.00584%	21.14	0.00530%	22	1.09	1.03	0.91
LINE/I_27	0.00589%	16.65	0.00575%	15.97	0.00526%	15.87	0.00548%	15.45	0.00577%	15.46	0.00531%	16.23	0.97	1.04	0.92
LINE/I_28	0.00586%	13.37	0.00629%	13.16	0.00649%	12.5	0.00654%	11.52	0.00670%	13.3	0.00582%	12.81	1.07	1.01	0.87
LINE/I_29	0.00585%	15.50	0.00700%	16.28	0.00600%	15.44	0.00566%	14.86	0.00594%	14.83	0.00619%	15.07	1.20	0.94	1.04
LINE/I_3	0.04698%	14.39	0.04863%	15.18	0.04238%	11.92	0.04117%	12.33	0.04373%	12.46	0.04038%	12.44	1.04	0.97	0.92
LINE/I_30	0.00571%	12.81	0.00656%	13.62	0.00566%	12.19	0.00617%	11.73	0.00582%	12.75	0.00504%	13.07	1.15	1.09	0.87
LINE/I_31	0.00562%	12.77	0.00551%	13.24	0.00189%	22.26	0.00247%	17.15	0.00269%	16.84	0.00372%	11.36	0.98	1.30	1.39
LINE/I_32	0.00560%	13.11	0.00574%	13.43	0.00529%	10.57	0.00523%	10.38	0.00482%	11.65	0.00400%	12.36	1.02	0.99	0.83
LINE/I_33	0.00535%	10.62	0.00506%	9.83	0.00460%	7.92	0.00522%	6.21	0.00485%	6.3	0.00438%	6.47	0.95	1.13	0.90
LINE/I_34	0.00521%	17.17	0.00546%	17.63	0.00529%	15.52	0.00533%	17.06	0.00524%	15.64	0.00501%	16.44	1.05	1.01	0.96
LINE/I_35	0.00497%	20.36	0.00530%	22.26	0.00423%	18.64	0.00482%	18.22	0.00458%	16.28	0.00408%	17.65	1.07	1.14	0.89
LINE/I_36	0.00486%	16.89	0.00505%	17.83	0.00507%	15.6	0.00498%	15.61	0.00425%	16	0.00406%	15.42	1.04	0.98	0.95
LINE/I_37	0.00461%	6.83	0.00557%	6.39	0.00462%	6.3	0.00540%	6.29	0.00510%	6.34	0.00379%	6.51	1.21	1.17	0.74
LINE/I_38	0.00451%	24.95	0.00589%	28.87	0.00441%	24.94	0.00435%	24.43	0.00458%	23.75	0.00454%	22.74	1.31	0.99	0.99
LINE/I_39	0.00447%	13.58	0.00496%	14.28	0.00479%	11.75	0.00438%	12.24	0.00439%	12.77	0.00449%	11.94	1.11	0.91	1.02
LINE/I_4	0.03742%	7.49	0.03189%	7.82	0.02962%	7.22	0.02807%	7.51	0.04682%	6.85	0.02876%	7.01	0.85	0.95	0.61
LINE/I_40	0.00419%	18.91	0.00485%	22.51	0.00425%	18.78	0.00484%	16.67	0.00405%	18.62	0.00374%	19.07	1.16	1.14	0.92
LINE/I_41	0.00413%	20.70	0.00434%	21.07	0.00348%	19.18	0.00356%	19.72	0.00373%	19.02	0.00342%	19.17	1.05	1.02	0.92
LINE/I_42	0.00390%	15.49	0.00396%	16.04	0.00349%	14.54	0.00364%	15.88	0.00369%	15.45	0.00333%	14.89	1.01	1.04	0.90
LINE/I_43	0.00386%	19.25	0.00370%	19.16	0.00398%	18.92	0.00363%	18.64	0.00373%	19.36	0.00357%	18.92	0.96	0.91	0.96
LINE/I_44	0.00292%	15.73	0.00307%	16.36	0.00280%	15.75	0.00285%	15.67	0.00252%	14.25	0.00242%	14.53	1.05	1.02	0.96
LINE/I_45	0.00284%	18.44	0.00285%	19.59	0.00285%	17.11	0.00285%	15.8	0.00328%	17.05	0.00289%	16.94	1.01	1.00	0.88
LINE/I_46	0.00281%	6.03	0.00319%	4.79	0.00263%	3.96	0.00129%	6.85	0.00120%	8.27	0.00164%	7.83	1.13	0.49	1.37
LINE/I_47	0.00271%	14.60	0.00301%	14.85	0.00336%	12.03	0.00269%	13.91	0.00257%	13.26	0.00269%	13.71	1.11	0.80	1.04
LINE/I_48	0.00264%	10.02	0.00289%	10.42	0.00249%	8.89	0.00284%	9.1	0.00261%	9.33	0.00256%	9.22	1.10	1.14	0.98
LINE/I_49	0.00249%	9.00	0.00256%	7.68	0.00251%	10.44	0.00269%	8.87	0.00302%	9.7	0.00252%	9.6	1.03	1.07	0.83
LINE/I_5	0.03207%	15.42	0.03372%	16.07	0.02870%	13.97	0.03249%	13.54	0.03089%	13.56	0.02882%	13.31	1.05	1.13	0.93
LINE/I_50	0.00245%	24.97	0.00248%	23.05	0.00169%	23.77	0.00204%	21.48	0.00204%	22.58	0.00194%	21.09	1.01	1.20	0.95
LINE/I_51	0.00241%	18.99	0.00297%	20.41	0.00248%	15.09	0.00320%	15.14	0.00274%	15.83	0.00209%	16.76	1.23	1.29	0.77

LINE/I_52	0.00225%	6.60	0.00227%	6.88	0.00120%	9.87	0.00139%	6.34	0.00079%	14.32	0.00099%	9.64	1.01	1.15	1.26
LINE/I_53	0.00208%	23.79	0.00226%	23.99	0.00125%	21.51	0.00131%	19.04	0.00139%	18.89	0.00142%	20.06	1.08	1.05	1.02
LINE/I_54	0.00198%	13.24	0.00183%	13.92	0.00208%	9.42	0.00188%	10.79	0.00125%	14.99	0.00137%	15.35	0.92	0.91	1.09
LINE/I_55	0.00185%	22.46	0.00241%	27.15	0.00143%	20.33	0.00150%	19.69	0.00132%	26.99	0.00146%	23.7	1.30	1.05	1.10
LINE/I_56	0.00180%	10.93	0.00201%	11.08	0.00186%	11.8	0.00212%	10.64	0.00179%	10.33	0.00167%	10.85	1.12	1.14	0.94
LINE/I_57	0.00180%	0.71	0.00164%	0.69	0.00315%	0.91	0.00283%	0.77	0.00051%	0.61	0.00079%	0.57	0.92	0.90	1.55
LINE/I_58	0.00173%	14.78	0.00177%	15.29	0.00146%	15.16	0.00133%	14.88	0.00176%	14.67	0.00171%	14.06	1.02	0.91	0.97
LINE/I_59	0.00168%	19.87	0.00200%	22.37	0.00154%	19.31	0.00144%	19.64	0.00163%	19.43	0.00159%	20.84	1.19	0.94	0.98
LINE/I_6	0.02941%	18.49	0.03016%	20.46	0.02794%	14.61	0.02762%	14.62	0.01642%	23.62	0.01921%	20.39	1.03	0.99	1.17
LINE/I_60	0.00135%	11.27	0.00148%	10.53	0.00132%	9.54	0.00105%	10.79	0.00157%	11.09	0.00141%	10.68	1.10	0.80	0.90
LINE/I_61	0.00133%	19.85	0.00134%	19.53	0.00158%	15.72	0.00137%	16.81	0.00143%	16.06	0.00138%	14.75	1.01	0.87	0.97
LINE/I_62	0.00030%	9.11	0.00034%	4.81	0.00063%	3.39	0.00061%	4.57	0.00008%	9.19	0.00022%	6.35	1.11	0.96	2.65
LINE/I_7	0.02263%	18.86	0.01471%	16.66	0.02101%	15.95	0.02043%	15.95	0.01758%	19.01	0.01749%	18.1	0.65	0.97	0.99
LINE/I_8	0.02154%	15.31	0.02319%	14.23	0.02155%	11.48	0.02256%	11.03	0.01912%	13.78	0.01831%	13.6	1.08	1.05	0.96
LINE/I_9	0.01793%	17.98	0.01833%	18.43	0.01568%	16.74	0.01585%	16.67	0.01281%	16.86	0.01619%	16.8	1.02	1.01	1.26
LINE/Jockey_1	0.17982%	7.14	0.19816%	8.14	0.16860%	7.24	0.17583%	7.14	0.21777%	7.25	0.16127%	7.4	1.10	1.04	0.74
LINE/Jockey_10	0.03580%	11.48	0.03649%	11.55	0.03084%	11.71	0.03105%	11.97	0.03607%	10.99	0.03120%	11.51	1.02	1.01	0.87
LINE/Jockey_100	0.00178%	20.66	0.00224%	20.04	0.00207%	13.15	0.00228%	15.86	0.00166%	19.23	0.00207%	17.1	1.26	1.10	1.25
LINE/Jockey_101	0.00162%	4.40	0.00121%	4.58	0.00116%	3.6	0.00085%	3.96	0.00082%	4.12	0.00090%	5.23	0.74	0.73	1.09
LINE/Jockey_102	0.00153%	15.86	0.00288%	14.36	0.00159%	12.34	0.00212%	12.89	0.00175%	12.43	0.00185%	13.17	1.88	1.33	1.06
LINE/Jockey_103	0.00100%	15.71	0.00090%	13.76	0.00097%	11.05	0.00114%	11.73	0.00140%	12.48	0.00093%	12.06	0.90	1.18	0.67
LINE/Jockey_104	0.00098%	8.48	0.00091%	7.92	0.00089%	9.56	0.00087%	8.84	0.00126%	8.84	0.00087%	8.46	0.92	0.99	0.69
LINE/Jockey_105	0.00091%	9.48	0.00131%	13.40	0.00089%	10.63	0.00108%	10.27	0.00127%	10.25	0.00110%	10.61	1.43	1.22	0.86
LINE/Jockey_106	0.00073%	9.39	0.00102%	14.38	0.00067%	9.27	0.00059%	12.16	0.00071%	8.98	0.00062%	11.22	1.40	0.88	0.87
LINE/Jockey_107	0.00063%	13.86	0.00065%	13.61	0.00138%	14.54	0.00159%	13.1	0.00170%	13.74	0.00153%	13.92	1.03	1.15	0.90
LINE/Jockey_108	0.00048%	21.31	0.00046%	22.25	0.00074%	17.97	0.00078%	17.75	0.00081%	16.95	0.00061%	16.1	0.96	1.06	0.75
LINE/Jockey_109	0.00046%	14.77	0.00052%	13.78	0.00071%	13.69	0.00063%	13.65	0.00072%	13.05	0.00064%	11.61	1.14	0.89	0.89
LINE/Jockey_11	0.03217%	14.88	0.02636%	13.92	0.02631%	11.55	0.02622%	11.33	0.03183%	11.55	0.02420%	12.32	0.82	1.00	0.76
*LINE/Jockey_110	0.00039%	19.95	0.00139%	8.14	0.00045%	11.3	0.00074%	12.43	0.00037%	16.01	0.00035%	13.91	3.58	1.63	0.95
LINE/Jockey_12	0.03109%	14.19	0.04310%	13.04	0.02867%	10.78	0.03160%	10.13	0.03066%	10.96	0.02576%	11.37	1.39	1.10	0.84
LINE/Jockey_13	0.03095%	4.03	0.02987%	3.89	0.02605%	4.85	0.02562%	4.94	0.03107%	4.77	0.02571%	4.99	0.97	0.98	0.83

LINE/Jockey_14	0.02971%	15.36	0.02953%	16.74	0.02617%	13.59	0.02823%	13.1	0.03260%	13.22	0.02550%	13.73	0.99	1.08	0.78
LINE/Jockey_15	0.02712%	11.63	0.02591%	11.85	0.02344%	10.95	0.02173%	11.18	0.02648%	10.89	0.02299%	10.92	0.96	0.93	0.87
LINE/Jockey_16	0.02679%	10.26	0.02546%	10.34	0.02191%	10.67	0.02197%	10.61	0.02584%	10.49	0.02211%	10.51	0.95	1.00	0.86
LINE/Jockey_17	0.02631%	13.27	0.02510%	13.44	0.02388%	11.64	0.02647%	11.96	0.03212%	12.42	0.02328%	12.72	0.95	1.11	0.72
LINE/Jockey_18	0.02556%	10.29	0.02890%	9.86	0.02361%	9.33	0.02491%	8.41	0.02862%	8.71	0.02457%	8.78	1.13	1.06	0.86
LINE/Jockey_19	0.02337%	3.74	0.02310%	3.67	0.02116%	3.3	0.02275%	3.28	0.02984%	3.2	0.02282%	3.24	0.99	1.07	0.76
LINE/Jockey_2	0.08186%	14.57	0.07829%	14.91	0.07039%	13.29	0.07375%	13.08	0.08841%	13.28	0.06610%	13.25	0.96	1.05	0.75
LINE/Jockey_20	0.02283%	10.49	0.02243%	10.39	0.01877%	9.75	0.02029%	9.5	0.02250%	9.28	0.01903%	9.5	0.98	1.08	0.85
LINE/Jockey_21	0.02259%	19.22	0.02242%	19.65	0.02104%	18.8	0.02177%	18.06	0.02091%	18.57	0.02027%	19.3	0.99	1.03	0.97
LINE/Jockey_22	0.02169%	19.51	0.02152%	20.19	0.01846%	16.77	0.01863%	16.83	0.02275%	17.11	0.01736%	17.57	0.99	1.01	0.76
LINE/Jockey_23	0.02094%	15.67	0.01910%	15.28	0.01944%	13.58	0.01972%	13.32	0.02472%	13.32	0.01854%	13.7	0.91	1.01	0.75
LINE/Jockey_24	0.02072%	3.79	0.01954%	3.93	0.02038%	3.47	0.01906%	3.82	0.02345%	3.69	0.01889%	3.64	0.94	0.94	0.81
LINE/Jockey_25	0.01956%	19.42	0.01614%	18.82	0.01600%	17.5	0.01589%	16.89	0.01936%	16.86	0.01485%	17.3	0.83	0.99	0.77
LINE/Jockey_26	0.01891%	15.81	0.01498%	15.87	0.01102%	12.86	0.01034%	11.98	0.01363%	17.22	0.00724%	15.55	0.79	0.94	0.53
LINE/Jockey_27	0.01873%	4.65	0.01803%	4.79	0.01495%	5.82	0.01429%	4.86	0.01498%	5.37	0.01445%	5.2	0.96	0.96	0.96
LINE/Jockey_28	0.01827%	9.21	0.01673%	9.62	0.01421%	8.82	0.01487%	9.42	0.01674%	8.92	0.01317%	9.04	0.92	1.05	0.79
LINE/Jockey_29	0.01817%	5.15	0.01707%	5.19	0.02044%	5.56	0.01981%	5.67	0.02408%	5.4	0.02021%	5.1	0.94	0.97	0.84
LINE/Jockey_3	0.07011%	8.96	0.07553%	8.82	0.06842%	8.42	0.06672%	8.26	0.07849%	8.18	0.06913%	8.41	1.08	0.98	0.88
LINE/Jockey_30	0.01740%	13.48	0.01528%	14.12	0.01810%	13.2	0.01896%	11.93	0.02276%	12.88	0.01796%	12.89	0.88	1.05	0.79
LINE/Jockey_31	0.01720%	11.29	0.01734%	11.24	0.01681%	9.71	0.01693%	9.4	0.01964%	9.66	0.01613%	9.8	1.01	1.01	0.82
LINE/Jockey_32	0.01716%	14.24	0.01699%	15.21	0.02045%	11.78	0.02053%	11.83	0.02557%	12.21	0.01787%	12.18	0.99	1.00	0.70
LINE/Jockey_33	0.01646%	15.18	0.01507%	15.90	0.01335%	12.88	0.01416%	12.18	0.01704%	12.32	0.01297%	13.21	0.92	1.06	0.76
LINE/Jockey_34	0.01564%	7.30	0.01492%	7.14	0.01405%	6.76	0.01321%	6.65	0.01528%	6.78	0.01306%	6.57	0.95	0.94	0.85
LINE/Jockey_35	0.01559%	21.99	0.01382%	22.96	0.01287%	19.67	0.01269%	19.43	0.01593%	18.6	0.01284%	19.64	0.89	0.99	0.81
LINE/Jockey_36	0.01541%	10.89	0.01339%	11.25	0.01633%	9.26	0.01869%	9.49	0.02204%	9.41	0.01513%	9.8	0.87	1.14	0.69
LINE/Jockey_37	0.01533%	13.78	0.01404%	14.04	0.01710%	12.67	0.01734%	12.23	0.02200%	12.47	0.01504%	12.7	0.92	1.01	0.68
LINE/Jockey_38	0.01497%	7.98	0.01368%	7.67	0.01807%	6.7	0.01838%	6.69	0.02287%	7.18	0.01629%	7.33	0.91	1.02	0.71
LINE/Jockey_39	0.01464%	12.30	0.01406%	12.28	0.01366%	11.4	0.01249%	11.18	0.01423%	11.43	0.01393%	11.29	0.96	0.91	0.98
LINE/Jockey_4	0.05239%	3.36	0.04941%	3.47	0.04902%	2.81	0.04797%	2.84	0.05252%	3.19	0.04502%	3.07	0.94	0.98	0.86
LINE/Jockey_40	0.01419%	15.18	0.01326%	15.73	0.01377%	14.34	0.01615%	13.74	0.01847%	13.97	0.01335%	14.14	0.93	1.17	0.72
LINE/Jockey_41	0.01412%	15.03	0.01216%	13.80	0.01560%	12.27	0.01720%	12.06	0.02039%	12.17	0.01536%	12.22	0.86	1.10	0.75

LINE/Jockey_42	0.01364%	16.24	0.02511%	14.24	0.01336%	11.02	0.01733%	10.93	0.01385%	12.59	0.01297%	12.14	1.84	1.30	0.94
LINE/Jockey_43	0.01356%	8.15	0.01233%	8.76	0.01345%	6.75	0.01388%	6.66	0.01567%	6.83	0.01218%	7.48	0.91	1.03	0.78
LINE/Jockey_44	0.01315%	10.67	0.01060%	8.91	0.01180%	9.35	0.01373%	8.32	0.01575%	9.15	0.01173%	9.25	0.81	1.16	0.74
LINE/Jockey_45	0.01232%	12.22	0.01195%	12.46	0.01071%	11.22	0.00994%	11.42	0.01217%	11.41	0.01041%	11.52	0.97	0.93	0.85
LINE/Jockey_46	0.01229%	12.27	0.01098%	12.12	0.01126%	11.01	0.01236%	11.73	0.01516%	11.47	0.01023%	10.99	0.89	1.10	0.68
LINE/Jockey_47	0.01226%	21.29	0.01305%	21.41	0.01115%	19.81	0.01069%	20.19	0.01235%	20.29	0.01078%	20.63	1.06	0.96	0.87
LINE/Jockey_48	0.01151%	11.35	0.01002%	11.95	0.01349%	10.87	0.01369%	10.79	0.01644%	10.63	0.01196%	11.24	0.87	1.02	0.73
LINE/Jockey_49	0.01133%	17.75	0.01007%	17.72	0.01107%	15.57	0.01083%	15.78	0.01228%	15	0.00980%	15.92	0.89	0.98	0.80
LINE/Jockey_5	0.04293%	13.58	0.03632%	13.04	0.03520%	10.98	0.03683%	10.84	0.04694%	11.02	0.03502%	11.19	0.85	1.05	0.75
LINE/Jockey_50	0.01110%	10.68	0.01086%	10.77	0.01087%	9.82	0.00964%	9.87	0.01006%	11.07	0.00914%	10.49	0.98	0.89	0.91
LINE/Jockey_51	0.01100%	15.41	0.01227%	15.98	0.01006%	13.61	0.00949%	13.54	0.00930%	15.71	0.00849%	15.49	1.12	0.94	0.91
LINE/Jockey_52	0.01092%	14.58	0.00923%	15.54	0.01406%	13.1	0.01451%	12.67	0.01781%	12.49	0.01163%	12.63	0.84	1.03	0.65
LINE/Jockey_53	0.01012%	14.21	0.00933%	13.70	0.01090%	13.4	0.01030%	12.91	0.01230%	13.6	0.00978%	13.61	0.92	0.94	0.80
LINE/Jockey_54	0.00961%	7.94	0.00969%	7.63	0.01207%	6.61	0.01082%	7.02	0.00796%	8.61	0.00796%	8.34	1.01	0.90	1.00
LINE/Jockey_55	0.00837%	9.26	0.00843%	10.38	0.00849%	9.2	0.00920%	9.15	0.01131%	9.03	0.00871%	9.23	1.01	1.08	0.77
LINE/Jockey_56	0.00836%	17.46	0.00810%	18.26	0.00828%	16.78	0.00816%	16.2	0.00964%	16.6	0.00749%	16.35	0.97	0.99	0.78
LINE/Jockey_57	0.00827%	15.94	0.00776%	15.85	0.00616%	13.74	0.00646%	13.43	0.00820%	13.73	0.00619%	13.48	0.94	1.05	0.76
LINE/Jockey_58	0.00823%	7.45	0.00785%	7.16	0.00769%	5.68	0.00788%	4.96	0.00909%	5.81	0.00664%	6.44	0.95	1.02	0.73
LINE/Jockey_59	0.00753%	13.21	0.00718%	12.62	0.00731%	11.21	0.00749%	11.53	0.00653%	14.28	0.00618%	13.47	0.95	1.02	0.95
LINE/Jockey_6	0.03976%	3.29	0.03747%	3.20	0.04000%	3.45	0.04019%	3.37	0.04837%	3.14	0.03936%	3.31	0.94	1.00	0.81
LINE/Jockey_60	0.00730%	8.81	0.00844%	8.02	0.00656%	7.76	0.00630%	7.39	0.00749%	7.53	0.00620%	7.91	1.16	0.96	0.83
LINE/Jockey_61	0.00712%	11.62	0.00528%	10.77	0.00606%	10.62	0.00712%	10.91	0.00820%	11.35	0.00605%	11.24	0.74	1.18	0.74
LINE/Jockey_62	0.00709%	8.44	0.00650%	8.14	0.00788%	6.64	0.00757%	7.24	0.01049%	6.74	0.00701%	6.65	0.92	0.96	0.67
LINE/Jockey_63	0.00701%	15.34	0.00647%	15.83	0.00688%	14.06	0.00818%	13.45	0.00928%	13.5	0.00703%	13.91	0.92	1.19	0.76
LINE/Jockey_64	0.00682%	11.91	0.00662%	12.00	0.00536%	9.87	0.00592%	10.49	0.00590%	10.73	0.00509%	10.26	0.97	1.10	0.86
LINE/Jockey_65	0.00668%	12.46	0.00552%	11.98	0.00650%	11.27	0.00664%	11.51	0.00810%	11.66	0.00583%	12.04	0.83	1.02	0.72
LINE/Jockey_66	0.00643%	12.63	0.00680%	13.13	0.00450%	11.1	0.00461%	10.1	0.00442%	9.49	0.00425%	10.11	1.06	1.02	0.96
LINE/Jockey_67	0.00626%	10.25	0.00586%	9.94	0.00451%	9.48	0.00462%	10.35	0.00553%	9.53	0.00466%	9.58	0.94	1.03	0.84
LINE/Jockey_68	0.00605%	13.27	0.00539%	13.01	0.00467%	11.96	0.00519%	11.93	0.00705%	12.32	0.00449%	12.47	0.89	1.11	0.64
LINE/Jockey_69	0.00605%	12.84	0.00591%	14.21	0.00728%	11.2	0.00738%	10.51	0.00895%	11.13	0.00645%	12.34	0.98	1.01	0.72
LINE/Jockey_7	0.03943%	11.72	0.03857%	12.03	0.03712%	10.44	0.03537%	10.49	0.03923%	10.1	0.03379%	10.1	0.98	0.95	0.86

LINE/Jockey_70	0.00586%	9.91	0.00539%	10.14	0.00570%	8.29	0.00626%	8.5	0.00692%	9.06	0.00529%	9.48	0.92	1.10	0.76
LINE/Jockey_71	0.00538%	16.89	0.00368%	14.90	0.00408%	13.8	0.00422%	13.73	0.00529%	13.34	0.00361%	13.9	0.68	1.03	0.68
*LINE/Jockey_72	0.00469%	18.31	0.01107%	13.32	0.00439%	15.77	0.00562%	13.86	0.00524%	12.72	0.00504%	12.91	2.36	1.28	0.96
LINE/Jockey_73	0.00460%	15.61	0.00443%	15.25	0.00434%	15.16	0.00417%	13.34	0.00541%	14.54	0.00418%	15.08	0.96	0.96	0.77
LINE/Jockey_74	0.00440%	21.78	0.00318%	21.08	0.00404%	17.96	0.00416%	17.27	0.00535%	18.19	0.00414%	18.2	0.72	1.03	0.77
LINE/Jockey_75	0.00423%	17.57	0.00271%	16.55	0.00414%	14.85	0.00392%	15.08	0.00499%	16.09	0.00408%	16.4	0.64	0.95	0.82
LINE/Jockey_76	0.00414%	11.36	0.00457%	15.25	0.00337%	10.67	0.00338%	10.05	0.00403%	10.2	0.00304%	11.4	1.10	1.00	0.75
LINE/Jockey_77	0.00403%	7.44	0.00418%	11.16	0.00309%	7.47	0.00351%	6.28	0.00214%	9.26	0.00201%	7.51	1.04	1.14	0.94
LINE/Jockey_78	0.00394%	7.61	0.00369%	8.65	0.00627%	5.56	0.00689%	4.66	0.00813%	5.51	0.00544%	6.15	0.94	1.10	0.67
LINE/Jockey_79	0.00384%	16.84	0.00312%	16.75	0.00332%	15.25	0.00333%	15.2	0.00393%	14.59	0.00315%	15.54	0.81	1.00	0.80
LINE/Jockey_8	0.03768%	12.91	0.03665%	13.38	0.03476%	10.69	0.03794%	10.51	0.04314%	11.13	0.03139%	11.76	0.97	1.09	0.73
LINE/Jockey_80	0.00384%	16.57	0.00355%	16.48	0.00392%	14.89	0.00484%	14.76	0.00544%	15.11	0.00416%	15.38	0.93	1.24	0.77
LINE/Jockey_81	0.00371%	15.70	0.00335%	15.75	0.00349%	15.36	0.00370%	15.66	0.00485%	15.49	0.00328%	15.68	0.90	1.06	0.68
LINE/Jockey_82	0.00371%	19.17	0.00281%	17.38	0.00360%	17.46	0.00409%	16.79	0.00429%	18.1	0.00346%	17.65	0.76	1.14	0.81
LINE/Jockey_83	0.00354%	16.29	0.00292%	15.04	0.00274%	14.41	0.00290%	14.38	0.00348%	14.5	0.00296%	14.47	0.82	1.06	0.85
LINE/Jockey_84	0.00335%	8.73	0.00331%	9.20	0.00315%	9.99	0.00301%	9.87	0.00346%	9.3	0.00241%	9.22	0.99	0.95	0.70
LINE/Jockey_85	0.00319%	19.30	0.00276%	19.60	0.00279%	16.82	0.00284%	16.4	0.00358%	16.83	0.00265%	17.04	0.87	1.02	0.74
LINE/Jockey_86	0.00318%	16.98	0.00290%	16.90	0.00307%	15.62	0.00343%	14.93	0.00424%	15.39	0.00324%	15.27	0.91	1.12	0.76
LINE/Jockey_87	0.00313%	12.79	0.00250%	13.79	0.00239%	12.32	0.00281%	11.9	0.00134%	15.58	0.00143%	14.76	0.80	1.18	1.06
LINE/Jockey_88	0.00302%	17.21	0.00312%	17.44	0.00236%	15.21	0.00259%	15.99	0.00264%	15.52	0.00232%	15.51	1.03	1.10	0.88
LINE/Jockey_89	0.00295%	17.43	0.00355%	17.92	0.00250%	16.75	0.00276%	17.12	0.00306%	16.67	0.00269%	16.76	1.20	1.10	0.88
LINE/Jockey_9	0.03693%	13.97	0.03463%	14.35	0.02986%	12.65	0.03224%	13.01	0.03667%	12.7	0.02825%	12.94	0.94	1.08	0.77
LINE/Jockey_90	0.00292%	18.55	0.00266%	18.13	0.00355%	15.76	0.00330%	16.56	0.00425%	15.43	0.00302%	16.72	0.91	0.93	0.71
LINE/Jockey_91	0.00290%	12.23	0.00266%	12.68	0.00333%	11.72	0.00331%	10.99	0.00378%	11.95	0.00266%	12.03	0.92	1.00	0.70
LINE/Jockey_92	0.00284%	16.91	0.00393%	18.62	0.00222%	16.16	0.00305%	12.9	0.00269%	13.94	0.00244%	14.49	1.38	1.37	0.91
LINE/Jockey_93	0.00282%	11.16	0.00320%	11.36	0.00266%	11.19	0.00296%	10.74	0.00312%	10.39	0.00292%	9.69	1.13	1.11	0.93
LINE/Jockey_94	0.00247%	9.75	0.00344%	17.78	0.00191%	10.39	0.00222%	10.54	0.00238%	8.93	0.00201%	8.95	1.39	1.16	0.85
LINE/Jockey_95	0.00245%	25.16	0.00239%	26.34	0.00197%	13.73	0.00178%	13.88	0.00236%	14.23	0.00133%	14.49	0.98	0.90	0.56
LINE/Jockey_96	0.00243%	20.33	0.00260%	21.71	0.00322%	19.32	0.00301%	18.92	0.00339%	19.09	0.00265%	19.75	1.07	0.93	0.78
LINE/Jockey_97	0.00232%	20.93	0.00205%	21.66	0.00219%	20.11	0.00198%	20.29	0.00265%	19.21	0.00209%	20.06	0.88	0.91	0.79
LINE/Jockey_98	0.00225%	23.67	0.00319%	23.61	0.00232%	20.26	0.00245%	18.3	0.00211%	20.15	0.00233%	16.14	1.42	1.06	1.10

LINE/Jockey_99	0.00216%	22.89	0.00233%	24.45	0.00241%	19.76	0.00236%	20.01	0.00285%	20.86	0.00208%	21.87	1.08	0.98	0.73
LINE/L1_1	0.10008%	8.18	0.09358%	8.79	0.07634%	7.52	0.08519%	7.42	0.08657%	8.02	0.10233%	7.72	0.94	1.12	1.18
LINE/L1_10	0.01988%	18.20	0.02249%	19.05	0.01566%	13.6	0.01535%	13.97	0.01814%	14.05	0.01687%	12.82	1.13	0.98	0.93
*LINE/L1_100	0.00030%	8.42	0.00043%	15.14	0.00011%	8.37	0.00030%	9.62	0.00040%	6.65	0.00036%	7.94	1.42	2.64	0.89
LINE/L1_11	0.01328%	17.04	0.01424%	19.03	0.01166%	13.33	0.01140%	13.45	0.01122%	14.36	0.01126%	13.48	1.07	0.98	1.00
LINE/L1_12	0.01226%	17.27	0.01278%	17.33	0.00962%	16.06	0.00960%	16.03	0.01051%	16.07	0.01051%	15.93	1.04	1.00	1.00
LINE/L1_13	0.01202%	17.21	0.01328%	17.70	0.01107%	15.54	0.01126%	15.9	0.01132%	15.81	0.01182%	15.7	1.11	1.02	1.04
LINE/L1_14	0.01058%	12.17	0.01117%	12.62	0.01131%	9.44	0.01050%	10.39	0.00536%	14.73	0.00782%	13.05	1.06	0.93	1.46
LINE/L1_15	0.00943%	13.65	0.00922%	13.68	0.00375%	11.28	0.00254%	11.6	0.00266%	12.47	0.00418%	11.59	0.98	0.68	1.57
LINE/L1_16	0.00906%	14.42	0.00370%	18.17	0.00293%	16.84	0.00247%	17.29	0.01221%	7.29	0.00280%	16.71	0.41	0.84	0.23
LINE/L1_17	0.00904%	12.31	0.00900%	11.77	0.00858%	11.65	0.00841%	11.04	0.00895%	11.77	0.00943%	10.86	1.00	0.98	1.05
LINE/L1_18	0.00867%	11.07	0.00939%	11.14	0.00810%	10.2	0.00765%	9.78	0.00803%	9.58	0.00816%	9.96	1.08	0.95	1.02
LINE/L1_19	0.00851%	17.28	0.00743%	20.74	0.00531%	13.34	0.00501%	12.21	0.00970%	9.3	0.00498%	13.04	0.87	0.94	0.51
LINE/L1_2	0.08307%	7.77	0.08672%	8.04	0.07582%	7.37	0.07727%	6.96	0.08719%	6.94	0.07261%	7.58	1.04	1.02	0.83
LINE/L1_20	0.00822%	11.76	0.00828%	10.68	0.00815%	7.49	0.00811%	8.99	0.00750%	9.39	0.00733%	8.02	1.01	0.99	0.98
LINE/L1_21	0.00738%	15.95	0.00163%	18.83	0.00120%	19.07	0.00157%	14.82	0.01272%	9.17	0.00136%	17.51	0.22	1.31	0.11
LINE/L1_22	0.00736%	16.68	0.00802%	16.59	0.00736%	15.68	0.00679%	15.33	0.00749%	15.37	0.00687%	15.76	1.09	0.92	0.92
LINE/L1_23	0.00695%	13.55	0.00665%	17.24	0.00497%	11.92	0.00536%	10.53	0.00845%	6.98	0.00488%	10.26	0.96	1.08	0.58
LINE/L1_24	0.00689%	12.56	0.00689%	14.06	0.00498%	12.71	0.00622%	13.02	0.00415%	15.94	0.00480%	15.25	1.00	1.25	1.16
LINE/L1_25	0.00647%	18.84	0.00670%	20.68	0.00472%	17.32	0.00492%	17.21	0.00448%	16.21	0.00434%	17.79	1.04	1.04	0.97
LINE/L1_26	0.00612%	6.29	0.00756%	6.44	0.00689%	5.98	0.00647%	5.78	0.00584%	5.65	0.00604%	5.31	1.24	0.94	1.03
LINE/L1_27	0.00591%	16.06	0.00608%	21.65	0.00370%	12.91	0.00409%	11.64	0.00668%	8.67	0.00345%	13.13	1.03	1.11	0.52
LINE/L1_28	0.00529%	23.47	0.00657%	25.55	0.00438%	19.67	0.00486%	21.34	0.00472%	19.77	0.00456%	17.89	1.24	1.11	0.97
LINE/L1_29	0.00525%	29.87	0.00640%	31.31	0.00377%	24.57	0.00377%	24.31	0.00444%	25.46	0.00374%	25.78	1.22	1.00	0.84
LINE/L1_3	0.05874%	4.13	0.06189%	3.92	0.05456%	3.55	0.05654%	3.74	0.06118%	3.76	0.05086%	3.83	1.05	1.04	0.83
LINE/L1_30	0.00508%	20.34	0.00610%	22.52	0.00434%	16.89	0.00495%	17.89	0.00461%	18.47	0.00436%	16.81	1.20	1.14	0.95
LINE/L1_31	0.00494%	18.81	0.00520%	20.09	0.00374%	16.95	0.00457%	18.82	0.00418%	15.77	0.00415%	16.77	1.05	1.22	0.99
LINE/L1_32	0.00483%	17.57	0.00474%	18.80	0.00407%	14.22	0.00470%	13.77	0.00403%	13.62	0.00372%	14.05	0.98	1.16	0.92
LINE/L1_33	0.00475%	18.56	0.00551%	22.03	0.00383%	18.88	0.00345%	19.26	0.00427%	17.32	0.00431%	14.44	1.16	0.90	1.01
LINE/L1_34	0.00442%	11.43	0.00502%	11.56	0.00445%	9.9	0.00438%	10.43	0.00443%	10.96	0.00458%	10.97	1.14	0.98	1.03
LINE/L1_35	0.00431%	15.70	0.00400%	16.53	0.00294%	13.31	0.00318%	12.58	0.00357%	14.45	0.00327%	13.7	0.93	1.08	0.91

LINE/L1_36	0.00415%	26.11	0.00504%	28.10	0.00381%	22.01	0.00384%	21.08	0.00342%	23.46	0.00309%	21.62	1.21	1.01	0.90
LINE/L1_37	0.00403%	18.08	0.00412%	17.45	0.00259%	14.15	0.00298%	12.45	0.00385%	14.39	0.00307%	15.37	1.02	1.15	0.80
LINE/L1_38	0.00389%	19.02	0.00456%	19.84	0.00323%	12.51	0.00371%	13.86	0.00333%	16.97	0.00294%	13.26	1.17	1.15	0.88
LINE/L1_39	0.00387%	12.68	0.00522%	9.98	0.00405%	10.56	0.00604%	7.73	0.00370%	11.23	0.00341%	10.27	1.35	1.49	0.92
LINE/L1_4	0.04093%	15.44	0.03698%	14.40	0.03312%	7.61	0.03474%	7.36	0.04377%	8.83	0.04317%	8.18	0.90	1.05	0.99
LINE/L1_40	0.00377%	13.33	0.00462%	15.15	0.00375%	10.93	0.00368%	12.63	0.00356%	11.93	0.00271%	12.42	1.22	0.98	0.76
LINE/L1_41	0.00368%	26.45	0.00372%	26.89	0.00203%	18.78	0.00259%	20.99	0.00258%	19.84	0.00228%	19.11	1.01	1.27	0.88
LINE/L1_42	0.00366%	17.55	0.00351%	19.13	0.00322%	17.85	0.00327%	17.85	0.00317%	14.43	0.00288%	16.42	0.96	1.02	0.91
LINE/L1_43	0.00357%	11.20	0.00353%	14.81	0.00264%	8.76	0.00287%	11	0.00247%	9.94	0.00254%	10.9	0.99	1.09	1.03
LINE/L1_44	0.00355%	19.35	0.00434%	19.06	0.00335%	15.83	0.00344%	16.08	0.00360%	16.8	0.00305%	15.96	1.22	1.03	0.85
LINE/L1_45	0.00355%	23.07	0.00373%	25.02	0.00317%	19.23	0.00292%	20.15	0.00267%	19.57	0.00283%	17.01	1.05	0.92	1.06
LINE/L1_46	0.00348%	23.64	0.00397%	24.45	0.00367%	21.59	0.00412%	21.22	0.00368%	21.19	0.00323%	20.39	1.14	1.12	0.88
LINE/L1_47	0.00346%	15.22	0.00426%	18.57	0.00369%	15.41	0.00432%	19.05	0.00331%	14.93	0.00349%	14.76	1.23	1.17	1.05
LINE/L1_48	0.00328%	27.58	0.00450%	28.68	0.00300%	24.96	0.00313%	27.17	0.00330%	24.05	0.00294%	24.83	1.37	1.04	0.89
LINE/L1_49	0.00316%	16.63	0.00264%	22.59	0.00228%	17.89	0.00237%	16.52	0.00366%	11.92	0.00210%	17.56	0.84	1.04	0.57
LINE/L1_5	0.03518%	8.83	0.03361%	10.29	0.03056%	7.64	0.03047%	8.05	0.02576%	9.59	0.02335%	9.89	0.96	1.00	0.91
LINE/L1_50	0.00315%	28.04	0.00362%	27.83	0.00286%	24.99	0.00371%	25.26	0.00322%	25.23	0.00298%	25.08	1.15	1.30	0.93
LINE/L1_51	0.00295%	21.72	0.00348%	24.71	0.00211%	22.68	0.00213%	21.11	0.00215%	19.79	0.00243%	19.89	1.18	1.01	1.13
LINE/L1_52	0.00289%	19.25	0.00352%	17.74	0.00279%	17.18	0.00420%	12.86	0.00279%	18.66	0.00311%	18.19	1.22	1.50	1.11
LINE/L1_53	0.00285%	22.13	0.00315%	24.69	0.00244%	18.27	0.00193%	21.08	0.00216%	17.99	0.00221%	17.49	1.11	0.79	1.02
LINE/L1_54	0.00278%	23.40	0.00244%	21.78	0.00169%	17.08	0.00158%	14.51	0.00285%	24.22	0.00156%	18.52	0.88	0.93	0.55
LINE/L1_55	0.00268%	28.81	0.00328%	29.89	0.00177%	26.64	0.00205%	26.55	0.00245%	27.26	0.00191%	26.13	1.22	1.16	0.78
LINE/L1_56	0.00258%	24.39	0.00325%	21.94	0.00210%	19.54	0.00206%	21.42	0.00237%	19.04	0.00208%	18.02	1.26	0.98	0.88
LINE/L1_57	0.00251%	15.03	0.00236%	20.55	0.00187%	12.04	0.00202%	13.32	0.00346%	11.04	0.00158%	14.47	0.94	1.08	0.46
LINE/L1_58	0.00248%	25.58	0.00326%	25.98	0.00201%	21.8	0.00204%	22.15	0.00241%	20.67	0.00194%	22.62	1.32	1.01	0.81
LINE/L1_59	0.00248%	10.62	0.00262%	9.98	0.00156%	8.95	0.00088%	13.45	0.00101%	10.79	0.00139%	10.03	1.06	0.57	1.38
LINE/L1_6	0.03297%	9.74	0.03595%	10.82	0.03452%	9.14	0.03171%	9.03	0.03421%	8.8	0.03602%	8.6	1.09	0.92	1.05
LINE/L1_60	0.00247%	25.76	0.00319%	27.73	0.00170%	24.36	0.00197%	23.92	0.00197%	24.17	0.00211%	23.17	1.29	1.16	1.07
LINE/L1_61	0.00233%	11.87	0.00243%	13.22	0.00230%	10.77	0.00204%	10.46	0.00234%	12.06	0.00198%	10.86	1.04	0.89	0.85
LINE/L1_62	0.00214%	5.55	0.00232%	7.24	0.00239%	5.19	0.00248%	6.38	0.00200%	6.15	0.00283%	5.57	1.08	1.04	1.41
LINE/L1_63	0.00213%	16.54	0.00168%	16.58	0.00129%	12.29	0.00146%	11.85	0.00182%	13.82	0.00117%	11.05	0.79	1.13	0.64

LINE/L1_64	0.00213%	16.48	0.00213%	17.86	0.00194%	10.47	0.00161%	11.51	0.00224%	10.65	0.00206%	8.95	1.00	0.83	0.92
LINE/L1_65	0.00212%	15.10	0.00235%	17.43	0.00190%	15.79	0.00216%	15.49	0.00222%	17.53	0.00203%	17.62	1.10	1.14	0.91
LINE/L1_66	0.00200%	10.25	0.00210%	12.21	0.00160%	8.94	0.00155%	8.89	0.00192%	7.21	0.00189%	7.55	1.05	0.97	0.98
LINE/L1_67	0.00200%	8.33	0.00199%	8.64	0.00214%	8.08	0.00198%	6.7	0.00187%	8.62	0.00157%	8.8	1.00	0.92	0.84
LINE/L1_68	0.00193%	16.33	0.00238%	14.90	0.00185%	13.2	0.00215%	12.16	0.00195%	14.37	0.00163%	17.07	1.23	1.16	0.84
LINE/L1_69	0.00191%	23.69	0.00233%	26.15	0.00203%	22.94	0.00281%	18.92	0.00198%	22.88	0.00187%	22.85	1.22	1.39	0.95
LINE/L1_7	0.03197%	17.54	0.03276%	19.05	0.02770%	17.37	0.02576%	17.33	0.02410%	19.81	0.02324%	19.38	1.02	0.93	0.96
LINE/L1_70	0.00183%	24.05	0.00182%	22.12	0.00145%	17.07	0.00167%	19.01	0.00144%	20.78	0.00139%	21.91	0.99	1.15	0.96
LINE/L1_71	0.00183%	15.99	0.00216%	17.40	0.00129%	14.68	0.00118%	14.18	0.00156%	14.49	0.00129%	14.57	1.18	0.92	0.83
LINE/L1_72	0.00177%	20.89	0.00210%	23.02	0.00175%	20.71	0.00196%	23.11	0.00206%	17.79	0.00178%	18.21	1.19	1.12	0.86
LINE/L1_73	0.00176%	24.66	0.00188%	22.29	0.00100%	21.16	0.00113%	18.12	0.00121%	17.8	0.00129%	16.07	1.07	1.13	1.07
LINE/L1_74	0.00173%	24.69	0.00192%	23.09	0.00111%	23.46	0.00154%	20.74	0.00122%	20.18	0.00142%	19.82	1.11	1.39	1.16
LINE/L1_75	0.00173%	23.98	0.00203%	25.84	0.00153%	23.88	0.00156%	22.73	0.00172%	20.36	0.00140%	23.4	1.18	1.02	0.81
LINE/L1_76	0.00168%	19.92	0.00207%	20.41	0.00131%	15.56	0.00138%	14.33	0.00139%	13.42	0.00123%	14.69	1.23	1.06	0.88
LINE/L1_77	0.00147%	25.25	0.00187%	25.31	0.00133%	22.96	0.00134%	22.53	0.00130%	24.33	0.00125%	24.18	1.27	1.00	0.96
LINE/L1_78	0.00145%	3.82	0.00156%	2.18	0.00050%	2.79	0.00037%	3.84	0.00039%	6.17	0.00064%	3.15	1.08	0.74	1.62
LINE/L1_79	0.00143%	22.29	0.00164%	22.80	0.00125%	21.18	0.00114%	22.35	0.00149%	21.48	0.00118%	22.11	1.15	0.91	0.79
LINE/L1_8	0.02855%	4.59	0.03082%	4.40	0.02828%	4.23	0.02896%	4.07	0.03107%	4.22	0.02588%	4.34	1.08	1.02	0.83
LINE/L1_80	0.00141%	27.30	0.00161%	31.60	0.00085%	21.04	0.00110%	23.39	0.00129%	22.94	0.00104%	22.45	1.15	1.29	0.81
LINE/L1_81	0.00140%	9.60	0.00162%	9.22	0.00103%	9.09	0.00113%	8.62	0.00146%	9.06	0.00105%	9.02	1.15	1.10	0.72
LINE/L1_82	0.00138%	17.56	0.00168%	14.49	0.00131%	11.17	0.00126%	9.13	0.00149%	12.42	0.00147%	12.55	1.21	0.96	0.99
LINE/L1_83	0.00137%	25.05	0.00163%	25.25	0.00090%	23.54	0.00123%	23.26	0.00127%	22.87	0.00122%	23.11	1.19	1.37	0.96
LINE/L1_84	0.00135%	14.78	0.00139%	14.69	0.00128%	11.69	0.00146%	11.21	0.00141%	12.14	0.00129%	12.75	1.03	1.14	0.92
LINE/L1_85	0.00134%	21.24	0.00187%	24.04	0.00142%	21.52	0.00172%	22.98	0.00212%	22.29	0.00174%	22.45	1.39	1.21	0.82
LINE/L1_86	0.00129%	28.41	0.00139%	29.39	0.00083%	26.2	0.00083%	25.8	0.00099%	23	0.00082%	24.26	1.08	1.00	0.83
LINE/L1_87	0.00122%	7.51	0.00110%	6.06	0.00108%	5.75	0.00096%	7.4	0.00123%	7.48	0.00092%	5.49	0.90	0.89	0.75
LINE/L1_88	0.00121%	14.76	0.00180%	14.22	0.00127%	9.85	0.00114%	12.55	0.00117%	12.85	0.00111%	10.75	1.49	0.90	0.95
LINE/L1_89	0.00121%	17.80	0.00144%	19.40	0.00122%	17.51	0.00121%	14.65	0.00124%	17.32	0.00131%	16.17	1.20	0.99	1.06
LINE/L1_9	0.02631%	18.76	0.02648%	18.78	0.02677%	17.63	0.02711%	17.73	0.02740%	17.55	0.02692%	17.42	1.01	1.01	0.98
LINE/L1_90	0.00120%	8.73	0.00111%	8.65	0.00102%	8.46	0.00100%	9.02	0.00129%	8.87	0.00120%	9.23	0.93	0.99	0.93
LINE/L1_91	0.00112%	10.52	0.00134%	10.51	0.00120%	10.97	0.00105%	9.07	0.00108%	9.95	0.00116%	10.49	1.20	0.88	1.07

LINE/L1_92	0.00110%	27.81	0.00130%	28.11	0.00086%	24.38	0.00110%	28.03	0.00150%	24.81	0.00118%	23.42	1.19	1.27	0.79
LINE/L1_93	0.00103%	15.13	0.00109%	16.94	0.00058%	15.67	0.00087%	11.2	0.00093%	8.17	0.00083%	12.69	1.07	1.51	0.89
LINE/L1_94	0.00094%	28.94	0.00179%	32.66	0.00083%	29.24	0.00132%	31.1	0.00131%	29.88	0.00127%	31.79	1.91	1.60	0.97
LINE/L1_95	0.00081%	11.69	0.00081%	13.78	0.00046%	15.23	0.00030%	12.22	0.00046%	11.39	0.00072%	9.86	1.00	0.64	1.56
LINE/L1_96	0.00074%	1.69	0.00066%	1.68	0.00051%	1.81	0.00065%	2.31	0.00078%	1.79	0.00066%	1.57	0.89	1.28	0.85
LINE/L1_97	0.00058%	4.84	0.00063%	10.22	0.00111%	7.86	0.00066%	10.72	0.00074%	7.75	0.00074%	7.54	1.09	0.59	0.99
LINE/L1_98	0.00036%	20.44	0.00048%	22.34	0.00041%	20.39	0.00051%	21.06	0.00064%	19.7	0.00050%	20.46	1.36	1.26	0.77
LINE/L1_99	0.00032%	24.02	0.00067%	29.05	0.00053%	25.32	0.00041%	19.16	0.00041%	26.18	0.00042%	25.78	2.08	0.77	1.04
LINE/L2_1	0.51704%	5.68	0.51709%	5.81	0.50339%	5.35	0.50358%	5.27	0.45882%	5.29	0.51087%	5.32	1.00	1.00	1.11
LINE/L2_10	0.02066%	2.22	0.02075%	1.97	0.02020%	1.62	0.01307%	2.11	0.01057%	2.72	0.01210%	2.65	1.00	0.65	1.14
LINE/L2_11	0.01982%	13.18	0.01988%	14.03	0.01401%	12.5	0.01293%	11.9	0.01182%	13.49	0.01279%	12.51	1.00	0.92	1.08
LINE/L2_12	0.01903%	13.68	0.01906%	16.66	0.01350%	13.28	0.01483%	13.52	0.00851%	21.98	0.01145%	17.2	1.00	1.10	1.35
LINE/L2_13	0.01472%	23.95	0.01550%	24.86	0.01321%	21.51	0.01270%	20.96	0.01016%	24	0.01226%	23.96	1.05	0.96	1.21
LINE/L2_14	0.01461%	17.18	0.01570%	16.81	0.01555%	16.48	0.01551%	16.99	0.01406%	17.33	0.01550%	17.1	1.07	1.00	1.10
LINE/L2_15	0.01378%	12.92	0.01466%	14.76	0.01070%	15.01	0.01048%	14.16	0.00696%	19.6	0.00836%	18.14	1.06	0.98	1.20
LINE/L2_16	0.01338%	12.67	0.01344%	14.18	0.01149%	15.45	0.01154%	13.8	0.01048%	16.08	0.01082%	15.14	1.00	1.00	1.03
LINE/L2_17	0.01313%	4.97	0.01321%	5.95	0.00968%	6.15	0.01035%	5.67	0.00407%	8.77	0.00782%	7.38	1.01	1.07	1.92
LINE/L2_18	0.01185%	19.52	0.01222%	20.11	0.01126%	16.07	0.01107%	16.75	0.00632%	22.18	0.00705%	20.88	1.03	0.98	1.12
LINE/L2_19	0.01088%	8.43	0.00992%	9.54	0.00824%	8.19	0.00900%	7.86	0.00506%	10.7	0.00731%	9.58	0.91	1.09	1.44
LINE/L2_2	0.32426%	10.30	0.32598%	10.61	0.31841%	9.61	0.32141%	9.55	0.29483%	9.69	0.32554%	9.59	1.01	1.01	1.10
LINE/L2_20	0.01047%	13.84	0.01060%	14.14	0.01107%	13.52	0.01032%	13.93	0.00989%	14.62	0.01032%	14.32	1.01	0.93	1.04
LINE/L2_21	0.01001%	13.86	0.01036%	14.22	0.01012%	13.59	0.00978%	12.74	0.00997%	13.14	0.01017%	13.3	1.03	0.97	1.02
LINE/L2_22	0.00988%	13.89	0.00980%	14.17	0.00900%	14.65	0.00964%	14.87	0.00954%	15.75	0.00843%	15.44	0.99	1.07	0.88
LINE/L2_23	0.00907%	16.96	0.00929%	17.93	0.00925%	11.36	0.00794%	12.66	0.00463%	19.1	0.00522%	17.75	1.02	0.86	1.13
LINE/L2_24	0.00895%	15.07	0.00918%	15.32	0.00982%	13.85	0.00902%	14.27	0.00892%	14.52	0.00950%	14.63	1.03	0.92	1.07
LINE/L2_25	0.00853%	16.24	0.00777%	17.82	0.00837%	12.43	0.00810%	13.21	0.00368%	23.24	0.00547%	19.34	0.91	0.97	1.49
LINE/L2_26	0.00821%	7.00	0.00802%	8.08	0.01337%	4.16	0.01157%	4.43	0.00916%	4.31	0.00866%	4.94	0.98	0.87	0.94
LINE/L2_27	0.00796%	10.98	0.00754%	11.47	0.00562%	11.65	0.00610%	11.33	0.00410%	15.24	0.00540%	12.21	0.95	1.09	1.32
LINE/L2_28	0.00787%	8.05	0.00674%	9.00	0.00667%	8.18	0.00599%	8.12	0.00346%	11.52	0.00387%	11.45	0.86	0.90	1.12
LINE/L2_29	0.00715%	12.68	0.00850%	14.93	0.00652%	11.51	0.00659%	12.23	0.00593%	11.7	0.00663%	11.64	1.19	1.01	1.12
LINE/L2_3	0.13414%	14.97	0.14078%	15.34	0.13201%	14.16	0.12880%	14.13	0.13085%	14.33	0.13413%	14.2	1.05	0.98	1.03

LINE/L2_30	0.00710%	10.51	0.00737%	11.81	0.00832%	9.32	0.00783%	9.12	0.00414%	12.97	0.00532%	12.24	1.04	0.94	1.29
LINE/L2_31	0.00700%	14.28	0.00750%	16.64	0.00815%	12.02	0.00763%	10.98	0.00298%	19.65	0.00386%	16.5	1.07	0.94	1.29
LINE/L2_32	0.00656%	9.07	0.00633%	9.50	0.00714%	9.84	0.00689%	10.45	0.00565%	11.84	0.00646%	11.41	0.97	0.96	1.14
LINE/L2_33	0.00637%	14.56	0.00691%	14.75	0.00608%	14.46	0.00635%	13.75	0.00580%	14.44	0.00651%	14.01	1.09	1.04	1.12
LINE/L2_34	0.00632%	11.80	0.00564%	12.10	0.00435%	9.91	0.00412%	8.64	0.00263%	14.63	0.00272%	12.07	0.89	0.95	1.03
LINE/L2_35	0.00630%	17.01	0.00705%	17.83	0.00645%	16.66	0.00638%	15.31	0.00502%	15.3	0.00650%	16.16	1.12	0.99	1.29
LINE/L2_36	0.00570%	12.76	0.00556%	13.28	0.00958%	8.52	0.01064%	8.06	0.00934%	8.51	0.00985%	8.54	0.98	1.11	1.05
LINE/L2_37	0.00565%	7.95	0.00576%	6.70	0.00461%	5.24	0.00536%	4.49	0.00440%	5.78	0.00410%	5.49	1.02	1.16	0.93
LINE/L2_38	0.00533%	5.06	0.00460%	6.10	0.00360%	5.47	0.00300%	5.86	0.00162%	9.34	0.00229%	7.8	0.86	0.83	1.41
LINE/L2_39	0.00532%	14.64	0.00578%	16.21	0.00482%	16.92	0.00550%	16.81	0.00271%	18.7	0.00411%	17.16	1.08	1.14	1.52
LINE/L2_4	0.08233%	14.89	0.09191%	15.47	0.08298%	13.21	0.07971%	13.49	0.08181%	13.57	0.08134%	13.62	1.12	0.96	0.99
LINE/L2_40	0.00476%	11.92	0.00556%	11.84	0.00450%	11.25	0.00386%	10.95	0.00493%	11.18	0.00441%	11.2	1.17	0.86	0.89
LINE/L2_41	0.00414%	3.71	0.00399%	4.34	0.00432%	2.98	0.00379%	3.63	0.00289%	3.35	0.00409%	3.22	0.96	0.88	1.42
LINE/L2_42	0.00346%	13.71	0.00349%	14.43	0.00357%	13.38	0.00401%	13.41	0.00363%	13.43	0.00349%	13.59	1.01	1.12	0.96
LINE/L2_43	0.00346%	10.81	0.00372%	12.25	0.00430%	9.87	0.00441%	7.83	0.00189%	14.71	0.00296%	11.7	1.08	1.03	1.56
LINE/L2_44	0.00314%	6.79	0.00280%	8.83	0.00339%	5.68	0.00338%	5.81	0.00189%	6.07	0.00265%	6.42	0.89	1.00	1.40
LINE/L2_45	0.00299%	10.33	0.00384%	12.00	0.00280%	8.7	0.00333%	8.78	0.00223%	10.19	0.00295%	8.08	1.28	1.19	1.32
LINE/L2_46	0.00263%	5.87	0.00237%	6.10	0.00244%	5.56	0.00229%	6.15	0.00246%	6.1	0.00261%	6.25	0.90	0.94	1.06
LINE/L2_47	0.00242%	22.83	0.00289%	23.90	0.00179%	20.16	0.00228%	19.97	0.00174%	20.88	0.00211%	19.5	1.19	1.27	1.22
LINE/L2_48	0.00234%	12.78	0.00266%	13.11	0.00285%	10.61	0.00251%	10.95	0.00160%	12.81	0.00204%	13.05	1.14	0.88	1.27
LINE/L2_49	0.00228%	4.68	0.00191%	5.28	0.00162%	5.22	0.00147%	5.46	0.00087%	10.23	0.00110%	10.14	0.84	0.91	1.26
LINE/L2_5	0.07183%	17.75	0.07701%	18.27	0.06999%	16.26	0.06605%	16.6	0.06260%	16.63	0.06981%	16.33	1.07	0.94	1.12
LINE/L2_50	0.00222%	12.99	0.00240%	13.69	0.00188%	9.37	0.00186%	10.07	0.00184%	10.27	0.00193%	11.88	1.08	0.99	1.05
LINE/L2_51	0.00205%	13.39	0.00196%	13.61	0.00248%	13.32	0.00281%	13.71	0.00236%	15.05	0.00280%	14.41	0.96	1.13	1.19
LINE/L2_52	0.00178%	13.82	0.00210%	13.66	0.00166%	11.2	0.00232%	10.87	0.00128%	13.47	0.00218%	13.28	1.18	1.40	1.71
LINE/L2_53	0.00177%	10.62	0.00210%	13.16	0.00215%	9.63	0.00222%	9.68	0.00108%	20.69	0.00121%	15.53	1.19	1.04	1.11
LINE/L2_54	0.00173%	11.28	0.00189%	12.78	0.00167%	10.64	0.00207%	10.61	0.00150%	11.34	0.00169%	11.74	1.09	1.24	1.13
LINE/L2_55	0.00161%	1.70	0.00131%	1.88	0.00187%	2.5	0.00188%	2.05	0.00040%	2.09	0.00071%	2.78	0.82	1.01	1.76
LINE/L2_56	0.00160%	3.66	0.00138%	3.87	0.00152%	3.19	0.00153%	2.61	0.00129%	3.37	0.00187%	3.54	0.86	1.01	1.45
LINE/L2_57	0.00155%	9.07	0.00172%	9.51	0.00137%	5.3	0.00146%	7.78	0.00100%	7.6	0.00150%	8.73	1.11	1.06	1.50
LINE/L2_58	0.00147%	15.24	0.00147%	17.01	0.00149%	12.71	0.00125%	12.87	0.00133%	12.48	0.00163%	13.16	1.00	0.84	1.22

LINE/L2_59	0.00142%	11.91	0.00148%	13.63	0.00118%	8.58	0.00111%	7.89	0.00103%	11.29	0.00112%	11.96	1.04	0.94	1.09
LINE/L2_6	0.03709%	0.97	0.03805%	0.84	0.01112%	1.62	0.00718%	2	0.01069%	2.9	0.01079%	2.32	1.03	0.65	1.01
LINE/L2_60	0.00141%	5.40	0.00093%	5.23	0.00096%	4.24	0.00102%	4.37	0.00040%	6.82	0.00073%	9.07	0.66	1.05	1.82
LINE/L2_61	0.00138%	12.71	0.00162%	15.32	0.00183%	12.93	0.00162%	12.67	0.00081%	14.17	0.00122%	13.75	1.18	0.89	1.51
LINE/L2_62	0.00131%	8.65	0.00165%	8.95	0.00137%	7.57	0.00138%	6.28	0.00110%	7	0.00128%	5.86	1.26	1.00	1.16
LINE/L2_63	0.00125%	2.48	0.00070%	3.95	0.00112%	8.26	0.00116%	9.96	0.00194%	6.51	0.00105%	7.99	0.56	1.03	0.54
LINE/L2_64	0.00125%	9.58	0.00144%	9.31	0.00135%	5.65	0.00160%	7.01	0.00082%	8.73	0.00121%	7.4	1.15	1.18	1.47
LINE/L2_65	0.00118%	15.71	0.00136%	16.62	0.00106%	13.29	0.00134%	11.99	0.00088%	10.16	0.00123%	9.75	1.15	1.27	1.39
LINE/L2_66	0.00114%	8.51	0.00114%	8.83	0.00102%	7.01	0.00104%	7.27	0.00077%	8.35	0.00124%	9.62	1.00	1.02	1.62
LINE/L2_67	0.00106%	12.32	0.00114%	13.14	0.00129%	13.07	0.00113%	16.53	0.00087%	18.83	0.00106%	18.14	1.07	0.87	1.22
LINE/L2_68	0.00103%	4.48	0.00130%	3.61	0.00141%	4.24	0.00146%	4.47	0.00099%	3.44	0.00127%	4.27	1.26	1.03	1.28
LINE/L2_69	0.00090%	5.74	0.00104%	6.29	0.00132%	3.88	0.00127%	5.22	0.00103%	5.35	0.00141%	5.11	1.16	0.96	1.36
LINE/L2_7	0.03362%	10.45	0.03315%	10.71	0.02995%	9.7	0.03072%	9.75	0.02675%	9.98	0.02958%	9.89	0.99	1.03	1.11
LINE/L2_70	0.00081%	15.27	0.00074%	15.39	0.00059%	8.5	0.00060%	8.59	0.00046%	9.57	0.00076%	9.31	0.92	1.02	1.66
LINE/L2_71	0.00075%	7.49	0.00097%	7.19	0.00065%	5.28	0.00128%	4.9	0.00054%	5.33	0.00076%	6.28	1.30	1.98	1.41
LINE/L2_72	0.00069%	4.04	0.00078%	6.77	0.00022%	5.21	0.00041%	4.31	0.00014%	13.42	0.00036%	5.56	1.13	1.90	2.67
LINE/L2_73	0.00057%	10.84	0.00062%	15.78	0.00063%	10.51	0.00077%	11.48	0.00036%	10.26	0.00054%	11.04	1.08	1.22	1.50
LINE/L2_74	0.00053%	14.32	0.00052%	13.92	0.00073%	10.58	0.00053%	11.49	0.00049%	14.52	0.00054%	11.8	0.98	0.73	1.08
LINE/L2_75	0.00049%	10.23	0.00040%	9.82	0.00050%	9.43	0.00062%	9.27	0.00028%	9.19	0.00041%	9.34	0.82	1.25	1.47
LINE/L2_76	0.00046%	17.79	0.00067%	22.44	0.00034%	17.79	0.00036%	16.56	0.00045%	18.48	0.00053%	17.27	1.46	1.05	1.17
LINE/L2_77	0.00046%	8.31	0.00040%	10.13	0.00046%	12.19	0.00057%	11.7	0.00020%	8.58	0.00050%	9.76	0.87	1.23	2.54
LINE/L2_8	0.03221%	14.76	0.03459%	15.33	0.03322%	14.12	0.03112%	14.09	0.03122%	14.34	0.03452%	14.32	1.07	0.94	1.11
LINE/L2_9	0.02116%	7.39	0.02202%	7.18	0.02052%	6.75	0.02091%	6.55	0.01705%	6.89	0.02070%	6.54	1.04	1.02	1.21
LINE/Penelope_1	0.72467%	6.30	0.71643%	6.44	0.70303%	5.74	0.69438%	5.71	0.72768%	5.72	0.66062%	5.95	0.99	0.99	0.91
LINE/Penelope_10	0.04739%	13.41	0.04654%	13.48	0.04422%	11.9	0.04245%	12.18	0.04463%	12.96	0.03983%	12.73	0.98	0.96	0.89
LINE/Penelope_100	0.00434%	11.35	0.00375%	12.55	0.00396%	11.9	0.00414%	11.93	0.00353%	13.39	0.00360%	12.67	0.86	1.05	1.02
LINE/Penelope_101	0.00424%	14.44	0.00463%	15.08	0.00396%	13.42	0.00407%	11.72	0.00407%	12.76	0.00405%	12.59	1.09	1.03	0.99
LINE/Penelope_102	0.00419%	9.78	0.00448%	10.57	0.00430%	9.5	0.00363%	9.4	0.00450%	8.86	0.00396%	9.35	1.07	0.84	0.88
LINE/Penelope_103	0.00399%	11.58	0.00376%	12.06	0.00353%	11.34	0.00378%	10.28	0.00393%	10.41	0.00364%	10.68	0.94	1.07	0.92
LINE/Penelope_104	0.00397%	12.97	0.00363%	13.90	0.00472%	11.46	0.00401%	11.33	0.00337%	14.06	0.00317%	14.27	0.91	0.85	0.94
LINE/Penelope_105	0.00396%	4.47	0.00279%	5.37	0.00250%	4.85	0.00197%	6.13	0.00142%	9.54	0.00182%	6.06	0.70	0.79	1.28

LINE/Penelope_106	0.00395%	14.98	0.00365%	15.56	0.00320%	14.02	0.00325%	14.02	0.00360%	14.18	0.00301%	13.99	0.92	1.01	0.84
LINE/Penelope_107	0.00389%	15.49	0.00390%	16.11	0.00331%	15.16	0.00327%	15.66	0.00328%	16.32	0.00315%	16.06	1.00	0.99	0.96
LINE/Penelope_108	0.00387%	15.78	0.00365%	15.66	0.00328%	12.01	0.00372%	12.9	0.00227%	19.84	0.00270%	17.49	0.94	1.14	1.19
LINE/Penelope_109	0.00373%	14.69	0.00399%	13.93	0.00324%	13.19	0.00297%	12.5	0.00364%	13.1	0.00317%	13.13	1.07	0.92	0.87
LINE/Penelope_11	0.04382%	9.81	0.04554%	10.40	0.04064%	8.13	0.03791%	8.44	0.04163%	8.26	0.03998%	9.23	1.04	0.93	0.96
LINE/Penelope_110	0.00368%	10.34	0.00365%	10.83	0.00408%	9.91	0.00371%	8.5	0.00409%	9.19	0.00357%	8.75	0.99	0.91	0.87
LINE/Penelope_111	0.00366%	24.02	0.00427%	26.89	0.00382%	22.99	0.00309%	23.17	0.00374%	23.55	0.00359%	23.59	1.17	0.81	0.96
LINE/Penelope_112	0.00361%	6.01	0.00371%	6.49	0.00370%	5.84	0.00337%	5.76	0.00292%	6.45	0.00338%	6.24	1.03	0.91	1.16
LINE/Penelope_113	0.00353%	18.75	0.00359%	18.50	0.00314%	15.19	0.00266%	16.5	0.00241%	20.58	0.00268%	19.36	1.02	0.85	1.11
LINE/Penelope_114	0.00342%	12.80	0.00351%	13.63	0.00342%	12.85	0.00334%	10.02	0.00373%	11	0.00395%	11.11	1.03	0.98	1.06
LINE/Penelope_115	0.00326%	13.03	0.00335%	13.24	0.00396%	12.22	0.00353%	12.34	0.00255%	13.98	0.00272%	13.22	1.03	0.89	1.07
LINE/Penelope_116	0.00325%	11.80	0.00368%	11.26	0.00290%	10.45	0.00301%	10.89	0.00331%	11.29	0.00340%	10.48	1.13	1.04	1.03
LINE/Penelope_117	0.00317%	14.16	0.00310%	13.58	0.00352%	12.94	0.00317%	12.87	0.00411%	13.39	0.00364%	12.75	0.98	0.90	0.89
LINE/Penelope_118	0.00313%	13.82	0.00185%	13.79	0.00166%	12.2	0.00169%	12.95	0.00440%	13.36	0.00186%	12.55	0.59	1.02	0.42
LINE/Penelope_119	0.00301%	9.59	0.00316%	10.88	0.00301%	10.29	0.00275%	10.89	0.00321%	9.57	0.00319%	8.58	1.05	0.91	0.99
LINE/Penelope_12	0.04268%	10.17	0.04423%	10.34	0.03833%	9.95	0.03879%	9.53	0.03711%	9.74	0.03947%	9.64	1.04	1.01	1.06
LINE/Penelope_120	0.00291%	16.31	0.00293%	16.67	0.00251%	15.9	0.00256%	14.96	0.00259%	14.32	0.00237%	14.88	1.01	1.02	0.92
LINE/Penelope_121	0.00286%	12.35	0.00255%	12.72	0.00203%	13.22	0.00205%	13.36	0.00231%	13.59	0.00207%	14.35	0.89	1.01	0.90
LINE/Penelope_122	0.00276%	11.16	0.00254%	13.55	0.00205%	8.82	0.00247%	10.73	0.00125%	14.24	0.00165%	12.64	0.92	1.20	1.32
LINE/Penelope_123	0.00271%	13.29	0.00270%	14.76	0.00296%	10.3	0.00277%	13.1	0.00283%	11.59	0.00215%	13.38	1.00	0.94	0.76
LINE/Penelope_124	0.00265%	8.66	0.00253%	10.13	0.00216%	8.42	0.00231%	8.25	0.00096%	14.71	0.00149%	11.16	0.96	1.07	1.54
LINE/Penelope_125	0.00261%	10.05	0.00250%	9.92	0.00199%	7.93	0.00195%	7.34	0.00205%	8.69	0.00204%	7.71	0.96	0.98	0.99
LINE/Penelope_126	0.00259%	13.26	0.00237%	13.22	0.00253%	13.38	0.00210%	12.32	0.00227%	12.09	0.00207%	12.6	0.91	0.83	0.91
LINE/Penelope_127	0.00241%	24.19	0.00269%	26.92	0.00222%	18.91	0.00193%	17.38	0.00197%	20	0.00194%	18.84	1.11	0.87	0.98
LINE/Penelope_128	0.00221%	25.12	0.00236%	24.49	0.00144%	22.33	0.00140%	22.06	0.00139%	20.62	0.00146%	20.53	1.07	0.97	1.05
LINE/Penelope_129	0.00211%	8.54	0.00182%	9.54	0.00117%	9.35	0.00082%	11.15	0.00050%	15.89	0.00071%	13.1	0.86	0.70	1.41
LINE/Penelope_13	0.04094%	10.81	0.04136%	11.01	0.04059%	10.42	0.03920%	10.21	0.03498%	10.03	0.03654%	9.94	1.01	0.97	1.04
LINE/Penelope_130	0.00207%	11.56	0.00210%	13.21	0.00161%	10.81	0.00200%	12.04	0.00186%	12.23	0.00222%	12.05	1.02	1.24	1.19
LINE/Penelope_131	0.00198%	21.13	0.00222%	22.43	0.00171%	19.38	0.00163%	18.5	0.00179%	20.15	0.00199%	20.62	1.12	0.95	1.12
LINE/Penelope_132	0.00195%	7.96	0.00227%	7.36	0.00192%	8.5	0.00231%	6.04	0.00231%	6.49	0.00191%	6.55	1.16	1.20	0.83
LINE/Penelope_133	0.00194%	18.00	0.00190%	20.61	0.00151%	15.93	0.00159%	12.11	0.00156%	15.73	0.00135%	17.35	0.98	1.05	0.87

LINE/Penelope_134	0.00182%	21.46	0.00180%	21.96	0.00131%	19.94	0.00122%	20.91	0.00131%	20.29	0.00112%	19.94	0.99	0.93	0.85
LINE/Penelope_135	0.00180%	27.27	0.00220%	28.98	0.00138%	19.78	0.00162%	21.02	0.00137%	21.75	0.00137%	22.26	1.22	1.18	1.00
LINE/Penelope_136	0.00171%	14.36	0.00185%	13.23	0.00108%	12.08	0.00108%	9.87	0.00113%	10.18	0.00113%	11.38	1.08	1.00	1.00
LINE/Penelope_137	0.00165%	11.49	0.00195%	14.33	0.00174%	8.18	0.00169%	10.39	0.00150%	10.68	0.00185%	8.98	1.18	0.97	1.23
LINE/Penelope_138	0.00159%	23.40	0.00184%	23.39	0.00117%	19.67	0.00104%	24.21	0.00141%	27.38	0.00126%	25.82	1.16	0.89	0.89
LINE/Penelope_139	0.00157%	5.26	0.00156%	7.11	0.00148%	5.15	0.00117%	4.92	0.00166%	4.43	0.00126%	7.27	0.99	0.79	0.76
LINE/Penelope_14	0.03918%	15.17	0.03907%	15.65	0.03581%	14.52	0.03770%	14.35	0.03528%	13.61	0.03436%	14.45	1.00	1.05	0.97
LINE/Penelope_140	0.00157%	9.75	0.00146%	10.65	0.00136%	13.61	0.00147%	11.72	0.00115%	16.61	0.00108%	13.9	0.93	1.08	0.93
LINE/Penelope_141	0.00154%	15.39	0.00132%	17.20	0.00166%	13.96	0.00202%	11.77	0.00075%	25.37	0.00110%	21.76	0.86	1.22	1.46
LINE/Penelope_142	0.00154%	6.10	0.00137%	7.86	0.00143%	6.03	0.00113%	6.74	0.00062%	12.99	0.00102%	10.23	0.89	0.79	1.63
LINE/Penelope_143	0.00150%	12.72	0.00145%	13.17	0.00378%	11.38	0.00353%	11.59	0.00393%	10.75	0.00334%	10.52	0.96	0.93	0.85
LINE/Penelope_144	0.00150%	12.70	0.00134%	10.95	0.00138%	12.77	0.00133%	15.29	0.00076%	19.36	0.00096%	13.94	0.90	0.97	1.26
LINE/Penelope_145	0.00144%	17.99	0.00128%	17.58	0.00189%	15.77	0.00168%	15.84	0.00160%	15.51	0.00200%	16.65	0.89	0.89	1.25
LINE/Penelope_146	0.00126%	12.29	0.00134%	12.75	0.00152%	10.17	0.00111%	10.64	0.00122%	9.27	0.00147%	11.16	1.06	0.73	1.21
LINE/Penelope_147	0.00121%	7.36	0.00127%	8.36	0.00135%	6.38	0.00100%	8.06	0.00042%	18.83	0.00067%	11.4	1.05	0.74	1.58
LINE/Penelope_148	0.00118%	18.96	0.00138%	18.60	0.00111%	12.31	0.00132%	14.03	0.00102%	14.07	0.00104%	14.52	1.17	1.20	1.02
LINE/Penelope_149	0.00116%	15.22	0.00112%	15.42	0.00086%	13.23	0.00100%	11.6	0.00096%	11.1	0.00088%	14.2	0.96	1.17	0.92
LINE/Penelope_15	0.03700%	12.21	0.03748%	12.69	0.03636%	11.57	0.03666%	10.95	0.03395%	10.44	0.03459%	11.65	1.01	1.01	1.02
LINE/Penelope_150	0.00111%	16.29	0.00098%	15.20	0.00076%	14	0.00078%	14.64	0.00061%	19.44	0.00068%	19.43	0.88	1.03	1.11
LINE/Penelope_151	0.00104%	11.23	0.00151%	11.62	0.00118%	10.73	0.00142%	12.59	0.00153%	11.41	0.00131%	12.13	1.45	1.21	0.86
LINE/Penelope_152	0.00103%	18.57	0.00106%	19.61	0.00079%	15.65	0.00096%	12.37	0.00085%	11.61	0.00110%	16.53	1.04	1.21	1.29
LINE/Penelope_153	0.00099%	14.45	0.00132%	15.36	0.00062%	13.86	0.00069%	14.41	0.00075%	11.73	0.00106%	11.06	1.33	1.11	1.41
LINE/Penelope_154	0.00092%	16.83	0.00104%	19.34	0.00100%	10.38	0.00087%	14.65	0.00098%	15.25	0.00096%	16.85	1.13	0.87	0.98
LINE/Penelope_155	0.00089%	9.90	0.00095%	14.44	0.00093%	9.86	0.00089%	9.19	0.00076%	11.4	0.00089%	9.53	1.07	0.96	1.16
LINE/Penelope_156	0.00084%	15.11	0.00105%	15.74	0.00081%	16.5	0.00102%	12.91	0.00094%	16.54	0.00106%	17.32	1.24	1.26	1.12
LINE/Penelope_157	0.00077%	9.48	0.00079%	10.44	0.00071%	9.17	0.00055%	10.4	0.00045%	12.07	0.00048%	13.02	1.02	0.78	1.05
LINE/Penelope_158	0.00077%	16.95	0.00097%	20.36	0.00054%	16.63	0.00054%	16.68	0.00074%	14.97	0.00094%	13.31	1.25	0.99	1.26
LINE/Penelope_159	0.00076%	19.97	0.00074%	21.62	0.00057%	17.77	0.00071%	19.05	0.00076%	18.04	0.00077%	15.25	0.97	1.24	1.01
LINE/Penelope_16	0.03661%	9.73	0.03882%	9.95	0.03672%	8.9	0.03759%	8.87	0.03919%	9.36	0.03331%	9.39	1.06	1.02	0.85
LINE/Penelope_160	0.00074%	15.20	0.00065%	14.98	0.00149%	10.57	0.00162%	10.67	0.00126%	12.42	0.00144%	11.5	0.88	1.09	1.14
LINE/Penelope_161	0.00067%	19.00	0.00057%	18.14	0.00091%	14.93	0.00089%	16.87	0.00075%	22.55	0.00087%	23.1	0.86	0.97	1.15

LINE/Penelope_162	0.00043%	14.39	0.00058%	11.21	0.00047%	11.39	0.00064%	10.33	0.00052%	11.45	0.00058%	17.51	1.33	1.37	1.11
LINE/Penelope_163	0.00039%	6.60	0.00031%	7.76	0.00146%	6.54	0.00125%	6.73	0.00104%	6.66	0.00153%	7.11	0.80	0.85	1.48
LINE/Penelope_164	0.00027%	9.40	0.00023%	14.02	0.00040%	6.52	0.00043%	6.22	0.00012%	23.72	0.00010%	19.87	0.84	1.08	0.77
LINE/Penelope_165	0.00009%	25.98	0.00005%	25.54	0.00006%	24.59	0.00015%	23.63	0.00008%	20.98	0.00012%	22.39	0.59	2.38	1.45
LINE/Penelope_166	0.00002%	18.85	0.00002%	17.99	0.00002%	5.08	0.00001%	7.84	0.00001%	14.62	0.00001%	30.01	1.29	0.30	1.28
LINE/Penelope_17	0.03531%	12.26	0.03765%	12.53	0.03182%	10.99	0.03188%	11.16	0.03563%	10.75	0.03419%	11	1.07	1.00	0.96
LINE/Penelope_18	0.03338%	11.12	0.03431%	11.73	0.02987%	10.42	0.03129%	10.24	0.03416%	9.82	0.03381%	9.99	1.03	1.05	0.99
LINE/Penelope_19	0.02958%	10.19	0.03136%	10.36	0.02799%	9.66	0.02969%	9.87	0.03097%	9.73	0.02951%	9.79	1.06	1.06	0.95
LINE/Penelope_2	0.23792%	8.56	0.24172%	8.69	0.22505%	8.1	0.23392%	8.01	0.20647%	7.69	0.22002%	8.12	1.02	1.04	1.07
LINE/Penelope_20	0.02911%	10.90	0.02887%	11.40	0.02694%	9.97	0.02646%	10.19	0.02913%	9.96	0.02550%	9.75	0.99	0.98	0.88
LINE/Penelope_21	0.02844%	10.39	0.03669%	12.25	0.02694%	9.43	0.02718%	10.38	0.02899%	8.48	0.03230%	9.46	1.29	1.01	1.11
LINE/Penelope_22	0.02765%	7.50	0.02783%	7.24	0.02437%	5.47	0.02454%	5.66	0.02682%	6.45	0.02482%	5.73	1.01	1.01	0.93
LINE/Penelope_23	0.02695%	9.95	0.02730%	10.38	0.02792%	8.38	0.02497%	8.32	0.02462%	9.05	0.02734%	8.15	1.01	0.89	1.11
LINE/Penelope_24	0.02690%	7.23	0.02659%	7.41	0.02302%	6.36	0.02304%	6.33	0.01952%	6.02	0.02099%	6.29	0.99	1.00	1.08
LINE/Penelope_25	0.02628%	11.48	0.02539%	12.00	0.03054%	9.99	0.02880%	10.38	0.02719%	12.53	0.02314%	11.8	0.97	0.94	0.85
LINE/Penelope_26	0.02616%	14.18	0.02654%	14.76	0.02513%	11.89	0.02358%	12.01	0.02470%	11.61	0.02421%	12	1.01	0.94	0.98
LINE/Penelope_27	0.02407%	15.01	0.02380%	15.65	0.01892%	13.14	0.01775%	13.59	0.01779%	14.5	0.01716%	14.32	0.99	0.94	0.96
LINE/Penelope_28	0.02115%	9.40	0.02154%	9.43	0.02397%	8.53	0.02486%	8.56	0.02532%	8.57	0.02373%	8.65	1.02	1.04	0.94
LINE/Penelope_29	0.01990%	9.22	0.01833%	9.19	0.02087%	8.6	0.02046%	8.34	0.01898%	9.37	0.01805%	9.27	0.92	0.98	0.95
LINE/Penelope_3	0.23074%	10.21	0.23134%	10.88	0.22115%	9.48	0.22533%	9.56	0.23047%	8.61	0.21160%	9.8	1.00	1.02	0.92
LINE/Penelope_30	0.01962%	20.63	0.02111%	21.81	0.01638%	21.17	0.01673%	21.02	0.01532%	23.05	0.01649%	22.6	1.08	1.02	1.08
LINE/Penelope_31	0.01741%	13.05	0.01839%	13.44	0.01539%	12.63	0.01638%	13.08	0.01366%	16.25	0.01406%	15.58	1.06	1.06	1.03
LINE/Penelope_32	0.01696%	13.58	0.01764%	15.17	0.02018%	12.16	0.01883%	13	0.01448%	14.28	0.01595%	14.03	1.04	0.93	1.10
LINE/Penelope_33	0.01666%	7.70	0.01722%	7.82	0.01509%	7.19	0.01581%	7.26	0.01724%	7.42	0.01550%	7.51	1.03	1.05	0.90
LINE/Penelope_34	0.01628%	12.29	0.01704%	11.38	0.01630%	10.1	0.01417%	9.8	0.01777%	8.86	0.01869%	9.3	1.05	0.87	1.05
LINE/Penelope_35	0.01607%	11.73	0.01488%	11.81	0.01439%	11.23	0.01380%	10.97	0.01377%	10.9	0.01469%	10.9	0.93	0.96	1.07
LINE/Penelope_36	0.01567%	9.22	0.01665%	9.64	0.01623%	8.26	0.01460%	7.81	0.01429%	8.7	0.01572%	8.28	1.06	0.90	1.10
LINE/Penelope_37	0.01468%	11.33	0.01506%	11.84	0.01465%	10.89	0.01314%	10.49	0.01484%	10.62	0.01494%	10.54	1.03	0.90	1.01
LINE/Penelope_38	0.01422%	12.63	0.01505%	13.84	0.01232%	12.02	0.01237%	12.37	0.01322%	12.59	0.01331%	12.09	1.06	1.00	1.01
LINE/Penelope_39	0.01399%	11.94	0.01501%	11.93	0.01232%	10.96	0.01224%	10.61	0.01260%	10.38	0.01267%	10.52	1.07	0.99	1.01
LINE/Penelope_4	0.06840%	9.45	0.06645%	9.53	0.05209%	8.95	0.05227%	8.95	0.05676%	8.98	0.05129%	9.12	0.97	1.00	0.90

LINE/Penelope_40	0.01394%	18.72	0.01497%	19.05	0.01526%	17.06	0.01528%	16.3	0.01252%	17.89	0.01529%	17.2	1.07	1.00	1.22
LINE/Penelope_41	0.01329%	10.59	0.01313%	11.20	0.01330%	9.83	0.01454%	9.05	0.01414%	9.68	0.01422%	9.66	0.99	1.09	1.01
LINE/Penelope_42	0.01282%	15.40	0.01481%	17.43	0.01209%	12.68	0.01184%	12.43	0.00997%	14.33	0.01217%	13.21	1.16	0.98	1.22
LINE/Penelope_43	0.01276%	20.77	0.01314%	22.57	0.01074%	17.85	0.01019%	19.75	0.01055%	18.97	0.00997%	19.27	1.03	0.95	0.95
LINE/Penelope_44	0.01253%	9.47	0.01187%	10.58	0.00901%	11.34	0.00915%	9.74	0.00494%	15.91	0.00669%	12.9	0.95	1.02	1.35
LINE/Penelope_45	0.01249%	12.54	0.01302%	12.58	0.01177%	12.38	0.01195%	11.64	0.01208%	11.78	0.01295%	11.58	1.04	1.02	1.07
LINE/Penelope_46	0.01232%	13.24	0.01231%	13.26	0.01161%	12.28	0.01124%	12.56	0.00984%	12.26	0.01253%	12.4	1.00	0.97	1.27
LINE/Penelope_47	0.01219%	9.72	0.01221%	9.56	0.01049%	8.85	0.00988%	8.93	0.01037%	9.4	0.01006%	9.4	1.00	0.94	0.97
LINE/Penelope_48	0.01202%	6.78	0.01170%	7.03	0.00982%	6.84	0.01085%	6.26	0.00909%	7.12	0.01094%	7.03	0.97	1.10	1.20
LINE/Penelope_49	0.01189%	11.07	0.01177%	10.92	0.01057%	10.24	0.00988%	10.64	0.00975%	10.66	0.01016%	10.5	0.99	0.93	1.04
LINE/Penelope_5	0.06370%	9.72	0.06226%	9.93	0.05952%	9.67	0.05680%	9.89	0.05515%	9.54	0.06051%	9.64	0.98	0.95	1.10
LINE/Penelope_50	0.01163%	10.09	0.01014%	10.83	0.01050%	8.94	0.01098%	9.26	0.00986%	9.12	0.01028%	9.91	0.87	1.05	1.04
LINE/Penelope_51	0.01158%	11.97	0.01188%	12.61	0.01430%	11.32	0.01279%	11.45	0.01030%	14.58	0.01113%	13.31	1.03	0.89	1.08
LINE/Penelope_52	0.01087%	7.33	0.01070%	7.20	0.01547%	7.05	0.01402%	6.87	0.01722%	6.96	0.01593%	7.02	0.98	0.91	0.92
LINE/Penelope_53	0.01073%	12.95	0.01108%	12.94	0.01006%	11.39	0.00966%	11.68	0.01016%	11.53	0.00946%	12	1.03	0.96	0.93
LINE/Penelope_54	0.01057%	17.44	0.01167%	18.13	0.01016%	14.7	0.00932%	15.12	0.00949%	14.7	0.01008%	14.68	1.10	0.92	1.06
LINE/Penelope_55	0.01056%	12.19	0.00997%	11.73	0.00820%	10.6	0.00858%	11.27	0.00830%	11.16	0.00821%	10.7	0.94	1.05	0.99
LINE/Penelope_56	0.01032%	9.26	0.00963%	9.39	0.01301%	8.07	0.01368%	8.1	0.00745%	13.03	0.00886%	10.83	0.93	1.05	1.19
LINE/Penelope_57	0.01008%	11.78	0.01033%	12.20	0.00962%	10.13	0.00963%	10.3	0.01064%	10.02	0.01027%	10.37	1.02	1.00	0.97
LINE/Penelope_58	0.00977%	10.39	0.01009%	10.08	0.00852%	10.32	0.00867%	10.16	0.00842%	10.16	0.00874%	10.31	1.03	1.02	1.04
LINE/Penelope_59	0.00975%	7.69	0.00879%	7.63	0.00665%	7.02	0.00683%	7.14	0.00481%	8.6	0.00496%	9.14	0.90	1.03	1.03
LINE/Penelope_6	0.06022%	11.41	0.06640%	11.70	0.05353%	9.27	0.05239%	8.92	0.04918%	10.67	0.04698%	10.87	1.10	0.98	0.96
LINE/Penelope_60	0.00955%	14.94	0.00465%	17.80	0.00441%	16.55	0.00419%	16.48	0.01560%	9.8	0.00433%	16.15	0.49	0.95	0.28
LINE/Penelope_61	0.00941%	7.42	0.01129%	7.50	0.00758%	8.06	0.00754%	8.37	0.00605%	8.43	0.00736%	8.77	1.20	0.99	1.22
LINE/Penelope_62	0.00914%	11.01	0.00932%	12.11	0.00954%	10.46	0.00870%	10.7	0.00834%	10.59	0.00983%	10.34	1.02	0.91	1.18
LINE/Penelope_63	0.00910%	13.51	0.00921%	13.77	0.00879%	13	0.00903%	12.59	0.00851%	12.95	0.00898%	13.45	1.01	1.03	1.06
LINE/Penelope_64	0.00821%	7.89	0.00954%	7.86	0.00795%	7.29	0.00806%	7.34	0.00766%	7.4	0.00845%	7.12	1.16	1.01	1.10
LINE/Penelope_65	0.00791%	10.48	0.00829%	10.36	0.00760%	9.13	0.00825%	8.81	0.00820%	9.52	0.00805%	8.56	1.05	1.09	0.98
LINE/Penelope_66	0.00778%	12.35	0.00830%	12.28	0.00743%	11.54	0.00662%	11.4	0.00704%	11.54	0.00721%	11.07	1.07	0.89	1.02
LINE/Penelope_67	0.00771%	11.65	0.00822%	11.47	0.00708%	10.62	0.00785%	10.31	0.00573%	13.21	0.00660%	12.6	1.07	1.11	1.15
LINE/Penelope_68	0.00759%	12.59	0.00735%	13.43	0.00506%	14.93	0.00605%	13.51	0.00402%	17.39	0.00483%	15.87	0.97	1.19	1.20

LINE/Penelope_69	0.00739%	9.68	0.00770%	10.26	0.00894%	7.51	0.00820%	7.61	0.00721%	9.55	0.00667%	9.45	1.04	0.92	0.93
LINE/Penelope_7	0.05961%	12.75	0.05984%	12.78	0.04262%	11.4	0.04138%	11.75	0.04548%	11.66	0.04240%	11.72	1.00	0.97	0.93
LINE/Penelope_70	0.00703%	13.14	0.00887%	14.15	0.00874%	8.65	0.00832%	9.63	0.00763%	12.33	0.00655%	11.02	1.26	0.95	0.86
LINE/Penelope_71	0.00681%	13.04	0.00642%	15.51	0.00489%	15.17	0.00483%	14.66	0.00473%	18.46	0.00488%	16.87	0.94	0.99	1.03
LINE/Penelope_72	0.00677%	10.08	0.00617%	10.25	0.00499%	9.65	0.00508%	9.69	0.00472%	8.98	0.00485%	9.25	0.91	1.02	1.03
LINE/Penelope_73	0.00666%	7.11	0.00631%	6.49	0.00796%	5.19	0.00715%	5.52	0.00187%	13.23	0.00323%	8.2	0.95	0.90	1.73
LINE/Penelope_74	0.00645%	12.70	0.00659%	13.39	0.00578%	10.88	0.00591%	11.77	0.00640%	10.48	0.00628%	11.61	1.02	1.02	0.98
LINE/Penelope_75	0.00614%	12.79	0.00638%	13.36	0.00756%	8.84	0.00653%	9.47	0.00391%	14.39	0.00417%	13.55	1.04	0.86	1.07
LINE/Penelope_76	0.00574%	9.99	0.00551%	10.85	0.00429%	10.04	0.00478%	8.89	0.00302%	11.61	0.00416%	11	0.96	1.11	1.38
LINE/Penelope_77	0.00554%	7.88	0.00444%	8.83	0.00383%	8.86	0.00419%	7.67	0.00219%	13.31	0.00287%	10.77	0.80	1.09	1.31
LINE/Penelope_78	0.00548%	10.96	0.00535%	11.36	0.00543%	10.19	0.00536%	11.21	0.00559%	10.16	0.00650%	9.85	0.97	0.99	1.16
LINE/Penelope_79	0.00544%	17.23	0.00533%	17.55	0.00467%	16.2	0.00480%	16.74	0.00514%	16.56	0.00524%	15.82	0.98	1.03	1.02
LINE/Penelope_8	0.05529%	11.21	0.05674%	11.35	0.05465%	11.41	0.05455%	11.03	0.05507%	11.19	0.05686%	11.04	1.03	1.00	1.03
LINE/Penelope_80	0.00535%	11.49	0.00562%	13.40	0.00485%	9.09	0.00468%	8.43	0.00544%	9.13	0.00521%	9.21	1.05	0.97	0.96
LINE/Penelope_81	0.00522%	13.44	0.00557%	13.10	0.00410%	11.2	0.00448%	11.15	0.00532%	10.83	0.00483%	10.96	1.07	1.09	0.91
LINE/Penelope_82	0.00521%	14.71	0.00566%	14.40	0.00420%	13.36	0.00436%	14.04	0.00468%	13.78	0.00428%	13.48	1.09	1.04	0.91
LINE/Penelope_83	0.00514%	11.35	0.00514%	12.74	0.00433%	9.7	0.00455%	10.51	0.00446%	9.62	0.00461%	10.78	1.00	1.05	1.03
LINE/Penelope_84	0.00511%	10.47	0.00570%	11.51	0.00454%	10.68	0.00466%	11.37	0.00484%	11.16	0.00501%	10.62	1.12	1.02	1.03
LINE/Penelope_85	0.00510%	9.19	0.00476%	9.27	0.00480%	9.15	0.00565%	9.08	0.00476%	9.42	0.00543%	9.03	0.93	1.18	1.14
LINE/Penelope_86	0.00507%	13.82	0.00337%	14.67	0.00281%	13.34	0.00304%	13.63	0.00676%	12.63	0.00299%	13.23	0.67	1.08	0.44
LINE/Penelope_87	0.00506%	13.29	0.00561%	13.79	0.00530%	13.65	0.00497%	13.02	0.00516%	12.72	0.00619%	12.29	1.11	0.94	1.20
LINE/Penelope_88	0.00498%	10.40	0.00492%	10.61	0.00558%	9.29	0.00538%	9.74	0.00613%	9.43	0.00568%	9	0.99	0.96	0.93
LINE/Penelope_89	0.00490%	24.51	0.00487%	24.60	0.00311%	23.2	0.00342%	19.51	0.00430%	20.18	0.00343%	20.34	0.99	1.10	0.80
LINE/Penelope_9	0.05165%	9.07	0.05592%	9.72	0.05399%	7.04	0.05347%	6.96	0.04488%	8.19	0.05281%	7.47	1.08	0.99	1.18
LINE/Penelope_90	0.00481%	12.35	0.00514%	13.14	0.00509%	13.7	0.00517%	12.76	0.00470%	13.68	0.00510%	13.09	1.07	1.02	1.09
LINE/Penelope_91	0.00476%	8.73	0.00420%	7.60	0.00247%	7.31	0.00222%	6.76	0.00308%	7.18	0.00241%	7.72	0.88	0.90	0.78
LINE/Penelope_92	0.00474%	12.60	0.00498%	13.50	0.00460%	11.41	0.00449%	11.61	0.00427%	12.1	0.00430%	11.27	1.05	0.98	1.01
LINE/Penelope_93	0.00470%	14.30	0.00448%	14.80	0.00522%	14.81	0.00511%	14.48	0.00548%	15.72	0.00478%	15.3	0.95	0.98	0.87
LINE/Penelope_94	0.00461%	11.52	0.00450%	12.90	0.00440%	10.33	0.00480%	10.9	0.00586%	11.02	0.00560%	10.6	0.98	1.09	0.96
LINE/Penelope_95	0.00459%	9.82	0.00436%	9.53	0.00395%	9.76	0.00409%	9.57	0.00414%	9.7	0.00437%	9.58	0.95	1.03	1.06
LINE/Penelope_96	0.00450%	5.35	0.00442%	4.99	0.00422%	4.83	0.00487%	4.44	0.00355%	5.51	0.00405%	4.65	0.98	1.15	1.14

LINE/Penelope_97	0.00445%	9.41	0.00422%	9.60	0.00506%	8.82	0.00501%	8.87	0.00502%	8.74	0.00498%	8.89	0.95	0.99	0.99
LINE/Penelope_98	0.00443%	10.86	0.00419%	12.75	0.00380%	12.73	0.00353%	11.83	0.00311%	13.61	0.00347%	12.44	0.95	0.93	1.12
LINE/Penelope_99	0.00438%	14.48	0.00405%	14.51	0.00333%	14.25	0.00406%	14.82	0.00353%	13.66	0.00316%	14.63	0.92	1.22	0.90
LINE/R1_1	0.08503%	19.49	0.09364%	20.31	0.05733%	19.52	0.05698%	19.03	0.07089%	18.91	0.06277%	19.32	1.10	0.99	0.89
LINE/R1_10	0.00981%	16.54	0.01051%	15.94	0.01576%	11.66	0.01334%	12.48	0.00674%	20.94	0.00805%	19.14	1.07	0.85	1.19
LINE/R1_11	0.00960%	19.00	0.01097%	20.56	0.00713%	15.5	0.00712%	13.88	0.00750%	16.3	0.00751%	16.32	1.14	1.00	1.00
LINE/R1_12	0.00939%	14.42	0.01011%	14.96	0.01481%	10.75	0.01400%	11.5	0.00526%	19.4	0.00694%	17.65	1.08	0.95	1.32
LINE/R1_13	0.00859%	19.66	0.00985%	20.95	0.00714%	19.13	0.00697%	18.75	0.00932%	17.73	0.00865%	17.71	1.15	0.98	0.93
LINE/R1_14	0.00857%	16.90	0.00796%	16.45	0.00385%	7.73	0.00245%	14.22	0.00280%	17.32	0.00384%	16.47	0.93	0.64	1.37
LINE/R1_15	0.00840%	15.43	0.00888%	16.68	0.00738%	15.86	0.00717%	15.54	0.00639%	17.74	0.00712%	17.18	1.06	0.97	1.11
LINE/R1_16	0.00824%	25.38	0.00864%	24.73	0.00417%	25.71	0.00462%	23.78	0.00586%	20.48	0.00664%	19.62	1.05	1.11	1.13
LINE/R1_17	0.00808%	10.29	0.00804%	10.50	0.00751%	7.24	0.00681%	8.84	0.00815%	9.03	0.00777%	8.48	1.00	0.91	0.95
LINE/R1_18	0.00794%	14.92	0.00836%	16.08	0.00724%	12.63	0.00685%	11.77	0.00676%	13.96	0.00736%	13.19	1.05	0.95	1.09
LINE/R1_19	0.00757%	22.84	0.00817%	21.99	0.00556%	20.52	0.00512%	19.65	0.00665%	20.06	0.00650%	19.11	1.08	0.92	0.98
LINE/R1_2	0.03191%	12.76	0.03296%	13.56	0.03112%	13.3	0.03206%	12.89	0.02941%	12.12	0.02995%	12.79	1.03	1.03	1.02
LINE/R1_20	0.00687%	9.19	0.00688%	10.45	0.00693%	8.18	0.00592%	7.79	0.00737%	7.67	0.00681%	8.3	1.00	0.85	0.92
LINE/R1_21	0.00674%	13.90	0.00671%	13.80	0.01012%	9.68	0.00909%	9.73	0.00379%	19.5	0.00483%	17.72	1.00	0.90	1.27
LINE/R1_22	0.00650%	14.20	0.00634%	14.18	0.01119%	10.56	0.00993%	11.8	0.00440%	19.64	0.00541%	18.3	0.98	0.89	1.23
LINE/R1_23	0.00600%	15.28	0.00569%	13.75	0.00281%	4.71	0.00252%	9.87	0.00205%	12.99	0.00330%	17.08	0.95	0.90	1.61
LINE/R1_24	0.00597%	21.64	0.00599%	21.97	0.00752%	18.26	0.00694%	18.93	0.00507%	23.25	0.00586%	21.8	1.00	0.92	1.16
LINE/R1_25	0.00573%	22.47	0.00567%	22.46	0.00422%	20.25	0.00417%	19.59	0.00457%	22.29	0.00424%	21.24	0.99	0.99	0.93
LINE/R1_26	0.00543%	17.10	0.00570%	17.84	0.00536%	16.27	0.00484%	15.63	0.00510%	16.45	0.00567%	16.09	1.05	0.90	1.11
LINE/R1_27	0.00469%	17.07	0.00491%	19.18	0.00183%	21.17	0.00141%	21.78	0.00358%	17.25	0.00278%	18.2	1.05	0.77	0.78
LINE/R1_28	0.00379%	15.55	0.00422%	13.55	0.00298%	8.81	0.00341%	9.62	0.00346%	10.9	0.00317%	9.33	1.11	1.15	0.92
LINE/R1_29	0.00361%	24.67	0.00387%	25.92	0.00293%	23.86	0.00291%	24.82	0.00337%	22.47	0.00315%	24.04	1.07	0.99	0.94
LINE/R1_3	0.02098%	11.47	0.02201%	11.25	0.02089%	9.35	0.01816%	9.81	0.01879%	10.24	0.02002%	9.71	1.05	0.87	1.07
LINE/R1_30	0.00349%	24.21	0.00479%	29.12	0.00195%	27.55	0.00255%	27.61	0.00266%	26.48	0.00292%	21.92	1.37	1.31	1.10
LINE/R1_31	0.00333%	4.84	0.00332%	5.87	0.00107%	10.87	0.00100%	6.69	0.00101%	6.06	0.00195%	4.54	1.00	0.94	1.93
LINE/R1_32	0.00313%	18.49	0.00396%	17.10	0.00302%	16.34	0.00266%	16.23	0.00329%	16.86	0.00314%	16.48	1.26	0.88	0.95
LINE/R1_33	0.00313%	11.66	0.00374%	10.79	0.00299%	9.51	0.00319%	10.37	0.00343%	9.54	0.00341%	8.97	1.20	1.07	1.00
LINE/R1_34	0.00291%	12.50	0.00316%	12.02	0.00254%	11.84	0.00275%	11.22	0.00281%	9.79	0.00304%	10.01	1.08	1.08	1.08

LINE/R1_35	0.00259%	17.46	0.00278%	17.61	0.00148%	20.05	0.00104%	19.97	0.00175%	15.33	0.00164%	16.48	1.07	0.70	0.94
LINE/R1_36	0.00215%	5.84	0.00208%	6.58	0.00179%	2.62	0.00087%	5.76	0.00085%	10.74	0.00144%	7.29	0.97	0.49	1.69
LINE/R1_37	0.00211%	27.19	0.00204%	27.00	0.00105%	24.53	0.00094%	26.19	0.00138%	23.05	0.00130%	22.9	0.97	0.90	0.94
LINE/R1_38	0.00203%	6.88	0.00217%	6.83	0.00190%	6.75	0.00177%	7.45	0.00193%	6.3	0.00189%	7	1.07	0.93	0.98
LINE/R1_39	0.00201%	19.39	0.00205%	18.04	0.00201%	18.26	0.00207%	21.08	0.00232%	19.08	0.00198%	19.31	1.02	1.03	0.86
LINE/R1_4	0.01743%	9.11	0.01632%	9.85	0.01423%	8.51	0.01480%	8.49	0.00839%	11.16	0.00939%	10.44	0.94	1.04	1.12
LINE/R1_40	0.00191%	15.22	0.00210%	15.16	0.00208%	12.86	0.00193%	13.6	0.00116%	18.51	0.00133%	17.01	1.10	0.93	1.15
LINE/R1_41	0.00191%	21.95	0.00206%	22.07	0.00116%	22.27	0.00163%	19.07	0.00172%	19.52	0.00161%	20.75	1.08	1.40	0.94
LINE/R1_42	0.00178%	17.30	0.00200%	18.39	0.00068%	17.95	0.00048%	15.35	0.00145%	18.26	0.00124%	18.37	1.13	0.71	0.86
LINE/R1_43	0.00166%	21.21	0.00194%	20.86	0.00191%	17.92	0.00157%	18.38	0.00152%	19.09	0.00181%	19.79	1.17	0.82	1.19
LINE/R1_44	0.00160%	8.07	0.00167%	8.33	0.00159%	6.02	0.00134%	5.31	0.00130%	9.58	0.00140%	8.21	1.04	0.85	1.08
LINE/R1_45	0.00124%	10.47	0.00169%	14.19	0.00053%	19.52	0.00050%	16.73	0.00115%	9.94	0.00114%	12.26	1.36	0.95	0.99
LINE/R1_46	0.00118%	17.76	0.00105%	15.55	0.00045%	23.4	0.00064%	18.94	0.00088%	11.39	0.00098%	12.17	0.89	1.42	1.11
LINE/R1_47	0.00100%	6.11	0.00091%	5.69	0.00098%	6.25	0.00102%	7.04	0.00093%	6.66	0.00065%	6.63	0.90	1.04	0.70
LINE/R1_5	0.01485%	10.58	0.01720%	10.85	0.01384%	7.77	0.01436%	7.28	0.01540%	8.08	0.01547%	8.08	1.16	1.04	1.00
LINE/R1_6	0.01356%	19.00	0.01537%	18.69	0.00875%	18.24	0.00852%	17.8	0.01062%	17.35	0.00959%	17.37	1.13	0.97	0.90
LINE/R1_7	0.01177%	16.65	0.01260%	17.17	0.01149%	16.13	0.01222%	14.93	0.01047%	14.28	0.01179%	15.11	1.07	1.06	1.13
LINE/R1_8	0.01048%	24.52	0.01300%	25.06	0.00824%	23.25	0.00851%	22.14	0.01001%	22.62	0.01027%	21.69	1.24	1.03	1.03
LINE/R1_9	0.01043%	11.90	0.01162%	11.68	0.01098%	9.33	0.01031%	9.38	0.01065%	9.59	0.00989%	8.99	1.11	0.94	0.93
LINE/R1-LOA_1	0.07956%	13.07	0.08155%	13.80	0.07293%	13.24	0.07658%	13.08	0.07018%	12.47	0.07181%	12.84	1.03	1.05	1.02
LINE/R2_1	0.02549%	8.04	0.02910%	8.04	0.01693%	7.35	0.01802%	7.42	0.02121%	7.3	0.01928%	7.07	1.14	1.06	0.91
LINE/R2_2	0.01324%	17.87	0.01512%	17.71	0.00467%	13.24	0.00430%	15.18	0.00355%	20.4	0.00553%	19.69	1.14	0.92	1.56
LINE/R2_3	0.01246%	17.59	0.01220%	17.07	0.00655%	15.89	0.00392%	16.74	0.00430%	16.22	0.00602%	16.43	0.98	0.60	1.40
LINE/R2_4	0.00908%	14.30	0.00980%	14.79	0.00598%	10.18	0.00354%	13.68	0.00355%	14.89	0.00478%	14.11	1.08	0.59	1.35
LINE/R2_5	0.00351%	14.91	0.00361%	14.73	0.00161%	16.08	0.00116%	16.61	0.00115%	19.97	0.00142%	18.28	1.03	0.72	1.24
LINE/R2_6	0.00255%	5.23	0.00274%	6.23	0.00114%	7.15	0.00103%	6.33	0.00159%	7.38	0.00146%	6.72	1.07	0.90	0.92
LINE/R2_7	0.00101%	7.19	0.00107%	6.02	0.00036%	8.11	0.00026%	7.02	0.00014%	12.43	0.00037%	8.67	1.06	0.74	2.74
LINE/RTE-BovB_1	4.01969%	10.96	4.01530%	11.64	3.90169%	10.86	3.85774%	10.86	4.23730%	10.59	3.83294%	10.97	1.00	0.99	0.90
LINE/RTE-BovB_2	2.41499%	9.88	2.32889%	10.25	2.23154%	9.47	2.12066%	9.4	2.40897%	9.32	2.11529%	9.69	0.96	0.95	0.88
LINE/RTE-BovB_3	0.00771%	2.63	0.00445%	2.23	0.02302%	2.31	0.01068%	2.29	0.00827%	2.3	0.01252%	2.3	0.58	0.46	1.51
LINE/Tx1_1	0.50536%	4.53	0.51318%	4.60	0.48826%	4.07	0.47219%	4.11	0.52363%	4.07	0.48417%	4.12	1.02	0.97	0.92

LTR/Copia_1	0.01618%	12.69	0.01713%	12.56	0.01133%	11.4	0.01040%	11.29	0.01258%	11.54	0.01149%	11.43	1.06	0.92	0.91
LTR/Copia_10	0.00152%	8.20	0.00149%	9.33	0.00143%	8.12	0.00153%	7.14	0.00130%	6.26	0.00149%	6.26	0.98	1.07	1.15
LTR/Copia_11	0.00099%	8.85	0.00095%	8.08	0.00081%	8.11	0.00071%	8.97	0.00098%	8.5	0.00079%	8.94	0.96	0.88	0.80
LTR/Copia_12	0.00074%	9.00	0.00085%	7.94	0.00069%	6.06	0.00051%	6.57	0.00043%	8.05	0.00086%	7.15	1.15	0.74	1.98
LTR/Copia_13	0.00073%	7.54	0.00068%	8.26	0.00069%	8.45	0.00082%	7.28	0.00037%	7.79	0.00067%	7.76	0.94	1.18	1.79
LTR/Copia_2	0.01612%	6.46	0.01611%	6.43	0.01262%	5.93	0.01390%	5.52	0.01415%	5.72	0.01395%	5.36	1.00	1.10	0.99
LTR/Copia_3	0.01188%	16.62	0.01338%	17.74	0.01611%	12.23	0.01329%	13.38	0.00937%	19.91	0.00953%	18.81	1.13	0.82	1.02
LTR/Copia_4	0.00738%	11.93	0.00604%	13.00	0.00512%	11.96	0.00476%	12.61	0.00607%	13.35	0.00476%	13.07	0.82	0.93	0.78
LTR/Copia_5	0.00455%	6.27	0.00444%	6.84	0.00518%	5.33	0.00525%	4.87	0.00100%	13.68	0.00245%	6.1	0.98	1.01	2.45
LTR/Copia_6	0.00377%	18.21	0.00398%	19.10	0.00314%	15.15	0.00296%	14.74	0.00253%	13.82	0.00336%	14.89	1.06	0.94	1.33
LTR/Copia_7	0.00210%	16.86	0.00218%	17.86	0.00228%	15.67	0.00248%	16.54	0.00245%	16.72	0.00226%	16.66	1.03	1.09	0.92
LTR/Copia_8	0.00186%	12.30	0.00177%	15.36	0.00159%	14.64	0.00158%	14.08	0.00110%	20.73	0.00113%	16.31	0.95	0.99	1.03
LTR/Copia_9	0.00166%	8.42	0.00184%	11.47	0.00147%	9.62	0.00190%	10.07	0.00194%	8.13	0.00204%	7.3	1.11	1.29	1.05
LTR/DIRS_1	0.00123%	19.68	0.00128%	21.80	0.00056%	13.66	0.00050%	9.48	0.00074%	10.53	0.00071%	12.63	1.04	0.89	0.96
LTR/ERV1_1	0.02812%	13.07	0.02825%	13.17	0.02652%	12.17	0.02747%	12.41	0.02333%	12.26	0.02898%	12.53	1.00	1.04	1.24
LTR/ERV1_2	0.01676%	16.13	0.01728%	16.84	0.01437%	16.55	0.01462%	15.97	0.01506%	17.02	0.01437%	16.8	1.03	1.02	0.95
LTR/ERVK_1	0.00563%	7.20	0.00603%	7.32	0.00464%	5.46	0.00639%	5.44	0.00414%	7.5	0.00463%	5.89	1.07	1.38	1.12
LTR/Gypsy_1	0.64376%	7.10	0.68613%	7.10	0.60223%	6.34	0.63828%	6.01	0.68515%	6.24	0.58577%	6.42	1.07	1.06	0.85
LTR/Gypsy_10	0.08017%	9.04	0.08759%	8.96	0.07296%	8.57	0.07753%	8.59	0.08349%	8.6	0.07727%	8.59	1.09	1.06	0.93
LTR/Gypsy_100	0.00613%	20.78	0.00678%	23.11	0.00666%	20.01	0.00564%	19.57	0.00453%	20.34	0.00588%	21.13	1.11	0.85	1.30
LTR/Gypsy_101	0.00610%	12.16	0.00577%	12.16	0.00539%	10.87	0.00570%	11.64	0.00418%	11.36	0.00557%	11.61	0.95	1.06	1.33
LTR/Gypsy_102	0.00583%	21.61	0.00607%	23.00	0.00511%	21.18	0.00491%	20.07	0.00399%	20.3	0.00456%	20.29	1.04	0.96	1.14
LTR/Gypsy_103	0.00577%	24.44	0.00556%	24.16	0.00430%	21.9	0.00380%	22.93	0.00476%	21.81	0.00394%	22.34	0.96	0.88	0.83
LTR/Gypsy_104	0.00576%	13.68	0.00604%	14.56	0.00672%	12.04	0.00665%	12.25	0.00731%	12.55	0.00660%	12.85	1.05	0.99	0.90
LTR/Gypsy_105	0.00570%	11.53	0.00587%	11.32	0.00461%	11.8	0.00499%	11.24	0.00588%	11.21	0.00544%	11.56	1.03	1.08	0.92
LTR/Gypsy_106	0.00558%	24.09	0.00698%	25.48	0.00453%	24.42	0.00411%	25.07	0.00611%	23.87	0.00522%	25.74	1.25	0.91	0.85
LTR/Gypsy_107	0.00554%	23.77	0.00590%	24.38	0.00604%	20.6	0.00552%	20.91	0.00554%	19.91	0.00583%	20.88	1.07	0.91	1.05
LTR/Gypsy_108	0.00534%	12.09	0.00582%	12.27	0.00478%	12.8	0.00515%	12.7	0.00518%	13.28	0.00534%	13.02	1.09	1.08	1.03
LTR/Gypsy_109	0.00534%	10.06	0.00466%	9.63	0.00458%	11	0.00415%	10.96	0.00553%	11.61	0.00430%	10.97	0.87	0.90	0.78
LTR/Gypsy_11	0.07004%	18.60	0.07482%	19.42	0.06244%	17.41	0.06331%	17.28	0.06229%	16.67	0.06624%	16.74	1.07	1.01	1.06
LTR/Gypsy_110	0.00519%	19.32	0.00497%	18.33	0.00535%	19.41	0.00461%	18.49	0.00391%	17.78	0.00561%	18.23	0.96	0.86	1.44

LTR/Gypsy_111	0.00507%	25.09	0.00570%	26.14	0.00489%	21.95	0.00481%	21.79	0.00309%	20.71	0.00468%	21.9	1.12	0.98	1.51
LTR/Gypsy_112	0.00477%	16.84	0.00479%	16.87	0.00454%	15.25	0.00468%	15.73	0.00453%	15.84	0.00490%	15.65	1.00	1.03	1.08
LTR/Gypsy_113	0.00476%	14.90	0.00470%	18.32	0.00247%	13.81	0.00310%	12.8	0.00211%	12.58	0.00260%	13.57	0.99	1.26	1.23
LTR/Gypsy_114	0.00469%	18.15	0.00491%	19.89	0.00496%	17.96	0.00456%	17.78	0.00372%	17.48	0.00515%	17.75	1.05	0.92	1.38
LTR/Gypsy_115	0.00465%	19.60	0.00453%	21.73	0.00354%	16.7	0.00353%	15.91	0.00285%	16.4	0.00409%	16.1	0.97	1.00	1.43
LTR/Gypsy_116	0.00449%	16.69	0.00439%	19.68	0.00401%	15.17	0.00339%	15.03	0.00381%	13.63	0.00380%	14.02	0.98	0.85	1.00
LTR/Gypsy_117	0.00448%	10.11	0.00465%	10.57	0.00385%	8.3	0.00392%	8.4	0.00464%	8.18	0.00380%	8.74	1.04	1.02	0.82
LTR/Gypsy_118	0.00447%	11.46	0.00420%	11.04	0.00407%	10.28	0.00339%	11.31	0.00413%	10.1	0.00354%	10.59	0.94	0.83	0.86
LTR/Gypsy_119	0.00446%	16.28	0.00487%	16.83	0.00424%	15.41	0.00370%	14.28	0.00427%	13.68	0.00404%	14.41	1.09	0.87	0.95
LTR/Gypsy_12	0.06813%	6.46	0.07105%	7.08	0.06520%	5.53	0.06446%	5.58	0.07807%	5.72	0.06127%	5.71	1.04	0.99	0.78
LTR/Gypsy_120	0.00435%	11.47	0.00464%	11.54	0.00370%	9.19	0.00359%	9.35	0.00425%	9.85	0.00389%	8.87	1.07	0.97	0.92
LTR/Gypsy_121	0.00434%	24.29	0.00452%	25.08	0.00432%	22.55	0.00354%	21.94	0.00362%	22.26	0.00445%	22.05	1.04	0.82	1.23
LTR/Gypsy_122	0.00423%	10.55	0.00398%	10.76	0.00447%	10.38	0.00390%	10.78	0.00509%	10.94	0.00462%	10.7	0.94	0.87	0.91
LTR/Gypsy_123	0.00403%	8.14	0.00411%	9.78	0.00488%	5.32	0.00467%	5.05	0.00084%	18.6	0.00238%	10.63	1.02	0.96	2.82
LTR/Gypsy_124	0.00382%	19.98	0.00392%	21.36	0.00352%	19.35	0.00344%	18.85	0.00261%	18.13	0.00399%	17.01	1.03	0.98	1.53
LTR/Gypsy_125	0.00378%	19.58	0.00340%	20.69	0.00303%	16.12	0.00326%	15.66	0.00344%	15.8	0.00326%	15.68	0.90	1.08	0.95
LTR/Gypsy_126	0.00363%	20.18	0.00408%	22.29	0.00344%	16.43	0.00335%	19.47	0.00385%	17.31	0.00360%	16.82	1.12	0.97	0.93
LTR/Gypsy_127	0.00362%	8.93	0.00350%	8.78	0.00430%	7.99	0.00411%	7.98	0.00500%	8.38	0.00436%	8.62	0.97	0.96	0.87
LTR/Gypsy_128	0.00306%	5.17	0.00316%	4.22	0.00428%	4.32	0.00392%	4.74	0.00160%	9.43	0.00189%	7.48	1.03	0.92	1.18
LTR/Gypsy_129	0.00305%	22.34	0.00308%	22.64	0.00288%	17.18	0.00308%	19.79	0.00196%	18.89	0.00290%	18.16	1.01	1.07	1.48
LTR/Gypsy_13	0.06441%	5.89	0.06876%	5.81	0.06220%	5.71	0.06356%	5.58	0.06948%	5.59	0.06402%	5.67	1.07	1.02	0.92
LTR/Gypsy_130	0.00305%	14.52	0.00293%	14.52	0.00249%	12.54	0.00248%	12.68	0.00308%	12.45	0.00240%	12.21	0.96	1.00	0.78
LTR/Gypsy_131	0.00299%	15.76	0.00299%	17.36	0.00260%	14.08	0.00262%	13.51	0.00298%	11.12	0.00288%	13.11	1.00	1.01	0.97
LTR/Gypsy_132	0.00296%	5.55	0.00346%	5.52	0.00214%	4.54	0.00206%	5.76	0.00225%	5.1	0.00231%	4.94	1.17	0.96	1.03
LTR/Gypsy_133	0.00293%	6.03	0.00361%	5.93	0.00222%	8.13	0.00226%	8.11	0.00221%	6.39	0.00335%	5.32	1.23	1.02	1.52
LTR/Gypsy_134	0.00290%	22.35	0.00312%	22.49	0.00238%	21.54	0.00252%	21.34	0.00212%	22	0.00256%	20.75	1.08	1.06	1.21
LTR/Gypsy_135	0.00284%	20.47	0.00282%	19.08	0.00224%	16.33	0.00234%	16.58	0.00193%	15.64	0.00223%	17.99	0.99	1.04	1.16
LTR/Gypsy_136	0.00281%	16.33	0.00295%	17.65	0.00258%	14.28	0.00263%	13.73	0.00288%	13.07	0.00256%	13.74	1.05	1.02	0.89
LTR/Gypsy_137	0.00249%	13.14	0.00239%	16.60	0.00271%	10.6	0.00203%	10.76	0.00270%	10.58	0.00253%	11.36	0.96	0.75	0.93
LTR/Gypsy_138	0.00234%	17.62	0.00236%	19.42	0.00276%	17.19	0.00287%	15.98	0.00302%	16.54	0.00270%	16.74	1.01	1.04	0.89
LTR/Gypsy_139	0.00218%	12.91	0.00214%	13.33	0.00205%	13.25	0.00218%	12.78	0.00236%	12.24	0.00211%	11.84	0.98	1.06	0.89

LTR/Gypsy_14	0.06392%	4.30	0.06385%	4.34	0.06796%	4.24	0.06517%	4.37	0.05950%	4.68	0.06319%	4.42	1.00	0.96	1.06
LTR/Gypsy_140	0.00182%	18.48	0.00187%	20.83	0.00121%	13.26	0.00132%	9.61	0.00114%	11.56	0.00118%	11.38	1.02	1.09	1.04
LTR/Gypsy_141	0.00181%	12.80	0.00184%	14.42	0.00161%	11.86	0.00155%	10.1	0.00172%	11.69	0.00144%	11.38	1.02	0.97	0.83
LTR/Gypsy_142	0.00140%	11.73	0.00136%	13.10	0.00168%	9	0.00142%	10.53	0.00068%	20.46	0.00102%	17.37	0.97	0.85	1.50
LTR/Gypsy_143	0.00129%	24.06	0.00133%	23.13	0.00085%	22.85	0.00103%	19.68	0.00095%	22.14	0.00080%	19.9	1.03	1.21	0.84
LTR/Gypsy_144	0.00099%	16.79	0.00096%	15.19	0.00077%	13.49	0.00055%	14.51	0.00092%	12.53	0.00091%	14.49	0.97	0.71	1.00
LTR/Gypsy_145	0.00090%	12.58	0.00106%	13.35	0.00060%	11.26	0.00137%	7.9	0.00100%	9	0.00068%	14.32	1.19	2.30	0.68
LTR/Gypsy_146	0.00088%	10.10	0.00076%	9.40	0.00091%	8.61	0.00080%	5.32	0.00043%	18.52	0.00061%	11.67	0.86	0.87	1.40
LTR/Gypsy_147	0.00072%	10.14	0.00087%	10.05	0.00048%	9.42	0.00100%	5.39	0.00060%	8.81	0.00046%	13.51	1.21	2.08	0.76
LTR/Gypsy_148	0.00067%	14.44	0.00060%	11.96	0.00067%	7.32	0.00064%	11.07	0.00046%	14.82	0.00055%	12.96	0.90	0.95	1.21
LTR/Gypsy_149	0.00060%	12.84	0.00088%	11.33	0.00072%	9.97	0.00078%	9.8	0.00025%	21.12	0.00045%	15.95	1.47	1.09	1.79
LTR/Gypsy_15	0.06176%	10.04	0.06437%	9.93	0.06468%	9.39	0.06417%	9.66	0.07542%	9.42	0.06439%	9.64	1.04	0.99	0.85
LTR/Gypsy_150	0.00050%	14.85	0.00058%	21.48	0.00040%	6.65	0.00075%	13.65	0.00027%	18.91	0.00038%	20.7	1.16	1.89	1.42
LTR/Gypsy_151	0.00049%	4.54	0.00054%	3.46	0.00051%	5.64	0.00069%	3.49	0.00041%	3.23	0.00030%	5.28	1.10	1.35	0.72
LTR/Gypsy_152	0.00042%	12.07	0.00056%	11.62	0.00051%	12.2	0.00053%	7.21	0.00039%	11.29	0.00037%	13.99	1.34	1.04	0.97
LTR/Gypsy_153	0.00041%	10.57	0.00056%	10.07	0.00045%	12.5	0.00053%	7.11	0.00052%	9.05	0.00050%	12.11	1.36	1.17	0.96
LTR/Gypsy_16	0.05792%	24.47	0.06127%	24.74	0.04859%	22.35	0.04633%	22.1	0.04626%	21.42	0.05022%	21.82	1.06	0.95	1.09
*LTR/Gypsy_17	0.05752%	9.37	0.07498%	8.22	0.04667%	7.89	0.05926%	6.91	0.04814%	7.92	0.04474%	8.08	1.30	1.27	0.93
LTR/Gypsy_18	0.05591%	13.45	0.05672%	13.48	0.05486%	12.32	0.05371%	12.33	0.05860%	12.51	0.05379%	12.64	1.01	0.98	0.92
LTR/Gypsy_19	0.05124%	14.13	0.06059%	14.37	0.05683%	13.34	0.05602%	13.6	0.06207%	13.56	0.05344%	13.41	1.18	0.99	0.86
LTR/Gypsy_2	0.40305%	9.50	0.41940%	9.29	0.40358%	8.86	0.43958%	8.84	0.40099%	8.79	0.36369%	8.82	1.04	1.09	0.91
LTR/Gypsy_20	0.04954%	17.59	0.05126%	18.12	0.05232%	16.67	0.05010%	16.7	0.03931%	16.42	0.05129%	16.44	1.03	0.96	1.30
LTR/Gypsy_21	0.04461%	10.26	0.04703%	10.18	0.05230%	11.88	0.04738%	11.07	0.04836%	10.33	0.04216%	10.09	1.05	0.91	0.87
LTR/Gypsy_22	0.04415%	13.27	0.04469%	13.51	0.06471%	9.78	0.06028%	10.31	0.05568%	10.71	0.04047%	10.95	1.01	0.93	0.73
LTR/Gypsy_23	0.04398%	19.63	0.04435%	20.20	0.04456%	18.07	0.04260%	18.14	0.03350%	18.39	0.04451%	18.58	1.01	0.96	1.33
LTR/Gypsy_24	0.04352%	11.68	0.04417%	11.73	0.04429%	10.31	0.04290%	10.16	0.05026%	10.08	0.04437%	10.02	1.02	0.97	0.88
LTR/Gypsy_25	0.03926%	9.14	0.04058%	9.40	0.03616%	8.88	0.03710%	8.98	0.04528%	7.98	0.03692%	8.8	1.03	1.03	0.82
LTR/Gypsy_26	0.03615%	14.39	0.03630%	14.70	0.03627%	13.24	0.03484%	13.41	0.03269%	12.82	0.03586%	12.96	1.00	0.96	1.10
LTR/Gypsy_27	0.03099%	13.14	0.03694%	12.94	0.03090%	12.29	0.03682%	12.22	0.02987%	12.07	0.02964%	12.33	1.19	1.19	0.99
LTR/Gypsy_28	0.03029%	9.15	0.03150%	9.22	0.02955%	8.98	0.02978%	8.8	0.03247%	8.93	0.02903%	8.79	1.04	1.01	0.89
LTR/Gypsy_29	0.02995%	11.73	0.03168%	12.98	0.03914%	12.25	0.04111%	12.45	0.02892%	10.65	0.02844%	11.67	1.06	1.05	0.98

LTR/Gypsy_3	0.20066%	8.41	0.23584%	8.53	0.20521%	7.64	0.22329%	7.16	0.21307%	7.18	0.21753%	7.59	1.18	1.09	1.02
LTR/Gypsy_30	0.02866%	13.87	0.03086%	14.22	0.02781%	12.34	0.02738%	12.23	0.02272%	12.7	0.02823%	12.1	1.08	0.98	1.24
LTR/Gypsy_31	0.02822%	8.09	0.02993%	7.98	0.02665%	7.83	0.02756%	8.02	0.03011%	7.78	0.02792%	7.99	1.06	1.03	0.93
LTR/Gypsy_32	0.02770%	15.31	0.02848%	15.46	0.02663%	14.04	0.02717%	13.97	0.02922%	14.04	0.02344%	13.91	1.03	1.02	0.80
LTR/Gypsy_33	0.02632%	24.41	0.02841%	25.12	0.02500%	22.43	0.02553%	21.85	0.01765%	21.15	0.02516%	21.41	1.08	1.02	1.43
LTR/Gypsy_34	0.02612%	10.44	0.02676%	10.34	0.02614%	10.42	0.02547%	10.54	0.02918%	10.45	0.02692%	10.5	1.02	0.97	0.92
LTR/Gypsy_35	0.02521%	11.56	0.02473%	11.88	0.02445%	10.49	0.02261%	10.61	0.02476%	10.41	0.02333%	10.49	0.98	0.92	0.94
LTR/Gypsy_36	0.02500%	14.02	0.02878%	13.42	0.02376%	11.59	0.02538%	11.54	0.01998%	12.27	0.02426%	12.41	1.15	1.07	1.21
LTR/Gypsy_37	0.02376%	14.60	0.02516%	14.89	0.02299%	13.62	0.02331%	13.48	0.02476%	13.47	0.02153%	13.84	1.06	1.01	0.87
LTR/Gypsy_38	0.02319%	18.17	0.02400%	18.24	0.01999%	16.71	0.02109%	17.08	0.02363%	16.95	0.02136%	17.04	1.04	1.05	0.90
LTR/Gypsy_39	0.02164%	10.84	0.02244%	10.77	0.01926%	9.61	0.02041%	9.48	0.02061%	9.49	0.02001%	9.21	1.04	1.06	0.97
LTR/Gypsy_4	0.16549%	8.70	0.16945%	9.38	0.16588%	8.43	0.16273%	8.49	0.18463%	8.21	0.16630%	8.29	1.02	0.98	0.90
LTR/Gypsy_40	0.02143%	13.23	0.02287%	13.25	0.01949%	12.68	0.01923%	12.68	0.02134%	12.66	0.01844%	12.69	1.07	0.99	0.86
LTR/Gypsy_41	0.02124%	13.11	0.02203%	13.33	0.02019%	12.22	0.02042%	12.36	0.02276%	12.29	0.02093%	12.24	1.04	1.01	0.92
LTR/Gypsy_42	0.02107%	13.72	0.02069%	13.49	0.01903%	13.69	0.01905%	13.74	0.02237%	13.74	0.02061%	13.74	0.98	1.00	0.92
LTR/Gypsy_43	0.02039%	15.97	0.02066%	15.78	0.01802%	15.25	0.01773%	15.16	0.02132%	15.1	0.01775%	15.34	1.01	0.98	0.83
LTR/Gypsy_44	0.01979%	15.91	0.02091%	17.87	0.02035%	14.1	0.01912%	14.46	0.01389%	14.68	0.01952%	13.9	1.06	0.94	1.41
LTR/Gypsy_45	0.01916%	12.64	0.01870%	12.63	0.01650%	12.06	0.01668%	11.67	0.01742%	11.97	0.01553%	11.83	0.98	1.01	0.89
LTR/Gypsy_46	0.01858%	14.12	0.02028%	14.01	0.01783%	13.14	0.01867%	13.01	0.01848%	13.07	0.01905%	13.19	1.09	1.05	1.03
LTR/Gypsy_47	0.01850%	20.69	0.02116%	21.35	0.01774%	19.39	0.01637%	18.76	0.01907%	18.7	0.01752%	19.05	1.14	0.92	0.92
LTR/Gypsy_48	0.01828%	26.66	0.02203%	27.76	0.01596%	24.82	0.01561%	24.54	0.01224%	24.33	0.01688%	24.98	1.20	0.98	1.38
LTR/Gypsy_49	0.01818%	11.19	0.01802%	11.06	0.01588%	8.29	0.01733%	8.6	0.01682%	8.42	0.01453%	8.64	0.99	1.09	0.86
LTR/Gypsy_5	0.12245%	7.88	0.13553%	7.67	0.11732%	7.35	0.12176%	6.95	0.12414%	7.07	0.11989%	7	1.11	1.04	0.97
LTR/Gypsy_50	0.01777%	12.47	0.02073%	12.45	0.01811%	11.12	0.01922%	10.98	0.01713%	11.65	0.01896%	11.56	1.17	1.06	1.11
LTR/Gypsy_51	0.01763%	5.54	0.01777%	5.96	0.01802%	5.36	0.01777%	5.3	0.02020%	5.43	0.01834%	5.37	1.01	0.99	0.91
LTR/Gypsy_52	0.01725%	15.21	0.01684%	15.29	0.01535%	13.54	0.01597%	13.61	0.01846%	13.12	0.01685%	13.48	0.98	1.04	0.91
LTR/Gypsy_53	0.01687%	9.78	0.01801%	9.66	0.01119%	8.78	0.01113%	9.28	0.01191%	9.26	0.01208%	8.86	1.07	0.99	1.01
LTR/Gypsy_54	0.01648%	10.86	0.01764%	10.68	0.01678%	9.8	0.01809%	9.77	0.01725%	9.83	0.01788%	9.94	1.07	1.08	1.04
LTR/Gypsy_55	0.01634%	10.58	0.01799%	10.33	0.01518%	9.51	0.01817%	8.7	0.01416%	9.63	0.01266%	9.29	1.10	1.20	0.89
LTR/Gypsy_56	0.01625%	8.05	0.01674%	7.80	0.01311%	6.7	0.01368%	6.61	0.01394%	6.46	0.01251%	7.08	1.03	1.04	0.90
LTR/Gypsy_57	0.01589%	10.05	0.01597%	9.91	0.01873%	9.69	0.01829%	9.78	0.01859%	10.01	0.01732%	10.04	1.01	0.98	0.93

LTR/Gypsy_58	0.01580%	24.20	0.01690%	25.36	0.01488%	22.18	0.01370%	21.73	0.01020%	20.64	0.01462%	21.12	1.07	0.92	1.43
LTR/Gypsy_59	0.01508%	13.75	0.01539%	13.66	0.01488%	12.81	0.01420%	13.32	0.01574%	13.39	0.01464%	13.27	1.02	0.95	0.93
LTR/Gypsy_6	0.10507%	17.16	0.09085%	14.66	0.13930%	16.11	0.14111%	15.9	0.15930%	15.62	0.16576%	15.7	0.86	1.01	1.04
LTR/Gypsy_60	0.01454%	20.05	0.01508%	20.09	0.01297%	18.24	0.01281%	17.31	0.01041%	18.22	0.01352%	17.75	1.04	0.99	1.30
LTR/Gypsy_61	0.01454%	24.14	0.01590%	24.83	0.01090%	18.18	0.01123%	19.11	0.01067%	18.77	0.01061%	17.68	1.09	1.03	0.99
LTR/Gypsy_62	0.01343%	10.34	0.01412%	10.03	0.01354%	9.44	0.01427%	9.53	0.01472%	8.89	0.01324%	9.31	1.05	1.05	0.90
LTR/Gypsy_63	0.01319%	12.64	0.01413%	12.28	0.01981%	7.86	0.01774%	8.7	0.00929%	16.59	0.01032%	14.49	1.07	0.90	1.11
LTR/Gypsy_64	0.01310%	7.42	0.01304%	7.93	0.01213%	6.95	0.01213%	6.84	0.01352%	7.04	0.01152%	7.13	1.00	1.00	0.85
LTR/Gypsy_65	0.01288%	14.00	0.01568%	12.66	0.01149%	11.75	0.01231%	11.06	0.00989%	11.53	0.01329%	11.87	1.22	1.07	1.34
LTR/Gypsy_66	0.01271%	10.42	0.01248%	10.51	0.01265%	8.82	0.01237%	8.96	0.00918%	9.31	0.01305%	8.78	0.98	0.98	1.42
LTR/Gypsy_67	0.01199%	9.31	0.01286%	10.50	0.01286%	8.21	0.01264%	8.28	0.00630%	13.64	0.00821%	11.96	1.07	0.98	1.30
LTR/Gypsy_68	0.01172%	10.23	0.01151%	10.48	0.01302%	10.11	0.01327%	9.65	0.01497%	9.56	0.01354%	9.92	0.98	1.02	0.90
LTR/Gypsy_69	0.01141%	22.52	0.01281%	22.99	0.01262%	22.03	0.01150%	22.1	0.00817%	21.19	0.01173%	22.28	1.12	0.91	1.44
LTR/Gypsy_7	0.10146%	10.49	0.10257%	11.04	0.08859%	10.2	0.08981%	9.69	0.10695%	8.71	0.09135%	9.8	1.01	1.01	0.85
LTR/Gypsy_70	0.01134%	12.56	0.01415%	14.82	0.01629%	14.13	0.01541%	15.04	0.01661%	14.07	0.01537%	13.74	1.25	0.95	0.93
LTR/Gypsy_71	0.01079%	21.41	0.01092%	21.10	0.00895%	19.52	0.00955%	18.36	0.00658%	18.45	0.00978%	18.55	1.01	1.07	1.49
LTR/Gypsy_72	0.01060%	13.78	0.01091%	14.26	0.01029%	12.43	0.00965%	12.87	0.01138%	12.31	0.01010%	12.48	1.03	0.94	0.89
LTR/Gypsy_73	0.00999%	21.30	0.01090%	22.81	0.00883%	17.38	0.00833%	16.88	0.00592%	17.95	0.00826%	16.21	1.09	0.94	1.40
LTR/Gypsy_74	0.00979%	11.05	0.00940%	10.65	0.00935%	10.57	0.01006%	10.53	0.00991%	10.76	0.00928%	10.74	0.96	1.08	0.94
LTR/Gypsy_75	0.00965%	7.65	0.01026%	7.44	0.00967%	6.64	0.00972%	7.47	0.01068%	7.35	0.00966%	7.11	1.06	1.01	0.90
LTR/Gypsy_76	0.00941%	7.65	0.01080%	11.53	0.01091%	7.18	0.01069%	7.76	0.00874%	9.18	0.01077%	7.31	1.15	0.98	1.23
LTR/Gypsy_77	0.00937%	9.75	0.00948%	10.04	0.00478%	9.95	0.00444%	10.54	0.00535%	10.02	0.00501%	10.55	1.01	0.93	0.94
LTR/Gypsy_78	0.00934%	14.97	0.00977%	15.91	0.00792%	13.37	0.00878%	12.84	0.00920%	13.08	0.00958%	12.95	1.05	1.11	1.04
LTR/Gypsy_79	0.00914%	11.57	0.00968%	11.72	0.00736%	10.01	0.00814%	11.01	0.00846%	9.89	0.00834%	10.14	1.06	1.11	0.99
LTR/Gypsy_8	0.09024%	17.06	0.09489%	17.49	0.08440%	15.23	0.08209%	15.38	0.08364%	14.66	0.08475%	15.31	1.05	0.97	1.01
LTR/Gypsy_80	0.00892%	6.39	0.00811%	7.92	0.00536%	7.78	0.00664%	6.21	0.00349%	10.78	0.00438%	10.09	0.91	1.24	1.25
LTR/Gypsy_81	0.00875%	13.39	0.00935%	13.90	0.00855%	12.7	0.00857%	12.8	0.00981%	12.85	0.00844%	13.02	1.07	1.00	0.86
LTR/Gypsy_82	0.00861%	8.91	0.00803%	10.92	0.00936%	7.14	0.00896%	7.34	0.00577%	8.41	0.00805%	7.66	0.93	0.96	1.40
LTR/Gypsy_83	0.00851%	16.73	0.00889%	16.60	0.00856%	16.08	0.00745%	15.62	0.00829%	15.92	0.00842%	15.67	1.04	0.87	1.02
LTR/Gypsy_84	0.00823%	13.37	0.00743%	12.89	0.00658%	10.94	0.00637%	10.31	0.00599%	11.08	0.00632%	11	0.90	0.97	1.05
LTR/Gypsy_85	0.00799%	13.55	0.00156%	16.78	0.00131%	15.53	0.00154%	14.31	0.01401%	8.21	0.00133%	14.98	0.20	1.18	0.09

LTR/Gypsy_86	0.00792%	17.47	0.00769%	17.31	0.00674%	16.67	0.00687%	17.55	0.00797%	16.71	0.00699%	17.35	0.97	1.02	0.88
LTR/Gypsy_87	0.00761%	13.16	0.00743%	13.38	0.00764%	12.59	0.00743%	12.65	0.00860%	13.64	0.00785%	12.99	0.98	0.97	0.91
LTR/Gypsy_88	0.00745%	9.73	0.00859%	11.95	0.00830%	8.24	0.00755%	7.98	0.00580%	9.99	0.00763%	9.37	1.15	0.91	1.32
LTR/Gypsy_89	0.00733%	9.80	0.00801%	9.19	0.00723%	9.36	0.00664%	8.66	0.00739%	8.67	0.00727%	8.9	1.09	0.92	0.98
LTR/Gypsy_9	0.08985%	7.30	0.09418%	7.32	0.09163%	6.97	0.08934%	6.57	0.09849%	6.18	0.09237%	6.52	1.05	0.98	0.94
LTR/Gypsy_90	0.00724%	16.33	0.00771%	16.27	0.00625%	14.31	0.00629%	13.65	0.00646%	14.01	0.00646%	15.63	1.06	1.01	1.00
LTR/Gypsy_91	0.00710%	20.84	0.00801%	22.31	0.00628%	17.15	0.00613%	16.67	0.00441%	17.96	0.00637%	18.49	1.13	0.98	1.45
LTR/Gypsy_92	0.00710%	19.16	0.00779%	20.00	0.00673%	17.31	0.00690%	18.23	0.00604%	18.96	0.00618%	19.38	1.10	1.02	1.02
LTR/Gypsy_93	0.00688%	19.84	0.00692%	20.52	0.00625%	17.79	0.00618%	16.16	0.00466%	17.57	0.00617%	16.79	1.01	0.99	1.32
LTR/Gypsy_94	0.00674%	10.00	0.00685%	11.18	0.00742%	7.82	0.00714%	9.11	0.00465%	13.87	0.00560%	12.96	1.02	0.96	1.20
LTR/Gypsy_95	0.00654%	29.59	0.00633%	29.66	0.00599%	26.09	0.00625%	27.01	0.00393%	26.72	0.00579%	25.75	0.97	1.04	1.47
LTR/Gypsy_96	0.00648%	22.81	0.00736%	24.46	0.00675%	19.88	0.00615%	21.36	0.00400%	20.09	0.00590%	21.39	1.14	0.91	1.47
LTR/Gypsy_97	0.00637%	16.67	0.00615%	17.75	0.00535%	11.7	0.00533%	12.96	0.00378%	11.72	0.00591%	11.57	0.96	1.00	1.56
LTR/Gypsy_98	0.00636%	18.32	0.00636%	18.13	0.00691%	16.89	0.00637%	16.3	0.00471%	15.3	0.00514%	15.67	1.00	0.92	1.09
LTR/Gypsy_99	0.00626%	16.61	0.00706%	18.84	0.00608%	15.45	0.00600%	15.51	0.00449%	16.94	0.00604%	15.82	1.13	0.99	1.34
LTR/Ngaro_1	0.01675%	14.92	0.01813%	15.58	0.01721%	14.63	0.01706%	14.38	0.01787%	14.26	0.01643%	14.54	1.08	0.99	0.92
LTR/Pao_1	0.15332%	11.75	0.15317%	11.95	0.13706%	10.65	0.13850%	10.6	0.13816%	10.79	0.13251%	10.88	1.00	1.01	0.96
LTR/Pao_10	0.01411%	12.42	0.01517%	12.41	0.01093%	11.52	0.01087%	11.57	0.01140%	11.01	0.01084%	11.4	1.08	0.99	0.95
LTR/Pao_11	0.01125%	11.84	0.01092%	12.18	0.00875%	12.08	0.00908%	11.45	0.00780%	12.66	0.00852%	12.46	0.97	1.04	1.09
LTR/Pao_12	0.01019%	13.28	0.00995%	14.59	0.01053%	12.55	0.00979%	12.68	0.00821%	14.63	0.00860%	13.7	0.98	0.93	1.05
LTR/Pao_13	0.00909%	9.03	0.00842%	9.36	0.00743%	9.43	0.00775%	8.98	0.00516%	11.68	0.00565%	11.18	0.93	1.04	1.09
LTR/Pao_14	0.00904%	11.53	0.00911%	11.86	0.00952%	10.9	0.01021%	11.35	0.01001%	11.72	0.01009%	11.62	1.01	1.07	1.01
LTR/Pao_15	0.00886%	11.69	0.00823%	11.73	0.00736%	12.06	0.00754%	11.65	0.00735%	13.4	0.00717%	12.48	0.93	1.02	0.98
LTR/Pao_16	0.00782%	17.37	0.00736%	18.26	0.00552%	12.8	0.00534%	13.83	0.00377%	18.37	0.00409%	17.6	0.94	0.97	1.08
LTR/Pao_17	0.00777%	18.85	0.00823%	20.25	0.01106%	13.39	0.01147%	13.69	0.01114%	13	0.01011%	14.03	1.06	1.04	0.91
LTR/Pao_18	0.00745%	14.57	0.00125%	17.58	0.00133%	17.22	0.00158%	14.45	0.01501%	9.37	0.00119%	13.99	0.17	1.19	0.08
LTR/Pao_19	0.00643%	12.22	0.00619%	13.55	0.00483%	11.48	0.00468%	13.09	0.00265%	15.77	0.00350%	15.31	0.96	0.97	1.32
LTR/Pao_2	0.06005%	18.33	0.05900%	18.65	0.04017%	15.97	0.04172%	15.89	0.03914%	16.82	0.03884%	16.15	0.98	1.04	0.99
LTR/Pao_20	0.00434%	17.66	0.00449%	18.36	0.00382%	16.47	0.00331%	17.68	0.00252%	21.2	0.00292%	18.38	1.03	0.87	1.16
LTR/Pao_21	0.00377%	9.66	0.00354%	11.01	0.00358%	11.89	0.00298%	9.97	0.00221%	14.12	0.00229%	13.76	0.94	0.83	1.04
LTR/Pao_22	0.00284%	12.08	0.00235%	10.54	0.00200%	9.56	0.00156%	11.1	0.00111%	16.93	0.00122%	13.47	0.83	0.78	1.10

LTR/Pao_23	0.00261%	11.57	0.00258%	12.48	0.00297%	10.15	0.00275%	9.96	0.00282%	10.03	0.00262%	10.67	0.99	0.92	0.93
LTR/Pao_24	0.00108%	10.24	0.00110%	10.14	0.00075%	11.55	0.00071%	9.71	0.00019%	12.25	0.00044%	9.95	1.02	0.96	2.35
LTR/Pao_3	0.06003%	20.89	0.06540%	21.74	0.06913%	15.67	0.06155%	16.23	0.04336%	23.82	0.04507%	22.3	1.09	0.89	1.04
LTR/Pao_4	0.05122%	13.20	0.04952%	13.11	0.05034%	12.72	0.05073%	12.57	0.05003%	12.81	0.04798%	12.61	0.97	1.01	0.96
LTR/Pao_5	0.02477%	14.57	0.02520%	14.70	0.02463%	13.73	0.02461%	13.8	0.02159%	15.85	0.02196%	15.19	1.02	1.00	1.02
LTR/Pao_6	0.02345%	16.69	0.02353%	17.09	0.02175%	14.14	0.02230%	14.04	0.01645%	20.78	0.01728%	18.63	1.00	1.03	1.05
LTR/Pao_7	0.02169%	11.45	0.02413%	12.03	0.03147%	9.09	0.03175%	9.54	0.03277%	8.95	0.03039%	8.84	1.11	1.01	0.93
LTR/Pao_8	0.01655%	10.25	0.01895%	10.37	0.01448%	10.28	0.01520%	10.09	0.01452%	9.9	0.01231%	10.11	1.14	1.05	0.85
LTR/Pao_9	0.01459%	15.05	0.01531%	15.97	0.01465%	14.28	0.01458%	13.67	0.01115%	15.49	0.01177%	15.84	1.05	0.99	1.06
RC/Helitron_1	0.28083%	1.09	0.28374%	1.04	0.16361%	1.52	0.12169%	1.87	0.15943%	1.65	0.15959%	1.61	1.01	0.74	1.00
RC/Helitron_10	0.01137%	14.97	0.01280%	17.62	0.01169%	11.92	0.01086%	12.16	0.00990%	12.79	0.01087%	12.91	1.13	0.93	1.10
RC/Helitron_11	0.00999%	16.89	0.01034%	18.04	0.00945%	16.19	0.00806%	16.46	0.00730%	18.82	0.00724%	18.99	1.04	0.85	0.99
RC/Helitron_12	0.00911%	10.01	0.00896%	10.63	0.00766%	9.44	0.00808%	10.4	0.00611%	12.78	0.00648%	11.63	0.98	1.05	1.06
RC/Helitron_13	0.00834%	8.67	0.00827%	8.74	0.00790%	8.62	0.00787%	7.97	0.00747%	8.22	0.00743%	8.26	0.99	1.00	0.99
RC/Helitron_14	0.00576%	10.32	0.00593%	11.60	0.00596%	9.23	0.00631%	10.18	0.00485%	12.37	0.00619%	11.75	1.03	1.06	1.28
RC/Helitron_15	0.00553%	6.20	0.00569%	6.65	0.00521%	5.79	0.00580%	6.02	0.00524%	6.36	0.00540%	6.63	1.03	1.11	1.03
RC/Helitron_16	0.00542%	8.33	0.00564%	8.40	0.00532%	8.35	0.00531%	8.16	0.00567%	8.47	0.00531%	8.2	1.04	1.00	0.94
RC/Helitron_17	0.00449%	13.83	0.00441%	14.62	0.00583%	14.44	0.00606%	14.39	0.00603%	13.95	0.00570%	14.3	0.98	1.04	0.95
RC/Helitron_18	0.00307%	14.64	0.00337%	16.68	0.00288%	12.97	0.00270%	14.02	0.00295%	13.33	0.00269%	13.13	1.10	0.94	0.91
RC/Helitron_19	0.00299%	7.31	0.00344%	7.79	0.00272%	7.15	0.00387%	5.55	0.00376%	6.23	0.00342%	7.01	1.15	1.42	0.91
RC/Helitron_2	0.22106%	1.24	0.22526%	1.17	0.14317%	1.97	0.10282%	2.44	0.13630%	2.08	0.12842%	2.01	1.02	0.72	0.94
RC/Helitron_20	0.00285%	12.10	0.00267%	12.46	0.00255%	11.41	0.00222%	10.64	0.00244%	10.92	0.00238%	11.02	0.94	0.87	0.98
RC/Helitron_21	0.00284%	6.97	0.00300%	7.06	0.00261%	6.24	0.00303%	6.48	0.00278%	6.69	0.00283%	6.52	1.06	1.16	1.02
RC/Helitron_22	0.00203%	8.50	0.00207%	8.99	0.00198%	9.02	0.00208%	9.04	0.00138%	9.52	0.00141%	9.11	1.02	1.05	1.02
RC/Helitron_23	0.00128%	16.16	0.00151%	15.16	0.00139%	13.24	0.00116%	11	0.00115%	13.77	0.00141%	13.11	1.18	0.84	1.22
RC/Helitron_3	0.15558%	4.04	0.13975%	3.83	0.16880%	7.01	0.17249%	6.98	0.16893%	7.62	0.18471%	7.55	0.90	1.02	1.09
RC/Helitron_4	0.08735%	5.44	0.09251%	7.30	0.07115%	5.03	0.07581%	5.79	0.07318%	5.98	0.08809%	6.15	1.06	1.07	1.20
RC/Helitron_5	0.04267%	1.82	0.04635%	1.64	0.01592%	1.79	0.01098%	1.4	0.01445%	2.22	0.01374%	2.1	1.09	0.69	0.95
RC/Helitron_6	0.03790%	16.62	0.04006%	17.16	0.03225%	16.23	0.03365%	16.23	0.03112%	16.65	0.03285%	16.49	1.06	1.04	1.06
RC/Helitron_7	0.03653%	17.95	0.03733%	18.68	0.03441%	18.53	0.03281%	18.49	0.03168%	19.11	0.03244%	19.04	1.02	0.95	1.02
RC/Helitron_8	0.02342%	12.45	0.02302%	12.59	0.02261%	11.71	0.02299%	11.73	0.01993%	11.32	0.02128%	11.73	0.98	1.02	1.07

RC/Helitron_9	0.02061%	16.58	0.02255%	17.27	0.02281%	17.12	0.02264%	17.15	0.01855%	17.4	0.01657%	17.13	1.09	0.99	0.89
RNA/RNA_1	0.02432%	4.68	0.02771%	3.96	0.01929%	4.08	0.01932%	3.97	0.04363%	4.11	0.03856%	4.19	1.14	1.00	0.88
RNA/RNA_2	0.00251%	4.01	0.00323%	4.12	0.00336%	3.91	0.00294%	3.53	0.00128%	6.81	0.00249%	3.03	1.29	0.87	1.95
RNA/tRNA_1	0.01728%	7.62	0.02106%	6.41	0.01684%	5.98	0.01617%	7.06	0.02759%	5.14	0.01664%	6.48	1.22	0.96	0.60
RNA/tRNA_10	0.00233%	1.12	0.00195%	1.30	0.00235%	1.36	0.00327%	1.14	0.00300%	1.05	0.00196%	1.29	0.84	1.39	0.65
RNA/tRNA_11	0.00212%	5.83	0.00367%	6.26	0.00313%	4.56	0.00334%	6.99	0.00279%	6.81	0.00388%	6.22	1.73	1.07	1.39
RNA/tRNA_12	0.00187%	0.82	0.00157%	0.76	0.00187%	0.78	0.00268%	1.08	0.00214%	1.09	0.00232%	0.72	0.84	1.44	1.09
RNA/tRNA_13	0.00179%	6.26	0.00198%	5.60	0.00175%	6.01	0.00137%	4.71	0.00410%	3.08	0.00345%	4.19	1.11	0.78	0.84
RNA/tRNA_14	0.00095%	5.85	0.00084%	5.12	0.00086%	3.7	0.00120%	3.01	0.00085%	3.28	0.00093%	3.66	0.88	1.39	1.09
RNA/tRNA_2	0.01674%	7.39	0.01612%	8.53	0.01937%	6.37	0.01481%	7.97	0.02101%	6.99	0.01774%	6.58	0.96	0.76	0.84
RNA/tRNA_3	0.01571%	2.43	0.02070%	1.63	0.01272%	2.32	0.01597%	1.81	0.03453%	1.42	0.02370%	1.84	1.32	1.26	0.69
RNA/tRNA_4	0.01259%	3.33	0.01323%	4.33	0.01176%	4.88	0.00857%	4.53	0.01566%	3.78	0.01192%	4.37	1.05	0.73	0.76
RNA/tRNA_5	0.00816%	6.01	0.00770%	6.44	0.00958%	5.76	0.00632%	8.42	0.00886%	6.19	0.00832%	5.61	0.94	0.66	0.94
RNA/tRNA_6	0.00634%	2.89	0.00791%	1.55	0.01413%	1.54	0.01105%	1.44	0.01054%	1.74	0.01202%	1.42	1.25	0.78	1.14
RNA/tRNA_7	0.00331%	2.81	0.00265%	4.46	0.00251%	3.26	0.00403%	2.28	0.00300%	2.22	0.00212%	3.49	0.80	1.60	0.71
RNA/tRNA_8	0.00251%	2.59	0.00255%	3.02	0.00235%	4.77	0.00194%	3.51	0.00313%	3.63	0.00189%	3	1.02	0.82	0.61
RNA/tRNA_9	0.00236%	10.80	0.00266%	10.24	0.00269%	5.12	0.00182%	4.76	0.00234%	7.46	0.00205%	8.19	1.13	0.68	0.88
SINE/7SL_1	0.00102%	1.79	0.00098%	1.86	0.00078%	1.85	0.00058%	3.24	0.00164%	15.84	0.00056%	3.58	0.96	0.74	0.34
SINE/Alu_1	0.00363%	1.39	0.00339%	1.02	0.00280%	2.01	0.00239%	1.35	0.00260%	2.96	0.00187%	1.5	0.93	0.85	0.72
SINE/ID_1	0.01420%	19.59	0.01489%	19.74	0.01653%	19.41	0.01598%	19.54	0.01457%	19.46	0.01654%	19.7	1.05	0.97	1.14
SINE/SINE_1	0.00056%	15.24	0.00074%	16.80	0.00075%	15.19	0.00067%	15.76	0.00077%	14.43	0.00064%	13.64	1.31	0.89	0.83
SINE/tRNA_1	0.21089%	7.88	0.19442%	7.88	0.08714%	7.15	0.08209%	7.11	0.10061%	7.04	0.07977%	7.23	0.92	0.94	0.79
SINE/tRNA_10	0.03805%	6.91	0.03586%	7.05	0.03379%	6.94	0.03411%	6.95	0.04117%	6.92	0.03257%	6.83	0.94	1.01	0.79
SINE/tRNA_100	0.00203%	11.10	0.00173%	12.61	0.00152%	12.71	0.00132%	10.57	0.00125%	13.89	0.00100%	13.77	0.85	0.87	0.80
SINE/tRNA_101	0.00202%	15.33	0.00202%	12.77	0.00308%	10.75	0.00250%	11.04	0.00115%	19.52	0.00117%	16.32	1.00	0.81	1.02
SINE/tRNA_102	0.00189%	18.04	0.00194%	19.56	0.00137%	16.06	0.00147%	13.2	0.00128%	18.41	0.00114%	16.27	1.03	1.07	0.89
SINE/tRNA_103	0.00181%	18.66	0.00177%	18.74	0.00082%	18.83	0.00090%	18.04	0.00099%	18.75	0.00103%	19.28	0.98	1.11	1.03
SINE/tRNA_104	0.00039%	17.03	0.00044%	23.68	0.00014%	6.11	0.00014%	5.93	0.00011%	19.03	0.00010%	15.06	1.13	1.01	0.89
SINE/tRNA_105	0.00019%	4.02	0.00020%	3.11	0.00018%	2.92	0.00026%	3.4	0.00006%	2.89	0.00009%	8.4	1.03	1.47	1.41
SINE/tRNA_11	0.03779%	12.02	0.03624%	11.83	0.02678%	10.85	0.02675%	10.67	0.02988%	10.49	0.02631%	10.65	0.96	1.00	0.88
SINE/tRNA_12	0.03710%	12.56	0.03502%	12.68	0.02731%	11.08	0.02721%	11.31	0.02675%	11.01	0.02344%	11.15	0.94	1.00	0.88

SINE/tRNA_13	0.03662%	8.92	0.03347%	9.08	0.03153%	8.11	0.03090%	7.89	0.03588%	7.94	0.03034%	7.81	0.91	0.98	0.85
SINE/tRNA_14	0.03611%	8.37	0.03310%	8.39	0.03907%	8.04	0.03856%	8.25	0.04672%	8.01	0.03836%	8.03	0.92	0.99	0.82
SINE/tRNA_15	0.03419%	7.58	0.03222%	7.61	0.02850%	5.73	0.02833%	5.61	0.03242%	5.97	0.02591%	5.91	0.94	0.99	0.80
SINE/tRNA_16	0.03400%	5.07	0.03348%	5.02	0.05212%	4.97	0.04973%	4.9	0.05871%	4.86	0.04856%	5.11	0.98	0.95	0.83
SINE/tRNA_17	0.03303%	12.75	0.03422%	12.88	0.03087%	12.44	0.02852%	12.45	0.03240%	12.48	0.03032%	12.47	1.04	0.92	0.94
SINE/tRNA_18	0.03130%	11.68	0.02875%	11.62	0.03710%	10.35	0.03618%	10.44	0.04199%	10.51	0.03483%	10.57	0.92	0.98	0.83
SINE/tRNA_19	0.02740%	12.23	0.02544%	12.09	0.02687%	11.99	0.02493%	12.08	0.02785%	11.51	0.02290%	11.69	0.93	0.93	0.82
SINE/tRNA_2	0.14823%	11.00	0.14464%	11.42	0.12927%	9.48	0.12304%	9.6	0.14349%	9.11	0.12020%	9.49	0.98	0.95	0.84
SINE/tRNA_20	0.02650%	8.52	0.02600%	8.57	0.03765%	8.47	0.03592%	8.45	0.04255%	8.35	0.03823%	8.6	0.98	0.95	0.90
SINE/tRNA_21	0.02137%	14.65	0.02173%	16.32	0.02154%	13.07	0.02061%	12.92	0.01087%	17.03	0.01606%	15.69	1.02	0.96	1.48
SINE/tRNA_22	0.01974%	11.24	0.01926%	11.34	0.01494%	10.66	0.01569%	10.73	0.01534%	11.12	0.01522%	11.13	0.98	1.05	0.99
SINE/tRNA_23	0.01875%	12.99	0.01707%	13.26	0.01332%	12.43	0.01326%	11.92	0.01077%	14.88	0.01071%	13.39	0.91	1.00	0.99
SINE/tRNA_24	0.01450%	10.09	0.01347%	9.76	0.01366%	9.67	0.01344%	9.87	0.01518%	10.17	0.01244%	10.01	0.93	0.98	0.82
SINE/tRNA_25	0.01335%	9.57	0.01241%	9.35	0.01206%	7.91	0.01143%	7.8	0.01312%	7.68	0.01165%	7.96	0.93	0.95	0.89
SINE/tRNA_26	0.01331%	13.73	0.01200%	13.52	0.01657%	12.93	0.01657%	13.1	0.01802%	12.99	0.01540%	13.07	0.90	1.00	0.85
SINE/tRNA_27	0.01281%	14.69	0.01368%	15.09	0.01274%	13.25	0.01356%	13.31	0.01231%	13.35	0.01178%	13.37	1.07	1.06	0.96
SINE/tRNA_28	0.01247%	10.47	0.01190%	10.98	0.01044%	9.32	0.01043%	9.06	0.01127%	8.64	0.01010%	9.29	0.95	1.00	0.90
SINE/tRNA_29	0.01228%	15.77	0.01174%	15.68	0.01103%	14.85	0.01057%	15.02	0.01245%	14.88	0.01076%	15.1	0.96	0.96	0.86
SINE/tRNA_3	0.09709%	7.12	0.09415%	7.19	0.09420%	6.54	0.09286%	6.54	0.11027%	6.27	0.09220%	6.44	0.97	0.99	0.84
SINE/tRNA_30	0.01133%	18.46	0.01009%	18.13	0.00812%	17.27	0.00812%	18.35	0.00768%	20.66	0.00726%	19.44	0.89	1.00	0.95
SINE/tRNA_31	0.01121%	16.12	0.01120%	16.11	0.00889%	14.33	0.00933%	14.99	0.00919%	15.37	0.00867%	15.07	1.00	1.05	0.94
SINE/tRNA_32	0.01119%	13.14	0.01010%	13.05	0.01082%	12.31	0.01070%	11.55	0.01192%	11.96	0.01077%	11.96	0.90	0.99	0.90
SINE/tRNA_33	0.01119%	12.20	0.01020%	13.14	0.00828%	13.56	0.00749%	13.58	0.00647%	15.96	0.00716%	15.65	0.91	0.90	1.11
SINE/tRNA_34	0.01085%	15.87	0.01023%	15.85	0.00844%	15.1	0.00804%	14.96	0.00912%	14.84	0.00826%	14.49	0.94	0.95	0.91
SINE/tRNA_35	0.01002%	15.42	0.00893%	16.55	0.00765%	13.86	0.00740%	13.34	0.00566%	18.87	0.00550%	17.74	0.89	0.97	0.97
SINE/tRNA_36	0.00948%	9.63	0.00926%	9.36	0.00974%	7.85	0.00927%	7.54	0.01143%	7.62	0.00938%	7.73	0.98	0.95	0.82
SINE/tRNA_37	0.00912%	12.77	0.00893%	12.60	0.00820%	11.77	0.00759%	11.15	0.00868%	11.73	0.00717%	11.89	0.98	0.93	0.83
SINE/tRNA_38	0.00896%	15.35	0.00805%	15.48	0.01126%	10.15	0.01010%	9.78	0.01113%	11.04	0.00928%	10.73	0.90	0.90	0.83
SINE/tRNA_39	0.00800%	15.64	0.00712%	16.16	0.00470%	17.86	0.00408%	16.74	0.00463%	16.3	0.00365%	17.21	0.89	0.87	0.79
SINE/tRNA_4	0.05557%	7.72	0.05131%	7.74	0.05504%	7.84	0.05530%	7.77	0.06308%	7.93	0.05328%	7.91	0.92	1.00	0.84
SINE/tRNA_40	0.00794%	17.11	0.00732%	17.70	0.00483%	15.21	0.00453%	16.09	0.00362%	18.28	0.00378%	18.36	0.92	0.94	1.04

SINE/tRNA_41	0.00785%	11.85	0.00793%	11.83	0.00945%	10.18	0.00907%	9.74	0.00958%	9.43	0.00846%	9.36	1.01	0.96	0.88
SINE/tRNA_42	0.00765%	12.98	0.00758%	13.33	0.00494%	11.34	0.00538%	11.47	0.00431%	13.6	0.00448%	12.62	0.99	1.09	1.04
SINE/tRNA_43	0.00760%	15.35	0.00739%	15.94	0.00847%	11.85	0.00793%	11.66	0.00827%	12.29	0.00763%	12.76	0.97	0.94	0.92
SINE/tRNA_44	0.00758%	13.94	0.00819%	15.54	0.00716%	15	0.00790%	14.99	0.00409%	19.2	0.00581%	17.66	1.08	1.10	1.42
SINE/tRNA_45	0.00737%	11.23	0.00701%	10.25	0.00578%	6.12	0.00471%	8.34	0.00235%	17.53	0.00334%	11.5	0.95	0.82	1.42
SINE/tRNA_46	0.00733%	13.95	0.00651%	13.52	0.00502%	11.63	0.00483%	12.33	0.00561%	11.9	0.00475%	12.14	0.89	0.96	0.85
SINE/tRNA_47	0.00713%	7.31	0.00670%	8.07	0.00675%	7.98	0.00696%	8.44	0.00556%	9.56	0.00644%	8.48	0.94	1.03	1.16
SINE/tRNA_48	0.00703%	13.92	0.00676%	14.02	0.00715%	12.74	0.00712%	11.71	0.00707%	11.78	0.00671%	12.07	0.96	1.00	0.95
SINE/tRNA_49	0.00699%	12.21	0.00637%	13.42	0.00489%	12.32	0.00510%	10.89	0.00457%	15.13	0.00433%	13.66	0.91	1.04	0.95
SINE/tRNA_5	0.05282%	10.95	0.04914%	10.79	0.02861%	10.82	0.02718%	10.83	0.03085%	10.81	0.02633%	10.57	0.93	0.95	0.85
SINE/tRNA_50	0.00683%	18.55	0.00659%	18.21	0.00644%	15.25	0.00669%	15.23	0.00732%	17.96	0.00568%	16.91	0.97	1.04	0.78
SINE/tRNA_51	0.00674%	14.00	0.00613%	14.39	0.00610%	12.38	0.00514%	12.43	0.00338%	15.47	0.00394%	14.73	0.91	0.84	1.17
SINE/tRNA_52	0.00652%	21.04	0.00723%	22.95	0.00484%	20.76	0.00503%	20.44	0.00428%	24.23	0.00413%	23.11	1.11	1.04	0.97
SINE/tRNA_53	0.00640%	12.22	0.00578%	12.00	0.00426%	12.01	0.00411%	11.88	0.00455%	11.25	0.00363%	12.14	0.90	0.96	0.80
SINE/tRNA_54	0.00630%	6.73	0.00831%	5.63	0.00606%	5.63	0.00690%	5.99	0.00530%	5.78	0.00635%	6.22	1.32	1.14	1.20
SINE/tRNA_55	0.00614%	13.32	0.00545%	13.74	0.00463%	14.17	0.00492%	13.04	0.00471%	13.52	0.00390%	14.26	0.89	1.06	0.83
SINE/tRNA_56	0.00608%	7.68	0.00573%	8.12	0.00568%	6	0.00603%	6.26	0.00236%	13.36	0.00332%	8.82	0.94	1.06	1.41
SINE/tRNA_57	0.00600%	12.85	0.00540%	14.56	0.00430%	12.63	0.00460%	11.76	0.00299%	15.5	0.00347%	14.67	0.90	1.07	1.16
SINE/tRNA_58	0.00596%	11.53	0.00579%	12.17	0.00659%	7.73	0.00638%	9.41	0.00574%	8.91	0.00500%	9.76	0.97	0.97	0.87
SINE/tRNA_59	0.00563%	14.52	0.00564%	14.53	0.00561%	12.32	0.00557%	12.62	0.00443%	14.85	0.00540%	13.68	1.00	0.99	1.22
SINE/tRNA_6	0.04417%	11.69	0.04316%	11.74	0.04201%	11.08	0.04032%	11.13	0.04633%	11	0.04264%	11.13	0.98	0.96	0.92
SINE/tRNA_60	0.00558%	15.62	0.00475%	14.96	0.00410%	12.06	0.00401%	10.76	0.00421%	12.61	0.00351%	12.22	0.85	0.98	0.83
SINE/tRNA_61	0.00546%	21.44	0.00092%	14.78	0.00190%	9.74	0.00159%	9.95	0.00091%	19.03	0.00090%	16.06	0.17	0.84	0.98
SINE/tRNA_62	0.00542%	17.09	0.00470%	17.73	0.00342%	17.56	0.00309%	15.82	0.00354%	16.53	0.00316%	17.85	0.87	0.91	0.89
SINE/tRNA_63	0.00538%	11.78	0.00542%	12.45	0.00376%	11.79	0.00375%	12.13	0.00398%	13.13	0.00366%	12.02	1.01	1.00	0.92
SINE/tRNA_64	0.00534%	14.53	0.00490%	14.73	0.00335%	15.58	0.00279%	14.13	0.00346%	14.33	0.00277%	14.18	0.92	0.83	0.80
SINE/tRNA_65	0.00526%	15.69	0.00483%	16.10	0.00475%	16.17	0.00466%	15.17	0.00388%	18.78	0.00385%	17.72	0.92	0.98	0.99
SINE/tRNA_66	0.00521%	14.00	0.00486%	13.58	0.00383%	13.41	0.00349%	13.62	0.00404%	13.34	0.00359%	13.72	0.93	0.91	0.89
SINE/tRNA_67	0.00519%	10.76	0.00522%	10.95	0.00486%	9.84	0.00503%	9.39	0.00409%	9.7	0.00465%	10.32	1.01	1.03	1.14
SINE/tRNA_68	0.00518%	14.06	0.00492%	15.36	0.02787%	9.29	0.02664%	9.06	0.03128%	8.96	0.02677%	9.34	0.95	0.96	0.86
SINE/tRNA_69	0.00512%	19.43	0.00552%	20.76	0.00410%	18.52	0.00470%	18	0.00369%	20.02	0.00372%	18.84	1.08	1.15	1.01

SINE/tRNA_7	0.04386%	10.01	0.04008%	9.85	0.02748%	9.5	0.02670%	9.69	0.03184%	9.41	0.02632%	9.37	0.91	0.97	0.83
SINE/tRNA_70	0.00488%	15.91	0.00375%	15.98	0.00528%	11.33	0.00532%	11.35	0.00570%	11.84	0.00535%	12.09	0.77	1.01	0.94
SINE/tRNA_71	0.00487%	14.30	0.00460%	14.57	0.00457%	14.11	0.00462%	13.93	0.00510%	14.62	0.00462%	14.9	0.94	1.01	0.90
SINE/tRNA_72	0.00467%	16.38	0.00537%	17.17	0.00360%	14.41	0.00361%	14.28	0.00399%	15.41	0.00380%	14.91	1.15	1.00	0.95
SINE/tRNA_73	0.00454%	8.80	0.00386%	9.27	0.00480%	5.91	0.00351%	7.45	0.00400%	7.39	0.00907%	5.44	0.85	0.73	2.27
SINE/tRNA_74	0.00444%	16.39	0.00482%	16.30	0.00380%	13.68	0.00385%	13.87	0.00433%	14.23	0.00367%	13.77	1.09	1.01	0.85
SINE/tRNA_75	0.00439%	13.55	0.00396%	13.76	0.00426%	12.12	0.00425%	11.98	0.00449%	12.26	0.00374%	12.57	0.90	1.00	0.83
SINE/tRNA_76	0.00439%	12.52	0.00458%	14.43	0.00633%	7.34	0.00524%	8.52	0.00244%	16.95	0.00275%	15.28	1.04	0.83	1.12
SINE/tRNA_77	0.00411%	18.05	0.00354%	18.08	0.00337%	15.38	0.00324%	15.39	0.00356%	16.06	0.00311%	14.89	0.86	0.96	0.87
SINE/tRNA_78	0.00404%	15.58	0.00388%	15.68	0.00427%	11.04	0.00409%	11.33	0.00459%	11.45	0.00403%	11.06	0.96	0.96	0.88
SINE/tRNA_79	0.00369%	16.87	0.00266%	17.46	0.00174%	13.86	0.00174%	14.92	0.00120%	19.25	0.00122%	17.31	0.72	1.00	1.02
SINE/tRNA_8	0.04133%	10.95	0.03986%	11.41	0.04218%	9.75	0.04363%	9.87	0.04896%	9.43	0.04139%	9.82	0.96	1.03	0.85
SINE/tRNA_80	0.00366%	16.75	0.00339%	16.85	0.00183%	17.74	0.00209%	17.17	0.00207%	17.89	0.00193%	17.48	0.92	1.14	0.94
SINE/tRNA_81	0.00365%	16.61	0.00357%	17.01	0.00264%	15.73	0.00221%	15.82	0.00273%	15.09	0.00219%	15.57	0.98	0.84	0.80
SINE/tRNA_82	0.00355%	6.42	0.00307%	6.84	0.00303%	6.34	0.00307%	6.07	0.00109%	10.49	0.00149%	7.35	0.86	1.02	1.37
SINE/tRNA_83	0.00348%	10.43	0.00339%	12.20	0.00252%	10.62	0.00281%	11.75	0.00251%	12.08	0.00238%	12.81	0.97	1.11	0.95
SINE/tRNA_84	0.00346%	20.11	0.00300%	19.39	0.00200%	18.49	0.00216%	18.23	0.00224%	17.98	0.00184%	18.55	0.87	1.08	0.82
SINE/tRNA_85	0.00341%	18.76	0.00323%	18.21	0.00300%	15.06	0.00260%	14.37	0.00207%	19.65	0.00180%	19.93	0.95	0.87	0.87
SINE/tRNA_86	0.00334%	20.85	0.00306%	22.00	0.00212%	19.93	0.00192%	20.41	0.00220%	20.86	0.00194%	20.67	0.92	0.91	0.88
SINE/tRNA_87	0.00332%	18.50	0.00279%	17.47	0.00187%	17.91	0.00197%	18.84	0.00218%	17.54	0.00209%	17.85	0.84	1.06	0.96
SINE/tRNA_88	0.00332%	14.60	0.00308%	15.66	0.00257%	11.64	0.00241%	11.64	0.00153%	16.99	0.00207%	14.53	0.93	0.94	1.35
SINE/tRNA_89	0.00317%	11.90	0.00272%	12.21	0.00246%	11.56	0.00223%	11.75	0.00177%	13.72	0.00194%	12.81	0.86	0.90	1.09
SINE/tRNA_9	0.03868%	8.06	0.03561%	7.85	0.02996%	7.91	0.02981%	8.01	0.03501%	7.83	0.02717%	7.98	0.92	0.99	0.78
SINE/tRNA_90	0.00299%	16.29	0.00279%	16.81	0.00249%	13.97	0.00238%	13.27	0.00244%	13.48	0.00222%	14.49	0.93	0.95	0.91
SINE/tRNA_91	0.00292%	11.43	0.00324%	10.24	0.00323%	8.95	0.00304%	8.68	0.00196%	9.93	0.00337%	8.07	1.11	0.94	1.72
SINE/tRNA_92	0.00289%	14.23	0.00267%	15.74	0.00180%	15.1	0.00216%	12.85	0.00179%	16.9	0.00160%	16.94	0.92	1.20	0.89
SINE/tRNA_93	0.00269%	19.13	0.00222%	19.49	0.00154%	16.49	0.00147%	17.37	0.00162%	16.98	0.00148%	17.93	0.83	0.95	0.91
SINE/tRNA_94	0.00268%	16.97	0.00244%	16.52	0.00154%	17.93	0.00155%	15.16	0.00163%	15.52	0.00152%	15.58	0.91	1.00	0.93
SINE/tRNA_95	0.00267%	7.22	0.00228%	8.00	0.00179%	8.52	0.00170%	8.19	0.00114%	10.61	0.00118%	9.26	0.85	0.95	1.04
SINE/tRNA_96	0.00257%	20.60	0.00255%	21.44	0.00188%	17.91	0.00208%	19.5	0.00220%	17.8	0.00157%	18.75	0.99	1.11	0.71
SINE/tRNA_97	0.00248%	12.54	0.00232%	12.75	0.00111%	18.73	0.00204%	8.26	0.00151%	17.46	0.00212%	12.31	0.94	1.85	1.40

SINE/tRNA_98	0.00242%	21.22	0.00198%	21.84	0.00141%	14.01	0.00124%	16.33	0.00128%	19.78	0.00110%	17.95	0.82	0.88	0.86
SINE/tRNA_99	0.00234%	16.32	0.00226%	17.34	0.00134%	10.82	0.00147%	11.04	0.00147%	11.53	0.00144%	11.14	0.96	1.10	0.98
SINE/tRNA-Deu-RTE_1	0.05633%	12.38	0.06058%	12.66	0.05294%	11.35	0.05217%	11.23	0.05173%	11.15	0.05209%	11.3	1.08	0.99	1.01
SINE/tRNA-L2_1	0.03700%	13.67	0.01696%	14.60	0.01530%	13.03	0.01896%	12.2	0.06259%	11.06	0.02050%	12.69	0.46	1.24	0.33
SINE/tRNA-L2_2	0.01569%	16.24	0.01690%	16.88	0.01680%	16.67	0.01676%	16.46	0.01768%	17.08	0.01742%	17.12	1.08	1.00	0.99
SINE/tRNA-L2_3	0.01287%	14.38	0.01277%	14.67	0.01181%	13.76	0.01282%	13.77	0.01259%	13.72	0.01319%	13.78	0.99	1.09	1.05
SINE/tRNA-L2_4	0.00686%	18.31	0.00668%	18.60	0.00815%	16.05	0.01022%	14.4	0.00594%	17.84	0.00964%	15.13	0.97	1.25	1.62
SINE/tRNA-RTE_1	0.15172%	16.12	0.15271%	16.51	0.12208%	14.88	0.11896%	14.94	0.13597%	14.89	0.11357%	15.12	1.01	0.97	0.84
SINE/tRNA-RTE_10	0.00549%	12.39	0.00561%	12.34	0.00598%	11.37	0.00605%	12.67	0.00647%	12.07	0.00632%	12.02	1.02	1.01	0.98
SINE/tRNA-RTE_11	0.00515%	17.42	0.00509%	19.52	0.00439%	15.5	0.00449%	16.61	0.00392%	16.95	0.00522%	15.19	0.99	1.02	1.33
SINE/tRNA-RTE_12	0.00211%	20.85	0.00240%	19.47	0.00209%	15.51	0.00183%	16.62	0.00116%	28.5	0.00140%	22.27	1.14	0.87	1.20
SINE/tRNA-RTE_13	0.00162%	8.56	0.00150%	13.88	0.00138%	9.25	0.00184%	10.91	0.00061%	20.8	0.00099%	15	0.93	1.33	1.64
SINE/tRNA-RTE_2	0.06521%	15.77	0.06900%	15.77	0.05851%	14.49	0.05730%	14.93	0.06224%	14.49	0.05607%	14.66	1.06	0.98	0.90
SINE/tRNA-RTE_3	0.02593%	6.97	0.02756%	6.79	0.02293%	5.66	0.02396%	5.69	0.02359%	5.76	0.02342%	5.68	1.06	1.05	0.99
SINE/tRNA-RTE_4	0.02180%	9.07	0.02165%	9.05	0.01815%	8.58	0.01820%	8.54	0.01945%	8.5	0.01723%	8.89	0.99	1.00	0.89
SINE/tRNA-RTE_5	0.01782%	12.37	0.01773%	12.82	0.02012%	11.16	0.02055%	10.48	0.01614%	14.71	0.01691%	13.22	1.00	1.02	1.05
SINE/tRNA-RTE_6	0.01141%	11.97	0.01172%	11.92	0.01238%	10.7	0.01196%	10.52	0.00997%	12.26	0.00961%	11.81	1.03	0.97	0.96
SINE/tRNA-RTE_7	0.01067%	12.64	0.01130%	12.67	0.00975%	11.59	0.00923%	11.67	0.00957%	11.44	0.00904%	11.73	1.06	0.95	0.94
SINE/tRNA-RTE_8	0.00726%	14.51	0.00694%	14.36	0.00766%	13.53	0.00719%	14.17	0.00697%	15.14	0.00726%	14.69	0.96	0.94	1.04
SINE/tRNA-RTE_9	0.00571%	4.84	0.00516%	5.65	0.00493%	5.79	0.00450%	5.83	0.00218%	6.13	0.00262%	5.77	0.90	0.91	1.20
SINE/tRNA-V_1	0.01345%	14.04	0.01309%	13.96	0.01308%	12.81	0.01193%	12.72	0.01261%	13.01	0.01298%	13.09	0.97	0.91	1.03
Unknown/Unknown_1	0.06244%	13.18	0.06327%	13.40	0.05760%	13.01	0.05625%	12.64	0.06250%	12.6	0.05784%	12.99	1.01	0.98	0.93
Unknown/Unknown_10	0.01003%	14.90	0.01052%	15.09	0.00828%	12.19	0.00840%	12.47	0.00734%	11.95	0.00702%	12.25	1.05	1.01	0.96
Unknown/Unknown_11	0.00951%	18.15	0.01040%	19.55	0.01068%	16.95	0.01034%	16.86	0.00785%	20.96	0.00817%	18.91	1.09	0.97	1.04
Unknown/Unknown_12	0.00770%	20.21	0.00762%	20.70	0.00648%	17.22	0.00532%	17.68	0.00409%	18.25	0.00754%	17.6	0.99	0.82	1.84
Unknown/Unknown_13	0.00682%	5.70	0.00745%	5.64	0.01552%	3.78	0.01324%	3.97	0.00245%	10.62	0.00370%	7.2	1.09	0.85	1.51
Unknown/Unknown_14	0.00680%	18.64	0.00721%	19.32	0.00604%	17.43	0.00563%	17.64	0.00550%	18.04	0.00608%	17.28	1.06	0.93	1.11
Unknown/Unknown_15	0.00560%	13.04	0.00521%	13.03	0.00457%	12.72	0.00382%	12.49	0.00572%	12.65	0.00500%	12.57	0.93	0.84	0.87
Unknown/Unknown_16	0.00462%	16.28	0.00487%	17.90	0.00353%	15.45	0.00348%	16.36	0.00255%	19.19	0.00284%	17.99	1.05	0.98	1.11
Unknown/Unknown_17	0.00347%	6.65	0.00326%	7.83	0.00241%	7.06	0.00275%	7.57	0.00192%	10.07	0.00217%	8.64	0.94	1.14	1.13
Unknown/Unknown_18	0.00347%	11.63	0.00340%	12.90	0.00244%	9.4	0.00296%	7.07	0.00137%	14.09	0.00150%	10.91	0.98	1.21	1.10

Unknown/Unknown_19	0.00321%	7.36	0.00299%	7.93	0.00334%	6.66	0.00284%	7.77	0.00247%	7.27	0.00295%	7.21	0.93	0.85	1.20
Unknown/Unknown_2	0.05050%	14.63	0.05219%	15.63	0.04101%	14.67	0.04291%	14.68	0.04799%	14.79	0.04312%	15.24	1.03	1.05	0.90
Unknown/Unknown_20	0.00296%	14.69	0.00284%	14.87	0.00694%	10.55	0.00661%	10.22	0.00839%	10.52	0.00711%	10.58	0.96	0.95	0.85
Unknown/Unknown_21	0.00271%	11.59	0.00270%	11.49	0.00285%	10.71	0.00271%	9.83	0.00258%	11.56	0.00274%	11.57	1.00	0.95	1.06
Unknown/Unknown_22	0.00234%	10.44	0.00244%	11.43	0.00215%	9.4	0.00218%	11.07	0.00225%	10.63	0.00248%	9.97	1.04	1.01	1.10
Unknown/Unknown_23	0.00188%	10.81	0.00172%	11.19	0.00170%	8.86	0.00188%	8.4	0.00201%	8.76	0.00188%	10.57	0.92	1.11	0.94
Unknown/Unknown_24	0.00165%	14.09	0.00154%	15.37	0.00143%	11.47	0.00147%	12.61	0.00136%	12.01	0.00130%	11.56	0.93	1.03	0.96
Unknown/Unknown_3	0.03233%	25.76	0.03203%	26.90	0.02584%	24.26	0.02523%	24.86	0.02835%	24.77	0.02480%	25.6	0.99	0.98	0.87
Unknown/Unknown_4	0.03166%	13.72	0.03365%	14.14	0.02876%	12.36	0.02722%	11.69	0.02836%	11.8	0.02830%	11.8	1.06	0.95	1.00
Unknown/Unknown_5	0.02878%	14.86	0.03030%	15.11	0.02581%	12.87	0.02691%	13.38	0.02466%	13.52	0.02631%	12.94	1.05	1.04	1.07
Unknown/Unknown_6	0.02098%	14.58	0.01871%	14.67	0.01895%	13.12	0.01807%	13.28	0.01990%	13.49	0.02009%	13.18	0.89	0.95	1.01
Unknown/Unknown_7	0.01961%	10.09	0.01593%	10.67	0.01246%	9.09	0.01147%	8.68	0.02646%	7.13	0.01407%	8.52	0.81	0.92	0.53
Unknown/Unknown_8	0.01186%	18.91	0.01163%	18.63	0.01048%	17.49	0.01072%	18.28	0.01124%	17.61	0.01127%	17.71	0.98	1.02	1.00
Unknown/Unknown_9	0.01026%	9.31	0.01141%	9.10	0.00938%	7.73	0.01097%	7.24	0.00813%	9	0.00921%	8.27	1.11	1.17	1.13
TEs total	47.28822%		47.37959%		44.51615%		43.69062%		45.78976%		42.65377%				
H3	0.00472%	1.12	0.00344%	1.02	0.00454%	0.59	0.00660%	0.72	0.01299%	0.67	0.00693%	0.84	0.73	1.45	0.53
18S rDNA	0.19480%	0.17	0.19597%	0.18	0.11444%	0.19	0.08331%	0.24	0.11028%	0.73	0.10476%	0.29	1.01	0.73	0.95
28S rDNA	0.39294%	0.19	0.40015%	0.18	0.20789%	0.19	0.14775%	0.25	0.20450%	1.12	0.19562%	0.31	1.02	0.71	0.96
5.8S rDNA	0.01423%	0.16	0.01416%	0.13	0.00853%	0.09	0.00647%	0.15	0.00781%	0.14	0.00802%	0.26	1.00	0.76	1.03
5S rDNA	0.00353%	5.98	0.00369%	6.58	0.00493%	4.97	0.00406%	5.48	0.00161%	7.31	0.00408%	4.82	1.05	0.82	2.54
U1 snDNA	0.00062%	11.58	0.00046%	11.26	0.00047%	11.46	0.00027%	10.8	0.00015%	11.17	0.00045%	11.79	0.74	0.58	2.97
*U2 snDNA	0.00125%	2.98	0.00229%	2.79	0.00115%	1.99	0.00110%	2.63	0.00127%	6.11	0.00032%	6.13	1.83	0.96	0.25
U6 snDNA	0.00085%	3.40	0.00115%	2.40	0.00099%	4.53	0.00061%	5.05	0.00077%	4.36	0.00052%	4.43	1.35	0.62	0.67
MFs total	0.61295%		0.62131%		0.34294%		0.25018%		0.33938%		0.32070%				
*Afl_SPSat01-179	1.73151%	4.09	1.56725%	4.07	1.81829%	4.46	1.52489%	4.38	2.45354%	4.31	4.37468%	4.26	0.91	0.84	1.78
Afl_SPSat02-391	0.68864%	2.34	0.60298%	2.32	0.61503%	2.47	0.58478%	2.42	0.64083%	3.11	0.72910%	2.75	0.88	0.95	1.14
Afl_SPSat03-17	0.54214%	24.46	0.51374%	24.82	0.39445%	24.33	0.40855%	24.24	0.40465%	24.3	0.42547%	24.3	0.95	1.04	1.05
Afl_SPSat04-161	0.51584%	3.58	0.40285%	3.50	0.86140%	3.06	0.94398%	3.02	0.44307%	3.5	0.64477%	3.87	0.78	1.10	1.46
Afl_SPSat05-437	0.18719%	2.16	0.17848%	2.20	0.12365%	2.7	0.11519%	2.21	0.19103%	2.36	0.18531%	2.16	0.95	0.93	0.97
Afl_SPSat06-265	0.10558%	3.68	0.09728%	3.52	0.22207%	3.31	0.19478%	3.19	0.12105%	3.59	0.17828%	3.76	0.92	0.88	1.47

Afl_SPSat07-36	0.07981%	3.26	0.06769%	3.11	0.01452%	8.27	0.00795%	10.84	0.04936%	7.03	0.17389%	3.59	0.85	0.55	3.52
Afl_SPSat08-184	0.07437%	5.62	0.07328%	5.72	0.08846%	4.64	0.09057%	4.62	0.08261%	4.88	0.08222%	4.9	0.99	1.02	1.00
Afl_SPSat09-187	0.06914%	3.17	0.07014%	3.22	0.07880%	3.11	0.08938%	3.09	0.07904%	3.06	0.09037%	3.24	1.01	1.13	1.14
Afl_SPSat10-297	0.06888%	7.57	0.06955%	7.95	0.04479%	8.21	0.03623%	9.09	0.03736%	7.12	0.06473%	8.02	1.01	0.81	1.73
Afl_SPSat11-407	0.06437%	18.12	0.02512%	22.84	0.02827%	21.78	0.02740%	21.38	0.13753%	9.43	0.02602%	21.59	0.39	0.97	0.19
Afl_SPSat12-237	0.03959%	8.05	0.02447%	8.57	0.08622%	8.07	0.13832%	7.75	0.03910%	9.16	0.03786%	8.7	0.62	1.60	0.97
Afl_SPSat13-177	0.02836%	8.06	0.02908%	8.04	0.02065%	7.19	0.02183%	7.29	0.02318%	7.46	0.01958%	7.51	1.03	1.06	0.84
Afl_SPSat14-110	0.02162%	20.72	0.02206%	21.35	0.02096%	17.43	0.02848%	15.48	0.02174%	16.72	0.02423%	16.53	1.02	1.36	1.11
Afl_SPSat15-299 / SF1	0.01881%	12.09	0.01864%	11.60	0.02417%	12.15	0.02292%	10.58	0.02175%	15.58	0.03029%	14.77	0.99	0.95	1.39
Afl_SPSat16-298 / SF1	0.01833%	10.56	0.01695%	10.58	0.03315%	7.5	0.02399%	9.36	0.03367%	16.29	0.03989%	14.27	0.92	0.72	1.19
Afl_SPSat17-231	0.01806%	15.98	0.01621%	17.43	0.01530%	13.94	0.01781%	14.42	0.01435%	14.38	0.01952%	11.71	0.90	1.16	1.36
Afl_SPSat18-7	0.01609%	3.36	0.01055%	3.27	0.11410%	3.1	0.12217%	3.09	0.04836%	3.12	0.03540%	3.29	0.66	1.07	0.73
Afl_SPSat19-17	0.01581%	11.59	0.01249%	11.81	0.01448%	11.32	0.01961%	10.07	0.01451%	10.66	0.01648%	11.14	0.79	1.35	1.14
Afl_SPSat20-233 / SF2	0.01510%	5.72	0.01394%	5.84	0.03657%	4.47	0.03925%	4.74	0.02148%	5.13	0.01871%	4.94	0.92	1.07	0.87
Afl_SPSat21-260	0.01458%	6.68	0.01460%	6.33	0.01459%	5.8	0.01566%	5.65	0.01621%	5.15	0.01442%	5.45	1.00	1.07	0.89
Afl_SPSat22-135	0.01455%	16.36	0.01364%	16.45	0.01692%	16.25	0.01865%	16.02	0.00267%	17.18	0.01018%	15.79	0.94	1.10	3.82
Afl_SPSat23-286	0.01357%	5.62	0.01227%	5.80	0.02017%	5.12	0.01883%	5.41	0.00960%	5.57	0.02141%	5.18	0.90	0.93	2.23
Afl_SPSat24-308	0.01354%	12.19	0.01310%	13.26	0.02479%	8.55	0.02128%	8.4	0.01398%	9.56	0.01772%	9.48	0.97	0.86	1.27
Afl_SPSat25-40	0.01343%	9.02	0.01077%	9.07	0.01476%	8.62	0.01866%	8.92	0.01976%	8.97	0.01459%	9.02	0.80	1.26	0.74
Afl_SPSat26-296 / SF1	0.01268%	8.99	0.00758%	9.62	0.01050%	9.69	0.00917%	10.19	0.02135%	7.97	0.02073%	7.87	0.60	0.87	0.97
Afl_SPSat27-609	0.01248%	2.44	0.00899%	2.84	0.00767%	2.84	0.00604%	3.09	0.00840%	2.94	0.00674%	3.01	0.72	0.79	0.80
Afl_SPSat28-247 / SF2	0.00975%	4.63	0.00854%	4.90	0.01166%	4.3	0.01069%	4.78	0.01921%	4.06	0.01719%	4.22	0.88	0.92	0.90
Afl_SPSat29-616	0.00948%	7.69	0.00866%	8.75	0.00726%	11.09	0.01004%	11.29	0.00596%	10.94	0.00860%	11.08	0.91	1.38	1.44
Afl_SPSat30-197	0.00852%	12.09	0.00838%	11.70	0.00851%	9.3	0.00839%	9.3	0.00593%	10.96	0.00503%	12.6	0.98	0.99	0.85
Afl_SPSat31-226	0.00698%	7.98	0.00659%	8.73	0.00997%	8.67	0.00992%	6.28	0.00450%	9.34	0.00853%	10.08	0.94	0.99	1.89
Afl_SPSat32-429	0.00646%	12.90	0.00769%	10.72	0.00403%	16.91	0.00638%	10	0.00427%	13.45	0.00478%	13.44	1.19	1.58	1.12
Afl_SPSat33-295	0.00640%	20.00	0.00630%	20.51	0.00489%	23.69	0.00429%	22.64	0.00430%	18.58	0.00613%	13.51	0.99	0.88	1.42
Afl_SPSat34-30	0.00612%	13.94	0.00422%	17.16	0.00865%	12.48	0.01221%	11.17	0.02149%	10.98	0.01590%	11.66	0.69	1.41	0.74
Afl_SPSat35-362	0.00585%	0.15	0.00304%	0.20	0.00749%	0.13	0.00610%	0.13	0.00287%	0.19	0.00248%	0.2	0.52	0.81	0.86
Afl_SPSat36-41	0.00501%	10.12	0.00538%	10.30	0.00433%	9.26	0.00490%	9.48	0.00449%	9.66	0.00490%	9.65	1.08	1.13	1.09
Afl_SPSat37-134	0.00488%	6.16	0.00380%	6.17	0.00888%	4.71	0.01103%	4.18	0.00702%	5.62	0.01265%	7.34	0.78	1.24	1.80

Afl_SPSat38-377	0.00483%	6.86	0.00439%	8.41	0.00489%	11.87	0.00426%	12.51	0.00454%	6.84	0.00798%	6.63	0.91	0.87	1.76
Afl_SPSat39-832	0.00455%	3.09	0.00690%	2.22	0.00710%	2.66	0.00656%	2.43	0.00862%	2.4	0.00429%	2.86	1.52	0.92	0.50
Afl_SPSat40-218	0.00431%	8.57	0.00452%	9.15	0.00517%	9.62	0.00513%	9.1	0.00566%	8.93	0.00568%	9.47	1.05	0.99	1.00
Afl_SPSat41-186	0.00376%	15.46	0.00603%	11.68	0.01089%	8.49	0.00652%	9.67	0.00465%	12.04	0.00454%	11.11	1.61	0.60	0.98
Afl_SPSat42-75	0.00374%	15.26	0.00434%	15.73	0.00318%	13.32	0.00314%	13.57	0.00247%	13.9	0.00242%	13.84	1.16	0.99	0.98
Afl_SPSat43-131	0.00329%	7.45	0.00410%	7.11	0.00652%	6.96	0.00573%	6.6	0.00165%	7.15	0.00587%	6.85	1.25	0.88	3.57
Afl_SPSat44-254	0.00297%	5.62	0.00277%	6.70	0.00888%	4.08	0.01036%	4.94	0.00360%	5.13	0.00489%	5.2	0.93	1.17	1.36
Afl_SPSat45-414	0.00288%	14.31	0.00439%	12.61	0.00243%	15.86	0.00198%	15	0.00251%	13.03	0.00291%	11.45	1.52	0.82	1.16
Afl_SPSat46-153	0.00285%	7.49	0.00272%	7.87	0.00226%	7.81	0.00313%	5.59	0.00394%	7.39	0.00194%	9.4	0.95	1.38	0.49
Afl_SPSat47-75	0.00224%	5.63	0.00221%	5.88	0.00436%	5.4	0.00417%	5.87	0.00175%	5.34	0.00570%	5.54	0.99	0.96	3.25
Afl_SPSat48-167	0.00194%	7.03	0.00248%	6.63	0.00426%	6.12	0.00358%	6.32	0.00318%	6.05	0.00409%	6.1	1.27	0.84	1.28
Afl_SPSat49-138	0.00133%	6.42	0.00161%	6.22	0.00302%	6.45	0.00307%	6.15	0.00088%	6.22	0.00337%	6.25	1.21	1.02	3.83
Afl_SPSat50-102	0.00104%	10.36	0.00097%	11.17	0.00228%	8.8	0.00219%	7.72	0.00145%	9.59	0.00120%	9.01	0.93	0.96	0.83
Afl_SPSat51-30	0.00089%	8.99	0.00083%	9.23	0.00110%	9.3	0.00104%	8.81	0.00032%	9.83	0.00164%	8.78	0.93	0.95	5.19
*Afl_SPSat52-23	0.00014%	10.02	0.00111%	10.53	0.00030%	9.92	0.00445%	9.73	0.00099%	9.52	0.00571%	10.68	8.03	14.70	5.76
Afl_SPSat53-17	0.00001%	30.79	0.00002%	22.89	0.00011%	22.26	0.00015%	20.64	0.00000%	0	0.00001%	9.54	1.60	1.37	1355.97
New_SatDNA described here															
*Afl_PESat01_7	0.00003%	22.45	0.00001%	32.69	0.18084%	3.23	0.22609%	3.19	0.00001%	6.79	0.00001%	28.19	0.31	1.25	1.78
Afl_PESat02_418	0.07967%	6.51	0.08069%	6.42	0.07384%	5.45	0.07531%	4.91	0.07744%	5.45	0.07395%	5.85	1.01	1.02	0.96
Afl_PESat03_80	0.01023%	16.23	0.01081%	16.09	0.00947%	16.2	0.00981%	15.21	0.00878%	16.39	0.01315%	16.39	1.06	1.04	1.50
Afl_PESat04_254	0.00200%	10.23	0.00181%	12.22	0.00618%	3.77	0.00479%	3.88	0.00379%	4.38	0.00414%	5.05	0.90	0.77	1.09
Afl_PESat05_131	0.00207%	3.15	0.00182%	2.99	0.00503%	1.94	0.00565%	1.78	0.00251%	3.54	0.00705%	2.15	0.88	1.12	2.80
Afl_PESat06_892	0.00464%	2.24	0.00454%	2.56	0.00430%	2.26	0.00438%	2.41	0.00634%	1.88	0.00315%	2.48	0.98	1.02	0.50
Afl_PESat07_205	0.00339%	16.61	0.00307%	16.41	0.00380%	14.47	0.00510%	11.1	0.00364%	14.66	0.00380%	14.12	0.91	1.34	1.04
Afl_ARGSat01_326	0.01061%	22.90	0.00818%	20.48	0.00577%	18.51	0.00570%	16.93	0.00843%	15.38	0.00645%	16.13	0.77	0.99	0.76
*Afl_ARGSat02_72	0.00002%	28.59	0.00004%	24.95	0.00003%	9.91	0.00004%	19.51	0.00002%	10.51	0.01000%	2.69	1.92	1.33	538.12
SatDNA total	4.63697%		4.13665%		5.19644%		5.05268%		5.20739%		7.59271%				
All repeats total	52.53814%		52.13754%		50.05553%		48.99347%		51.33654%		50.56719%				

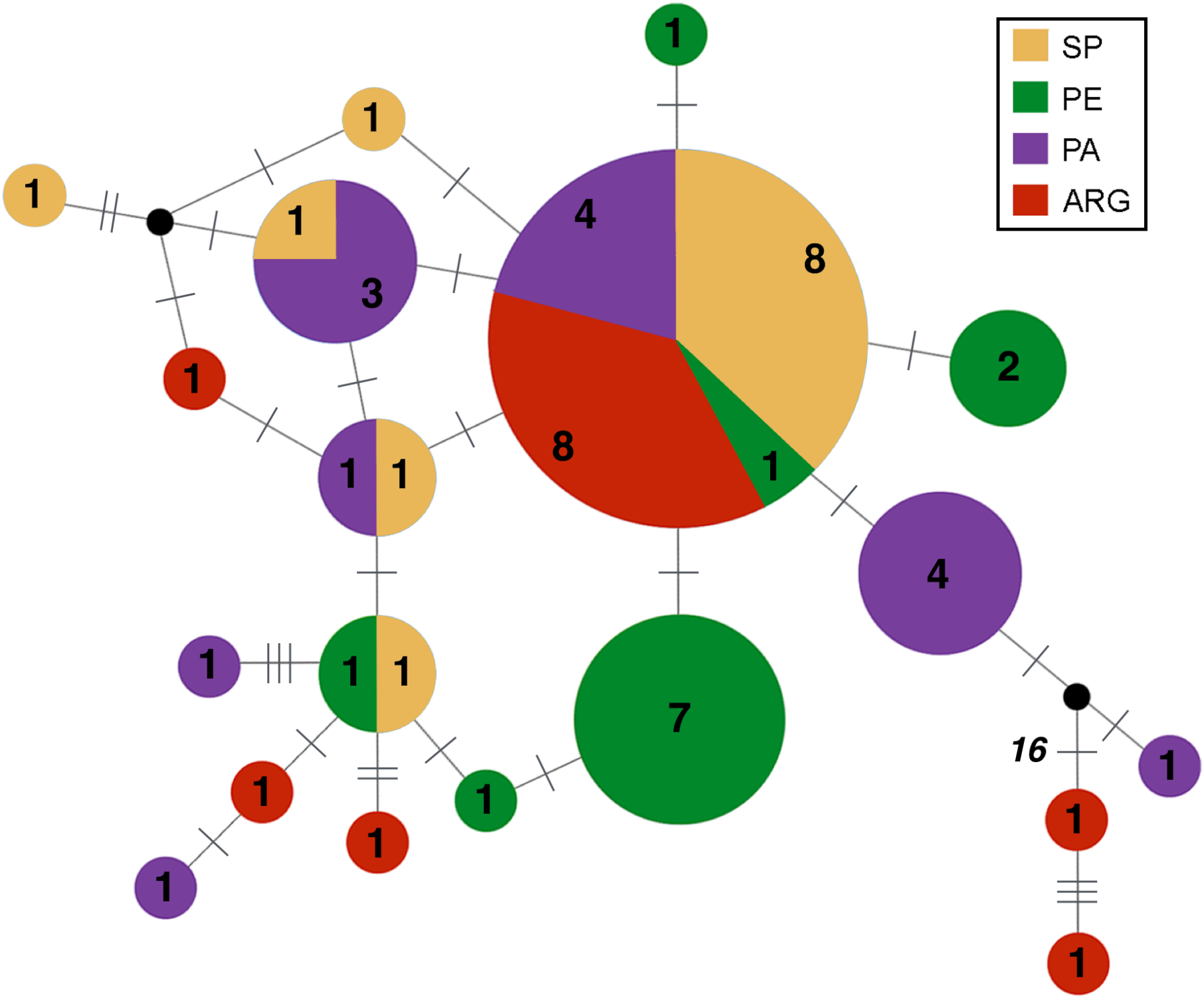
SP
PE
PA
ARG
1
1
1
1
3
4
8
2
1
8
1
1
1
4
1
1
1
7
1
1
1
1
16
1
1
1

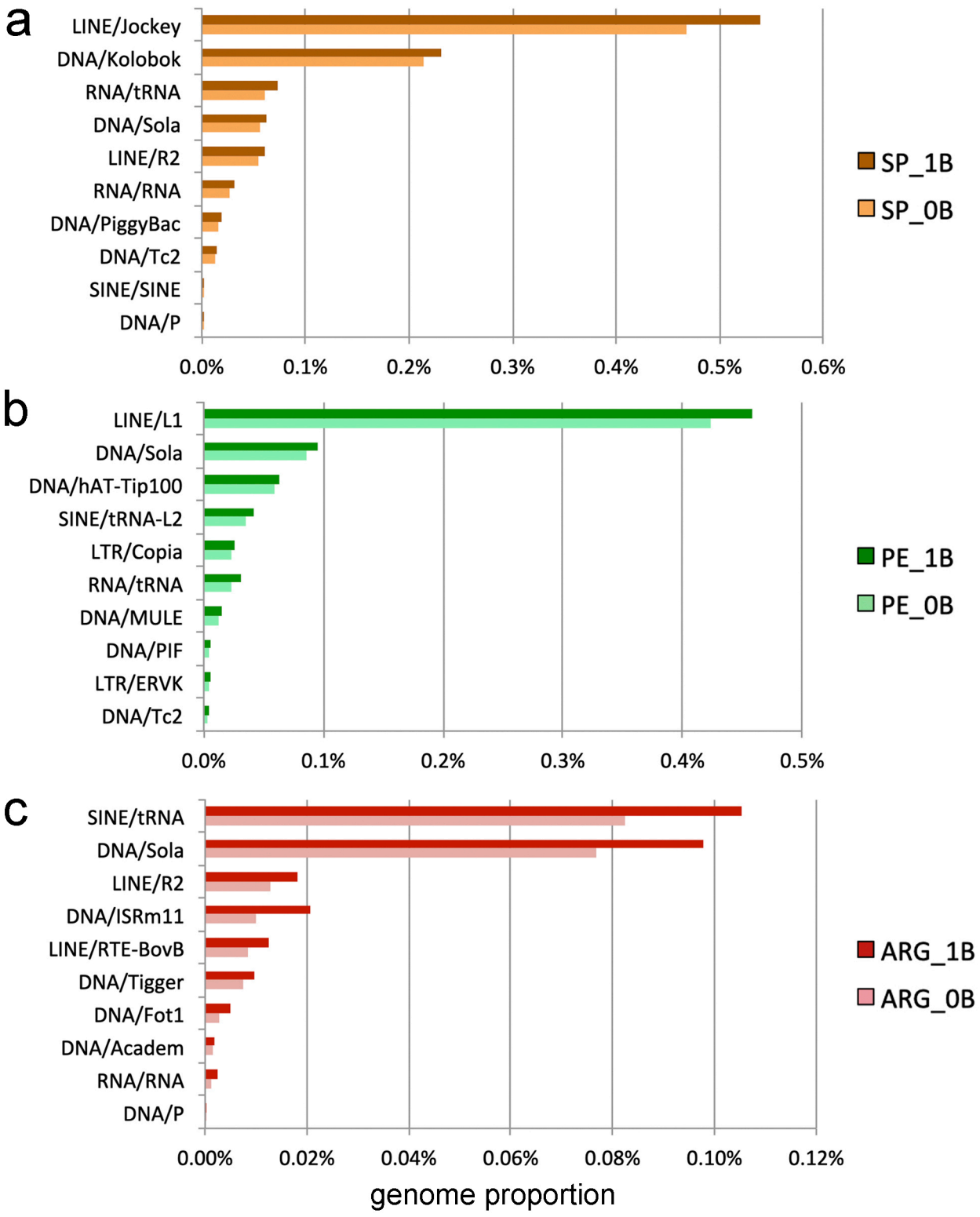
a
LINE/Jockey
DNA/Kolobok
RNA/tRNA
DNA/Sola
LINE/R2
RNA/RNA
DNA/PiggyBac
DNA/Tc2
SINE/SINE
DNA/P
0.0%
0.1%
0.2%
0.3%
0.4%
0.5%
0.6%
SP_1B
SP_0B
b
LINE/L1
DNA/Sola
DNA/hAT-Tip100
SINE/tRNA-L2
LTR/Copia
RNA/tRNA
DNA/MULE
DNA/PIF
LTR/ERVK
DNA/Tc2
0.0%
0.1%
0.2%
0.3%
0.4%
0.5%
PE_1B
PE_0B
c
SINE/tRNA
DNA/Sola
LINE/R2
DNA/ISRm11
LINE/RTE-BovB
DNA/Tigger
DNA/Fot1
DNA/Academ
RNA/RNA
DNA/P
0.00%
0.02%
0.04%
0.06%
0.08%
0.10%
0.12%
genome proportion
ARG_1B
ARG_0B

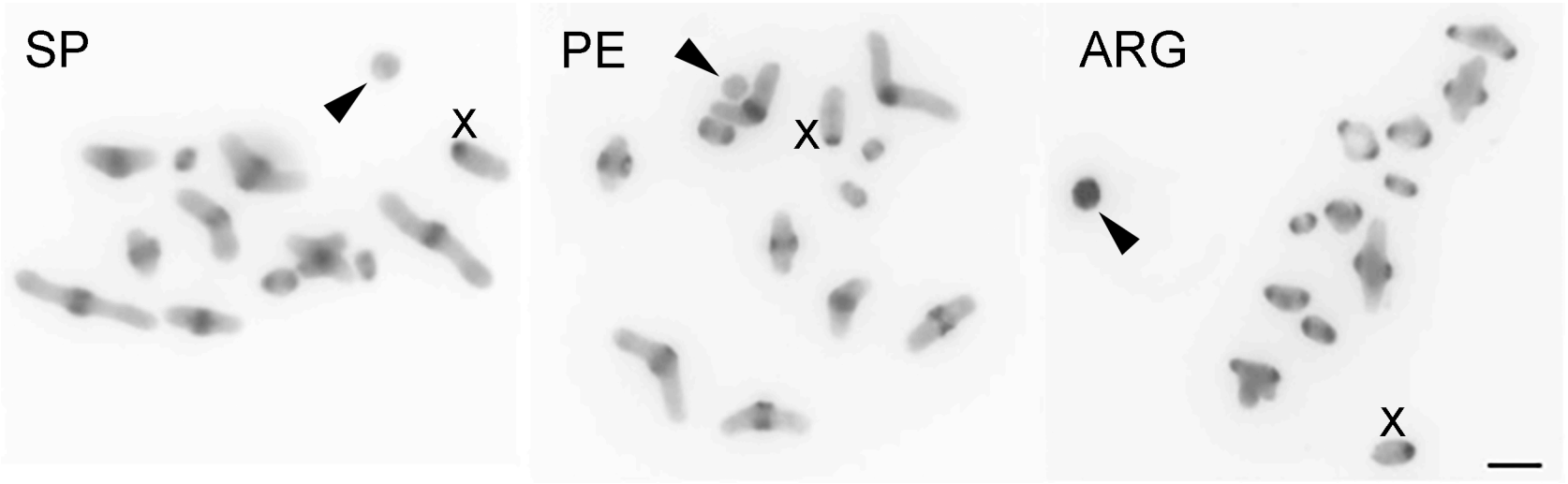
SP
X
PE
X
ARG
X

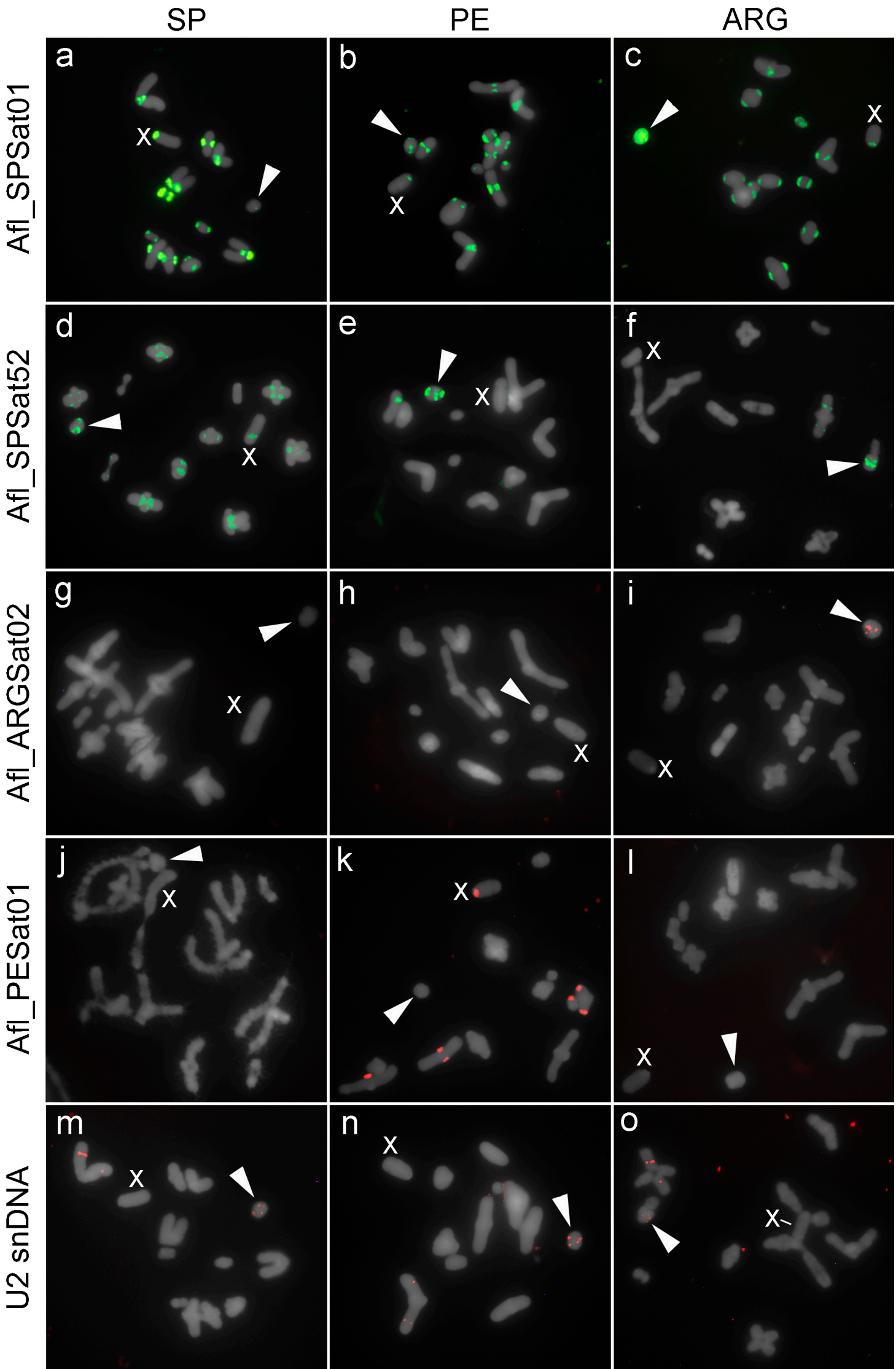
SP
PE
ARG
Afl_SPSat01
Afl_SPSat52
Afl_ARGSat02
Afl_PESat01
U2 snDNA
a
b
c
d
e
f
g
h
i
j
k
l
m
n
o
x

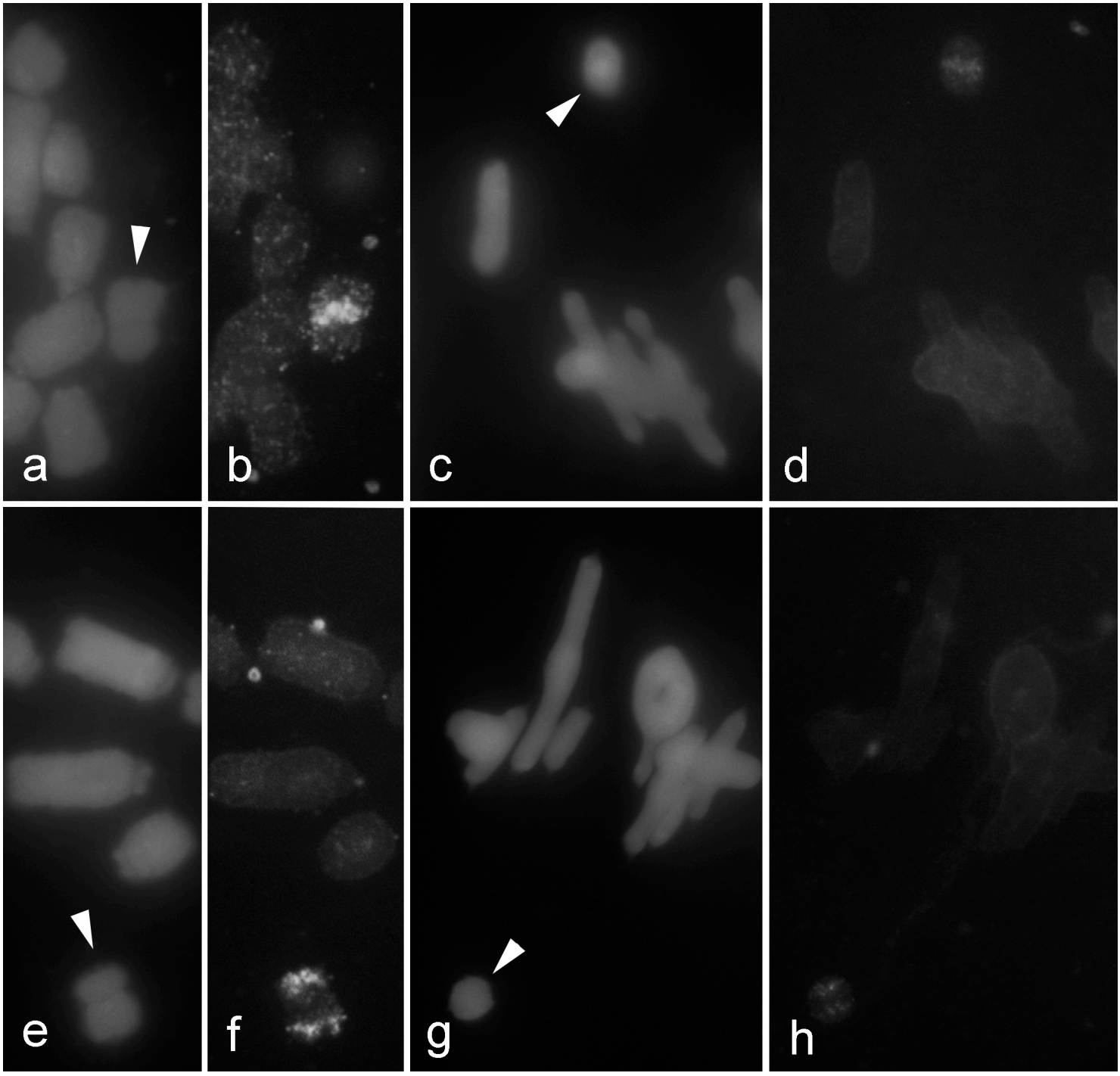
a
b
c
d
e
f
g
h

5. CONCLUSIONS

The main objective of this thesis was to investigate the structure, molecular composition and the evolutionary process involved in the origin of B chromosomes of Neotropical grasshoppers. Since this group of species presents some difficulties to explore its genomic content, such as giant genome size, high abundance in repetitive DNA and lack of available public databases, this certainly place a challenge for genome assembly and B chromosome genomic content examination. Therefore, this research was mainly approached through a comparative integration of cytogenetic and genomic data of the most abundant repetitive DNA families within this group of insects, isolated mainly through sequenced DNA and molecular cytogenetic assays using B-carrying and B-lacking individuals from different species and populations.

The findings of the present work provide support for intraspecific origin of the B chromosome in different grasshoppers species, which appears to be a common feature for this group. Moreover, the majority of the species studied here and other grasshoppers sustain the recurrent involvement of small chromosomes in the B chromosome origin (TERUEL et al., 2014; RUIZ-RUANO et al., 2016b, 2018). For *R. brasiliensis*, evidences of its B chromosome origin points to be from pair S11, despite the possible involvement of pair M7 by the sharing of some satDNAs. In *S. rubiginosa*, the autosomal origin for B chromosome from the pair S9 is suggested by the sharing of five satDNAs. Furthermore, the satDNA content and distribution in the B chromosome of *X. d. angulatus* indicate primarily that the pair S10 shares the most satDNAs with B chromosome (three satDNAs families), and it seems to be the ancestral pair involved in its B chromosome origin (see chapter 1). However, the most recent and unpublished data that is not present in this thesis with new information about satDNAs composition in this B chromosome also suggest the involvement of the pair S9. It seems that the case of *X. d. angulatus* brings a more complex panorama of B chromosome evolution and origin than in *R. brasiliensis* and *S. rubiginosa*, regarding additional steps of chromosomal rearrangements and accumulation/deletion of repeats after the B chromosome origin, as reported for other studies (LORETO et al., 2008; BERNARDINO et al., 2017).

Intriguingly, the B chromosome from *Abracris flavolineata* from Rio Claro/SP population is uncommonly not enriched in repetitive DNAs and totally C-negative, mostly because this B chromosome arose from the L1 autosome, probably passing

through misdivision and isochromosome formation process. This B chromosome is enriched particularly only by few repetitive elements and absent of B-specific satDNAs, suggesting that this B chromosome is young currently being in an initial step of heterochromatinization.

Deepening the knowledge about the B from *A. flavolineata*, our analysis of the repeatome collection of this species explored in distinct populations, provided evidences of a unique origin for the B chromosomes and intense turnover in repeat composition, resulting in the establishment of distinct variants at the interpopulation level. Despite highly differentiated, we proposed the single origin of the B variants through L1 autosome pair by the sharing of multiple elements in the B chromosome among the populations, such as U2 snDNA, Afl_SPSat01 and 52 and LINE/Jockey_72. Our data also suggests that the B variants of SP and PE are more similar to each other in relation to the ARG, which presented higher content of satDNAs, transposable elements of LINE subclass and totally C-positive pattern. Howoever, all three variants not showed enrichment of general repeat content in B-carrying genomes suggesting its resemblance to A complement and reinforcing our proposed hypothesis that the B chromosome of *A. flavolineata* is a young element. Nonetheless, the presence of a highly amplified and chromosome specific repeat in the B chromosome of ARG population was detected (Afl_ARGSat02), indicating a certain degree of differentiation to A complement.

6. REFERENCES

ÅGREN, J.A.; WRIGHT, S.I. Co-evolution between transposable elements and their hosts: a major factor in genome size evolution? **Chromosome research**, v. 19 n. 6, p. 777-786, 2011.

AHMAD, S.F.; JEHANGIR, M.; CARDOSO, A.L.; WOLF, I.R.; MARGARIDO, V.P.; CABRAL-DE-MELLO, D.C. et al. B chromosomes of multiple species have intense evolutionary dynamics and accumulated genes related to important biological processes. **BMC Genomics**, v. 21, p. 656, 2020.

AHMAD, S.F.; MARTINS, C. The modern view of B chromosomes under the impact of high scale omics analyses. **Cells**, v. 8 n. 2, p. 156, 2019.

AKBARI, O.S.; ANTOSHECHKIN, I.; HAY, B.A.; FERREE, P.M. Transcriptome profiling of *Nasonia vitripennis* testis reveals novel transcripts expressed from the selfish B chromosome, paternal sex ratio. **G3: Genes, Genomes, Genetics**, v. 3 n. 9, p. 1597-1605, 2013.

AMOS, A.; DOVER, G. The distribution of repetitive DNAs between regular and supernumerary chromosomes in species of *Glossina* (Tsetse): a two-step process in the origin of supernumeraries. **Chromosoma**, v. 81, p. 673–690, 1981.

ANDREWS, S. FastQC. A quality control tool for high throughput sequence data http://www.bioinformatics.babraham.ac.uk/projects/fastqc/. 2012.

ANJOS, A.; LORETO, V.; CABRAL-DE-MELLO, D.C. Organization of some repetitive DNAs and B chromosomes in the grasshopper *Eumastusia koebelei koebelei* (Rehn, 1909) (Orthoptera, Acrididae, Leptysminae). **Comparative Cytogenetics**, v. 10 n. 2, p. 219, 2016.

BAKKALI, M.; CABRERO, J.; LÓPEZ-LEÓN, M.D.; PERFECTTI, F.; CAMACHO, J.P.M. The B chromosome polymorphism of the grasshopper *Eyprepocnemis plorans* in North Africa. I. B variants and frequency. **Heredity**, v. 83 n. 4, p. 428-434, 1999.

BAKKALI, M.; PERFECTTI, F.; CAMACHO, J.P.M. The B chromosome polymorphism of the grasshopper *Eyprepocnemis plorans* in North Africa. II. Parasitic and neutralized B1 chromosomes. **Heredity**, v. 88, p. 14–18, 2002.

BANAEI-MOGHADDAM, A.M.; MARTIS, M.M.; MACAS, J.; GUNDLACH, H.; HIMMELBACH, A.; ALTSCHMIED, L. et al. Genes on B chromosomes: old questions revisited with new tools. **Biochimica et Biophysica Acta (BBA)-Gene Regulatory Mechanisms**, v. 1849 n. 1, p. 64-70, 2015.

BANAEI-MOGHADDAM, A.M.; MEIER, K., KARIMI-ASHTIYANI, R., HOUBEN, A. Formation and expression of pseudogenes on the B chromosome of rye. **The Plant Cell**, v. 25 n. 7, p. 2536-2544, 2003.

BELYAYEV, A.; RASKINA, O. Chromosome evolution in marginal populations of *Aegilops speltoides*: causes and consequences. **Annals of botany**, v. 111 n. 4, p. 531-538, 2013.

BERNARDINO, A.C.; CABRAL-DE-MELLO, D.C.; MACHADO, C.B.; PALACIOS-GIMENEZ, O.M.; SANTOS, N.; LORETO, V. Chromosome variants of the grasshopper *Xyleus discoideus angulatus* are potentially derived from pericentromeric DNA. **Cytogenetic and Genome Research**, v. 152 n. 4, p. 213-221, 2017.

BEUKEBOOM, L.W. Bewildering Bs: an impression of the 1st B–Chromosome Conference. **Heredity**, v. 73, p. 328–336, 1994.

BIDAU, C.J.; MARTI, D.A. B chromosomes and Robertsonian fusions of *Dichroplus pratensis* (Acrididae): intraspecific support for the centromeric drive theory. **Cytogenetic and Genome Research**, v. 106 n. 2-4, p. 347-350, 2004.

BIÉMONT, C.; VIEIRA, C. Junk DNA as an evolutionary force. **Nature**, v. 443 n. 7111, p. 521-524, 2006.

BISCOTTI, M.A.; CANAPA, A.; FORCONI, M.; OLMO, E.; BARUCCA, M. Transcription of tandemly repetitive DNA: functional roles. **Chromosome Research**, v. 23 n. 3, p. 463-477, 2015b.

BISCOTTI, M.A.; OLMO, E.; HESLOP-HARRISON, J.P. Repetitive DNA in eukaryotic genomes. **Chromosome Research**, v. 3 n. 23, p. 415-420, 2015a.

BOLGER, A.M.; LOHSE, M.; USADEL, B. Trimmomatic: a flexible trimmer for Illumina sequence data. **Bioinformatics**, v. 30, p. 2114–2120, 2014.

BOURQUE, G.; BURNS, K.H.; GEHRING, M.; GORBUNOVA, V.; SELUANOV, A.; HAMMELL, M. et al. Ten things you should know about transposable elements. **Genome biology**, v. 19 n. 1, p. 1-12, 2018.

BOWEN, N.J.; JORDAN, I.K. Transposable elements and the evolution of eukaryotic complexity. **Current Issues in Molecular Biology**, v. 4 n. 3, p. 65-76, 2002.

BRAJKOVIĆ, J.; FELICIELLO, I.; BRUVO-MAĐARIĆ, B.; UGARKOVIĆ, Đ. Satellite DNA-like elements associated with genes within euchromatin of the beetle *Tribolium castaneum*. **G3: Genes Genomes Genetics**, v. 2 n. 8, p. 931-941, 2012.

BUENO, D.; PALACIOS-GIMENEZ, O.M.; CABRAL-DE-MELLO, D.C. Chromosomal mapping of repetitive DNAs in the grasshopper *Abracris flavolineata* reveal possible ancestry of the B chromosome and H3 histone spreading. **PloS One**, v. 8 n. 6, p. e66532, 2013.

BUGROV, A.G.; KARAMYSHEVA, T.V.; RUBTSOV, D.N.; ANDREENKOVA, O.V.; RUBTSOV, N.B. Comparative FISH analysis of distribution of B chromosome repetitive DNA in A and B chromosomes in two subspecies of *Podisma sapporensis* (Orthoptera, Acrididae). **Cytogenetic and Genome Research**, v. 106 n. 2-4, p. 284-

288, 2004.

CABRAL-DE-MELLO, D.C.; MAREC, F. Universal fluorescence in situ hybridization (FISH) protocol for mapping repetitive DNAs in insects and other arthropods. **Molecular Genetics Genomics**, v. 296, p. 513–526. 2021.

CABRAL-DE-MELLO, D.C.; OLIVEIRA, S.G.; DE MOURA, R.C., MARTINS, C. Chromosomal organization of the 18S and 5S rRNAs and histone H3 genes in Scarabaeinae coleopterans: insights into the evolutionary dynamics of multigene families and heterochromatin. **BMC Genetics**, v. 12 n. 1, p. 1-12, 2011.

CABRERO, J.; BAKKALI, M.; BUGROV, A.; WARCHALOWSKA-SLIWA, E.; LÓPEZ-LEÓN, M.D.; PERFECTTI, F. et al. Multiregional origin of B chromosomes in the grasshopper *Eyprepocnemis plorans*. **Chromosoma**, v. 112 n. 4, p. 207-211, 2003.

CABRERO, J.; LÓPEZ-LEÓN, M.D.; RUÍZ-ESTÉVEZ, M.; GÓMEZ, R.; PETITPIERRE, E.; RUFAS, J.S. et al. B1 was the ancestor B chromosome variant in the western Mediterranean area in the grasshopper *Eyprepocnemis plorans*. **Cytogenetic and Genome Research**, v. 142 n. 1, p. 54-58, 2014.

CAMACHO, J.P.M. B chromosomes. In: The evolution of the genome (p. 223-286). Academic Press, 2005.

CAMACHO, J.P.M.; RUIZ-RUANO, F.J.; MARTÍN-BLÁZQUEZ, R.; LÓPEZ-LEÓN, M.D.; CABRERO, J.; LORITE, P. et al. A step to the gigantic genome of the desert locust: chromosome sizes and repeated DNAs. **Chromosoma**, v. 124 n. 2, p. 263-275, 2015.

CAMACHO, J.P.M.; SHARBEL, T.F.; BEUKEBOOM, L.W. B-chromosome evolution. **Philosophical Transactions of the Royal Society of London. Series B: Biological Sciences**, v. 355 n. 1394, p. 163-178, 2000.

CAZAUX, B.; CATALAN, J.; JUSTY, F.; ESCUDÉ, C.; DESMARAIS, E.; BRITTON-DAVIDIAN, J. Evolution of the structure and composition of house mouse satellite DNA sequences in the subgenus *Mus* (Rodentia: Muridea): a cytogenomic approach. **Chromosoma**, v. 122 n. 3, p. 209-220, 2013.

CHARLESWORTH, B.; SNIEGOWSKI, P.; STEPHAN, W. The evolutionary dynamics of repetitive DNA in eukaryotes. **Nature**, v. 371 n. 6494, p. 215-220, 1994.

CLARK, F.E.; CONTE, M.A.; KOCHER, T.D. Genomic characterization of a B chromosome in Lake Malawi cichlid fishes. **Genes**, v. 9 n. 12, p. 610, 2018.

COAN, R.L.; MARTINS, C. Landscape of transposable elements focusing on the B chromosome of the cichlid fish *Astatotilapia latifasciata*. **Genes**, v. 9 n. 6, p. 269, 2018.

COLEMAN, J.J.; ROUNSLEY, S.D.; RODRIGUEZ-CARRES, M.; KUO, A.; WASMANN, C.C.; GRIMWOOD, J. et al. The genome of *Nectria haematococca*:

contribution of supernumerary chromosomes to gene expansion. **PLoS Genetics**, v. 5 n. 8, p. e1000618, 2009.

D'AMBROSIO, U.; ALONSO-LIFANTE, M.P.; BARROS, K.; KOVAŘÍK, A.; DE XAXARS, G.M.; GARCIA, S. B-chrom: A database on B-chromosomes of plants, animals and fungi. **New Phytologist**, v. 216 n. 3, p. 635-642, 2017.

DHERAWATTANA, A.; SADANAGA, K. Cytogenetics of a crown rust-resistant hexaploid oat with 42 + 2 fragment chromosomes. **Crop Science**, v. 13, p. 591–594, 1973.

DOUGLAS, R.N.; YANG, H.; ZHANG, B.; CHEN, C.; HAN, F.; CHENG, J. et al. De novo centromere formation on chromosome fragments with an inactive centromere in maize (*Zea mays*). **Chromosome Research**, p. 1-13, 2021.

DRUMMOND, A.J., ASHTON, B., CHEUNG, M., HELED, J., KEARSE, M. Geneious v.4.8.5, biomatters ltd. Aukland, New Zealand. http://www.geneious.com. 2009.

EBRAHIMZADEGAN, R.; HOUBEN, A.; MIRZAGHADERI, G. Repetitive DNA landscape in essential A and supernumerary B chromosomes of *Festuca pratensis* Huds. **Scientific Reports**, v. 9 n. 1, p. 1-11, 2019.

EDGAR, R.C. MUSCLE: multiple sequence alignment with high accuracy and high throughput. **Nucleic Acids Research**, v. 32, p. 1792–1797, 2004.

EIRÍN-LÓPEZ, J. M., REBORDINOS, L., ROONEY, A. P., ROZAS, J. The birth-and-death evolution of multigene families revisited. **Repetitive DNA**, v. 7, p. 170-196, 2012.

FANTINATTI, B.E.; MAZZUCHELLI, J.; VALENTE, G.T.; CABRAL-DE-MELLO, D.C.; MARTINS, C. Genomic content and new insights on the origin of the B chromosome of the cichlid fish *Astatotilapia latifasciata*. **Genetica**, v. 139 n. 10, p. 1273-1282, 2011.

FEDOROFF, N.V. Transposable elements, epigenetics, and genome evolution. **Science**, v. 338 n. 6108, p. 758-767, 2012.

FELICIELLO, I., AKRAP, I., UGARKOVIĆ, Đ. Satellite DNA modulates gene expression in the beetle *Tribolium castaneum* after heat stress. **PLoS Genetics**, v. 11 n. 8, p. e1005466, 2015.

FESCHOTTE, C., PRITHAM, E. J. DNA transposons and the evolution of eukaryotic genomes. **Annual Review Genetics**, v. 41, p. 331-368, 2007.

FINNEGAN, D.J. Eukaryotic transposable elements and genome evolution. **Trends in Genetics**, v. 5, p. 103-107, 1989.

GARCÍA, G.; RÍOS, N.; GUTIÉRREZ, V. Next-generation sequencing detects repetitive elements expansion in giant genomes of annual killifish genus *Austrolebias*

(Cyprinodontiformes, Rivulidae). **Genetica**, v. 143 n. 3, p. 353-360, 2015.

GORDON, A.; HANNON, G.J. Fastx-toolkit. FASTQ/A short-reads pre-processing tools http://hannonlab.cshl.edu/fastx_toolkit. 2010.

GOUBERT, C.; MODOLO, L.; VIEIRA, C.; VALIENTEMORO, C.; MAVINGUI, P.; BOULESTEIX, M. De novo assembly and annotation of the Asian tiger mosquito (*Aedes albopictus*) repeatome with dnaPipeTE from raw genomic reads and comparative analysis with the yellow fever mosquito (*Aedes aegypti*). **Genome Biology Evolution**, v. 7, p. 1192–1205, 2015.

GRABHERR, M.G.; HAAS, B.J.; YASSOUR, M.; LEVIN, J.Z.; THOMPSON, D.A.; AMIT, I. et al. Trinity: reconstructing a full-length transcriptome without a genome from RNA-Seq data. **Nature Biotechnology**, v. 29, p. 644, 2011.

GRAPHODATSKY, A.S.; KUKEKOVA, A.V.; YUDKIN, D.V.; TRIFONOV, V.A.; VOROBIEVA, N.V.; BEKLEMISHEVA, V.R. et al. The proto-oncogene C-KIT maps to canid B-chromosomes. **Chromosome Research**, v. 13 n. 2, p. 113-122, 2005.

GREEN DM. Muller's Ratchet and the evolution of supernumerary chromosomes. **Genome**, v. 33, p. 818–824, 1990.

GREEN, D.M. Cytogenetics of the endemic New Zealand frog, *Leiopelma hochstetteri*: extraordinary supernumerary chromosome variation and a unique sex-chromosome system. **Chromosoma**, v. 97, p. 55–70, 1988.

HAHN, C.; BACHMANN, L.; CHEVREUX, B. Reconstructing mitochondrial genomes directly from genomic next-generation sequencing reads—a baiting and iterative mapping approach. **Nucleic Acids Research**, v. 41, p. e129–e129, 2013.

HANLON, S.L.; MILLER, D.E.; ECHE, S.; HAWLEY, R.S. Origin, composition, and structure of the supernumerary B chromosome of *Drosophila melanogaster*. **Genetics**, v. 210 n. 4, p. 1197-1212, 2018.

HEITKAM, T.; PETRASCH, S.; ZAKRZEWSKI, F.; KÖGLER, A.; WENKE, T.; WANKE, S.; SCHMIDT, T. Next-generation sequencing reveals differentially amplified tandem repeats as a major genome component of Northern Europe's oldest *Camellia japonica*. **Chromosome Research**, v. 23 n. 4, p. 791-806, 2015.

HEWITT, G.M. Grasshopper and crickets. In: John B ed. Animal Cytogenetics, v. 3, Insecta 1 Orthoptera. Berlin, Stuttgart: Gebruder Borntraeger, 1979.

HEWITT, G.M. The integration of supernumerary chromosomes into the orthopteran genome. **Cold Spring Harbor Symposia on Quantitative Biology**, v. 38, p. 183–194, 1973.

HOLMES, D.S.; BOUGOURD, S.M. B-chromosome selection in Allium schoenoprasum. I. Natural populations. **Heredity**, 63(1), 83-87, 1989.

HOUBEN, A. B chromosomes–a matter of chromosome drive. **Frontiers in Plant Science**, v. 8, p. 210, 2017.

HOUBEN, A.; BANAEI-MOGHADDAM, A.M.; KLEMME, S.; TIMMIS, J.N. Evolution and biology of supernumerary B chromosomes. **Cellular and Molecular Life Sciences**, v. 71 n. 3, p. 467-478, 2014.

HOUBEN, A.; THOMPSON, N.; AHNE, R.; LEACH, C.R.; VERLIN, D.; TIMMIS, J.N. A monophyletic origin of the B chromosomes of *Brachycome dichromosomatica* (Asteraceae). **Plant Systematics and Evolution**, v. 219 n. 1, p. 127-135, 1999.

HUANG, W.; DU, Y.; ZHAO, X.; JIN, W. B chromosome contains active genes and impacts the transcription of A chromosomes in maize (*Zea mays* L.). **BMC Plant Biology**, v. 16 n. 1, p. 1-14, 2016.

HUGHES, A.L.; NEI, M. Maintenance of MHC polymorphism. **Nature**, v. 355, n. 6359, p. 402-403, 1992.

JACKSON, R.C.; NEWMARK, K.P. Effects of supernumerary chromosomes on production of pigment in *Haplopappus gracilis*. **Science**, v. 132, p. 1316–1317, 1960.

JAMILENA, M.; RUIZ REJÓN, C.; RUIZ REJÓN, M. A molecular analysis of the origin of the *Crepis capillaris* B chromosome. **Journal of Cell Science**, v. 107 n. 3, p. 703-708, 1994.

JANG, T.S.; PARKER, J.S.; WEISS-SCHNEEWEISS, H. Structural polymorphisms and distinct genomic composition suggest recurrent origin and ongoing evolution of B chromosomes in the *Prospero autumnale* complex (Hyacinthaceae). **New Phytologist, v.** 210 n. 2, p. 669-679, 2016.

JONES, N.; HOUBEN, A. B chromosomes in plants: escapees from the A chromosome genome? **Trends in Plant Science**, v. 8 n. 9, p. 417-423, 2003.

JONES, R.N. Are B chromosomes selfish? In: Cavalier-Smith T ed. The Evolution of Genome Size. London: Wiley, p. 397–425, 1985.

JONES, R.N. B-chromosome drive. **The American Naturalist**, v. 137, p. 430–442, 1991.

JONES, R.N. New species with B chromosomes discovered since 1980. **The Nucleus**, v. 60 n. 3, p. 263-281, 2017.

JONES, R.N. Tansley review no. 85: B chromosomes in plants. **New Phytologist**, v. 131, p. 411–434, 1995.

JONES, R.N.; REES, H. B Chromosomes. New York: Academic Press. 1982.

KAPITONOV, V.V.; JURKA, J. Self-synthesizing DNA transposons in eukaryotes. **Proceedings of the National Academy of Sciences**, v. 103 n. 12, p. 4540-4545, 2006.

KARAFIÁTOVÁ, M.; BEDNÁŘOVÁ, M.; SAID, M.; ČÍŽKOVÁ, J.; HOLUŠOVÁ, K.; BLAVET, N. et al. The B chromosome of *Sorghum purpureosericeum* reveals the first pieces of its sequence. **Journal of Experimental Botany**, v. 72 n. 5, p. 1606-1616, 2021.

KAYANO, H. Cytogenetic studies in *Lillium callosum*. III. Preferential segregation of a supernumerary chromosome in EMCs. **Proceedings Japan Academy**, v. 33, p. 553–558, 1957.

KICHIGIN, I.G.; LISACHOV, A.P.; GIOVANNOTTI, M.; MAKUNIN, A.I.; KABILOV, M.R.; O'BRIEN, P.C. et al. First report on B chromosome content in a reptilian species: The case of *Anolis carolinensis*. **Molecular Genetics and Genomics**, v. 294 n. 1, p. 13-21, 2019.

KIDWELL, M.G. Transposable elements. In: The evolution of the genome. Academic Press, p. 165-221, 2005.

KLEMME, S.; BANAEI-MOGHADDAM, A.M.; MACAS, J.; WICKER, T.; NOVÁK, P.; HOUBEN, A. High-copy sequences reveal distinct evolution of the rye B chromosome. **New Phytologist**, v. 199 n. 2, p. 550-558, 2013.

KOJIMA, K.K.; JURKA, J. Crypton transposons: identification of new diverse families and ancient domestication events. **Mobile DNA**, v. 2 n. 1, p. 1-17, 2011.

KOPECNA, O.; KUBICKOVA, S.; CERNOHORSKA, H.; CABELOVA, K.; VAHALA, J.; MARTINKOVA, N.; RUBES, J. Tribe-specific satellite DNA in non-domestic Bovidae. **Chromosome Research**, v. 22 n. 3, p. 277-291, 2014.

KOUR, G.; KAUL, S.; DHAR, M.K. Molecular characterization of repetitive DNA sequences from B chromosome in *Plantago lagopus* L. **Cytogenetic and Genome Research**, v. 142 n. 2, p. 121-128, 2014.

KUHN, G.C.S. Satellite DNA transcripts have diverse biological roles in *Drosophila*. **Heredity**, v. 115 n. 1, p. 1, 2015.

KUMKE, K.; MACAS, J.; FUCHS, J.; ALTSCHMIED, L.; KOUR, J.; DHAR, M.K.; HOUBEN, A. *Plantago lagopus* B chromosome is enriched in 5S rDNA-derived satellite DNA. **Cytogenetic and Genome Research**, v. 148 n. 1, p. 68-73, 2016.

LAMB, J.C.; KATO, A.; BIRCHLER, J.A. Sequences associated with A chromosome centromeres are present throughout the maize B chromosome. **Chromosoma**, v. 113 n. 7, p. 337-349, 2005.

LAMB, J.C.; RIDDLE, N.C.; CHENG, Y.M.; THEURI, J.; BIRCHLER, J.A. Localization and transcription of a retrotransposon-derived element on the maize B chromosome. **Chromosome Research**, v. 15 n. 3, p. 383-398, 2007.

LANGDON, T.; SEAGO, C.; JONES, R.N.; OUGHAM, H.; THOMAS, H.; FORSTER, J.W. et al. De novo evolution of satellite DNA on the rye B

chromosome. **Genetics**, v. 154 n. 2, p. 869-884, 2000.

LI, W.; GODZIK, A. Cd-hit: a fast program for clustering and comparing large sets of protein or nucleotide sequences. **Bioinformatics**, v. 22 n. 13, p. 1658-1659, 2006.

LIBRADO, P.; ROZAS, J. DnaSP v5: a software for comprehensive analysis of DNA polymorphism data. **Bioinformatics**, v. 25 n. 11, p. 1451-1452, 2009.

LÓPEZ-FLORES, I.; GARRIDO-RAMOS, M.A. The repetitive DNA content of eukaryotic genomes. **Repetitive DNA**, v. 7, p. 1-28, 2012.

LÓPEZ-LEÓN, M.D.; CABRERO, J.; PARDO, M.C.; VISERAS, E.; CAMACHO, J.P.M.; SANTOS, J.L. Generating high variability of B chromosomes in *Eyprepocnemis plorans* (grasshopper). **Heredity**, v. 71 n. 4, p. 352-362, 1993.

LÓPEZ-LEÓN, M.D.; NEVES, N.; SCHWARZACHER, T.; HESLOP-HARRISON, J.P.; HEWITT, G.M.; CAMACHO, J.P.M. Possible origin of a B chromosome deduced from its DNA composition using double FISH technique. **Chromosome Research**, v. 2 n. 2, p. 87-92, 1994.

LORETO, V.; CABRERO, J.; LÓPEZ-LEÓN, M.D.; CAMACHO, J.P.M.; SOUZA, M.J. Possible autosomal origin of macro B chromosomes in two grasshopper species. **Chromosome Research**, v. 16 n. 2, p. 233-241, 2008.

MACAS, J.; NEUMANN, P.; NOVÁK, P.; JIANG, J. Global sequence characterization of rice centromeric satellite based on oligomer frequency analysis in large-scale sequencing data. **Bioinformatics**, v. 26 n. 17, p. 2101-2108, 2010.

MAKUNIN, A.I.; DEMENTYEVA, P.V.; GRAPHODATSKY, A.S.; VOLOBOUEV, V.T.; KUKEKOVA, A.V.; TRIFONOV, V.A. Genes on B chromosomes of vertebrates. **Molecular Cytogenetics**, v. 7 n. 1, p. 1-10, 2014.

MAKUNIN, A.I.; KICHIGIN, I.G.; LARKIN, D.M.; O'BRIEN, P.C.; FERGUSON-SMITH, M.A.; YANG, F. et al. Contrasting origin of B chromosomes in two cervids (Siberian roe deer and grey brocket deer) unravelled by chromosome-specific DNA sequencing. **BMC Genomics**, v. 17 n. 1, p. 1-14, 2016.

MARQUES, A.; BANAEI-MOGHADDAM, A.M.; KLEMME, S.; BLATTNER, F.R.; NIWA, K.; GUERRA, M.; HOUBEN, A. B chromosomes of rye are highly conserved and accompanied the development of early agriculture. **Annals of Botany**, v. 112 n. 3, p. 527-534, 2013.

MARQUES, A.; KLEMME, S.; HOUBEN, A. Evolution of plant B chromosome enriched sequences. **Genes**, v. 9 n. 10, p. 515, 2018.

MARSCHNER, S.; MEISTER, A.; BLATTNER, F.R.; HOUBEN, A. Evolution and function of B chromosome 45S rDNA sequences in *Brachycome dichromosomatica*. **Genome**, v. 50 n. 7, p. 638-644, 2007.

MARTINS, C.; TRIFONOV, V.; HOUBEN, A. Addressing long-standing questions

with advanced approaches: The 4th B chromosome conference. **Cytogenetic and Genome Research**, v. 160 n. 3, p. 111-117, 2020.

MARTIS, M.M.; KLEMME, S.; BANAEI-MOGHADDAM, A.M.; BLATTNER, F.R.; MACAS, J.; SCHMUTZER, T. et al. Selfish supernumerary chromosome reveals its origin as a mosaic of host genome and organellar sequences. **Proceedings of the National Academy of Sciences**, v. 109 n. 33, p. 13343-13346, 2012.

MCALLISTER, B.F. Isolation and characterization of a retroelement from B chromosome (PSR) in the parasitic wasp *Nasonia vitripennis*. **Insect Molecular Biology**, v. 4 n. 4, p. 253-262, 1995.

MCALLISTER, B.F.; WERREN, J.H. Hybrid origin of a B chromosome (PSR) in the parasitic wasp *Nasonia vitripennis*. **Chromosoma**, v. 106 n. 4, p. 243-253, 1997.

MENEZES-DE-CARVALHO, N.Z.; PALACIOS-GIMENEZ, O.M.; MILANI, D.; CABRAL-DE-MELLO, D.C. High similarity of U2 snDNA sequence between A and B chromosomes in the grasshopper *Abracris flavolineata*. **Molecular Genetics and Genomics**, v. 290 n. 5, p. 1787-1792, 2015.

MILANI, D.; CABRAL-DE-MELLO, D.C. Microsatellite organization in the grasshopper *Abracris flavolineata* (Orthoptera: Acrididae) revealed by FISH mapping: remarkable spreading in the A and B chromosomes. **PLoS One**, v. 9 n. 5, p. e97956, 2014.

MILANI, D.; PALACIOS-GIMENEZ, O.M.; CABRAL-DE-MELLO, D.C. The U2 snDNA is a useful marker for B chromosome detection and frequency estimation in the grasshopper *Abracris flavolineata*. **Cytogenetic and Genome Research**, v. 151 n. 1, p. 36-40, 2017.

MILANI, D.; RUIZ-RUANO, F.J.; CAMACHO, J.P.M.; CABRAL-DE-MELLO, D.C. Out of patterns, the euchromatic B chromosome of the grasshopper *Abracris flavolineata* is not enriched in high-copy repeats. **Heredity**, v. 127, p. 475-483, 2021.

MONTIEL, E.E.; CABRERO, J.; CAMACHO, J.P.M.; LÓPEZ-LEÓN, M.D. Gypsy, RTE and Mariner transposable elements populate *Eyprepocnemis plorans* genome. **Genetica**, v. 140 n. 7-9, p. 365-374, 2012.

MONTIEL, E.E.; CABRERO, J.; RUIZ-ESTÉVEZ, M.; BURKE, W.D.; EICKBUSH, T.H.; CAMACHO, J.P.M.; LÓPEZ-LEÓN, M.D. Preferential occupancy of R2 retroelements on the B chromosomes of the grasshopper *Eyprepocnemis plorans*. **PLoS One**, v. 9 n. 3, p. e91820, 2014.

NAVARRO-DOMÍNGUEZ, B.; MARTÍN-PECIÑA, M.; RUIZ-RUANO, F.J.; CABRERO, J.; CORRAL, J.M.; LÓPEZ-LEÓN, M.D. et al. Gene expression changes elicited by a parasitic B chromosome in the grasshopper *Eyprepocnemis plorans* are consistent with its phenotypic effects. **Chromosoma**, v. 128 n. 1, p. 53-67, 2019.

NAVARRO-DOMÍNGUEZ, B.; RUIZ-RUANO, F.J.; CABRERO, J.; CORRAL, J.M.; LÓPEZ-LEÓN, M.D.; SHARBEL, T.F. et al. Protein-coding genes in B

chromosomes of the grasshopper *Eyprepocnemis plorans*. **Scientific Reports**, v. 7 n. 1, p. 1-12, 2017.

NEI, M.; GU, X.; SITNIKOVA, T. Evolution by the birth-and-death process in multigene families of the vertebrate immune system. **Proceedings of the National Academy of Sciences**, v. 94 n. 15, p. 7799-7806, 1997.

NEI, M.; ROONEY, A.P. Concerted and birth-and-death evolution of multigene families. **Annual Review Genetics**, v. 39, p. 121-152, 2005.

NERGADZE, S.G.; BELLONI, E.; PIRAS, F.M.; KHORIAULI, L.; MAZZAGATTI, A.; VELLA, F. et al. Discovery and comparative analysis of a novel satellite, EC137, in horses and other equids. **Cytogenetic and Genome Research**, v. 144 n. 2, p. 114-123, 2014.

NORMARK, B.B. Phylogeny and evolution of parthenogenetic weevils of the *Aramigus tessellates* species complex (Coleoptera: Curculionidae: Naupactini): Evidence form mitochondrial DNA sequences. **Evolution**, v. 50, p. 734-745, 1996.

NOVÁK, P.; NEUMANN, P.; MACAS, J. Graph-based clustering and characterization of repetitive sequences in next-generation sequencing data. **BMC bioinformatics**, v. 11 n. 1, p. 1-12, 2010.

NOVÁK, P.; NEUMANN, P.; PECH, J.; STEINHAISL, J.; MACAS, J. RepeatExplorer: a galaxy- based web server for genome-wide characterization of eukaryotic repetitive elements from next-generation sequence reads. **Bioinformatics**, v. 29, p. 792–793, 2013.

NUR, U. A mitotically unstable supernumerary chromosome with an accumulation mechanism in a grasshopper. **Chromosoma**, v. 14, p. 407–422, 1963.

NUR, U. Maintenance of a "parasitic" B chromosome in the grasshopper *Melanoplus* femur–rubrum. **Genetics**, v. 87, p. 499–512, 1977.

NUR, U. The effect of supernumerary chromosomes on the development of mealy bugs. **Genetics**, v. 54, p. 1239–1249, 1966.

OLIVEIRA, N.L.; CABRAL-DE-MELLO, D.C.; ROCHA, M.F.; LORETO, V.; MARTINS, C.; MOURA, R.C. Chromosomal mapping of rDNAs and H3 histone sequences in the grasshopper *Rhammatocerus brasiliensis* (Acrididae, Gomphocerinae): extensive chromosomal dispersion and co-localization of 5S rDNA/H3 histone clusters in the A complement and B chromosome. **Molecular Cytogenetics**, v. 4 n. 1, p. 1-7, 2011.

ORGEL, L.E.; CRICK, F.H. Selfish DNA: the ultimate parasite. **Nature**, v. 284 n. 5757, p. 604-607, 1980.

ÖSTERGREN G. Parasitic nature of extra fragment chromosomes. **Botany Notiser**, v. 2, p. 157–163, 1945.

PALESTIS, B.G.; CABRERO, J.; TRIVERS, R.; CAMACHO, J.P.M. Prevalence of B chromosomes in Orthoptera is associated with shape and number of A chromosomes. **Genetica**, v. 138 n. 11-12, p. 1181-1189, 2010.

PALESTIS, B.G.; TRIVERS, R.; BURT, A.; JONES, R.N. The distribution of B chromosomes across species. **Cytogenetic and Genome Research**, v. 106 n. 2-4, p. 151-158, 2004.

PALOMEQUE, T.; LORITE, P. Satellite DNA in insects: a review. **Heredity**, v. 100 n. 6, p. 564-573, 2008.

PARDO, M.C.; LÓPEZ-LEÓN, M.D.; VISERAS, E.; CABRERO, J.; CAMACHO, J.P.M. Mitotic instability of B chromosomes during embryo development in *Locusta migratoria*. **Heredity**, v. 74 n. 2, p. 164-169, 1995.

PARKER, J.S.; JONES, G.H.; EDGAR, L.A.; WHITEHOUSE, C. The population cytogenetics of *Crepis capillaris* IV. The distribution of B-chromosomes in British populations. **Heredity**, v. 66 n. 2, p. 211-218, 1991.

PENG, S.F.; CHENG, Y.M. Characterization of satellite CentC repeats from heterochromatic regions on the long arm of maize B-chromosome. **Chromosome Research**, v. 19 n. 2, p. 183-191, 2011.

PERFECTTI, F.; WERREN, J.H. The interspecific origin of B chromosomes: experimental evidence. **Evolution**, v. 55 n. 5, p. 1069-1073, 2001.

PERVAIZ, N.; SHAKEEL, N.; QASIM, A.; ZEHRA, R.; ANWAR, S.; RANA, N. et al. Evolutionary history of the human multigene families reveals widespread gene duplications throughout the history of animals. **BMC Evolutionary Biology**, v. 19 n. 1, p. 1-11, 2019.

PEZER, Ž.; BRAJKOVIĆ, J.; FELICIELLO, I.; UGARKOVIĆ, Đ. Transcription of satellite DNAs in insects. In: Long Non-Coding RNAs. Springer, Berlin, Heidelberg, p. 161-178, 2011.

PLOHL, M.; LUCHETTI, A.; MEŠTROVIĆ, N.; MANTOVANI, B. Satellite DNAs between selfishness and functionality: structure, genomics and evolution of tandem repeats in centromeric (hetero) chromatin. **Gene**, v. 409 n .1-2, p. 72-82, 2008.

PLOHL, M.; MEŠTROVIĆ, N.; MRAVINAC, B. Satellite DNA evolution. **Repetitive DNA**, v. 7, p. 126-152, 2012.

POLETTO, A.B.; FERREIRA, I.A.; CABRAL-DE-MELLO, D.C.; NAKAJIMA, R.T.; MAZZUCHELLI, J.; RIBEIRO, H.B. et al. Chromosome differentiation patterns during cichlid fish evolution. **BMC Genetics**, v. 11 n. 1, p. 1-12, 2010.

POULTER, R.T.; BUTLER, M.I. Tyrosine recombinase retrotransposons and transposons. **Microbiology Spectrum**, v. 3 n. 2, p. 3-2, 2015.

PRITHAM, E.J. Transposable elements and factors influencing their success in

eukaryotes. **Journal of Heredity**, v. 100 n. 5, p. 648-655, 2009.

PRITHAM, E.J.; PUTLIWALA, T.; FESCHOTTE, C. Mavericks, a novel class of giant transposable elements widespread in eukaryotes and related to DNA viruses. **Gene**, v. 390 n. 1-2, p. 3-17, 2007.

RUBAN, A.; SCHMUTZER, T.; SCHOLZ, U.; HOUBEN, A. How next-generation sequencing has aided our understanding of the sequence composition and origin of B chromosomes. **Genes**, v. 8 n. 11, p. 294, 2017.

RUIZ-ESTÉVEZ, M.; BADISCO, L.; BROECK, J.V.; PERFECTTI, F.; LÓPEZ-LEÓN, M.D.; CABRERO, J. et al. B chromosomes showing active ribosomal RNA genes contribute insignificant amounts of rRNA in the grasshopper *Eyprepocnemis plorans*. **Molecular Genetics Genomics**, v. 289 n. 6, p. 1209-1216, 2014.

RUIZ-RUANO, F.J.; CABRERO, J.; LÓPEZ-LEÓN, M.D.; CAMACHO, J.P.M. Satellite DNA content illuminates the ancestry of a supernumerary (B) chromosome. **Chromosoma**, v. 126 n. 4, p. 487–500, 2016b.

RUIZ-RUANO, F.J.; CABRERO, J.; LÓPEZ-LEÓN, M.D.; SÁNCHEZ, A.; CAMACHO, J.P.M. Quantitative sequence characterization for repetitive DNA content in the supernumerary chromosome of the migratory locust. **Chromosoma**, v. 127 n. 1, p. 45–57, 2018.

RUIZ-RUANO, F.J.; CUADRADO, Á.; MONTIEL, E.E.; CAMACHO, J.P.M.; LÓPEZ-LEÓN, M.D. Next generation sequencing and FISH reveal uneven and nonrandom microsatellite distribution in two grasshopper genomes. **Chromosoma**, v. 124 n. 2, p. 221-234, 2015.

RUIZ-RUANO, F.J.; LÓPEZ-LEÓN, M.D.; CABRERO, J.; CAMACHO, J.P.M. High-throughput analysis of the satellitome illuminates satellite DNA evolution. **Scientific Reports**, v. 6, p. 28333, 2016a.

RUSSELL, D.W.; SAMBROOK, J. Molecular cloning: a laboratory manual. Cold Spring Harbor, NY: Cold Spring Harbor Laboratory, v. 1, p. 112, 2001.

RUTISHAUSER, A.; RÖTHLISBERGER, E. Boosting mechanism of B chromosomes in *Crepis capillaris*. **Chromosomes Today**, v. 1, p. 28–30, 1966.

SAHA, S.; BRIDGES, S.; MAGBANUA, Z.V.; PETERSON, D.G. Empirical comparison of ab initio repeat finding programs. **Nucleic Acids Research**, v. 36 n. 7, p. 2284-2294, 2008.

SCHMIEDER, R.; EDWARDS, R. Fast identification and removal of sequence contamination from genomic and metagenomic datasets. **PloS One**, v. 6 n. 3, p. e17288, 2011.

SERRANO-FREITAS, É.A.; SILVA, D.M.Z.A.; RUIZ-RUANO, F.J.; UTSUNOMIA, R.; ARAYA-JAIME, C.; OLIVEIRA, C. et al. Satellite DNA content of B chromosomes in the characid fish *Characidium gomesi* supports their origin

from sex chromosomes. **Molecular Genetics and Genomics**, v. 295 n. 1, p. 195-207, 2019.

SHAPIRO, J.A.; VON STERNBERG, R. Why repetitive DNA is essential to genome function. **Biological Reviews**, v. 80 n. 2, p. 227-250, 2005.

SHARBEL, T.F.; GREEN, D.M.; HOUBEN, A. B-chromosome origin in the endemic New Zealand frog *Leiopelma hochstetteri* through sex chromosome devolution. **Genome**, v. 41 n. 1, p. 14-22, 1998.

SHAW, M.W.; HEWITT, G.M. B chromosomes, selfish DNA and theoretical models: where next? **Oxford Surveys in Evolutionary Biology**, v. 7, p. 197-223, 1990.

SILVA, D.M.D.A.; PANSONATO-ALVES, J.C.; UTSUNOMIA, R.; ARAYA-JAIME, C.; RUIZ-RUANO, F.J.; DANIEL, S.N. et al. Delimiting the origin of a B chromosome by FISH mapping, chromosome painting and DNA sequence analysis in *Astyanax paranae* (Teleostei, Characiformes). **PLoS One**, v. 9 n. 4, p. e94896, 2014.

SILVA, D.M.Z.A., UTSUNOMIA, R., RUIZ-RUANO, F. J., DANIEL, S. N., PORTO-FORESTI, F., HASHIMOTO, D. T. et al. High-throughput analysis unveils a highly shared satellite DNA library among three species of fish genus *Astyanax*. **Scientific Reports**, v. 7, p. 12726, 2017.

SILVA, D.M.Z.A.; RUIZ-RUANO, F.J.; UTSUNOMIA, R.; MARTÍN-PECIÑA, M.; CASTRO, J.P.; FREIRE, P.P. et al. Long-term persistence of supernumerary B chromosomes in multiple species of *Astyanax* fish. **BMC Biology**, v. 19 n. 1, p. 1-17, 2021.

SMIT, A.F.A.; HUBLEY, R.; GREEN, P. RepeatMasker Open-4.0. http://www.repeatmasker.org. 2017.

SMITH, G.P. Evolution of repeated DNA sequences by unequal crossover. **Science**, v. 191 n. 4227, p. 528-535, 1976.

SONG, H.; FOQUET, B.; MARIÑO-PÉREZ, R.; WOLLER, D. Phylogeny of locusts and grasshoppers reveals complex evolution of density-dependent phenotypic plasticity. **Scientific Reports**, v. 7, p. 1–13, 2017.

STATON, S.E.; BURKE, J.M. Evolutionary transitions in the Asteraceae coincide with marked shifts in transposable element abundance. **BMC Genomics**, v. 16 n. 1, p. 1-13, 2015.

STAUB, R.W. Leaf striping correlated with the presence of B chromosomes in maize. **Journal of Heredity**, v. 78, p. 71–74, 1987.

SUMNER, A.T. A simple technique for demonstrating centromeric heterochromatin. **Expo Cell Research**, v. 75, p. 304-306, 1972.

SUN, C.; MUELLER, R.L. Hellbender genome sequences shed light on genomic expansion at the base of crown salamanders. **Genome Biology and Evolution**, v. 6 n.

7, p. 1818-1829, 2014.

TAMURA, K.; PETERSON, D.; PETERSON, N.; STECHER, G.; NEI, M.; KUMAR, S. MEGA5: molecular evolutionary genetics analysis using maximum likelihood, evolutionary distance, and maximum parsimony methods. **Molecular Biology and Evolution**, v. 28 n. 10, p. 2731-2739, 2011.

TENAILLON, M.I.; HUFFORD, M.B.; GAUT, B.S.; ROSS-IBARRA, J. Genome size and transposable element content as determined by high-throughput sequencing in maize and *Zea luxurians*. **Genome Biology and Evolution**, v. 3, p. 219-229, 2011.

TERUEL, M.; CABRERO, J.; MONTIEL, E.E.; ACOSTA, M.J.; SÁNCHEZ, A.; CAMACHO, J.P.M. Microdissection and chromosome painting of X and B chromosomes in *Locusta migratoria*. **Chromosome Research**, v. 17 n. 1, p. 11-18, 2009a.

TERUEL, M.; CABRERO, J.; PERFECTTI, F.; ACOSTA, M.J.; SÁNCHEZ, A.; CAMACHO, J.P.M. Microdissection and chromosome painting of X and B chromosomes in the grasshopper *Eyprepocnemis plorans*. **Cytogenetic and genome research**, v. 125 n. 4, p. 286-291, 2009b.

TERUEL, M.; CABRERO, J.; PERFECTTI, F.; CAMACHO, J.P.M. B chromosome ancestry revealed by histone genes in the migratory locust. **Chromosoma**, 119(2), 217-225, 2010.

TERUEL, M.; RUIZ-RUANO, F.J.; MARCHAL, J.A.; SÁNCHEZ, A.; CABRERO, J.; CAMACHO, J.P.M. et al. Disparate molecular evolution of two types of repetitive DNAs in the genome of the grasshopper *Eyprepocnemis plorans*. **Heredity**, v. 112, p. 531–542, 2014.

THOMAS, J.; PRITHAM, E.J. Helitrons, the eukaryotic rolling-circle transposable elements. **Microbiology Spectrum**, v. 3 n. 4, p. 3-4, 2015.

TOPP, C.N.; ZHONG, C.X.; DAWE, R.K. Centromere-encoded RNAs are integral components of the maize kinetochore. **Proceedings of the National Academy of Sciences, v.** 101 n. 45, p. 15986-15991, 2004.

TOSTA, V.C.; MARTHE, J.B.; TAVARES, M.G.; FERNANDES-SALOMÃO, T.M.; POMPOLO, S.G.; RECCO-PIMENTEL, S.M. et al. Possible introgression of B chromosomes between bee species (genus *Partamona*). **Cytogenetic and Genome Research**, v. 144 n. 3, p. 220-226, 2014.

TRIFONOV, V.A.; DEMENTYEVA, P.V.; LARKIN, D.M.; O'BRIEN, P.C.; PERELMAN, P.L.; YANG, F. et al. Transcription of a protein-coding gene on B chromosomes of the Siberian roe deer (*Capreolus pygargus*). **BMC Biology**, v. 11 n. 1, p. 1-11, 2013.

TSOUMANI, K.T.; DROSOPOULOU, E.; MAVRAGANI-TSIPIDOU, P.; MATHIOPOULOS, K.D. Molecular characterization and chromosomal distribution of a species-specific transcribed centromeric satellite repeat from the olive fruit fly,

Bactrocera oleae. **PLoS One**, v. 8 n. 11, p. e79393, 2013.

UGARKOVIĆ, Đ. Functional elements residing within satellite DNAs. **EMBO Reports**, v. 6 n. 11, p. 1035-1039, 2005.

UGARKOVIĆ, Đ.; PLOHL, M. Variation in satellite DNA profiles—causes and effects. **The EMBO journal**, v. 21 n. 22, p. 5955-5959, 2002.

UNTERGASSER, A.; CUTCUTACHE, I.; KORESSAAR, T.; YE, J.; FAIRCLOTH, B.C.; REMM, M. et al. Primer3—new capabilities and interfaces. **Nucleic Acids Research**, v. 40, p. e115– e115, 2012.

UTSUNOMIA, R.; SILVA, D.M.Z.D.A.; RUIZ-RUANO, F.J.; ARAYA-JAIME, C.; PANSONATO-ALVES, J.C.; SCACCHETTI, P.C. et al. (2016). Uncovering the ancestry of B chromosomes in *Moenkhausia sanctaefilomenae* (Teleostei, Characidae). **PLoS One**, v. 11 n. 3, p. e0150573, 2016.

VALENTE, G.T.; CONTE, M.A.; FANTINATTI, B.E.; CABRAL-DE-MELLO, D.C.; CARVALHO, R.F.; VICARI, M.R. et al. Origin and evolution of B chromosomes in the cichlid fish *Astatotilapia latifasciata* based on integrated genomic analyses. **Molecular Biology and Evolution**, v. 31 n. 8, p. 2061-2072, 2014.

VALENTE, G.T.; NAKAJIMA, R.T.; FANTINATTI, B.E.; MARQUES, D.F.; ALMEIDA, R.O.; SIMÕES, R.P. et al. B chromosomes: from cytogenetics to systems biology. **Chromosoma**, v. 126 n. 1, p. 73-81, 2017.

VITTORAZZI, S.E.; LOURENÇO, L.B.; RECCO-PIMENTEL, S.M. Long-time evolution and highly dynamic satellite DNA in leptodactylid and hylodid frogs. **BMC Genetics**, v. 15 n. 1, p. 1-11, 2014.

VU, G.T.; SCHMUTZER, T.; BULL, F.; CAO, H.X.; FUCHS, J.; TRAN, T.D. et al. Comparative genome analysis reveals divergent genome size evolution in a carnivorous plant genus. **Plant Genome**, v. 8 n. 3, p. 1-14, 2015.

WEBB, G.C.; WHITE, M.J.D.; CONTRERAS, N.; CHENEY, J. Cytogenetics of the partheno- genetic grasshopper *Warramaba* (formely Moraba) virgo and its bisexual rela- tives. IV. Chromosome banding studies. **Chromosoma**, v. 67, p. 309–339, 1978.

WEISS-SCHNEEWEISS, H.; LEITCH, A.R.; MCCANN, J.; JANG, T.S.; MACAS, J. Employing next generation sequencing to explore the repeat landscape of the plant genome. **Next Generation Sequencing in Plant Systematics. Regnum Vegetabile**, v. 157, p. 155-179, 2015.

WELLS, J.N.; FESCHOTTE, C. A field guide to eukaryotic transposable elements. **Annual Review Genetics**, v. 54, p. 539-561, 2020.

WERREN, J.H.; NUR, U.; EICKBUSH, D. An extrachromosomal factor causing loss of paternal chromosomes. **Nature**, v. 327 n. 6117, p. 75-76, 1987.

WHITE, W.J.D. Animal Cytology and Evolution, 3rd ed. London: Cambridge

University Press, 1973.

WILSON, E.B. The supernumerary chromosomes of Hemiptera. **Science**, NY v. 26 p. 870–871, 1907.

WONG, W.Y.; SIMAKOV, O.; BRIDGE, D.M.; CARTWRIGHT, P.; BELLANTUONO, A.J.; KUHN, A. et al. Expansion of a single transposable element family is associated with genome-size increase and radiation in the genus *Hydra*. **Proceedings of the National Academy of Sciences**, v. 116 n. 46, p. 22915-22917, 2019.

YOSHIDA, K.; TERAI, Y.; MIZOIRI, S.; AIBARA, M.; NISHIHARA, H.; WATANABE, M. et al. B chromosomes have a functional effect on female sex determination in Lake Victoria cichlid fishes. **PLoS Genetics**, v. 7 n. 8, p. e1002203, 2011.

YUAN, Y.W.; WESSLER, S.R. The catalytic domain of all eukaryotic cut-and-paste transposase superfamilies. **Proceedings of the National Academy of Sciences**, v. 108 n. 19, p. 7884-7889, 2011.

YUDKIN, D.V;, TRIFONOV, V.A.; KUKEKOVA, A.V.; VOROBIEVA, N.V.; RUBTSOVA, N.V.; YANG, F. et al. Mapping of KIT adjacent sequences on canid autosomes and B chromosomes. **Cytogenetic and Genome Research**, v. 116 n. 1-2, p. 100-103, 2007.

ZHOU, Q.; ZHU, H.M.; HUANG, Q.F.; ZHAO, L.; ZHANG, G.J.; ROY, S.W. et al. Deciphering neo-sex and B chromosome evolution by the draft genome of *Drosophila albomicans*. **BMC Genomics**, v. 13 n. 1, p. 1-12, 2012.

ZIEGLER, C.G.; LAMATSCH, D.K.; STEINLEIN, C.; ENGEL, W.; SCHARTL, M.; SCHMID, M. The giant B chromosome of the cyprinid fish *Alburnus alburnus* harbours a retrotransposon-derived repetitive DNA sequence. **Chromosome Research**, v. 11 n. 1, p. 23-35, 2003.

7. OTHER PUBLICATIONS PUBLISHED DURING PhD

1. PEREIRA, J. A.; **MILANI, D.**; FERRETTI, A. B. S. M.; BARDELLA, V. B. CABRAL-DE-MELLO, D. C.; LOPES, D. M. The extensive amplification of heterochromatin in *Melipona* bees revealed by high throughput genomic and chromosomal analysis. **Chromosoma** (accepted for publication).

2. **MILANI, D.**; RUIZ-RUANO, F. J.; CAMACHO, J. P. M.; CABRAL-DE-MELLO, D. C. Out of patterns, the euchromatic B chromosome of the grasshopper *Abracris flavolineata* is not enriched in high-copy repeats. **Heredity**, v. 127, p. 475-483, 2021.

3. MENEZES, R. S. T.; CABRAL-DE-MELLO, D. C.; **MILANI, D.**; BARDELLA, V. B.; ALMEIDA, E. A. B. The relevance of chromosome fissions for major ribosomal DNA dispersion in hymenopteran insects. **Journal of Evolutionary Biology**, v. 34-9, p. 1466-1476, 2021.

4. MARTI, E.; **MILANI, D.**; BARDELLA, V. B.; ALBUQUERQUE, L.; SONG, H.; PALACIOS-GIMENEZ, O. M.; CABRAL-DE-MELLO, D. C. Cytogenomic analysis unveils mixed molecular evolution and recurrent chromosome rearrangements shaping the multigene families on *Schistocerca* grasshopper genomes. **Evolution**, v. 75-8, p. 2027–2041, 2021.

5. PALACIOS-GIMENEZ, O. M.; **MILANI, D.**; SONG, H.; MARTI, D. A.; LÓPEZ-LEÓN, M. D.; RUIZ-RUANO, F. J.; CAMACHO, J. P. M.; CABRAL-DE-MELLO, D. C. Eight Million Years of Satellite DNA Evolution in Grasshoppers of the Genus *Schistocerca* Illuminate the Ins and Outs of the Library Hypothesis. **Genome Biology and Evolution**, v. 12, p. 88-102, 2020.

6. FERRETTI, A. B. S. M.; **MILANI, D.**; PALACIOS-GIMENEZ, O. M.; RUIZ-RUANO, F. J.; CABRAL-DE-MELLO, D. C. High dynamism for neo-sex chromosomes: satellite DNAs reveal complex evolution in a grasshopper. **Heredity**, v. 1365-2, p. 1, 2020.

7. BARDELLA, V. B.; **MILANI, D.**; CABRAL-DE-MELLO, D. C. Analysis of *Holhymenia histrio* genome provides insight into the satDNA evolution in an insect with holocentric chromosomes. **Chromosome Research**, v. 1, p. 1, 2020.

8. FERRETTI, A. B. S. M.; RUIZ-RUANO, F. J.; **MILANI, D.**; LORETO, V.; MARTI, D. A.; RAMOS, E.; MARTINS, C.; CABRAL-DE-MELLO, D. C. How dynamic could be the 45S rDNA cistron? An intriguing variability in a grasshopper species revealed by integration of chromosomal and genomic data. **Chromosoma**, v. 128, p. 165-175, 2019.

9. PALACIOS-GIMENEZ, O. M.*; **MILANI, D.***; LEMOS, B.; CASTILLO, E. R.; MARTÍ, D. A.; RAMOS, E.; MARTINS, C; CABRAL-DE-MELLO, D. C. Uncovering the evolutionary history of neo-XY sex chromosomes in the grasshopper *Ronderosia bergii* (Orthoptera, Melanoplinae) through satellite DNA analysis. **BMC Evolutionary Biology**, v. 18, p. 1-10, 2018.
*co-first authors

10. **MILANI, D.**; BARDELLA, V. B.; FERRETTI, A. B. S. M.; PALACIOS-GIMENEZ, O. M.; MELO, A. S.; MOURA, R. C.; LORETO, V.; SONG, H.; CABRAL-DE-MELLO, D. C. Satellite DNAs unveil clues about the ancestry and composition of B chromosomes in three grasshopper species. **Genes**, v. 9, p. 523, 2018.